Contract No:

This document was prepared in conjunction with work accomplished under Contract No. DE-AC09-08SR22470 with the U.S. Department of Energy (DOE) Office of Environmental Management (EM).

Disclaimer:

SRNL-STI-2013-00160
Revision 0

Keywords:
Waste Treatment Plant,
SuperLig 639,
Adsorption Isotherm,
Column Modeling

Retention:
Permanent

Upgrade to Ion Exchange Modeling for Removal of Technetium from Hanford Waste Using SuperLig® 639 Resin

L. L. Hamm
F. G. Smith, III
S. E. Aleman
D. J. McCabe

May 2013

Savannah River National Laboratory
Savannah River Nuclear Solutions, LLC
Aiken, SC 29808

Prepared for the U.S. Department of Energy under contract number DE-AC09-08SR22470.

DISCLAIMER

Printed in the United States of America

Prepared for
U.S. Department of Energy

REVIEWS AND APPROVALS

AUTHOR:

L. L. Hamm, Process Modeling and Computational Chemistry Date

F. G. Smith, Process Modeling and Computational Chemistry Date

S. E. Aleman, Threat Assessments Date

D. J. McCabe, Advanced Characterization and Process Development Date

TECHNICAL REVIEW:

W. D. King, Advanced Characterization and Process Development Date

APPROVAL:

M. B. Gorensek, Acting Manager Date
Process Modeling and Computational Chemistry

F. M. Pennebaker, Manager Date
Advanced Characterization and Process Development

S. L. Marra, Manager Date
E&CPT Research Programs

R.A. Robbins, Washington River Protection Solutions Date

TABLE OF CONTENTS

LIST OF TABLES

LIST OF FIGURES

LIST OF ACRONYMS

IDF	Integrated Disposal Facility
LAW	Low Activity Waste
PA	Performance Assessment
PNNL	Pacific Northwest National Laboratory
PNWD	Pacific Northwest Division
SRNL	Savannah River National Laboratory
SRS	Savannah River Site
WRPS	Washington River Protection Solutions
WTP	Waste Treatment Plant

1.0 Executive Summary

This report documents the development and application of computer models to describe the sorption of pertechnetate [TcO_4^-], and its surrogate perrhenate [ReO_4^-], on SuperLig® 639 resin. Two models have been developed: 1) A thermodynamic isotherm model, based on experimental data, that predicts [TcO_4^-] and [ReO_4^-] sorption as a function of solution composition and temperature and 2) A column model that uses the isotherm calculated by the first model to simulate the performance of a full-scale sorption process. The isotherm model provides a synthesis of experimental data collected from many different sources to give a best estimate prediction of the behavior of the pertechnetate-SuperLig® 639 system and an estimate of the uncertainty in this prediction. The column model provides a prediction of the expected performance of the plant process by determining the volume of waste solution that can be processed based on process design parameters such as column size, flow rate and resin physical properties.

Technetium-99 (^{99}Tc) is a long-lived radionuclide with a half-life of 210,000 years and is a significant fission product from nuclear reactors. Over fifty years of nuclear materials production at the DOE Hanford facility has generated waste containing approximately 26,500 Curies of ^{99}Tc, which is predominantly soluble, and will be processed as Low Activity Waste (LAW). The primary chemical form of ^{99}Tc found in LAW is the pertechnetate anion (TcO_4^-), which will not be removed from the aqueous waste in the Hanford Waste Treatment and immobilization Plant (WTP), and will primarily end up immobilized in the LAW glass, which will be disposed in the Integrated Disposal Facility (IDF). Removal of technetium from the LAW would eliminate a key risk contributor for the IDF PA for potential acceptance of supplemental waste forms, and has potential to reduce treatment and disposal costs. Elutable ion exchange has been developed for removing ^{99}Tc from LAW at Hanford, but the technology is not fully matured. One aspect of that maturation is updating the computer modeling of the ion exchange process to better estimate design of a system. This is one element of an overall strategy of managing technetium in Hanford tank waste.

SRNL previously performed preliminary computer modeling of technetium removal from Hanford Low Activity Waste (LAW) streams using ion exchange (Hamm, et al., 2000). Since this original modeling report was issued, additional laboratory data has been generated that was included as part of performing the updated model predictions reported here. The key tasks performed and key results from the current analysis are:

1. Updating the equilibrium model for technetium ion-exchange using SuperLig® 639[1] resin by including additional laboratory data.

   Data sources referenced in the preliminary 2000 study and in the current study are listed in Section 12. The preliminary study included data from 14 experimental studies. Eight of these 14 data sets were selected based on data consistency and included in the current modeling study along with data from nine experimental studies completed after the preliminary modeling was performed. The resulting data base was used to develop isotherm models for adsorption of pertechnetate and perrhenate on SuperLig® 639 at ~25 °C.

[1] SuperLig is a trademark of IBC Advanced Technologies, Inc., American Fork, UT

Some key results from this analysis are:

- The Technetium-SuperLig® 639 system operates as a sorption process where sorption of strong electrolytes dominates the equilibrium state. The concept of an anion-exchange process utilized in the preliminary study is replaced with the concept of sorption of neutral species (strong electrolytes).
- The new isotherm model addresses resin behavior with regard to ionic strength. In this analysis report, the isotherm model is limited to the loading phase only, but has the potential to also describe equilibrium behavior under elution conditions as well. Future effort to generalize this approach to include elution conditions is viable and could aid in process optimization.
- A potassium ion (K^+) enhancer effect was suspected during column studies and analyses performed in 2002. The more complete analysis provided in this report indicates that neutral species based on K^+ ion versus Na^+ ion are 50-to-75 times more favorable for sorption onto SuperLig® 639. The overwhelming evidence from batch contact tests, column loading tests, and column elution studies strongly confirms this observation.
- The average estimated value for the total sorption capacity for pertechnetate from the five different batches of SL-639 analyzed in this report is ~0.58 mmole $[TcO_4^-]/g_{resin}$. Sorption capacity varied from 0.30 to 0.96 mmole $[TcO_4^-]/g_{resin}$ for these batches.
- Given the importance of the batch-specific total sorption capacity and the minimal amount of experimental data available, measurement of this important parameter should be included in future testing plans.

2. Demonstration of the performance of the updated ion-exchange column model at different scales by comparison of model predictions to the observed performance of experimental columns.
    - Twelve column benchmark cases were chosen that range over the 6 resin batches of interest. The VERSE-LC column cycles were continued to where the lead column is nearly saturated (i.e., completely loaded). No effort was made to adjust VERSE-LC breakthrough predictions for these benchmark cases. The VERSE-LC predictions in general closely followed the experimental results.
3. Prediction of full-scale LAW ion-exchange performance during cycling in a two-column carousel arrangement with the currently projected average waste composition.

    A model was developed using the VERSE-LC code to simulate operation of the proposed full-scale LAW ion-exchange column using the TcO_4^- isotherm predicted from the analyses performed in items 1 and 2. The model predicts that a typical lead/lag column cycle using two columns with resin bed volumes of one cubic meter and bed length to diameter ratios of 3:1 is able to process approximately 27,000 gallons (102 bed volumes) of waste when operating at 25 °C. A cycle is terminated when the cumulative average concentration of pertechnetate in the effluent collected from the lag column reaches 1% of the concentration in the feed stream (i.e, a decontamination factor of 100). Breakthrough curves for the SL-639 TcO_4^- system were predicted to be relatively gradual. Using a 1% decontamination criterion based on the cumulative average effluent

concentration instead of on the instantaneous concentration measured at the exit of the lag column allows the system to process about 60% more waste volume in each cycle. Resin degradation during repeated sorption and elution cycles was not modeled.

- The prediction of overall performance for the Full-Scale column is lower in this report than that provided in the 2000 Report. The reduced performance is not the result of the newer analysis but is caused by differences between the original projected LAW composition and the current projected composition due to the inclusion of additional waste tanks. The feed compositions used in the 2000 Report (Envelope-A and Envelope-B feeds) had higher K+ (enhancer effect) and Na+ (ionic strength effect) concentrations along with lower NO_3^- (competitor effect) concentrations than the HTWOS System Plan 6 (Certa et al., 2011) average 5 M feed composition employed in this report.
- Full-Scale column performance is projected to achieve 40% to 50% breakthrough in the lead column before elution is required. Therefore, the ability to accurately predict not just the initial breakthrough but up to ~50% breakthrough is of importance. The column benchmarking suggests that the current VERSE-LC parameter settings provide reasonable estimates of column performance up to this level of breakthrough. Future improvements in column performance predictions/reliability should focus on mass transfer limiting aspects.
- As noted above, resin batch specific sorption capacity varied by about ±50% from the nominal value used in the column simulations. As a first approximation, the amount of waste that can be processed is directly proportional to the total sorption capacity.

2.0 Introduction and Background

The primary chemical form of ^{99}Tc found in Hanford Low Activity Waste (LAW) is the pertechnetate anion (TcO_4^-). Pertechnetate is highly soluble in water, and is mobile if released to the environment. Pertechnetate will not be removed from the aqueous waste in the Hanford Waste Treatment Plant, and will primarily end up immobilized in the LAW glass waste form, which will be disposed in the Integrated Disposal Facility (IDF). Because ^{99}Tc has a very long half-life and is highly mobile (Icenhower, 2008, 2010), it has the potential to be a major dose contributor to the Performance Assessment (PA) of the IDF (Mann, 2003). Due to the soluble properties of pertechnetate, and the potential for impact to the PA, effective management of ^{99}Tc is important to the overall success of the River Protection Project mission.

Removal, followed by off-site disposal of technetium from the LAW, would eliminate a key risk contributor for the IDF PA for supplemental waste forms, and has the potential to reduce treatment and disposal costs. Washington River Protection Solutions (WRPS) is developing conceptual flow sheets for LAW treatment and disposal that could benefit from technetium removal. One of these flow sheets will specifically examine removing TcO_4^- from the LAW feed stream to supplemental immobilization. To enable an informed decision regarding the viability of technetium removal, further maturation of available technologies will be performed. One of the technologies, SuperLig® 639, is an elutable ion exchange resin available from a commercial vendor.

This document describes an update to the computer modeling performed for maturation of the use of SuperLig® 639 for treatment of LAW at Hanford. A preliminary analysis report was issued in 2000 (referred to in this report as the "2000 Report"; (Hamm et al., 2000) where essentially all available batch contact and column studies were incorporated into the analysis effort. Updating this model will enable projection of performance with a wider range of feed compositions than was assumed in the original model and better estimates of full-scale performance. Ultimately, this will assist in projecting the size and throughput of a technetium treatment process to improve confidence in the design assumptions. Using a detailed computer model is vital in maturing the concept of a technetium ion exchange process because the impact from the wide-ranging chemistry of the many waste tanks at Hanford cannot be determined experimentally. Unlike most applications of ion exchange, the LAW feed composition will vary dramatically, and measuring behavior with each waste tank is not feasible and is cost prohibitive. A robust, comprehensive model can be used as a tool to evaluate design and operating options versus the waste feed composition and the results can be used in decision-making.

2.1 Insight from 2002 Analysis Efforts

Within the Executive Summary (Section 1) of the 2000 Report it was stated that "significant uncertainty exists in understanding the causes of column performance variability (i.e., it is believed that the majority of uncertainties reside with unknown factors influencing the isotherm model)." In the preliminary work, an estimate for the relative affinities of SuperLig® 639 resin for ion-exchange was $TcO_4^- > NO_3^- >> (SO_4^{2-}, Cl^-, OH^-, NO_2^-$, and $CO_3^{2-})$, while the relative affinity for other potential competitors had not yet been determined. The affinities for $NaTcO_4$ and $KTcO_4$ were assumed to be equal.

After that preliminary report was published in 2000, further experimental studies of the Technetium-SuperLig® 639 system were undertaken both at SRNL and PNNL. During the 2002

timeframe additional modeling analysis efforts were initiated but were terminated in late 2002 due to DOE's change of focus with regard to technetium removal in the WTP. A significant result of the 2002 modeling analysis was quantifying the Technetium-SuperLig® 639 system as a sorption process where sorption of strong electrolytes dominates the equilibrium state. In the present work, the concept of an anion-exchange process is replaced with the concept of sorption of neutral species (i.e., here strong electrolytes). The sorption of strong electrolytes complicates the creation of isotherm models since now multiple ion-pair combinations can exist on the solid phase. For example: $Na^+XO_4^-$, $K^+XO_4^-$, $Na^+NO_3^-$, $K^+NO_3^-$, $Na^+NO_2^-$, and $K^+NO_2^-$ are all neutral species that can potentially exist on the solid phase. We then have "enhancer" and "competitor" effects to contend with. To illustrate these aspects, consider a simple solution containing only the mono-valent cations Na^+ and K^+ and the mono-valent anions XO_4^- and NO_3^- where X is either Re or Tc. Further assume that a finite number of sorption sites exist per unit mass of dry resin. For Tc the following four mass-action processes would apply where L represents a site on the resin and the overbar indicates solid phase species:

$$\overline{L} + Na^+ + TcO_4^- \xleftrightarrow{K_{eq,1}} \overline{L - NaTcO_4}\,, \tag{2-1}$$

$$\overline{L} + K^+ + TcO_4^- \xleftrightarrow{K_{eq,2}} \overline{L - KTcO_4}\,, \tag{2-2}$$

$$\overline{L} + Na^+ + NO_3^- \xleftrightarrow{K_{eq,3}} \overline{L - NaNO_3}\,, \text{ and} \tag{2-3}$$

$$\overline{L} + K^+ + NO_3^- \xleftrightarrow{K_{eq,4}} \overline{L - KNO_3}\,. \tag{2-4}$$

Eq. (2-2) indicates that K^+ has the potential to "enhance" the TcO_4^- loading performance of the resin, while both Eqs. (2-3) and (2-4) represent "competition" of NO_3^- for sorption sites. The degree of enhancement and/or competition is determined by the various thermodynamic equilibrium constants. The equilibrium constant for the key reaction in Eq. (2-1) is:

$$K_{eq,1}(T) \equiv \left(\frac{\left[\overline{L - NaTcO_4}\right]}{\left[\overline{L}\right]\left[Na^+\right]\left[TcO_4^-\right]} \right)\left(\frac{1}{\gamma_{Na}\gamma_{TcO4}} \right) = \left(\hat{K}(T,\bar{c})\right)\left(\frac{1}{\gamma_{Na}\gamma_{TcO4}} \right), \tag{2-5}$$

In Eq. (2-5), γ_{Na} and γ_{TcO4} are liquid phase activity coefficients, non-ideality of the solid phase has been neglected, and the $\hat{K}(T,\bar{c})$ term represents an "effective" selectivity coefficient which becomes temperature and composition dependent.

Further experimental support for the above concept came from both SuperLig® 639 column loading and elution studies performed by Burgeson et al. (2002) and King et al. (2003). Table 2-1 provides some of the key aspects of the six column tests performed in 2002. From elution eluent, King et al. (2003) measured the concentration of Na^+ and K^+ exiting three columns over time using an online monitoring device. Figure 2-1 is a plot of their measurements. Three different column studies are shown where the initially loaded column was obtained using Hanford waste simulants for AN-105 (Envelope-A[1]), AZ-102 (Envelope-B), and AN-107

[1] Waste "Envelopes" were waste composition ranges defined in the early phase of Waste Treatment Plant Privatization contract. Envelope "A" referred to high nitrate/hydroxide dissolved salt solution; Envelope "B" referred to high sulfate dissolved salt solution; Envelope "C" referred to high soluble organic dissolved salt solution (a.k.a. "complex concentrate" waste); Envelope "D" referred to sludge.

(Envelope-C). If K^+ is to have an important enhancer effect then we would expect to see it within the eluent most likely for AZ-102 since its presence in that feed is the greatest. As Figure 2-1 illustrates, a clear presence of K^+ can be seen. Within the measurement errors of the techniques employed, its presence in the other two column eluents was not observed.

In order to predict XO_4^- breakthrough curves for the loading phase, VERSE requires simple algebraic isotherms. In the 2002 modeling analysis effort, new and improved algebraic isotherm models were created that took into account the enhancer and competitor effects mentioned above. Here, non-ideality within both liquid and solid phases is neglected. The following is a brief description of how the improved 2002 algebraic isotherm model was developed.

A three step development approach was employed where:

- Step 1 the "Enhancer" effect was considered;
- Step 2 a single "Competitor" effect was considered; and
- Step 3 the "Enhancer" effect and multiple "Competitor" effects were combined.

In Step 1, the following four equations were solved analytically:

$$K_{nx} = \frac{Q_{nx}}{Q_L c_n c_x}, \tag{2-6}$$

$$K_{kx} = \frac{Q_{kx}}{Q_L c_k c_x}, \tag{2-7}$$

$$Q_x = Q_{nx} + Q_{kx}, \tag{2-8}$$

$$Q_T = Q_x + Q_L. \tag{2-9}$$

Where: Q is solid phase loading (mmol/g) and n=Na, k=K, x=Re or x=Tc. The final isotherm becomes:

$$Q_x = \frac{Q_T c_x}{c_x + \beta}, \tag{2-10}$$

where

$$\beta = \frac{1}{K_{nx} c_n + K_{kx} c_k}. \tag{2-11}$$

In Step 2, the following five equations were solved analytically:

$$K_{nx} = \frac{Q_{nx}}{Q_L c_n c_x}, \tag{2-12}$$

$$K_{no} = \frac{Q_{no}}{Q_L c_n c_o}, \tag{2-13}$$

$$Q_x = Q_{nx}, \tag{2-14}$$

$$Q_o = Q_{no}, \tag{2-15}$$

$$Q_T = Q_x + Q_o + Q_L \quad . \tag{2-16}$$

where o = NO_3. The final isotherm becomes:

$$Q_x = \frac{Q_T c_x}{c_x + \beta} \quad , \tag{2-17}$$

where

$$\beta = \frac{1 + K_{no} c_n c_o}{K_{nx} c_n} \quad . \tag{2-18}$$

In Step 3, Eqs. (2-11) and (2-18) were combined to provide an estimated beta parameter that can be expressed as:

$$\beta = \frac{1 + (K_{no} c_n + K_{ko} c_k) c_o + (K_{np} c_n + K_{kp} c_k) c_p}{K_{nx} c_n + K_{kx} c_k} \quad . \tag{2-19}$$

where p = NO_2 which was considered to be a potential competitor because of its high concentration in most waste solutions. Note that Eq. (2-17) has the functional form of a traditional Langmuir isotherm which assumes a fixed number of sites that are also homogeneous.

Equations (2-17) and (2-19) were employed in the 2002 modeling analysis effort. Fitting methods similar to those employed in the 2000 Report were used to determine new selectivity coefficients for predicting "effective" single-component isotherm models. The K^+ effect, as seen in the simulant column elution studies by King et al. (2003), were checked against the column loading experiments with actual Hanford tank waste made by Burgeson et al. (2002). VERSE predictions of these new loading breakthrough curves were created using both the 2000 Report isotherm model and the newer 2002 analysis model.

A comparison of the predicted versus measured Tc breakthrough curves are shown in Figure 2-2. As can be seen in Table 2-1, a K^+ enhancer effect, if present, should be seen most clearly in the AP-101 (Envelope-A) column breakthrough results. In Figure 2-2 the results for AP-101 are shown as: (1) red circles representing the measured data, (2) a solid red curve that represents prediction using the 2000 Report isotherm model, and (3) a dashed red curve that represents prediction using the newer 2002 isotherm model which contains the K^+ enhancer effect. As Figure 2-2 indicates, a significant improvement in the predicted breakthrough behavior is achieved once the K^+ enhancer effect is included.

From the 2002 assessment it was determined that the above concept of sorption of strong electrolytes on a resin bed with a fixed number of sorption sites is a more valid representation than the earlier 2000 Report ion-exchange concept. As such, it is this newer concept that is used and improved on in this analysis report.

It should also be pointed out that the newer concept automatically addresses resin behavior with regard to ionic strength. This resin is elutable under lower ionic strength conditions (e.g., adequate elution occurs with water) as demonstrated by experimentation. The new model has this basic aspect built into it; even though, no effort is made to exploit this feature in this report. This analysis report is limited to the loading phase only. Future effort to generalize this approach to include elution conditions is plausible and would aid in system optimization.

2.2 Ion Exchange Modeling

The technetium ion-exchange system is one of many unit operations within the larger process flowsheet. Experimental efforts are required to characterize the resin and performance of the ion-exchange process in support of the overall design. Modeling the ion-exchange process in detail provides key supporting information needed to establish the overall flowsheet. For example, the ion exchange cycle time required to achieve the specified decontamination factor is needed at the overall flowsheet level. Separate (off-line) detailed transient column modeling can provide this information where the detail of the analysis is not restricted due to constraints imposed by runtime and storage requirements for the entire flowsheet.

2.3 Report Overview

This report focuses on the technetium-loading phase of a complete ion exchange process cycle. A preliminary analysis methodology was developed by Hamm et al. (2000) where as much of the available and pertinent data on the Technetium-SuperLig® 639 system was incorporated. This analysis effort updates the original 2000 effort by improving the isotherm model itself by (1) incorporating post-2000 Report column and batch contact data and (2) employing a more comprehensive numerically based isotherm modeling approach.

This document represents an updated status report on our current knowledge and capability to model the ion-exchange process for the Technetium-SuperLig® 639 system under various Hanford feed conditions. The methodology, its justification, assessment, and application to a possible facility are discussed in the following sections. Supporting information has also been provided in several appendices and wherever possible references to available published data/information pertinent to the discussion has been cited.

The theoretical approach and modeling calculations used in this work were cross-checked by the authors. A technical review of the modeling approach, ion-exchange chemistry, and a check of the work performed against that described in the Task Technical and Quality Assurance Plan (McCabe and Hamm, 2012) was also performed independently by Advanced Characterization and Process Development personnel.

Table 2-1. Key column studies performed during 2002 supporting the strong electrolyte sorption concept (SRNL experiments used simulants PNNL experiments used actual waste)

Lab	PI	XO4-	T (C)	Hanford Waste Envelope	Waste/ Simulant	Resin Batch number	Na+ [M]	K+ [M]	NO3- [M]
SRNL	**King**	**Re**	**25**	**A**	**AN-105**	5	4.866	0.094	1.073
SRNL	**King**	**Re**	**25**	**B**	**AZ-102**		4.665	0.147	0.472
SRNL	**King**	**Re**	**25**	**C**	**AN-107**		5.742	0.035	2.564
PNNL	**Burgeson**	**Tc**	**24-28**	**A**	**AP-101**	3	4.810	0.750	1.880
PNNL	**Burgeson**	**Tc**	**24-28**	**B**	**AZ-101**		4.260	0.090	0.850
PNNL	**Burgeson**	**Tc**	**24-28**	**C**	**AN-102**		4.780	0.028	1.730

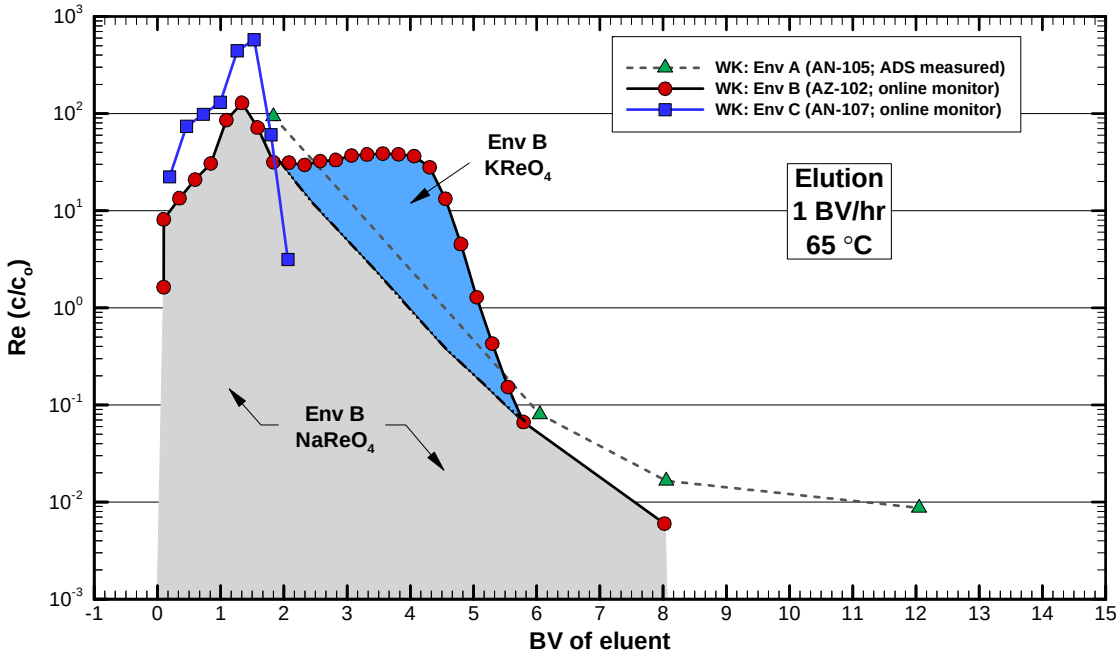

Figure 2-1. Measured eluent concentrations taken from the elution of three bench-scale columns partially loaded with Envelope A (AN-105), B (AZ-102), and C (AN-107) simulants (King et al., 2000) and eluted with water. All three columns were created using Resin Batch 5 and were loaded at 25 °C.

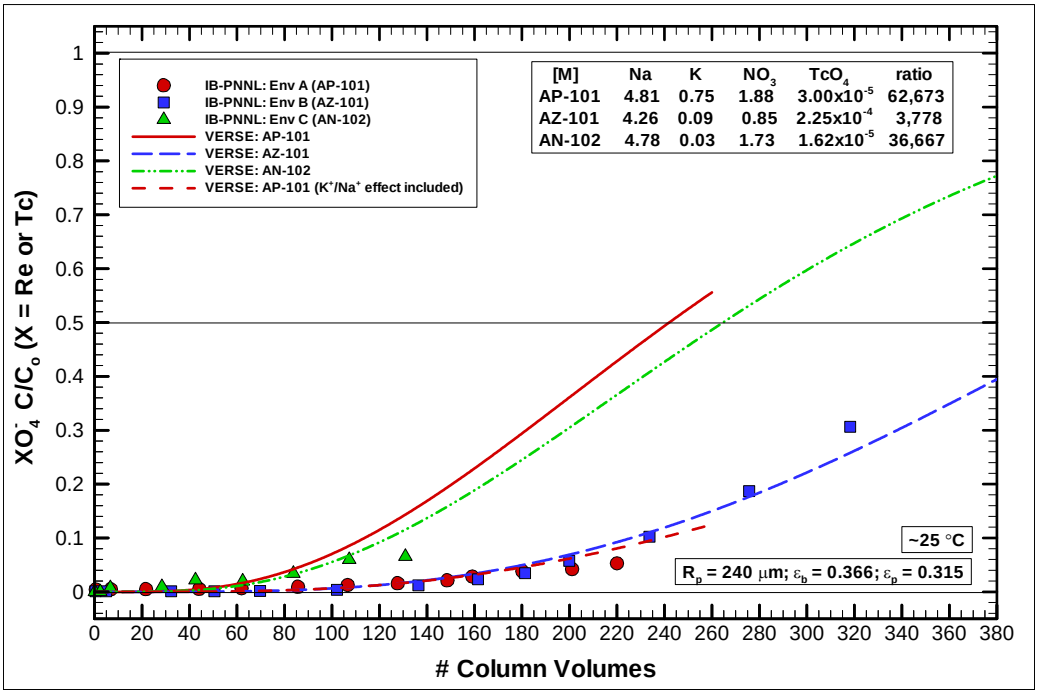

Figure 2-2. Measured and predicted exit concentrations taken from the loading-phase of three columns partially loaded with Envelope A (AP-101), B (AZ-101), and C (AN-102) (Burgeson et al., 2002). All three column experiments used samples of actual tank waste, Resin Batch 3, and were loaded at ~26 °C.

3.0 Column Model Formulations

The modeling of ion exchange columns is typically divided into two fundamental areas:

1. Determination of an equilibrium isotherm model generally empirical in nature but based on experimental data, and
2. A column model based on one-dimensional solute transport through a porous sorption material.

See Hamm et al. (2000) Section 3 for details on the baseline approach.

In the 2000 Report, algebraic isotherm models were generated employing a "Maximum Likelihood Algorithm" (Anderson et al., 1978) by fitting selected (experimentally obtained) batch contact data to simple non-linear isotherm equations. This approach provided limited flexibility to assess new batches and different feed compositions. In that analysis effort, it was believed that the majority of uncertainties associated with predicting column performance resided within the isotherm model.

In the upgraded approach presented in this report, a more chemistry-based model for the creation of isotherms has been developed. This improved isotherm model (a numerically based algorithm named "CERMOD") is employed to perform "numerical" batch contact experiments whose goal is the creation of simple "effective" single-component sorption isotherms (CERMOD can also be used to create mult-component isotherms). The improved method reduces overall uncertainties and increases the range of prediction with regard to feed compositions. Section 4 of this report addresses the improved equilibrium isotherm model (i.e., the "effective" single-component isotherm model and its chemistry-based numerical model - CERMOD). Details about CERMOD can be found in Appendix B.

The basis and justification for use of a simpler "effective" single-component column model was provided in the 2000 Report and remains valid for this analysis effort as well (Hamm et al., 2000 Section 3).

To take into account the various mechanisms for ion transport and adsorption as it travels down an ion exchange column, a porous particle solute transport formulation has experienced widespread use and acceptability. For this class of column models, five basic aspects of the ion exchange column must be addressed. In order of their importance with respect to predicting exit breakthrough curves for the Technetium-SuperLig® 639 system, they are:

- **Bed Definition** (high impact) – column size, geometry, and resin mass have a very direct impact on overall column performance, with particle geometry having a slightly less important impact (shifts entire breakthrough curve with respect to number of column volumes required to reach a specified concentration level).
- **Adsorption Isotherms** (high impact) – resin affinities for the various competing ions of interest have a very direct impact on overall column performance (shifts entire breakthrough curve with respect to number of column volumes required to reach a specified concentration level and for non-linear isotherms alters breakthrough curve shape as well as its sensitivity with respect to inlet feed conditions).

- **Pore Diffusion** (moderate impact) – intra-particle mass transport by pore diffusion to available surface sites has a moderate impact on overall column performance, with particle geometry having a slightly less important impact (under non-limiting mass transfer conditions it alters the shape of exit breakthrough curves typically by a rotation about the ~50% relative concentration level with slight shifting; under limiting mass transfer conditions the rotation is generally at a point higher than 50%).
- **Film Diffusion** (low impact) – liquid mass transport by film diffusion across the particle-to-bed boundary has a low impact on overall column performance (alters the shape of exit breakthrough curves typically by a rotation about the ~50% relative concentration level with slight shifting).
- **Axial Dispersion** (low impact) – mass transport along the column by axial dispersion has a low impact on overall column performance (alters the shape of exit breakthrough curves typically by a rotation about the ~50% relative concentration level with slight shifting).

The levels of impact indicated above are based on sensitivity studies and are relative values. Mechanisms such as surface migration or adsorption kinetics are not included in our column model since their impacts were considered to be negligible (e.g. fast kinetics) or already indirectly incorporated into the other features during the parameter estimation process.

4.0 Equilibrium Adsorption Isotherms

The development of an upgraded isotherm model consumed the major portion of the effort performed in this revised analysis. As pointed out earlier, a major weakness of the preliminary analyses presented in the 2000 Report was the algebraic isotherm models employed. In this section we will discuss the new isotherm modeling approach which is significantly more complicated than the prior approach; however, this newer approach provides more assurance and flexibility in addressing a range of feed compositions to which little (if any) isotherm data exists.

In our column modeling approach we assume that the rate of chemical adsorption is very fast when compared to the rates of diffusion within the pore fluid and mass transfer across the liquid film at the outer boundaries of the particles. In other words, we assume that local equilibrium exists between the pore fluid and its neighboring surface sites (i.e., very fast surface reaction kinetics). With this assumption an algebraic expression relating ionic (or neutral species) concentrations between the pore fluid and the solid resin (i.e., surface sites) can be established. No explicit attempt is, or has been, made to verify this assumption. In an indirect manner this assumption is either verified or incorporated into some of the modeling parameters. In addition, we assume that the resin contains a fixed number of homogeneous adsorption sites whose concentration (sites per gram of dry resin) is independent of total ionic strength or solution composition. As with any resin, it is possible that manufactured resin batches have some variability in the total sorption capacity. Therefore, as part of the isotherm model development, the total sorption capacity is considered to be an additional parameter that is estimated based on selected batch specific column loading data included into the available batch equilibrium contact data.

The original Langmuir-like isotherm from Section 2 is:

$$Q_x = \frac{Q_T c_x}{c_x + \beta} \ , \qquad (2\text{-}17)$$

The same functional form as shown in Eq. (2-17) is being employed in this analysis effort as was employed in the 2000 Report. The main difference between the two efforts is in how the beta parameter is being estimated:

- In the 2000 Report the beta parameter was curve fitted to a subset of batch contact experiments that were chosen based on composition limitations. The total capacity term was adjusted to account for column performance aspects.
- In this analysis effort the beta parameter is computed from a series of "numerical" batch contact tests (using CERMOD) where the model parameters (e.g., chemical equilibrium constants) are based on a large composite database. Best estimate values for total capacity and the other modeling parameters are estimated during an optimization activity prior to application to any specific feed composition. Feed compositions are not limited to the same degree as in the earlier effort.

In the isotherm development below, and later in its application in Section 9, we are assuming that the total ionic exchange capacity of the resin (i.e., number of active adsorption sites in milli-moles per gram of resin on a dry basis) is independent of the liquid-phase total ionic strength and the composition of competing anions. We are assuming that batch differences are primarily

related to improvements (or process variances) in the engineering/manufacturing of the SuperLig® 639 resin (i.e., number of sites per gram), not alterations in the chemistry.

4.1 Overview of Experimental Data

Equilibrium batch contact data and column performance data for adsorption of pertechnetate and perrhenate on SuperLig® 639 were obtained from the sources listed in Section 12.1. A summary of these data sets is given in Tables 4-1 and 4-2. Table 4-1 lists the different batches of SuperLig® 639 resin that were used in the experiments. Five different batches of SL-639 produced by IBC were used and a sixth batch was created by blending a 50:50 mixture of two batches to provide enough material for large scale column experiments. Because some variability in the performance of different resin batches is expected, having six batches represented in the database potentially introduces significant variation into the data. Batch-to-batch variability was accounted for by estimating a capacity for pertechnetate or perrhenate adsorption for each batch.

Table 4-2 lists the data sets and the number of batch contact and column experiments conducted, separated into the experiments using TcO_4^- and ReO_4^-, and by the temperature of the experiment. The temperatures listed in Table 4-2 are nominal values and conditions varied for each experiment and sometimes within each experiment. Data at the nominal temperature of 25 °C actually includes data taken over a range of temperatures from 19 °C to 26 °C which also introduces a degree of variability into the results. Including TcO_4^- and ReO_4^- data, 154 batch contact results are available at a nominal temperature of 25 °C. Typically the batch contacts were run in duplicate and the duplicate data has been included in the isotherm analysis.

One data set (Rapko et al., 2003) contained results from 20 batch contact experiments (12 pertechnetate and eight perrhenate) at 65 °C. Other than these results, the only data at temperatures other than 25 °C consists of one perrhenate batch contact experiment and two column runs at 35 °C and another batch contact experiment with two column runs at 45 °C conducted with AN-105 simulant at SRNL (Duffey et al., 2003 and King et al., 2003). Although not done as part of this work, these data sets could be used to estimate the temperature dependence of the isotherm.

Table 4-3 lists the various column tests considered in the determination of a batch specific total sorption capacity. All column testing was conducted with simulated or actual Hanford waste, except for one test conducted with SRS waste.

4.2 Equilibrium Batch Contact Tests

Batch contact test data was taken from the 2000 Report and additional data created after issuing the 2000 Report was included. A brief summary of the batch contact database is provided in Tables A-1 through A-7 where only those key parameters of interest are listed. The database is arranged by the first author of each technical report reviewed:

- King (22 Re tests and 2 Tc tests)
- Duffey (9 Re tests)
- Rapko (8 Re tests and 32 Tc tests)
- Hassan (25 Tc tests)
- Burgeson (22 Tc tests)

- Blanchard (12 Tc tests)
- Kurath (15 Tc tests)

A total of 147 batch contact tests constitute the database with an additional 12 isotherm points obtained from key column experiments (see Section 9 for details). From this total database of 159 data points, 9 batch contact tests were later excluded from the database due to potential conflicts (outliers) during the optimization process.

Here, *batch contact* test refers to a specific type of test employed to estimate a point on an isotherm. A brief description of an "experimental" batch contact test is provided which is consistent with the methods employed in the creation of all 147 tests referred to above. Also, a description is provided for what we refer to as a "numerical" batch contact test and then a simple example is given to illustrate both.

Experimental batch contact tests are performed where equilibrium is assumed to occur in 24, 48, and sometimes as long as 72 hours after initial contact while continual mechanical mixing is ongoing (e.g., shaker or orbital tables). During an individual batch contact test, a small amount of SuperLig® 639 resin (i.e., 0.05 to 0.18 g of resin) is placed into a beaker containing a known amount of a liquid-solution (i.e., 3.7 to 19.4 ml of either an envelope sample or its simulant). Typically the phase ratio of liquid to solid is designed to be approximately 100 ml/g (i.e., dry phase ratio values in database range from 9.7 up to 207.3 ml/g dry resin). A listing of the minimum to maximum parameter values within the batch contact database (i.e., 147 test points) is provided below:

Parameter	Min Value	Max Value
Initial K+ [M]	0.0000	0.7500
Initial Na+ [M]	0.0293	6.5900
Initial NO2- [M]	0.0000	1.2800
Initial NO3- [M]	0.0018	2.2090
Initial OH- [M]	0.0054	4.9000
Initial XO4- [M]	1.191E-07	2.417E-03
Vol (ml)	3.663	120.0
Resin (g)	0.0406	1.0
F factor	0.7643	1.0
T (C)	19.0	26.0
dry phase ratio	9.71	207.33
Final XO4- [M]	5.272E-09	1.071E-03
Final Loading (mmol/g)	9.374E-06	2.164E-01
Final Kd (ml/g)	13.46	3129.28
Final NO3 final [M]	1.735E-03	2.206E+00
Final NO3/ReO4	1.092E+01	4.605E+07

The parameters shaded in orange are the initial batch contact conditions, while those shaded in cyan are final equilibrium values. Only the final XO_4^- concentration is directly measured. The remaining parameters are computed values. As the above table indicates a broad range of concentrations have been tested.

The initial composition of the liquid-sample is known either through analytical means for envelope samples or based on its creation for simulant samples. For the isotherm modeling effort in the 2000 Report the liquid-solution's initial nitrate and pertechnetate (or perrhenate) ion concentrations had to be known. For the new isotherm model presented in this report (and based

on CERMOD) a potential larger number of ions should be defined. Below is the list of possible liquid-phase ions to be specified:

Cations	Anions	
Ca++	Al(OH)4-	NO2-
Cd++	C2O4--	NO3-
H+	CH3COO-	OH-
K+	Cl-	ReO4-
Mg++	COOH-	SO4--
Na+	CO3--	TcO4-
Pb++	F-	
Zn++	HPO4--	

The shaded ions represent those ions that are candidates for combining into neutral species and then being sorbed onto the resin. The concentrations of the other species are used to calculate solution ionic strength and ion activities. Nitrite (NO_2^-) is not currently considered as a potential ion for sorption onto the resin. From eluent analyses by King et al. (2003) NO_2^- does not appear in any significant amounts and based on these results was not included in the isotherm model coded into CERMOD.

From the measured initial and final states of the liquid-solution, along with the phase ratio of the liquid-to-solid quantities tested, K_d and surface loading values can be computed. Here the solid-phase concentrations are computed based on material balances where it is assumed that liquid-phase concentration changes occur only due to sorption. Helfferich (1962) indicates that this approach offers considerable advantages when these effects are negligible, but warns that equilibrium data taken in this manner can be unreliable. Based on both the 2000 analysis effort and this newer effort we see significant scatter within the batch contact database which might be contributable to the effects mentioned by Helfferich (1962).

From an error analysis perspective, we should anticipate increased scatter (i.e., increased residuals) in computed K_d values when compared to their corresponding observed (measured) values. This is easily seen when we note that the K_d value is computed from:

$$K_d = \frac{Q_x}{c_x} = \frac{\phi(c_o - c_x)}{c_x} \quad . \tag{4-1}$$

As Eq. (4-1) indicates, uncertainties in measured liquid-phase concentrations can have a different impact in K_d value uncertainties depending on the isotherm location.

The above "experimental" batch contact test can be conceptually illustrated on a simple xy diagram as provided in Figure 4-1. The blue curve represents the actual isotherm. Here, isotherm implies an "effective" single-component isotherm at a specific temperature where all species that interact with the solid-phase are at fixed concentrations except XO_4^-. The isotherm has the characteristic convex shape of a Langmuir isotherm. The red line represents the linear operating line (i.e., a material balance between the liquid and solid phases). For the batch contact tests considered here, the solid phase (i.e., resin) is initially completely unloaded with regard to XO_4^-. The slope of the operating line is equal to the phase ratio:

$$\phi = \frac{V_L}{m_{dry}} = \frac{V_L}{m_{wet} f} \quad , \tag{4-2}$$

where a reference state for wet resin is established based on a f-factor technique. During the equilibration process the aqueous concentration, starting at the red circle in Figure 4-1, migrates up this operating line until final equilibrium is achieved at the crossing point on the isotherm (i.e., the blue circle in Figure 4-1). Measurement errors in the phase ratio along with initial and final XO_4^- liquid concentrations result in estimated error in solid-phase XO_4^- loading as illustrated in Figure 4-1 by the dashed blue ellipse.

The "numerical" batch contact test is very similar in nature to the "experimental" one. Here the "experimental" batch contact inputs (i.e., phase ratio and initial liquid phase composition) are specified and CERMOD then computes an estimated XO_4^- loading value as shown in Figure 4-1 as the orange circle. Several key modeling parameters within CERMOD must be defined prior to the "numerical" batch contact simulation. These parameters are obtained by an appropriate optimization process to be discussed in a subsequent subsection. The basic idea is to optimize the model parameter values by looking at some large "experimental" batch contact test database where the residuals (i.e., computed minus observed XO_4^- loadings) from each test are minimized. CERMOD provides a list of functions that can be used for optimization and a specific one such as the sum of squares of the residuals is chosen for a particular calculation.

The creation of an isotherm unique to some chosen liquid feed composition is obtained by running CERMOD over a range of liquid-phase XO_4^- concentrations. The output from each specific run creates a point on this isotherm. Once a series of isotherm points have been generated, CERMOD fits these isotherm points to an algebraic model of the Freundlich/Langmuir Hybrid form:

$$Q_{XO_4^-} = \frac{a\left[c_{XO_4^-}\right]^b}{\left[c_{XO_4^-}\right]^d + \beta} \quad , \tag{4-3}$$

where the best estimate values of a, b, d, β are computed in the least-squares sense. An example of the results from this process can be seen in Figure 4-2 where the "numerical" batch contact points defining an isotherm are shown as red circles. The least-squares fitting is shown as the black curve. For the Technetium-SuperLig® 639 system, and the modeling assumptions made within CERMOD, the computed isotherms are very close to Langmuir in shape and typically the fitting process is restricted to this algebraic form (i.e., parameters b and d are fixed to unity).

4.3 The Isotherm Model

The numerical batch contact approach to modeling the solid-liquid equilibrium process has been coded into a FORTRAN based code CERMOD (see Appendix B for more details). Below the basic equations that constitute the model are briefly described. Numerous experiments confirmed that NO_3^- is a prime competitor for adsorption sites and a neutral species sorption process materialized. The experiments indicated that the neutral species needed to consider K^+, as well as Na^+, to the list of ions of interest. From SRNL and PNNL testing, a short list of strong electrolytes was established.

For each strong electrolyte (i.e., neutral species) that can possibly adsorb onto the resin a mass-action equation is required. The four strong electrolytes ($NaXO_4$, $NaNO_3$, KXO_4, KNO_3) currently being considered yield:

mass-action $$K_{11}(T) = \frac{\hat{\gamma}_{NaXO_4} Q_{NaXO_4}}{\xi Q_L \gamma_{Na^+} m_{Na^+} \gamma_{XO_4^-} m_{XO_4^-}} \quad (4\text{-}4)$$

mass-action $$K_{12}(T) = \frac{\hat{\gamma}_{NaNO_3} Q_{NaNO_3}}{Q_L \gamma_{Na^+} m_{Na^+} \gamma_{NO_3^-} m_{NO_3^-}} \quad (4\text{-}5)$$

mass-action $$K_{21}(T) = \frac{\hat{\gamma}_{KXO_4} Q_{KXO_4}}{\xi Q_L \gamma_{K^+} m_{K^+} \gamma_{XO_4^-} m_{XO_4^-}} \quad (4\text{-}6)$$

mass-action $$K_{22}(T) = \frac{\hat{\gamma}_{KNO_3} Q_{KNO_3}}{Q_L \gamma_{K^+} m_{K^+} \gamma_{NO_3^-} m_{NO_3^-}} \quad (4\text{-}7)$$

Material balances for the four ionic species loaded onto the solid (ϕ = phase ratio) are:

ionic solid loading $$Q_{Na^+} = Q^{\circ}_{Na^+} + (c^{\circ}_{Na^+} - c_{Na^+})\phi \quad (4\text{-}8)$$

ionic solid loading $$Q_{K^+} = Q^{\circ}_{K^+} + (c^{\circ}_{K^+} - c_{K^+})\phi \quad (4\text{-}9)$$

ionic solid loading $$Q_{XO_4^-} = Q^{\circ}_{XO_4^-} + (c^{\circ}_{XO_4^-} - c_{XO_4^-})\phi \quad (4\text{-}10)$$

ionic solid loading $$Q_{NO_3^-} = Q^{\circ}_{NO_3^-} + (c^{\circ}_{NO_3^-} - c_{NO_3^-})\phi \quad (4\text{-}11)$$

Only three of these ionic loading equations are independent. Four ionic balances on the solid-phase are:

ion balance $$Q_{Na^+} = Q_{NaXO_4} + Q_{NaNO_3} \quad (4\text{-}12)$$

ion balance $$Q_{K^+} = Q_{KXO_4} + Q_{KNO_3} \quad (4\text{-}13)$$

ion balance $$Q_{XO_4^-} = Q_{NaXO_4} + Q_{KXO_4} \quad (4\text{-}14)$$

ion balance $$Q_{NO_3^-} = Q_{NaNO_3} + Q_{KNO_3} \quad (4\text{-}15)$$

Only three of these ionic balances are independent. The solid-phase charge balance becomes:

solid phase charge balance $$Q_{Na^+} + Q_{K^+} = Q_{XO_4^-} + Q_{NO_3^-} \quad (4\text{-}16)$$

The liquid-phase charge balance becomes:

liquid phase charge balance $$\sum_{i=1}^{\text{cations}} z_i m_i = \sum_{j=1}^{\text{anions}} z_j m_j \quad (4\text{-}17)$$

The total number of resin sites becomes:

total resin sites $$Q_T = Q_L + Q_{Na^+} + Q_{K^+} \quad (4\text{-}18)$$

The dissociation reaction for water becomes:

dissociation water
$$K_w(T) = \frac{\gamma_{H^+} m_{H^+} \gamma_{OH^-} m_{OH^-}}{a_w} \tag{4-19}$$

An overall (solid plus liquid phase) hydrogen balance becomes:

H-balance
$$\begin{aligned} & 2n_w^o + V_L\left(c^\circ_{H^+} + c^\circ_{OH^-} + 4c^\circ_{Al(OH)_4^-} + 3c^\circ_{CH_3O_2^-} + c^\circ_{COOH^-} + c^\circ_{HCO_3^-} + c^\circ_{HPO_4^-} \right) \\ & = 2n_w + \frac{n_w}{\Omega}\left(m_{H^+} + m_{OH^-} + 4m_{Al(OH)_4^-} + 3m_{CH_3O_2^-} + m_{COOH^-} \right. \\ & \left. + m_{HCO_3^-} + m_{HPO_4^-} \right) \end{aligned} \tag{4-20}$$

An overall (solid plus liquid phase) oxygen balance becomes:

O-balance
$$\begin{aligned} & n_w^o + V_L\left(c^\circ_{OH^-} + 4c^\circ_{Al(OH)_4^-} + 2c^\circ_{CH_3O_2^-} + 2c^\circ_{COOH^-} + 3c^\circ_{HCO_3^-} + 4c^\circ_{HPO_4^-} \right) + m_s\left(4Q^o_{XO_4^-} + 3Q^o_{NO_3^-} \right) \\ & = n_w + \frac{n_w}{\Omega}\left(m_{OH^-} + 4m_{Al(OH)_4^-} + 2m_{CH_3O_2^-} + 2m_{COOH^-} + 3m_{HCO_3^-} + 4m_{HPO_4^-} \right) \\ & + m_s\left(4Q_{XO_4^-} + 3Q_{NO_3^-} \right) \end{aligned} \tag{4-21}$$

From the above list of equations 16 of them are independent and the following is a list of the 16 unknowns:

16 unknowns
$$\begin{bmatrix} n_w, m_{H^+}, m_{OH^-}, m_{Na^+}, m_{K^+}, m_{XO_4^-}, m_{NO_3^-}, Q_{Na^+}, Q_{K^+}, Q_{XO_4^-}, Q_{NO_3^-}, Q_L, \\ Q_{NaXO_4}, Q_{NaNO_3}, Q_{KXO_4}, Q_{KNO_3} \end{bmatrix} \tag{4-22}$$

The liquid-phase nonideality factors are computed using the Pitzer correlation and available correlation coefficients were taken from the literature (see Appendix B for more details about CERMOD). The equilibrium constant for the dissociation reaction of water is specified from literature values as well.

For closure in the above set of equations the following parameters must also be specified in order to perform a numerical batch contact simulation:

$K_{11}(T)$ - Equilibrium constant for $NaXO_4$ sorption (4-23a)

$K_{12}(T)$ - Equilibrium constant for $NaNO_3$ sorption (4-23b)

$K_{21}(T)$ - Equilibrium constant for KXO_4 sorption (4-23c)

$K_{22}(T)$ - Equilibrium constant for KNO_3 sorption (4-23d)

ξ - Selectivity ratio between ReO_4^- versus TcO_4^- (4-23e)

Q_T - Total sorption capacity (batch dependent) (4-23f)

Once the above six parameters have been specified, CERMOD can perform a numerical batch contact simulation for SuperLig® 639 and any specified liquid-phase composition of interest. The result of this individual simulation is a computed point on an isotherm consistent with major constituents of the liquid solution. A series of these individual numerical batch contact simulations can be run over several liquid solutions ranging in XO_4^- concentration to create an "effective" single component Langmuir isotherm:

$$Q_x = \frac{Q_T c_x}{c_x + \beta} , \tag{2-17}$$

where CERMOD output provides the user with the estimated fitted parameters (Q_T, β). Figure 4-2 compares the CERMOD computed isotherm points (i.e., numerical batch contact simulations) to the final Langmuir fit of this generated data set. The isotherm predictions shown correspond to the Avg. feed composition employed later in Full-Scale column performance analyses. As Figure 4-2 illustrates, the isotherm predictions by CERMOD result in an isotherm that closely resembles a Langmuir isotherm. This is not surprising given the fixed and finite number of available adsorption sites assumed in the above set of equations.

4.4 Impact of Total Ionic Strength

As noted in Section 4.4 of the 2000 Report, liquid-phase activity coefficients are dependent upon the total ionic strength of a solution. For example, the thermodynamic equilibrium constant can be broken up into selectivity and activity coefficients:

$$K_{21}(T) = \left[\tilde{K}_{21}(T, \bar{c})\right]\left[\tilde{K}_{\gamma}(T, \bar{c})\right] \tag{4-24}$$

Therefore, the "averaged" estimated values for the binary selectivity coefficients provided in the 2000 Report depended upon the total ionic strength. This ionic strength effect in the 2000 Report was addressed through use of an empirical relation expressed as

$$\tilde{K}_{21}(T) \approx \frac{A(T)}{\mu(\bar{c})} \tag{4-25}$$

In the newer CERMOD model described in an earlier subsection (details provided in Appendix B) liquid-phase activity coefficients are being addressed directly using literature-based coefficients to the Pitzer correlation (i.e., binary coefficients and in some case terniary coefficients). The ionic strength effect is implicitly handled in CERMOD requiring no additional post-processing of results.

4.5 Batch Specific Total Sorption Capacity

Unfortunately, there are no batch contact test results available specifically designed to address the total sorption capacity of any of the particular batches being considered. A simple algebraic form for the XO_4^- isotherm was developed in Section 2 given by:

$$Q_{XO_4^-} = \frac{Q_T c_{XO_4^-}}{c_{XO_4^-} + \beta} \tag{2-17}$$

where

Q_T - Total sorption capacity for XO_4^- that is batch dependent and represents the total number of available (active) sites per gram of dry resin (mmole/g).

β - Beta parameter that is sorption site specific and represents the combined effect of enhancer and competitor impacts (mole/L).

In developing Eq. (2-17) it was assumed that a fixed number of homogenous sites exist per unit mass of dry resin and that the selectivity coefficients were approximately constant over the range of the isotherm under consideration.

We view the total sorption capacity as an engineered quantity while the beta parameter accounts for a resin's unique selectivity (i.e., chemical) aspects. With this view batch variability is considered to be primarily a result of variations in total sorption capacity while the chemical behavior is basically unchanged from batch to batch.

In order to capture the unchanging ("true") chemical selectivity of SuperLig® 639, a method must be devised to pin down the batch variability (i.e., batch specific total capacities) for every unique batch considered. The batch contact database consists of five unique batches and one mixture batch. One or more column studies exist for each of these six batches. One may view the batch contact database as having biases at the batch level that must be eliminated in order to extract out acceptable chemical selectivity.

In principle when a column is operated beyond its complete exhaustion (i.e., total breakthrough point), the area above this breakthrough curve represents its total loading capacity for the specific feed composition employed. This represents a point on its loading isotherm. Helfferich (1962) points out that isotherm data taken in this manner are far more reliable than data obtained using the batch contact methods typically employed. Figure 4-3 is a cartoon illustrating the principles being discussed here. From this insight, batch variability can potentially be handled by estimating batch total capacities from individual column breakthrough data. In essence, the biasing effect of batch variability is extracted out of the batch contact database by including column derived isotherm points. This is the approach being employed within this analysis effort whose results indicate that it is a successful strategy.

Unfortunately, few of the SRNL or PNNL column experiments were run to a complete (100%) breakthrough condition. However, complete breakthrough curves for each column experiment can be estimated either graphically or in some cases with the assistance of VERSE runs. One example of this technique can be seen in Figure 4-4 for the perrhenate-SuperLig® 639 column run by King at al. (2000a) where the area above the exit breakthrough curve represents a point on the isotherm for the feed conditions tested. Once this area has been estimated a point on the isotherm can be computed based on the following approximations.

Looking at the molar balance for XO_4^- over one entire column, the total column loading versus time can be expressed by:

$$\frac{dn}{dt} = F\left(c_o - c(t)\right) \quad , \tag{4-26}$$

where in column volume terms use can be made of

$$\tau = \frac{Ft}{V_T}$$

Integration of (4-26), assuming initially a fresh column, yields:

$$n(\tau) = V_T c_o \int_0^{\tau} \left[1 - \frac{c(\tau')}{c_o} \right] d\tau' \quad , \tag{4-27}$$

The total loading of the column at any point in time is the sum of both loading onto the solid and within the liquid phases:

$$n(\tau) = n_S(\tau) + n_L(\tau) \quad , \tag{4-28}$$

These loadings (in moles or mmoles) can be expressed in terms of concentrations and bed parameters as:

$$n_L(\tau) = V_T c_o \left[1 - (1 - \varepsilon_b)(1 - \varepsilon_p) \right] \quad , \tag{4-29}$$

and

$$n_S(\tau) = V_T \rho_b Q_S \quad . \tag{4-30}$$

An expression for the solid loading on the bed can now be derived from the above equations as:

$$Q_S = \frac{c_o}{\rho_b} \left[\int_0^{\tau} \left[1 - \frac{c(\tau')}{c_o} \right] d\tau' - \left[1 - (1 - \varepsilon_b)(1 - \varepsilon_p) \right] \right] \quad , \tag{4-31}$$

For resin beds with a high affinity for the sorbent of interest, the second term is small and can be neglected to yield:

$$Q_S \cong \frac{c_o}{\rho_b} \left[\int_0^{\tau} \left[1 - \frac{c(\tau')}{c_o} \right] d\tau' \right] \quad . \tag{4-32}$$

Thus, once the area (as illustrated in the cartoon of Figure 4-2 and in the actual case of Figure 4-4) has been estimated, Eq. (4-32) provides us with one point on an isotherm (c_o, Q_S).

Twelve column experiments were selected where all six batches were included (three in triplicate). Table 9-1 lists the selected column experiments and provides some of their key attributes. Results of the above column strategy are provided in Table 9-1 where the feed concentration of XO_4^- is listed along with the estimated XO_4^- loading based on Eq. (4-25). Each of these feed concentrations of XO_4^- and column loadings (at saturated conditions) represents an isotherm point on a specific isotherm at their given feed composition and temperature.

4.6 Isotherm Parameter Estimations

As mentioned in the above subsection, CERMOD requires the specification of six modeling parameters (i.e., five are related to chemical selectivity while the last one is batch specific). CERMOD has built into it the capability of performing an optimization process to estimate these parameters based on several cost functions (i.e., in CERMOD icost option = 0, 1 ,2, …, or 7). For the optimization results provided in this report the following cost function option was employed:

$$\text{Cost}(\bar{\theta}) = \sum_{i=1}^{N_{BC}} (w_i \cdot r_i)^2 \quad , \tag{4-33}$$

where for icost=0 (log-difference q residual option)

$$r_i(\bar{\theta}) = \ln(Q_i^{obs}) - \ln(Q_i^{mod}) \quad , \tag{4-34}$$

and w_i represents weighting of data points. In this analysis effort uniform weighting was employed (i.e., $w_i = 1$). During the optimization activity several of the other cost function options were viewed to see if the parameter estimations would differ significantly. Given the broad range (i.e., over 4 orders of magnitude) in Q loading values, the log-based cost function option (icost=0) appeared to handle the database more evenly.

The original database employed in the optimization process was $N_{BC} = 159$ (i.e., 147 traditional batch contact experiments and 12 column based isotherm points). During the initial scoping runs 9 batch contact data points were omitted from the final optimization due to significant outlier residuals being seen for these particular data points. Identifying the root cause for each of these batch contact experiments yielding outlier residuals is not plausible at this time. However, some of these experiments were multi-batch sequential contacts, where errors could propagate.

The remaining 150 data points range over a wide range of conditions. Unfortunately, temperatures ranged from 19 to 26 °C with the majority of them near 25 °C. Each batch contact experiment was assumed to be at 25 °C where the estimated parameters are then assumed to represent average values at 25 °C. Future efforts should update CERMOD to allow each batch contact point to operate at its own temperature and the parameters to be estimated would then become temperature dependent terms.

A listing of all 147 experimental batch contact tests is provided in Appendix A. Tables A-1 through A-7 provide the key data associated with each experiment grouped by the lead author. The final optimization run with CERMOD is shown in Table A-8 as its parameter output file. In that file the final best estimate parameter values are listed and are also listed below:

$K_{11}(T = 25C) = 1{,}436.055$ - Equilibrium constant for $NaXO_4$ sorption

$K_{12}(T = 25C) = 1.093978$ - Equilibrium constant for $NaNO_3$ sorption

$K_{21}(T = 25C) = 107{,}094.2$ - Equilibrium constant for KXO_4 sorption

$K_{22}(T = 25C) = 51.04232$ - Equilibrium constant for KNO_3 sorption

$\xi = 0.5050$ - Selectivity ratio between ReO_4^- versus TcO_4^-

Qtot = 0.6472 - Total resin sorption loading

Qfrac = Batch dependent sorption capacity relative to Qtot

Batch	Batch ID	Qfrac
1	981015DHC-720011	1.001
2	990420DHC-720067	0.498
3	010227CTC-9-23	1.488
4	980624001DC	0.459
5	I-R2-03-27-02-20-45	1.030
6	50%Batch1 50%Batch2	0.758

The resulting six batch dependent total sorption capacities are listed in Table 4-4 and in Table A-8. Table 4-4 also lists the batch ID's and batch indexing employed for the five individual batches, as well as the one mixture batch, considered. The estimated total XO_4^- sorption capacities (in mmole/g of dry resin) for each of the six batches are also provided. As Table 4-5 indicates, the estimated total capacities have significant variability (i.e., 51% to 166% of their

averaged value). All six of these estimated batch capacities were obtained during the model optimization process and not entirely with experiments, as discussed within the section. Note that the estimated value for the mixture batch number 6 is very close to a simple arithmetic average of batches 1 and 2 (i.e., 0.4906 versus the average value of 0.4851). This suggests that a reasonable estimate for "effective" total capacities for mixtures can be estimated by their weighted averaging. For column conditions the mixture should be reasonably uniform. The average estimated value is listed in Table 4-4 of ~0.58 mmole/g_{resin}

The K^+ enhancer effect was observed during column studies and analyses back in the 2002 time frame as discussed in Section 2 above. The best estimate thermodynamic equilibrium constants listed above show the expected trend. The ratios of these equilibrium constants provide us with some indication of SuperLig® 639 preference for K^+ over Na^+ in its sorbed neutral species:

$$\frac{K_{21}}{K_{11}} = 75.6 \quad \text{- } KXO_4 \text{ versus } NaXO_4 \text{ sorption}$$

$$\frac{K_{22}}{K_{12}} = 46.7 \quad \text{- } KNO_3 \text{ versus } NaNO_3 \text{ sorption}$$

As the above ratios indicate neutral species based on K^+ versus Na^+ are 50+ times more favorable for sorption onto SuperLig® 639. The overwhelming evidence from batch contact tests, column loading tests, and column elution tests strongly confirms this loading aspect.

CERMOD also writes out observed and computed loadings and residuals (%errors) for:

- XO_4^- ionic solid-phase loadings (mmol/g of dry resin)
- XO_4^- ionic liquid-phase concentrations [M]
- XO_4^- Kd values (ml/g of dry resin)

Statistical quantities are computed by CERMOD to help assess the actual estimated fitted parameters. For sub-groups of the database the following two statistical quantities are computed:

$$RMS = \sqrt{\frac{\sum_i \varepsilon_i^2}{N_{sub}}} \quad , \tag{4-35}$$

$$AVG = \frac{\sum_i \varepsilon_i}{N_{sub}} \quad , \tag{4-36}$$

where $$\varepsilon_i = \frac{X_i^{mod} - X_i^{obs}}{X_i^{obs}} \quad \text{for} \quad X \equiv Q, c, K_d \quad .$$

Each of these quantities for the 150 (i.e., 159 - 9) data points is listed in Table 4-5 and Table A-8. At the bottom of Table A-8 is a summary of the statistics of the fitting process which has also been copied into Table 4-5. Table 4-5 is a summary of the statistics containing root-mean-square (RMS) and average deviation (AVG) results for various sub-groups of isotherm data. Specifically,

- First three lines – RMS values for all 150 data points, just for those data points for Re, and then just for Tc data points;

- Next three lines – AVG deviations for all data points, just Re data points, then just Tc data points;
- Next six pair of lines – RMS and AVG values for all data points associated with a given batch.

For example, in Table 4-5 the overall statistics (that includes all 150 data points) is given as:

- (6.7% RMS; 0.9% AVG) XO4- ionic solid-phase loadings (mmol/g of dry resin)
- (27.6% RMS; -2.4% AVG) XO4- ionic liquid-phase concentrations [M]
- (35.3% RMS; 11.8% AVG) XO4- Kd values (ml/g of dry resin)

The above numbers indicate that a reasonably large scatter in K_d values exists. As expected (and discussed in Appendix A) variances in K_d are a combined result of variances in Q and c due to the constraint of each batch contact operating along a fixed operating line. However, given the range of and number of data contained within the database (assuming that biases have been extracted out), there is reasonable confidence in CERMOD's ability to estimate an isotherm.

To better assess the predictive capability of CERMOD several graphical plots were created and are illustrated in Figures 4-5 through 4-10. In each figure the batch contact tests are color coded based on the lead author and the 12 column based isotherm points are color coded by batch ID. As the above statistics imply, the predicted loading (Q) values versus the observed Q values lie close to the 45 degree line as shown in Figure 4-5. The RMS value is 6.7% with an average deviation value of 0.9%. In Figure 4-5, a 25% confidence band is shown as a dashed black line. Note that the chosen optimization function is based on the Q values and our smallest RMS should be on this variable.

A very similar residual plot for liquid-phase concentrations (c) is shown in Figure 4-6 where 25% and 50% confidence bands are provided. The RMS value is 27.6% with an average deviation value of -2.4%. The residual plot for K_d values is shown in Figure 4-7. The RMS value is 35.5% with an average deviation value of 11.8%. That is, there is an average bias of 11.8% higher in computed K_d values. To better see the spread in K_d residuals, a subset of the data in Figure 4-7 is replotted in linear-linear coordinates in Figure 4-8. Figure 4-8 does not show all of the observed values. This figure has been cut off at 2000 ml/g while observed values as high as 3000 ml/g exist within the database.

In the 2000 Report, data was typically shown in a loading (Q) versus the NO_3/XO_4 molar ratio coordinates (e.g., see Figure 4-7 in the 2000 Report). A similar plot is shown in Figure 4-9 where the entire new database is provided. The data sets at low NO_3/XO_4 molar ratios do not follow the general trend shown by the rest of the data at higher ratio values. This deviation from the trend did not show up in the original 88 batch contact tests employed in the 2000 Report. This new effect comes from data taken by Rapko (2003) using a very simple simulant. The CERMOD predictions of these values is fairly good (i.e., CERMOD shows the same trend as the data) as can be seen in the Figure 4-10 where only Rapko (2003) data is shown. This data is color coded (blue for Tc data and red for Re data) where open symbols reflect computed values. This data is from batch contacts conducted at very low ionic strengths and low concentrations of the key anions.

4.6.1 Rhenium as a Technetium Surrogate

In Section 4.3.3 of the 2000 Report, information was provided with regard to rhenium being chosen as a non-radioactive surrogate for technetium. Limited analyses in that report estimated that the impact on selectivity coefficients of Re versus Tc was (see Figure 4-7 of the 2000 Report):

$$\frac{\widetilde{K}_{21}\Big|_{Re}}{\widetilde{K}_{21}\Big|_{Tc}} \cong 0.568 \qquad (4\text{-}15)$$

In the parameter estimation process employed in this report the batch contact database (total of 147 data points) yielded the following best estimate value:

$$\frac{K_{11}(T \approx 25C)\Big|_{Re}}{K_{11}(T \approx 25C)\Big|_{Tc}} = \frac{K_{21}(T \approx 25C)\Big|_{Re}}{K_{21}(T \approx 25C)\Big|_{Tc}} \cong 0.505 \qquad (4\text{-}15)$$

Note that in the 2000 Report, average selectivity coefficients were employed where in this newer analysis thermodynamic equilibrium coefficients are being considered. The above two values are very consistent (i.e., ~13%) providing additional confidence in our ability to employ rhenium column studies in the understanding of various aspects of technetium column behavior.

4.6.2 Mixed Batch Column Performance

Three of the twelve column benchmark cases employed a 50:50 wt% mixture of Batches 1 and 2 (i.e., referred to in this report as Batch 6). One of these column studies was the pilot-scale facility. The Full-Scale column predictions to be discussed in Section 10 also employ Batch 6.

During the parameter estimation process, batch total sorption capacities were also estimated. In this estimation process, all six batch IDs were allowed to vary independently (i.e., Batch 6 was not constrained to be a 50:50 mix of Batches 1 and 2). The optimized values are provided in Table 4-2. The 50:50 average value of Batches 1 and 2 becomes 0.4851 mmole/g, while the independently derived value for Batch 6 was 0.4906 mmole/g (i.e., difference of ~1%). From this assessment, it appears that a column packed with resin that is made up of multiple batches can have its total sorption capacity estimated as the weighted sum of the individual total capacities.

4.7 Application Using VERSE-LC

VERSE-LC has several equilibrium adsorption isotherm models to choose from (see user manual by Whitley and Wang, 1996). As discussed in the Section 4 of the 2000 Report, for the equilibrium isotherms of interest here the VERSE-LC option of a Freundlich/Langmuir Hybrid (option F) can conform to its functional form. As pointed out by Hamm et al. (1999), in VERSE-LC input the surface concentration (e.g., in units of gmole/g_{resin}) is expected to be pre-multiplied by the bed density of the active column (e.g., resulting in gmole/L_{CV}). This basically establishes the total number of available sorption sites within the column.

For input to VERSE-LC we use the conversion:

$$\hat{Q}_{XO_4^-} = \rho_b Q_{XO_4^-} \ . \qquad (4\text{-}18)$$

For the column simulations performed within this report the Freundlich/Langmuir Hybrid model can be used for an effective single component case. Here all other ionic concentrations throughout the column are assumed to be at their feed concentration levels. This approximation has been demonstrated to be adequate in Hamm et al. (1999 and 2000b). For the "effective" single-component pertechnetate (or perrhenate) isotherm, Eq. (2-17) under these conditions in VERSE-LC notation becomes:

$$\hat{Q}_{XO_4^-} = \frac{a_1 c_{pl}^{M_{ai}}}{b_1 c_{pl}^{M_{bl}} + \beta} \Rightarrow \frac{\rho_b c_{XO_4^-}}{c_{XO_4^-} + \beta} \quad , \tag{4-21}$$

where the beta parameter for pertechnetate (or perrhenate) becomes dependent upon the ionic feed concentrations (other than pertechnetate or perrhenate). The general Freundlich/Langmuir Hybrid isotherm model in VERSE-LC is reduced down to the simpler Langmuir isotherm as shown in Eq. (4-21).

For the various batch ID's and waste envelopes to be considered in this report, the computed parameter values for Eq. (4-21) are listed in Table 9-3. This includes the twelve benchmark cases and the Full-Scale column design. It is assumed that the resin mixture has been adequately well mixed.

4.8 New versus Old Isotherm Models

As pointed out earlier in this section, the new approach at deriving an "effective" single-component isotherm model is significantly different from the approach employed in the 2000 Report. In this subsection, a comparison is made of the predicted isotherms employed in the Full-Scale column predictions presented in the 2000 Report, versus the predicted isotherm employed in the Full-Scale column predictions presented in this report. Supporting analyses are presented to verify that the differences observed are indeed justifiable.

In the 2000 Report Full-Scale column performance predictions were made using two feeds (i.e., Env-A and Env-B feeds taken from King et al. (2000a) and Hassan et al., (2000b), respectively). In Figure 4-11 a comparison is made of the isotherm models employed in the 2000 Report versus the HTWOS SP6 Average feed isotherm employed in this report. The feed concentration of pertechnetate is shown for each feed as a color-coded circle. The HTWOS SP6 baseline average feed composition is an averaged mixture of all the waste tank feeds to be processed in WTP as defined in System Plan 6 (Certa et al., 2011). As Figure 4-11 indicates, the loading performance associated with the Avg. feed isotherm is about a factor of two lower than the others.

To better understand the source of this difference a comparison was made of the isotherm model and column predictions for the benchmark case by Hassan et al. (2000a). The 2000 Report isotherm model and column predictions are shown in Figures 4-12 and 4-13, respectively. For comparison purposes the same set of predictions were computed using the methods presented in this report. The new versus old isotherms, as shown in Figure 4-12, are very close. As expected, given the similar isotherm predictions for this relatively low potassium feed, the new versus old column predictions, as shown in Figure 4-13, are very close to each other. Given these results, it appears that the new HTWOS SP6 baseline average feed composition results in a much more unfavorable isotherm than either the old Env-A or Env-B feed compositions.

A direct comparison of the isotherm predicted using the 2000 Report Env-A feed composition versus the HTWOS SP6 average feed composition in this report is provided in Figure 4-14. Here both isotherms were computed using the methods developed in this report. As Figure 4-14 indicates a significant difference results directly from the feed composition differences. A comparison between both feeds showing key ions that dominate loading behavior is shown below:

ion	AN-103 feed [M]	HTWOS SP6 Avg feed [M]
K^+	0.121	0.033
Na^+	5.250	5.002
NO_3^-	1.571	1.622

As the above table indicates for the AN-103 (Env-A) feed:

- K^+ is up (enhancer effect that can be significant)
- Na^+ is up (ionic strength effect)
- NO_3^- is down (competitor effect)

All three of these effects increase the AN-103 loading performance versus the HTWOS SP6 average feed. Thus, the prediction of overall performance for the Full-Scale columns will generally be lower in this report than those provided in the 2000 Report. The reduced performance is not the result of the newer analysis but is caused by composition differences.

4.9 Isotherm Models for Column Benchmarking

Section 9 shows five column benchmarking case studies for pertechnetate feeds. A comparison of the isotherms corresponding to these five column studies versus the Avg. feed employed in the Full-Scale predictions is provided in Figure 4-15. The impact of feed composition, as well as batch variability, can be observed. Key ions for each of these feeds are listed below:

ion	loading effect	Hassan AN-103	Burgeson AP-101	Burgeson AZ-101	Burgeson AN-102	King SRS Tank-44F	HTWOS SP6 Avg
K+	enchancer	0.121	0.750	0.090	0.028	0.057	0.033
Na+	ionic strength	5.250	4.810	4.260	4.780	5.275	5.002
NO_3-	competitor	1.571	1.880	0.850	1.730	0.370	1.622
Batch ID	-	1	3	3	3	6	6
Q total	mmol/g	0.6478	0.9630	0.9630	0.9630	0.4906	0.4906

At high pertechnetate concentration levels the isotherms approach their total sorption capacity as provided in the above table. Figure 4-15 also indicates that the isotherm based on the HTWOS SP6 baseline average feed is the lowest performer within the set of feeds being considered. This low performance is a combination of feed composition and the choice of resin batch to be employed. The highest loading is observed for the SRS Tank 44 sample which has the lowest nitrate concentration.

4.10 Non-Pertechnetate to Pertechnetate Ratio

Uncertainties associated with the pertechnetate batch contact studies can become large because of the unknown fraction of non-pertechnetate technetium contained within an actual waste sample. This is especially true when a series of re-contact tests are conducted where the finite

sample volume continues to concentrate the non-pertechnetate species. Under these conditions, the calculated final concentration of pertechnetate in the liquid sample after each contact period becomes progressively more sensitive to the error in the analysis from the growing fraction of non-pertechnetate within the liquid-sample. However, several re-contact tests in series can potentially help to determine what the original liquid-sample non-pertechnetate fraction was (or at least set its upper bound). A detailed discussion on this topic was provided in Appendix A of the 2000 Report where material balances for equilibrium batch contact tests were considered. The calculational strategy presented in the 2000 Report was reviewed and was found to be functionally correct and its implementation consistent.

Data taken since the 2000 Report was issued was reviewed to see if improved estimates of the non-pertechnetate fractions could be achieved. The majority of the newer batch contact tests were performed with either diluted non-pertechnetate fractions or with perrhenate which has no non-perrhenate concerns. In most cases, experimenters estimated the non-pertechnetate fraction in samples of actual tank waste using tracer techniques. Blanchard et al. (2000b) report two measurements of pertechnetate (using a Tc-95m tracer) and total Tc-99 removal from AN-107. The average removal of total Tc-99 was 22% while 80% removal of pertechnetate was achieved indicating that a large fraction of Tc-99 in solution was not in the pertechnetate form. On the other hand, two experiments conducted by Burgeson et al. using waste samples AP-101 (2002) and AZ-101 (2003b) reported fractional removals of pertechnetate equal to or only slightly less than that for total technetium. This would indicate that the technetium in these samples was predominantly in the pertechnetate form. A third experiment conducted by Burgeson et al. (2003a) using a mixed waste sample AN-102/C-104 reported 38% removal of total technetium and 85% removal of pertechnetate. Kurath et al. (1999) report non-pertechnetate fractions in AW-101 of 2.9% or less but 76.8% in AN-107. The data appears to show that the fraction of technetium in the non-pertechnetate form can vary widely in samples of actual waste.

This modeling study only considered pertechnetate removal data as presented in the experimental studies. No attempt was made to calculate removal of technetium not in the pertechnetate form. The modeling makes the assumption that technetium in the non-pertechnetate form remains as non-pertechnetate and does not participate in species equilibrium with SL-639 resin.

Table 4-1. Six SuperLig® 639 resin batches used in experiments.

Batch ID	SuperLig-639 Batch	Batch ID	SuperLig-639 Batch
1	981015DHC-720011	4	980624001DC
2	990420DHC-720067	5	I-R2-03-27-02-20-45
3	010227CTC-9-23	6	50% 981015DHC-720011 50% 990420DHC-720067

Table 4-2. Summary of data used to derive and benchmark isotherms.

				Batch Contact Experiments						
			SL-639	Technetium		Rhenium				
PNNL	Reference	Waste/Simulant	Batch ID	25 °C	65 °C	25 °C	35 °C	45 °C	65 °C	**Column Runs**
1[1]	Burgeson 2002	AP-101	6	6						
			3	2						1
2[1]	Burgeson 2003	AN-102/C-104	3	6						1
3[1]	Burgeson 2004	AZ-101	3	8						1
4[1]	Blanchard 2000a	AW-101	4	6						1
5[1]	Blanchard 2000b	AN-107	4	6						1
6	Kurath 1999	AW-101	4	11						
		AN-107	4	4						
7[1]	Rapko 2003	AN-105 (Simulant)	3	32	12	8			8	
			SL-639	Technetium		Rhenium				
SRNL	Reference	Waste/Simulant	Batch ID	25 °C	65 °C	25 °C	35 °C	45 °C	65 °C	**Column Runs**
1	Hassan 2000a	AN-103	1	8						1
2	Hassan 2000b	AN-102	1	6						1
3	Hassan 2000c	AZ-102	1	8						1
4[1]	Hassan 2003	AW-101	5	4						5
5	King 2000a	Env. A (Simulant)	1			2				
		Env. A (Simulant)	4			8				4
		Env. A (Simulant)	2			12				
		Env. A (Simulant)	6							1
6	King 2000b	Tank 44	1	2						1
7	King 2001	AN-102	1	6						
		AN-102	6							1
8[1]	King 2003	AN-105 (Simulant)	2							4[2]
		AN-105 (Simulant)	5							3[2]
		AZ-102 (Simulant)	5							1
		AN-107 (Simulant)	5							1
9	Steimke 2000	Env. A (Simulant)	6							9
10[1]	Duffey 2003	AN-105	5			7	1	1		
		AZ-102	5			1				
		AN-107	5			1				
Total Number of Experiments Performed				115	12	39	1	1	8	38

[1] Data set not available for the preliminary full-scale column analysis performed in 2000.
[2] Column experiments conducted at nominal temperatures of 25, 35 and 45 °C, all others at 25 °C.

Table 4-3. Nomenclature used to identify various column experiments discussed throughout this report. Orange shading indicates those column experiments included since the 2000 Report.

Batch ID	Waste envelope (simulant)	Specific test case	anion	Column Scale	Reference report
1	AN-103 (Env A)	-	Tc	Lab	Hassan et al., 2000a
2	AN-105 (Env A)	Exp. 1	Re	Lab	King et al., 2003
3	AP-101 (Env A)	-	Tc	Lab	Burgeson et al., 2002
	AZ-101 (Env B)	-	Tc	Lab	Burgeson et al., 2004
	AN-102/C-104 (Env C)	-	Tc	Lab	Burgeson et al., 2003a
4	AN-105 (Env A)	Exp. 1	Re	Bench	King et al., 2000a
5	AN-105 (Env A)	Exp. 5	Re	Lab	King et al., 2003
	AZ-102 (Env B)	Exp. 8	Re	Bench	King et al., 2003
	AN-107 (Env C)	Exp. 9	Re	Bench	King et al., 2003
6	AN-105 (Env A)	Exp. 5	Re	Bench	King et al., 2000a
	SRS Tank 44F	-	Tc	Bench	King et al., 2000b
	AN-105 (Env A)	Run 9	Re	Pilot	Steimke et al., 2000
6	Avg. Hanford Feed	-	Tc	Full	This Report

Table 4-4. Summary of estimated total sorption capacities for the various batches considered within this report.

Batch Index	SuperLig® 639 Batch ID	Total capacity (mmole/g)	Ratio (batch-to-average)	Comments
1	981015DHC720011	0.6478	1.12	Considered in 2000 Report.
2	990420DHC720067	0.3223	0.56	Considered in 2000 Report.
3	010227CTC-9-23	0.9630	1.66	New batch with the highest total capacity.
4	980624001DC	0.2971	0.51	Batch considered in 2000 Report.
5	I-R2-03-27-02-20-45	0.6666	1.15	New batch.
6	50:50 Batch-1 & 2	0.4906	0.85	Considered in 2000 Report. Mixture of batches 1 and 2 used in both batch contact and column studies. Simple averaging of Batch 1 & 2 yields estimated value of 0.4851, close in value to value obtained during optimization process.
Avg.	-	0.5794	1.0	Average total capacity for comparing batch variability.

Table 4-5. Statistics of final optimization process broken out into groups.

Population Considered	Number of Data Points	Type of Statistic	XO4- Ionic Loadings (mmol/g)	XO4- Ionic Concentrations [M]	XO4- Kd Values (ml/g)
All	150	RMS	6.7	27.6	35.3
ReO4- only	46	RMS	7.8	24.9	26.9
TcO4- only	104	RMS	6.2	28.8	38.5
All	150	AVG	0.9	-2.4	11.8
ReO4- only	46	AVG	1.6	-1.0	8.4
TcO4- only	104	AVG	0.6	-3.1	13.4
Batch 1	30	RMS	7.1	29.5	57.6
		AVG	5.3	-23.2	45.1
Batch 2	3	RMS	14.5	76.0	46.8
		AVG	-11.5	61.9	-37.9
Batch 3	56	RMS	4.7	20.1	28.6
		AVG	1.4	-7.4	14.3
Batch 4	37	RMS	8.0	25.1	24.9
		AVG	-1.7	11.8	-7.7
Batch 5	14	RMS	7.3	14.7	21.6
		AVG	-0.1	-2.8	5.7
Batch 6	10	RMS	5.6	47.1	23.9
		AVG	-0.3	16.0	-5.9

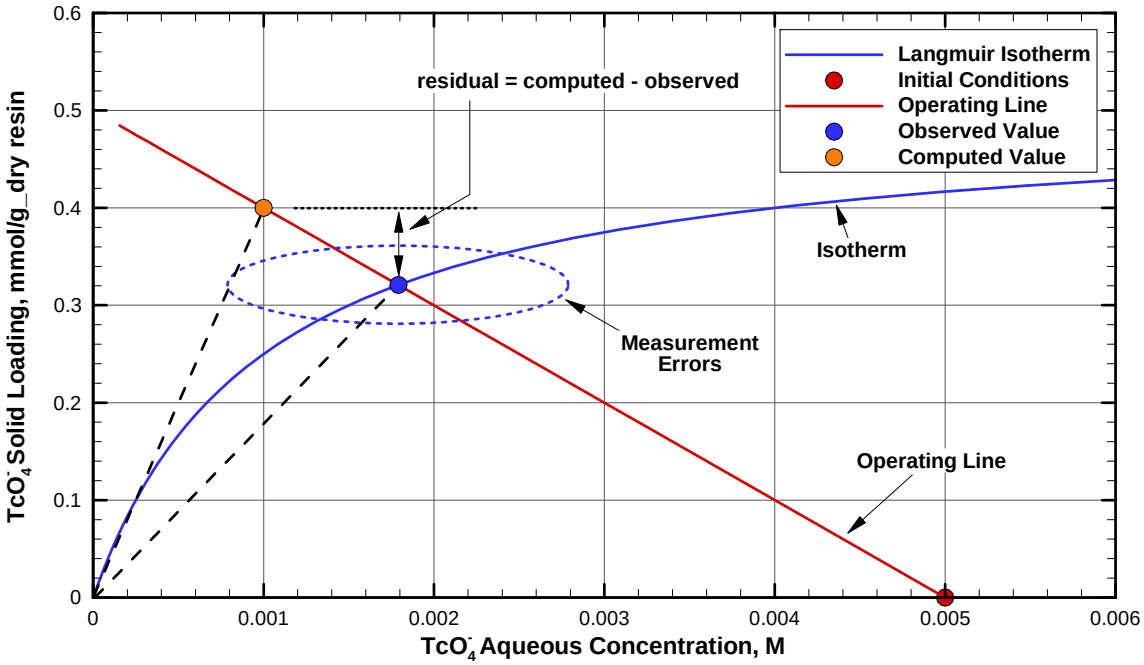

Figure 4-1. Illustration of the path taken during a typical "experimental" and "numerical" batch contact test. Operating line represent the transient path taken while circles represent equilibrium points.

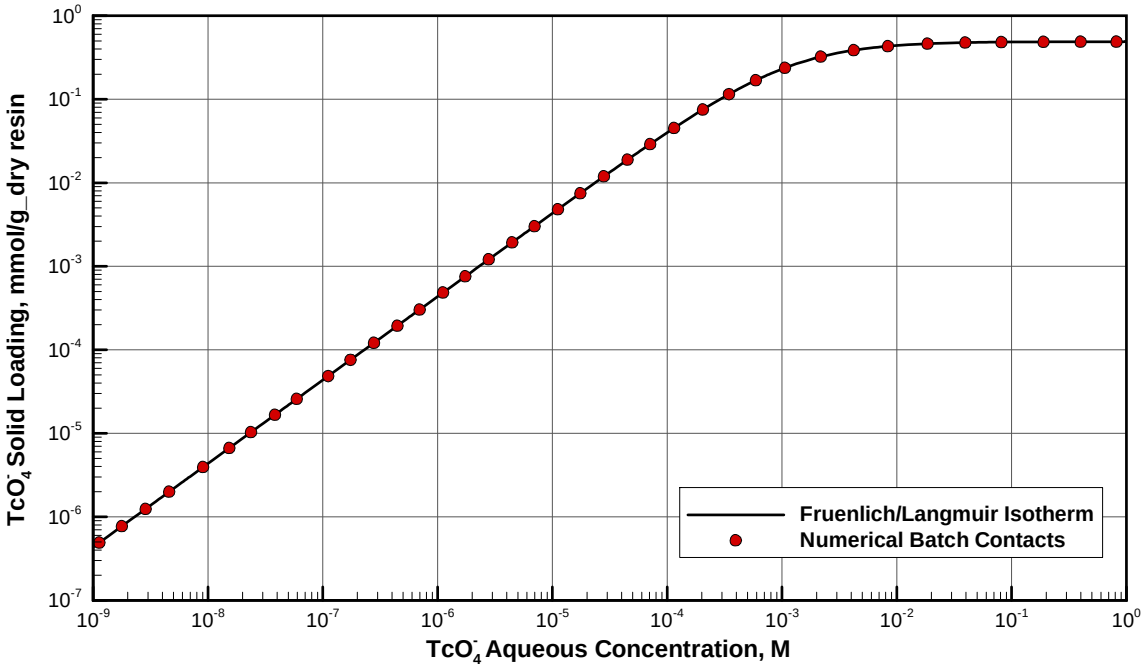

Figure 4-2. Langmuir isotherm fit to a series of CERMOD generated numerical batch contact simulations for the Avg. feed to the Full-Scale columns.

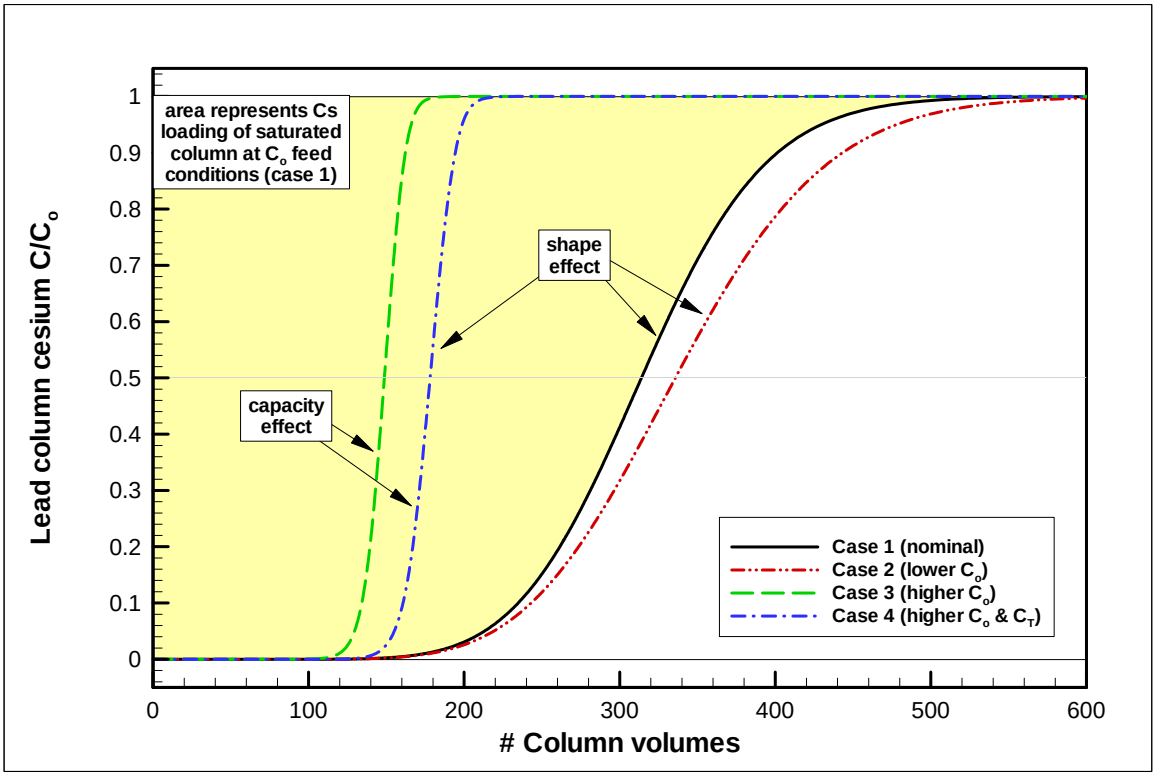

Figure 4-3. Characteristic column breakthrough curves for varying inlet feed concentrations showing shaded in yellow the total column loading capacity under nominal feed conditions.

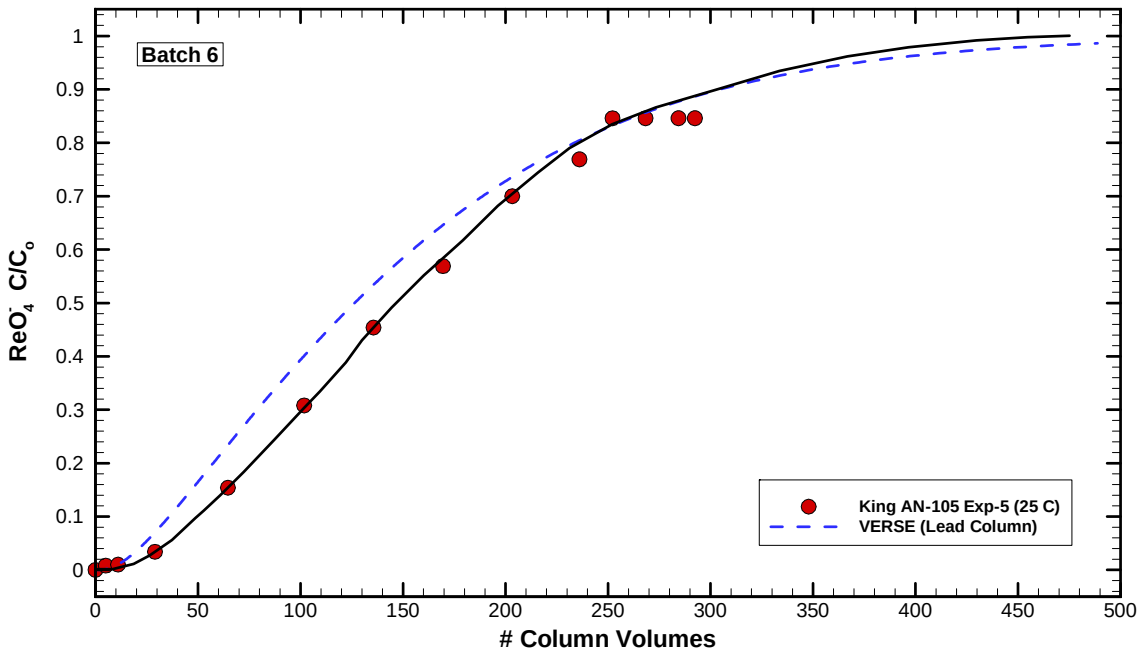

Figure 4-4. Comparison of exit breakthrough curve for experimental column data (red circles), graphical approximation (solid black line), and VERSE estimation (dashed blue line).

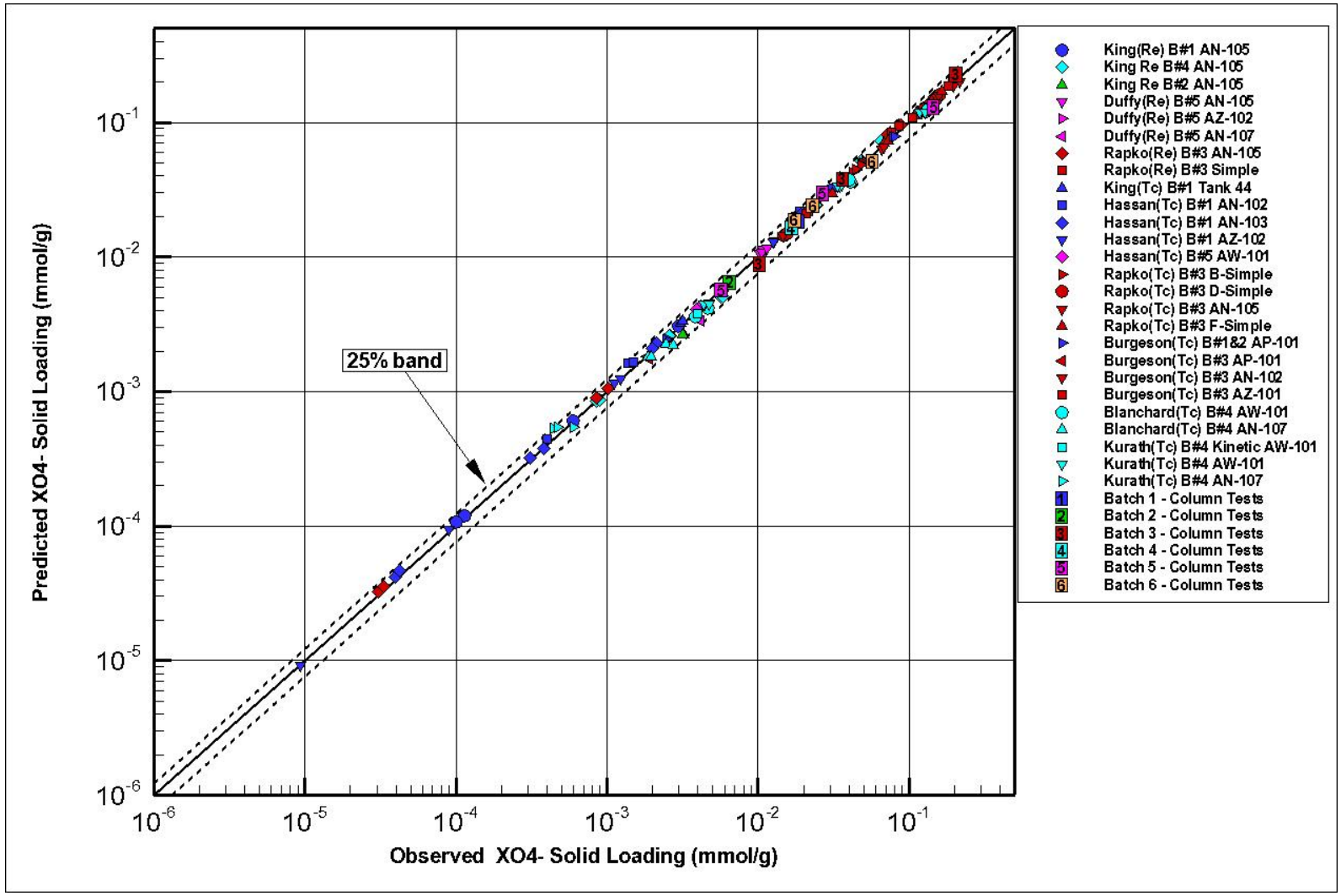

Figure 4-5. Variation in measured pertechnetate and perrhenate loading on SuperLig® 639 resin with respect to computed values. The database shown was taken from two different sites (SRNL and PNNL) and six different batches for a total of 150 data points (138 batch contacts and 12 column tests). Colors coded by batch ID.

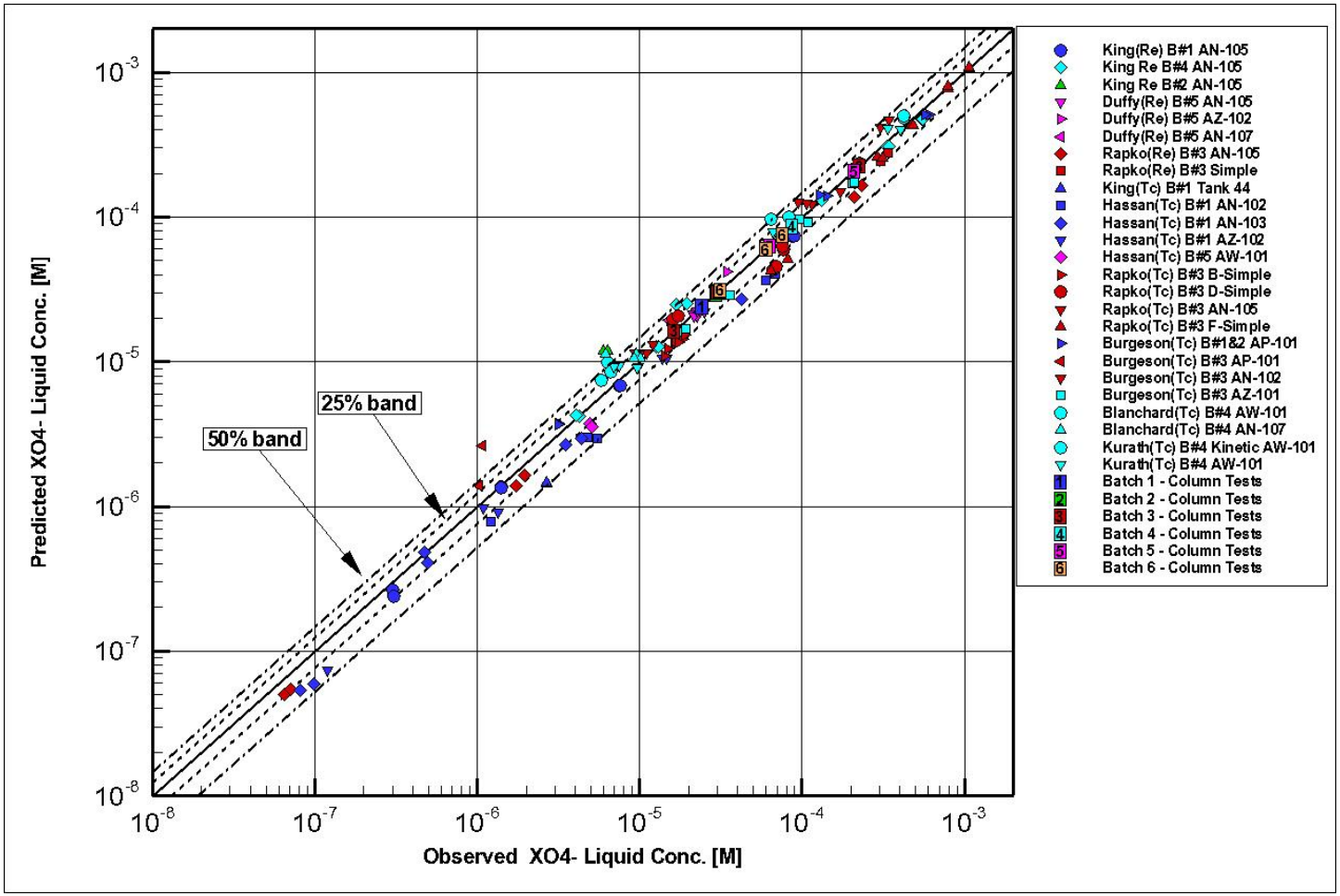

Figure 4-6. Variation in measured pertechnetate and perrhenate concentration on SuperLig® 639 resin with respect to computed values. The database shown was taken from two different sites (SRNL and PNNL) and six different batches for a total of 150 data points (138 batch contacts and 12 column tests). Colors coded by batch ID.

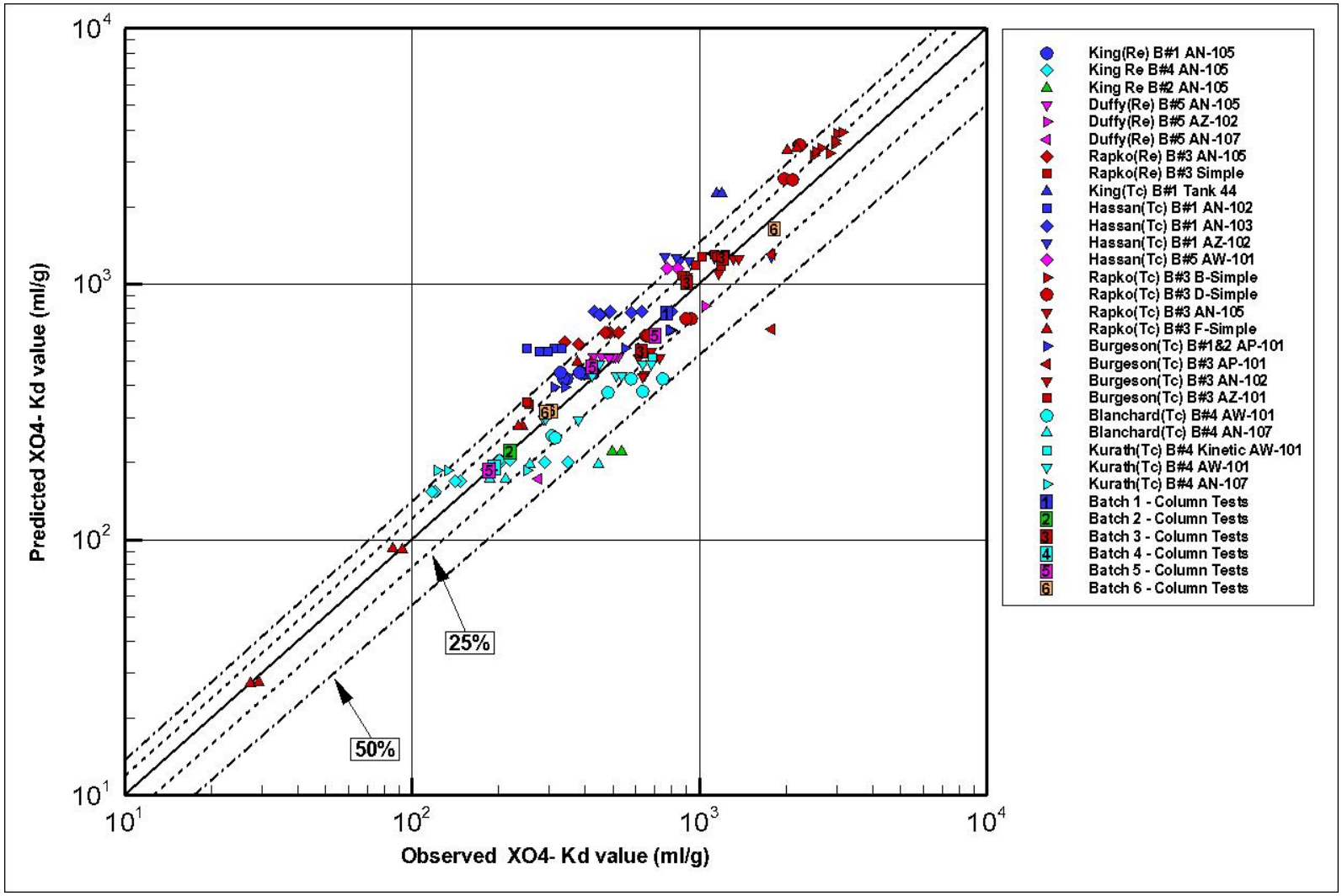

Figure 4-7. Variation in measured pertechnetate and perrhenate Kd values on SuperLig® 639 resin with respect to computed values. The database shown was taken from two different sites (SRNL and PNNL) and six different batches for a total of 150 data points (138 batch contacts and 12 column tests). Colors coded by batch ID.

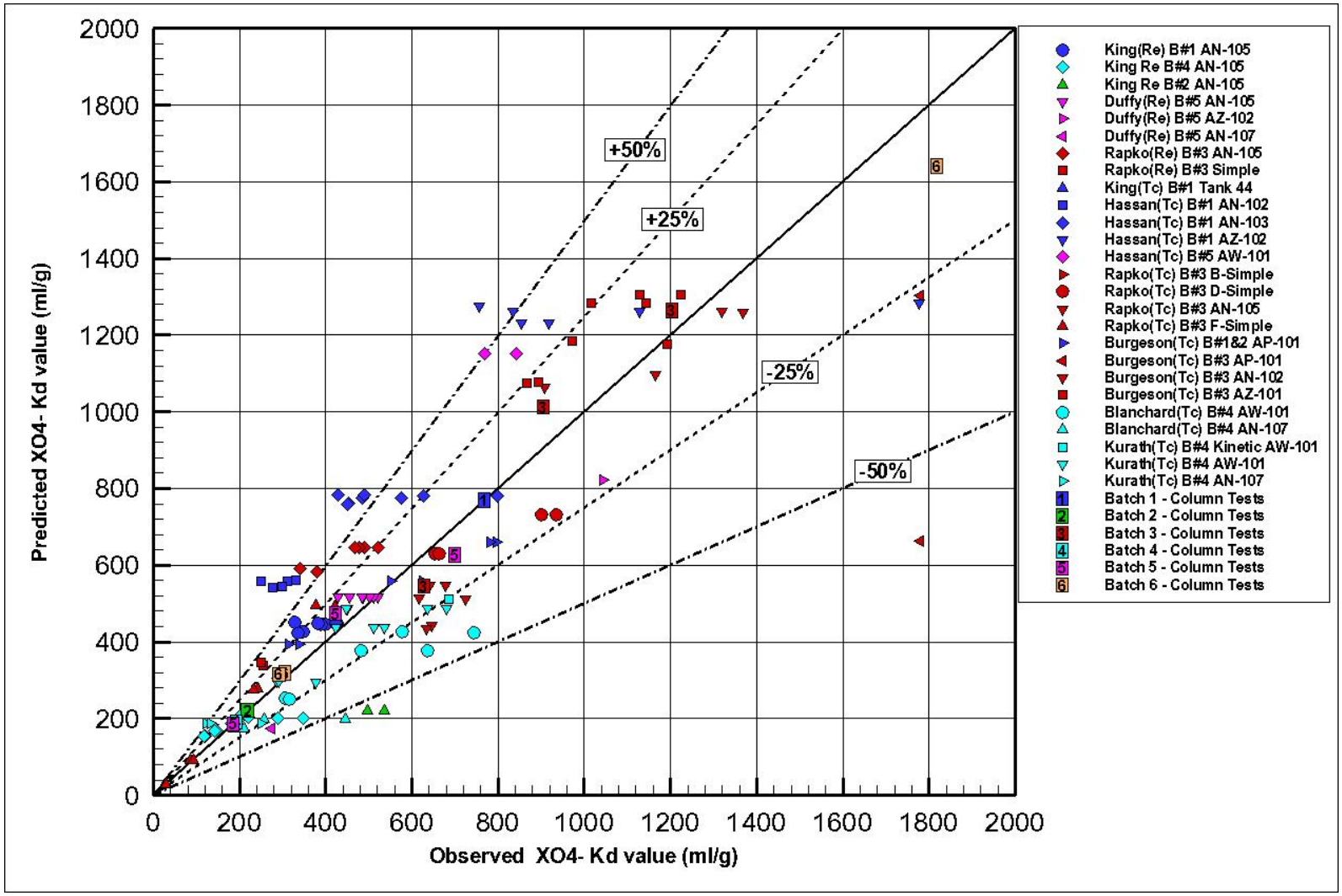

Figure 4-8. Variation in measured pertechnetate and perrhenate Kd values on SuperLig® 639 resin with respect to computed values (continued). Close-up in a linear-linear coordinate system and colors coded by batch ID.

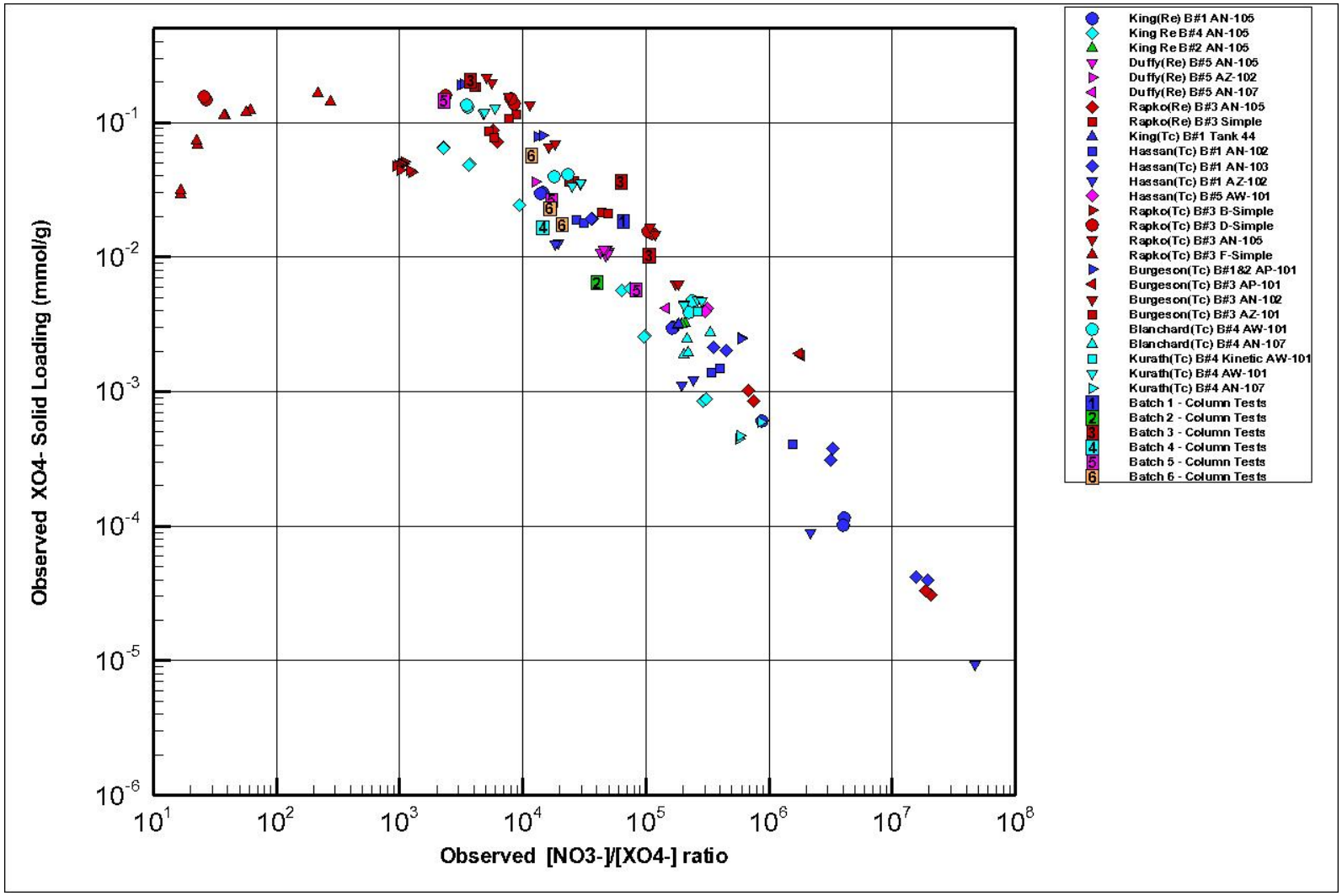

Figure 4-9. Variation in measured pertechnetate and perrhenate loading on SuperLig® 639 resin with respect to final molar ratio of nitrate to pertechnetate and perrhenate ions. The database shown was taken from two different sites (SRNL and PNNL) and six different batches for a total of 150 data points (138 batch contacts and 12 column tests). Colors coded by batch ID.

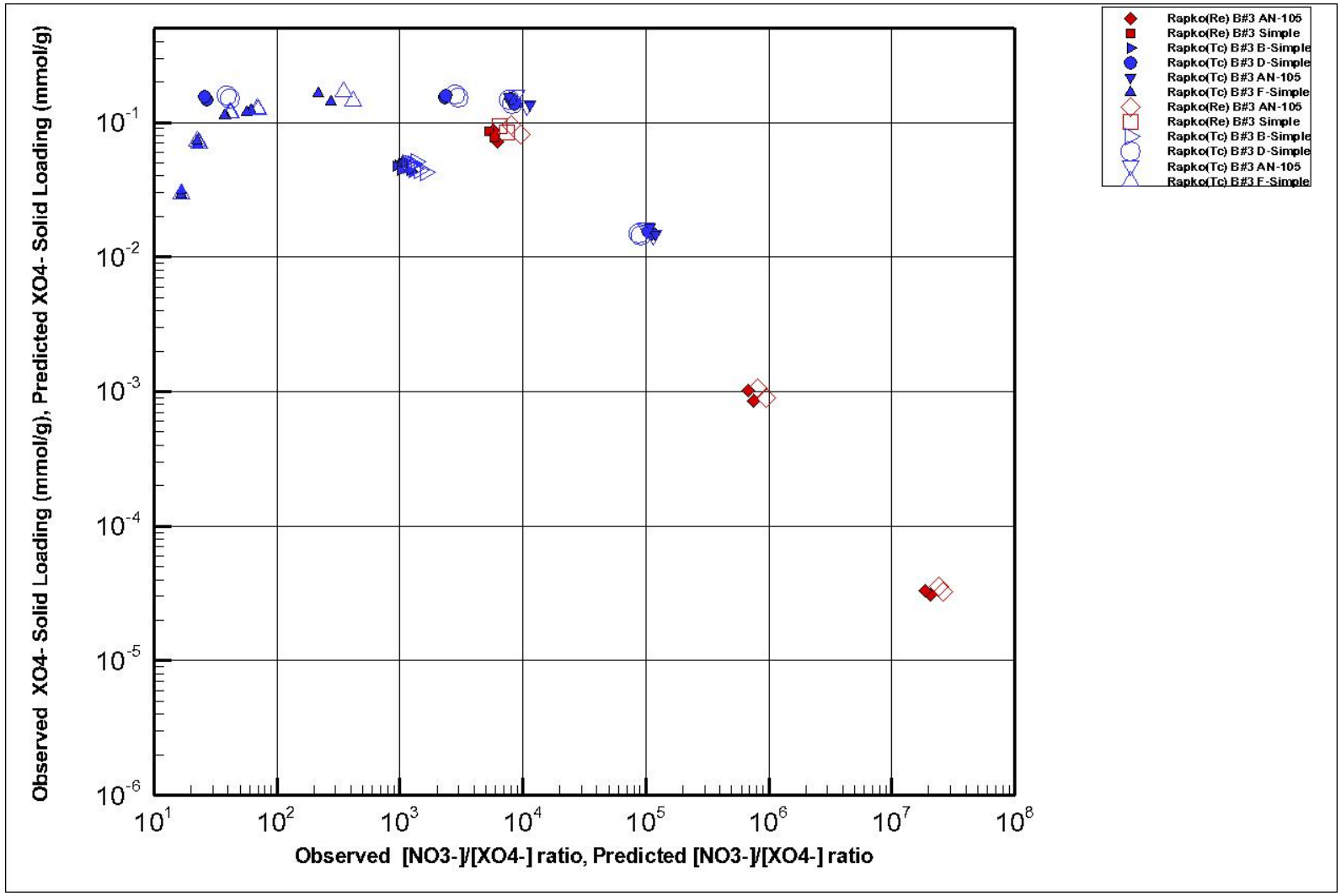

Figure 4-10. Variation in measured pertechnetate and perrhenate loading on SuperLig® 639 resin with respect to final molar ratio of nitrate to pertechnetate and perrhenate ions. The database shown reduced to only Rapko (2003) data. Color coded by Re versus Tc.

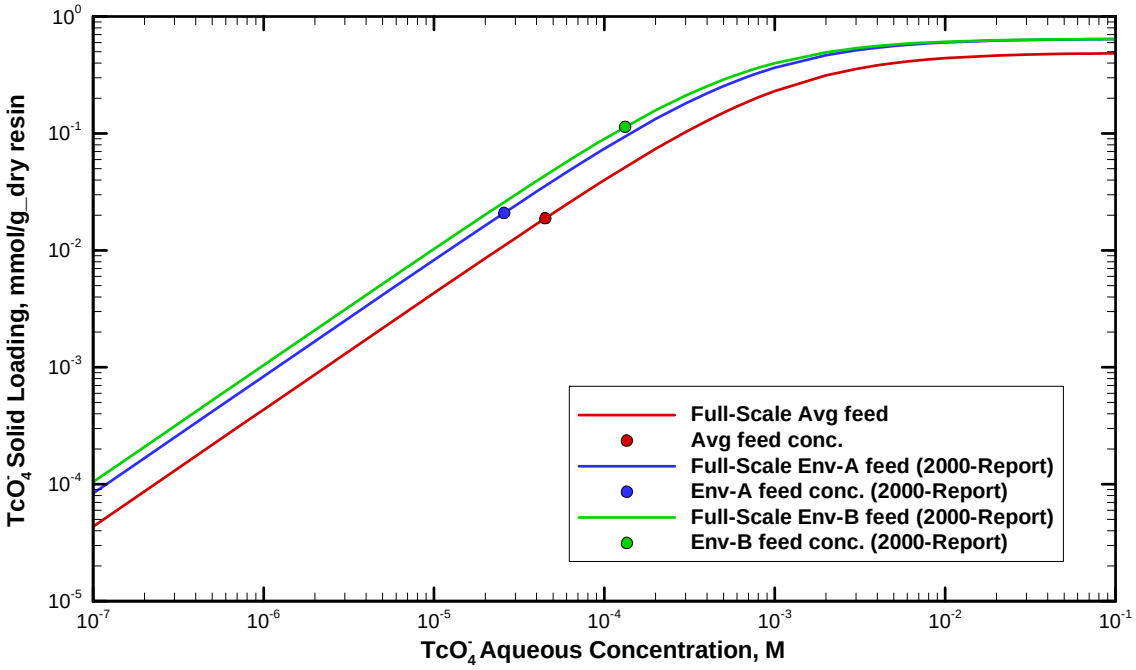

Figure 4-11. Comparison of 25 °C isotherms (i.e., pertechnetate loadings on SuperLig® 639 resin) used to predict Full-Scale performance for the HTWOS SP6 Avg. feed composition employed in this report to the Env-A and Env-B feeds considered in the 2000 Report.

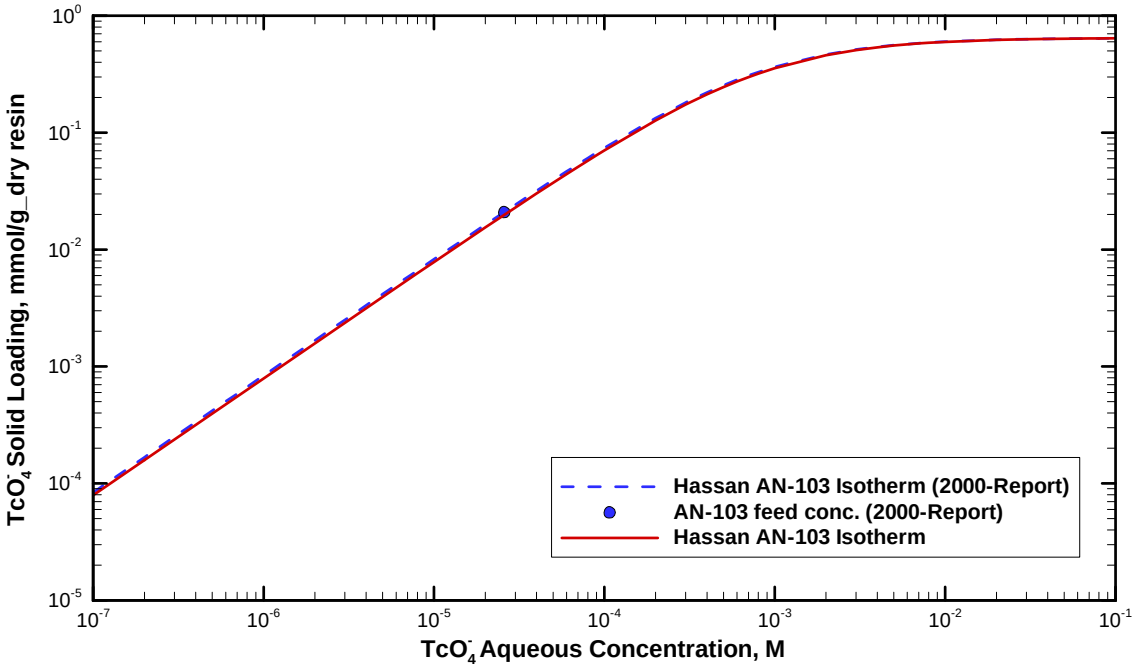

Figure 4-12. Comparison of 25 °C isotherms (i.e., pertechnetate loadings on SuperLig® 639 resin) for the AN-103 (Env-A) simulant employed in column test by Hassan et al. (2000a). Isotherm predictions based on the 2000 Report (dashed curve) and this report (solid curves).

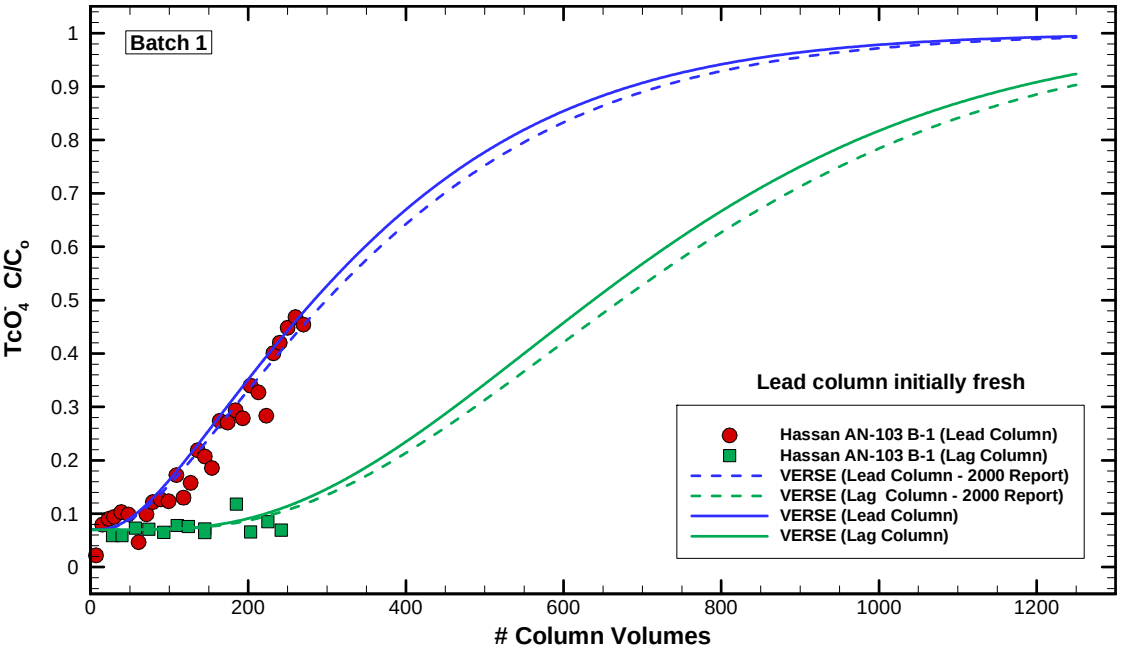

Figure 4-13. Comparison of measured versus predicted pertechnetate lead and lag column breakthrough curves for a Env-A feed composition (Hassan et al., 2000a). Predictions based on the 2000 Report's isotherm model (dashed curves) and this report's isotherm model (solid curves).

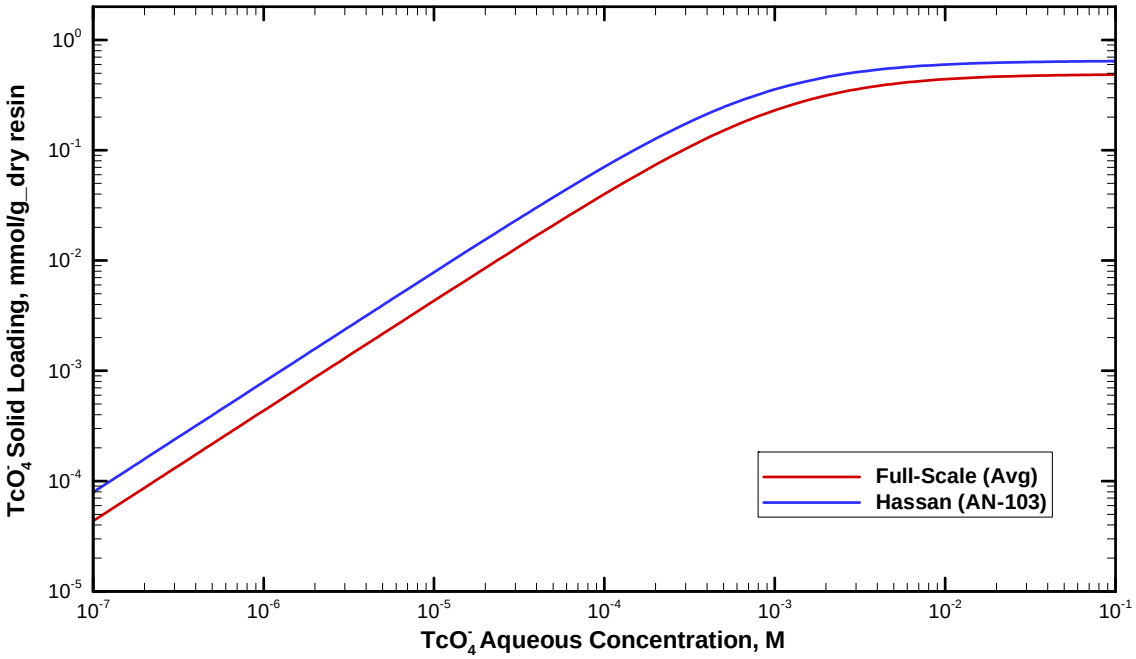

Figure 4-14. Comparison of 25 °C isotherms (i.e., pertechnetate loadings on SuperLig® 639 resin) for the AN-103 (Env-A) simulant employed in column test by Hassan et al. (2000a) versus the HTWOS SP6 Avg. feed composition employed in this report for Full-Scale performance.

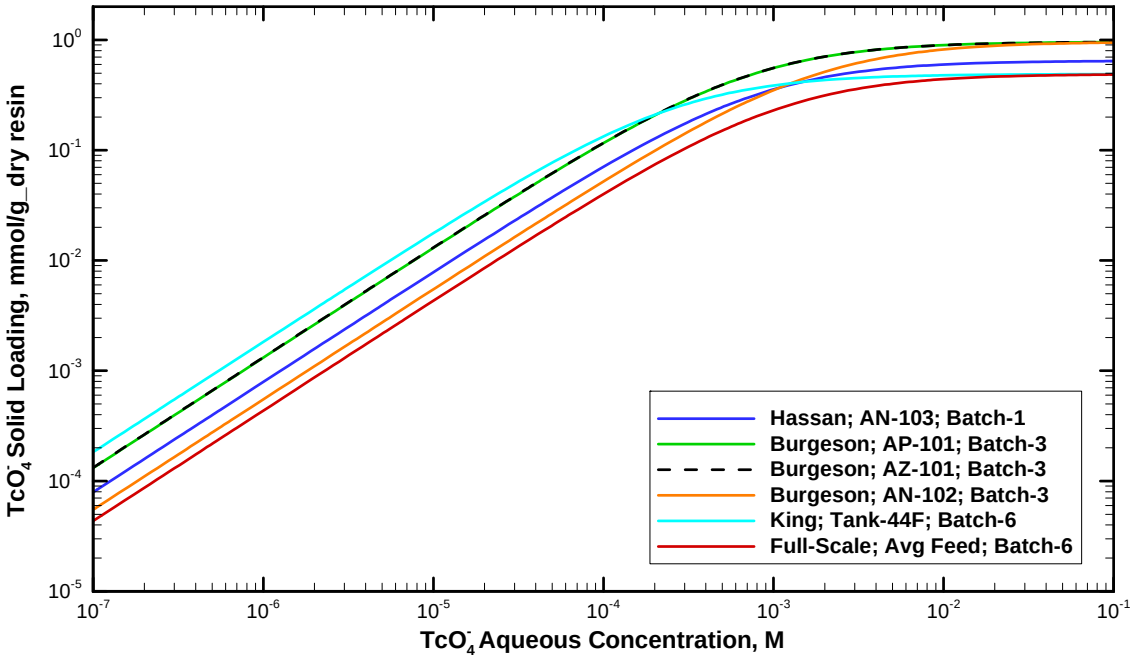

Figure 4-15. Comparison of 25 °C isotherms (i.e., pertechnetate loadings on SuperLig® 639 resin) for various column studies considered in this report. The impact of feed composition, as well as batch variability, can be observed

5.0 Column Properties

Column properties (i.e., bed and particle porosities, particle and bed densities) were either directly taken from the 2000 Report for the original batch ID's considered or taken from appropriate experimental reports for the new batch ID's. See Hamm et al. (2000b) Section 5 for more details.

6.0 Particle Size Distributions

Average particle radius values were taken directly from the 2000 Report. See Hamm et al. (2000b) Section 6 for more details.

7.0 Pore Diffusion

Pore diffusion parameters and associated parameters were either directly taken from the 2000 Report or were computed based on the methodology presented in the 2000 Report. See Hamm et al. (2000b) Section 7 for more details.

8.0 Axial Dispersion and Film Diffusion

Axial dispersion and film diffusion parameters, along with their associated parameters, were either directly taken from the 2000 Report or were computed based on the methodology presented in the 2000 Report. See Hamm et al. (2000b) Section 8 for more details.

9.0 Multi-Scale Column Assessments

Numerous laboratory-scale column experiments have been performed to measure the technetium removal capability (in the form of pertechnetate and using a surrogate perrhenate) of the SuperLig® 639 resin for feed conditions typical of a range of Hanford waste types (i.e., Envelopes A, B, and C). A listing of the pilot-scale, intermediate-scale, and small-scale column studies considered in this section is provided in Table 9-1. Twelve specific tests are considered where five were taken from the preliminary report issued in 2000 (i.e., Hamm et al., 2000b) and seven were tests performed after that report was issued. Table 4-3 provides a listing of column experiments where the seven column tests included since the 2000 Report was issued are shaded in orange. The selected column performance database covers a wide range of conditions such as:

- Five different resin batches and one 50:50 mix of two of these batches (six batches in total).
- Seven different feeds representing Hanford tank compositions and one feed composition taken from a SRS tank. Both actual and simulant feeds were used.
- Column volumes ranging from lab-scale (5 to 10 ml), intermediate (bench)-scale (50 to 75 ml), up to pilot-scale (1200 ml).
- Geometric aspects varied such as L/D ratios from 2 to 86 and the column-to-particle diameter ratios from 15 to 35.
- Throughput varied from 1.5 to 3.36 CV/hr (column volumes per hour are sometimes expressed as bed volumes per hr – BV/hr). Flow in the full-scale column simulation was set to 3.25 CV/hr while a value of 3.0 CV/hr was employed in the 2000 Report.
- Both pertechnetate and perrhenate feed conditions were addressed.
- 18 to 28 °C temperature variation among the column tests. This specific impact was not explicitly incorporated into the isotherm's thermodynamic equilibrium constants (i.e., isotherm parameters were averaged values assumed to be acceptable over the range considered and representing ~25 °C estimates).

For comparison purposes, the full-scale columns are listed in Table 9-1. Key features associated with each column are also given in Table 9-1.

VERSE-LC was used to model 12 of these column experiments where pertechnetate (or its surrogate perrhenate) breakthrough curves were experimentally measured for the SuperLig® 639 resin (several differing batch IDs were tested along with corresponding equilibrium contact tests). Comparisons of these model calculations to the corresponding experimental data are provided in the following subsections. The VERSE-LC input files for each of the 12 simulations are listed in Appendix C.

None of the transport parameter settings were altered during the assessment phase discussed below. The transport properties were established by means other than fitting to the column data directly (e.g., the binary dispersion coefficient for perrhenate was assumed to be equal to the value for pertechnetate which is based on batch kinetics data as discussed in Section 7 of Hamm et al. (2000b)).

As stated in the earlier analysis report (i.e., see Section 9 of Hamm et al. (2000b)), "initial efforts to generalize the binary adsorption isotherm model to account for batch variability and waste types were unsuccessful. Therefore, binary isotherm models for pertechnetate (and perrhenate)

were created for each unique batch ID and waste type (i.e., differing total ionic strengths and compositions)." In this updated analysis effort, this shortcoming was revisited as discussed in Section 4. Here the isotherm model was established based on fitting model parameters over a wide range of batch contact experiments (i.e., six different resin batches) and numerically derived isotherm points for each column assessment case. See Section 4 for further general discussions on the isotherm fitting technique employed.

Chemical equilibrium between the various potential chemical forms of technetium (or rhenium) is not accounted for in the following simulations. Even though VERSE-LC has the capability to address liquid-phase reactions between various feed constituents, no quantitative information regarding the various types of forms (or their reaction equilibrium) is available. Therefore, non-pertechnetate (or non-perrhenate) feed just passes through the columns as an inert species and is not being considered (or recognized) by VERSE-LC during these simulations.

9.1 Algebraic Isotherms

In order to run VERSE-LC column simulations, each benchmark case must have as input an algebraic isotherm (here an "effective" single component isotherm) that is unique to the column's feed composition and temperature. Given the model parameters obtained during the CERMOD optimization process as discussed in Section 4, isotherms for each column test can be generated. The compositions of each column test feed (i.e., only those ions considered in the CERMOD model) are listed in Table 9-2. As mentioned in Section 4, a series of CERMOD numerical batch contact tests were performed and then fitted to an algebraic isotherm for each feed composition. The results of these CERMOD runs are listed in Table 9-3.

Isotherm comparisons are graphically shown for the:

- Five Tc isotherms in Figure 9-1;
- Seven Re isotherms in Figure 9-2; and
- Tc versus Re isotherms for the HTWOS SP6 Avg. Feed in Figure 9-3.

Each of these iostherms is employed in the 12 benchmark cases discussed below. As mentioned earlier, VERSE-LC input files for each case are provided in Appendix C.

9.2 Column Benchmark Cases

Twelve column benchmark cases were chosen that range over the six resin batches of interest. Table 9-4 provides a summary of some of the key geometry and flow conditions. Below, a brief discussion, along with a graphical comparison of data to VERSE-LC predictions, is provided. The VERSE-LC runs were performed to the point where the lead column is nearly saturated (i.e., completely loaded). No effort was made to adjust VERSE-LC breakthrough predictions for these benchmark cases. Transport parameters used in the modeling were taken from the prior analysis performed 2000 and 2002. As Section 10 results will indicate, Full-Scale column performance during the carousel process results in lead columns reaching breakthrough levels of 40% to 50% at the point when a carousel "rotation" is required, where the lead column is removed from service and eluted, and a fresh column is placed in the lag sequence. Therefore, the ability to accurately predict up to ~50% breakthrough is of substantial importance.

9.2.1 "Hot" Lab-Scale Pertechnetate (Batch 1) Test

Column tests were performed using an actual sample of Hanford Envelope A Waste taken from Hanford Tank 241-AN-103. The removal of pertechnetate from the sample was tested using SuperLig® 639 Batch 1 and the test results are documented by Hassan et al. (2000a). This case was also considered in the 2000 Report. A nonpertechnetate fraction of ~7% was assumed in the analyses consistent with the very early on breakthrough behavior measured. The results, as shown in Figure 9-4, conform fairly consistently with the early on breakthrough data for both columns.

9.2.2 Lab-Scale Perrhenate (Batch 2) Test

Column tests were performed using a simulant of Hanford Envelope A Waste representing Hanford Tank 241-AN-105. The removal of perrhenate from the simulant was tested using SuperLig® 639 Batch 2 and the test results are documented by King et al. (2003). These tests were obtained after the 2000 Report, but were examined during a 2002 analysis effort. Here the Exp-1 column test is considered. As shown in Figure 9-5 the breakthrough data suggests that early on breakthrough may have occurred. This could have resulted from channeling in the packed bed. The VERSE-LC simulation assumes a well packed bed. Beyond the first 20 column volumes results conform fairly consistently with the breakthrough data for this column.

9.2.3 "Hot" Lab-Scale Pertechnetate (Batch 3) Test

Column tests were performed using an actual sample of Hanford Envelope A Waste taken from Hanford Tank 241-AP-101. The removal of pertechnetate from the sample was tested using SuperLig® 639 Batch 3 and the test results are documented by Burgeson et al. (2002). This test was after the 2000 Report, but was examined during a 2002 analysis effort where the K^+ enhancer effect was further confirmed. The AP-101 K^+ ion concentration is perhaps the highest value for all the Hanford waste tanks and the K^+ ion enhancer effect should be clearly observable. The results as shown in Figure 9-6 conform fairly consistently with the breakthrough data for this column.

9.2.4 "Hot" Lab-Scale Pertechnetate (Batch 3) Test

Column tests were performed using an actual sample of Hanford Envelope B Waste taken from Hanford Tank 241-AZ-101. The removal of pertechnetate from the sample was tested using SuperLig® 639 Batch 3 and the test results are documented by Burgeson et al. (2004). This test was after the 2000 Report, but was examined during a 2002 analysis effort. The results as shown in Figure 9-7 conform fairly consistently with the early on breakthrough data for this column. Breakthrough data near 250 to 300 CVs appears to be showing a sharper concentration front than predictions.

9.2.5 "Hot" Lab-Scale Pertechnetate (Batch 3) Test

Column tests were performed using an actual sample of Hanford Envelope C Waste taken from Hanford Tank 241-AN-102 supernate and solids from Tank 241-C-104. The removal of pertechnetate from the sample was tested using SuperLig® 639 Batch 3 and the test results are documented by Burgeson et al. (2003a). This test was after the 2000 Report, but was examined

during a 2002 analysis effort. As shown in Figure 9-8 the early on breakthrough performance of the column appears to be better than the VERSE-LC predictions.

9.2.6 Bench-Scale Perrhenate (Batch 4) Test

Column tests were performed using a simulant of Hanford Envelope A Waste representing Hanford Tank 241-AN-105. The removal of perrhenate from the simulant was tested using SuperLig® 639 Batch 4 and the test results are documented by King et al. (2000a). This case was also considered in the 2000 Report. Here the Exp-1 column test is considered. The results as shown in Figure 9-9 conform fairly consistently with the breakthrough data for this column. Discrepancies early on suggest that transport properties employed in VERSE-LC are not sufficiently limiting mass transfer rates here. Late breakthrough data shows a steady-state offset indicating that the feed concentration value employed in normalizing the data is suspect.

9.2.7 Lab-Scale Perrhenate (Batch 5) Test

Column tests were performed using a simulant of Hanford Envelope A Waste representing Hanford Tank 241-AN-105. The removal of perrhenate from the simulant was tested using SuperLig® 639 Batch 5 and the test results are documented by King et al. (2003). These tests were after the 2000 Report, but were employed during 2002 analysis efforts. Here the Exp-5 column test is considered. The results shown in Figure 9-10 conform fairly consistently to the breakthrough data for this column. A slight early-on breakthrough can be seen in the data.

9.2.8 Bench-Scale Perrhenate (Batch 5) Test

Column tests were performed using a simulant of Hanford Envelope B Waste representing Hanford Tank 241-AZ-102. The removal of perrhenate from the simulant was tested using SuperLig® 639 Batch 5 and the test results are documented by King et al. (2003). These tests were after the 2000 Report, but were employed during 2002 analysis efforts. Here the Exp-8 column test is considered. The results shown in Figure 9-11 are significantly different in shape suggesting that transport parameter settings should need to be revisited.

9.2.9 Bench -Scale Perrhenate (Batch 5) Test

Column tests were performed using a simulant of Hanford Envelope C Waste representing Hanford Tank 241-AN-107. The removal of perrhenate from the simulant was tested using SuperLig® 639 Batch 5 and the test results are documented by King et al. (2003). These tests were after the 2000 Report, but were employed during 2002 analysis efforts. Here the Exp-9 column test is considered. The results shown in Figure 9-12 conform fairly consistently with the breakthrough data for this column. Slight rates of mass transfer discrepancies appear to be observed where the actual column data suggests more limiting conditions exist.

9.2.10 Bench-Scale Perrhenate (Batch 6) Test

Column tests were performed using a simulant of Hanford Envelope A Waste representing Hanford Tank 241-AN-105. The removal of perrhenate from the simulant was tested using SuperLig® 639 Batch 6 and the test results are documented by King et al. (2000a). This case was also considered in the 2000 Report. Here the Exp-5 column test is considered. The results shown in Figure 9-13 conform fairly consistently with the breakthrough data for this column.

9.2.11 Bench-Scale Perrhenate (Batch 6) Test

Initial interest in treating the SRS sample for pertechnetate removal resulted from the similarity between the Tank 44F supernate composition and the Hanford Envelope A supernate solutions, as discussed by King et al. (2000b). Column tests were performed using a SRS waste sample from Tank 44F. The removal of pertechnetate from the sample was tested using SuperLig® 639 Batch 6 and the test results are documented by King et al. (2000b). This case was also considered in the 2000 Report. The results shown in Figure 9-14 conform fairly consistently with the breakthrough data for this column. Again, slight discrepancies in calculated mass transfer rates may account for the difference between model predictions and observed breakthrough behavior.

9.2.12 Pilot-Scale Perrhenate (Batch 6) Test

Column tests were performed using a simulant of Hanford Envelope A waste representing Hanford Tank 241-AN-105. The removal of perrhenate from the simulant was tested using SuperLig® 639 Batch 6 and the test results are documented by Steimke et al. (2000). This case was also considered in the 2000 Report. Here the Run-9 column test is included. That test utilized a fresh lead and lag column arrangement. The results, shown in Figure 9-15, conform fairly consistently to the breakthrough data for this column.

9.2.13 HTWOS SP6 2013 LAW (5 M Average)

The projected LAW feed composition used in this report for the full-scale modeling was derived from a computer model of the Hanford Waste Treatment Plan (WTP) effluent vector for the life of the mission. This was done using the Hanford Tank Waste Operations Simulator (HTWOS) using the System Plan 6 (Certa et al., 2011) baseline case. This averaged the composition of the Cs-decontaminated LAW for processing the waste tank contents, and normalized to 5.0 M [Na^+] salt content and subsequently adjusted for cation-anion balance and solubility. The composition is shown in the far-right column of Table 9-2.

Table 9-1. Key features of Pertechnetate (perrhenate)-SuperLig® 639 fixed bed full-, pilot-, intermediate-, and small-scale columns.

Column Index	Lab	PI	timing	XO4-	T (C)	Scale	Simulant	Resin Batch	Q total (mmole/g)	Bed density (g/ml)	Feed inlet XO4- conc. [M][a]	Total Solid Loading (mmole/ml)
1	SRNL	Hassan	old	Tc	26	Lab	AN-103	1	0.6478	0.468	2.4015E-05	1.8445E-02
2	SRNL	King	new	Re	25	Lab	AN-105	2	0.3223	0.479	2.9430E-05	6.4338E-03
3	PNNL	Burgeson	new	Tc	24-28	Lab	AP-101	3	0.9630	0.4564	2.9997E-05	3.6101E-02
4	PNNL	Burgeson	new	Tc	24-28	Lab	AZ-101			0.4564	2.2498E-04	2.0358E-01
5	PNNL	Burgeson	new	Tc	24-28	Lab	AN-102			0.4564	1.6248E-05	1.0208E-02
6	SRNL	King	old	Re	20-23	Bench	AN-105	4	0.2971	0.489	8.5929E-05	1.6554E-02
7	SRNL	King	new	Re	25	Lab	AN-105	5	0.6666	0.622	6.2700E-05	2.6513E-02
8	SRNL	King	new	Re	25	Bench	AZ-102			0.622	2.0700E-04	1.4479E-01
9	SRNL	King	new	Re	25	Bench	AN-107			0.622	3.0600E-05	5.6620E-03
10	SRNL	King	old	Re	20-23	Bench	AN-105	6	0.4906	0.4735	7.5188E-05	2.2951E-02
11	SRNL	Steimke	old	Re	18	Pilot	AN-105			0.527	5.9613E-05	1.7354E-02
12	SRNL	King	old	Tc	23-27	Bench	Tank-44F			0.4735	3.1232E-05	5.6780E-02
13	HTWOS*	-	new	Tc	25	Full	Avg. Feed	6	0.4906	0.5003[b]	4.5000E-05	-

[a] For certain column studies perrhenate (ReO_4^-) was used as a surrogate for pertechnetate ($^{99}TcO_4^-$).
[b] Average of 0.4735 and 0.527 measured bed densities for Batch 6.
*HTWOS System Plan 6 5 M [Na^+] average baseline composition

Table 9-2. Species feed concentrations required in CERMOD and lower bound estimates[a] for the total ionic strength (in molar units) for those column performance predictions presented in this report.

Species ID	Hassan 2000 (AN-103) (TcO_4^-) [M]	King 2002 (AN-105) (ReO_4^-) [M]	Burgeson 2002 (AP-101) (TcO_4^-) [M]	Burgeson 2002 (AN-101) (TcO_4^-) [M]	Burgeson 2002 (AN-102) (TcO_4^-) [M]	King 2000 (AN-105) (ReO_4^-) [M]	King 2002 (AN-105) (ReO_4^-) [M]	King 2002 (AN-107) (ReO_4^-) [M]	King 2002 (AZ-102) (ReO_4^-) [M]	King 2000 (AN-105) (ReO_4^-) [M]	King 2000 (Tk-44F) (TcO_4^-) [M]	Steimke 2000 (AN-105) (ReO_4^-) [M]	HTWOS SP6 2013 (5 M Avg) (TcO_4^-) [M]
Batch ID	**1**	**2**		**3**		**4**		**5**			**6**		**6**
Cations													
Ca^{2+}	0.000E+0	4.820E-4	0.000E+0	0.000E+0	4.000E-3	0.000E+0	1.500E-5	1.710E-3	3.560E-3	0.000E+0	0.000E+0	6.750E-4	0.000E+0
Cd^{2+}	0.000E+0	2.640E-5	0.000E+0	0.000E+0	0.000E+0	0.000E+0	2.020E-5	0.000E+0	0.000E+0	0.000E+0	0.000E+0	0.000E+0	0.000E+0
H^+	0.000E+0	0.000E+0	0.000E+0	0.000E+0	0.000E+0	0.000E+0	0.000E+0	0.000E+0	0.000E+0	0.000E+0	0.000E+0	0.000E+0	0.000E+0
K^+	1.210E-1	9.500E-2	7.500E-1	9.000E-2	2.800E-2	9.000E-2	9.400E-2	1.470E-1	3.500E-2	9.000E-2	5.700E-2	8.920E-2	3.280E-2
Mg^{2+}	0.000E+0	0.000E+0	0.000E+0	0.000E+0	0.000E+0	0.000E+0	0.000E+0	0.000E+0	0.000E+0	0.000E+0	0.000E+0	1.050E-4	0.000E+0
Na^+	5.250E+0	4.959E+0	4.810E+0	4.260E+0	4.780E+0	4.993E+0	4.866E+0	4.665E+0	5.742E+0	4.993E+0	5.400E+0	4.973E+0	5.002E+0
Pb^+	0.000E+0	8.180E-4	0.000E+0	0.000E+0	0.000E+0	0.000E+0	8.070E-4	0.000E+0	0.000E+0	0.000E+0	0.000E+0	0.000E+0	0.000E+0
Zn^{2+}	0.000E+0	0.000E+0	0.000E+0	0.000E+0	2.015E-1	0.000E+0	0.000E+0	0.000E+0	0.000E+0	0.000E+0	0.000E+0	0.000E+0	0.000E+0
Anions													
$Al(OH)_4^-$	7.000E-1	5.480E-1	2.500E-1	1.900E-1	2.900E-1	6.900E-1	5.560E-1	4.800E-2	9.000E-3	6.900E-1	2.393E-1	6.900E-1	3.070E-1
$C_2O_4^{2-}$	6.000E-3	2.000E-3	2.000E-2	1.000E-2	1.600E-2	3.000E-3	2.000E-3	1.300E-2	0.000E+0	3.000E-3	7.000E-4	3.300E-3	0.000E+0
CH_3COO^-	0.000E+0	0.000E+0	0.000E+0	0.000E+0	0.000E+0	0.000E+0	0.000E+0	0.000E+0	0.000E+0	0.000E+0	0.000E+0	0.000E+0	3.850E-2
Cl^-	6.098E-2	6.255E-1	3.997E-2	3.775E-3	5.098E-2	1.200E-1	6.873E-1	2.047E-1	0.000E+0	1.200E-1	9.299E-3	1.859E-1	4.215E-2
$COOH^-$	0.000E+0	3.200E-2	0.000E+0	0.000E+0	0.000E+0	3.000E-2	3.100E-2	1.680E-1	1.430E-1	3.000E-2	2.200E-3	3.000E-2	0.000E+0
CO_3^{2-}	4.200E-2	5.408E-2	4.900E-1	4.900E-1	7.600E-1	2.600E-2	6.367E-2	9.640E-1	8.250E-1	2.600E-2	2.600E-2	6.850E-2	2.740E-1
F^-	0.000E+0	0.000E+0	0.000E+0	1.000E-1	3.300E-1	0.000E+0	0.000E+0	7.200E-2	0.000E+0	0.000E+0	3.000E-4	4.700E-3	3.160E-2
HPO_4^{2-}	7.000E-3	2.000E-3	1.000E-2	1.700E-2	2.300E-2	3.000E-3	2.000E-3	1.100E-2	2.700E-2	3.000E-3	3.100E-3	2.800E-3	4.899E-2
NO_2^-	1.037E+0	1.130E+0	7.800E-1	1.182E+0	9.000E-1	1.130E+0	1.124E+0	1.131E+0	8.470E-1	1.130E+0	4.760E-01	1.132E+00	5.650E-01
NO_3^-	1.571E+0	1.183E+0	1.880E+0	8.500E-1	1.730E+0	1.250E+0	1.073E+0	4.720E-1	2.564E+0	1.250E+0	4.950E-1	1.247E+0	1.622E+0
OH^-	1.876E+0	1.410E+0	1.510E+0	6.300E-1	1.800E-1	1.791E+0	1.345E+0	1.835E-1	5.171E-1	1.791E+0	4.173E+0	1.617E+0	1.611E+0
ReO_4^-	-	2.943E-5	-	-	-	8.593E-5	6.270E-5	2.070E-4	3.060E-5	7.519E-5	-	5.961E-5	-
SO_4^{2-}	8.000E-3	6.000E-3	3.000E-2	1.800E-1	7.000E-2	3.800E-3	5.000E-3	2.800E-1	0.000E+0	3.800E-3	1.300E-3	3.800E-3	8.600E-2
TcO_4^-	2.401E-5	-	3.000E-5	2.250E-4	1.625E-5	-	-	-	-	-	3.123E-5	-	4.500E-5
Total ionic strength[M]	> 5.37	> 5.06	> 5.56	> 4.35	> 5.22	> 5.08	> 4.96	> 4.82	> 5.78	> 5.08	> 5.40	> 5.06	> 5.04

[a] Only rough estimates (i.e., lower bounds) for the total ionic strength can be computed since a complete listing of the anions and cations in solution is not available. The total ionic strength is computed based on molar units.

Table 9-3. Parameter settings for an "effective" single component Freundlich/Langmuir Hybrid equilibrium isotherm model for Pertechnetate (or perrhenate) on SuperLig® 639 based on the "effective" single component approach.

Lab	PI	timing	XO4-	Scale	Simulant	Batch number	$\rho_b Q_T$ (gmole/ml)	β [M]
SRNL	Hassan	old	Tc	Lab	AN-103	1	0.30317	8.17736×10^{-4}
SRNL	King	new	Re	Lab	AN-105	2	0.15438	1.43021×10^{-3}
PNNL	Burgeson	new	Tc	Lab	AP-101	3	0.43950	7.31694×10^{-4}
PNNL	Burgeson	new	Tc	Lab	AZ-101			7.26774×10^{-4}
PNNL	Burgeson	new	Tc	Lab	AN-102			1.74938×10^{-3}
SRNL	King	old	Re	Bench	AN-105	4	0.41463	1.34504×10^{-3}
SRNL	King	new	Re	Lab	AN-105	5	0.41460	1.46318×10^{-3}
SRNL	King	new	Re	Bench	AZ-102			8.56092×10^{-4}
SRNL	King	new	Re	Bench	AN-107			3.55316×10^{-3}
SRNL	King	old	Re	Bench	AN-105	6	0.23230	1.46318×10^{-3}
SRNL	King	old	Tc	Bench	Tank-44F			3.06846×10^{-4}
SRNL	Steimke	old	Re	Pilot	AN-105		0.25855	1.49735×10^{-3}
HTWOS	-	new	Tc	Full-Scale	Avg. Feed	6	0.24545	1.12753×10^{-3}
HTWOS	-	new	Re	Full-Scale	Avg. Feed			2.23280×10^{-3}

Table 9-4. Geometry and flow conditions for the various columns considered.

Column Index	Lab	PI	dia (cm)	length (cm)	vol (ml)	flow (ml/min)	flow (CV/hr)	Co [M]	L/D
1	SRNL	Hassan	1.10	10.73	10.20	0.2550	1.50	2.401E-05	9.76
2	SRNL	King	1.60	5.02	10.10	0.5016	2.98	2.943E-05	3.14
3	PNNL	Burgeson	1.50	3.10	5.48	0.2739	3.00	3.000E-05	2.07
4	PNNL	Burgeson	1.50	3.10	5.48	0.2739	3.00	2.250E-04	2.07
5	PNNL	Burgeson	1.50	3.10	5.48	0.2739	3.00	1.625E-05	2.07
6	SRNL	King	2.69	8.99	51.10	2.8984	3.40	8.593E-05	3.34
7	SRNL	King	1.45	6.10	10.07	0.5016	2.99	6.270E-05	4.21
8	SRNL	King	2.50	15.19	74.58	3.6669	2.95	2.070E-04	6.08
9	SRNL	King	2.50	15.19	74.58	3.7539	3.02	3.060E-05	6.08
10	SRNL	King	2.69	8.80	50.00	2.4438	2.93	7.519E-05	3.27
11	SRNL	Steimke	2.61	223.66	1200.00	67.167	3.36	5.961E-05	85.57
12	SRNL	King	2.70	8.75	50.10	2.5885	3.10	3.123E-05	3.24
13	HTWOS *	-	77.00	225.00	1047741	56781	3.25	4.500E-05	2.92
*HTWOS System Plan 6 5 M [Na^+] average baseline composition									

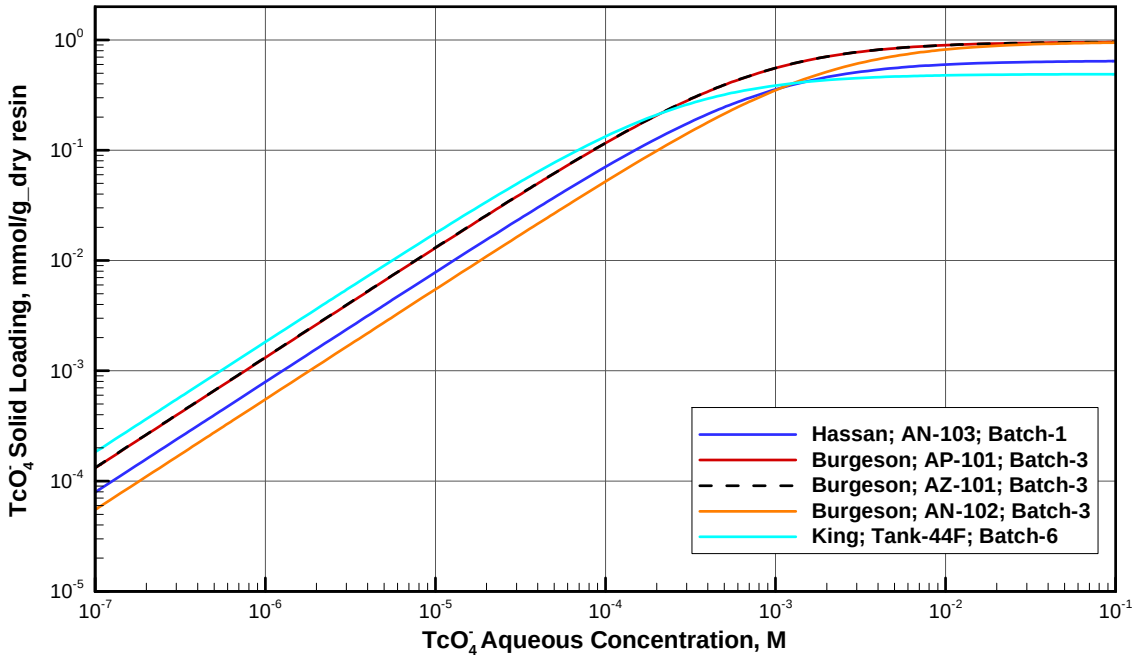

Figure 9-1. A comparison of predicted loadings on SuperLig® 639 resin for the five different pertechnetate column tests considered.

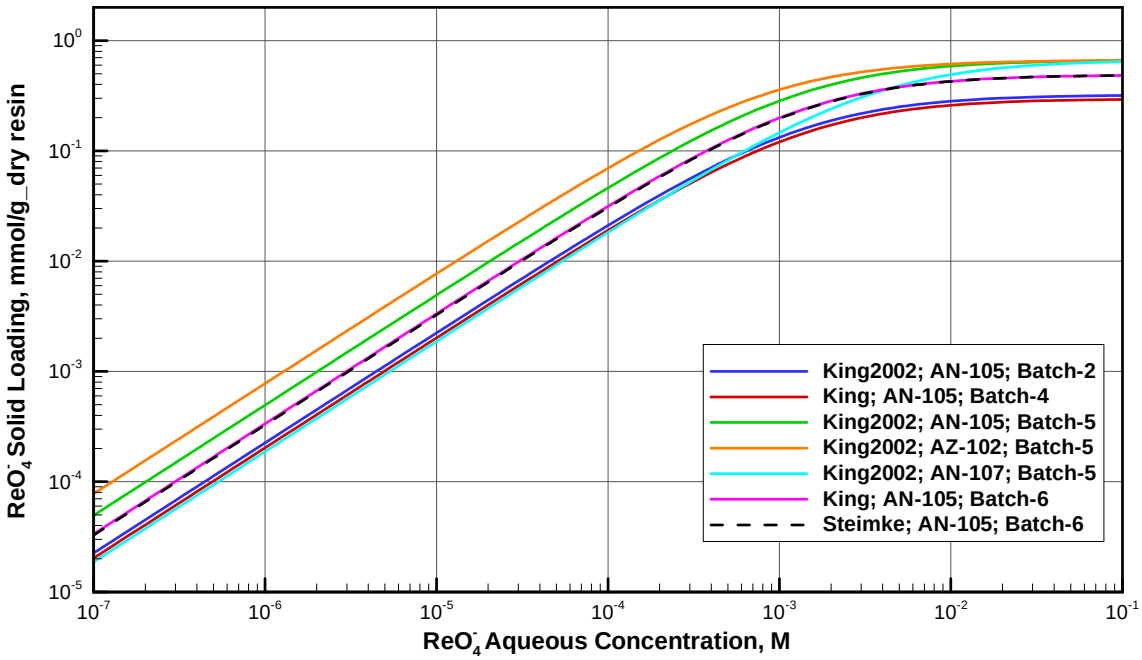

Figure 9-2. A comparison of predicted loadings on SuperLig® 639 resin for the seven different perrhenate column tests considered.

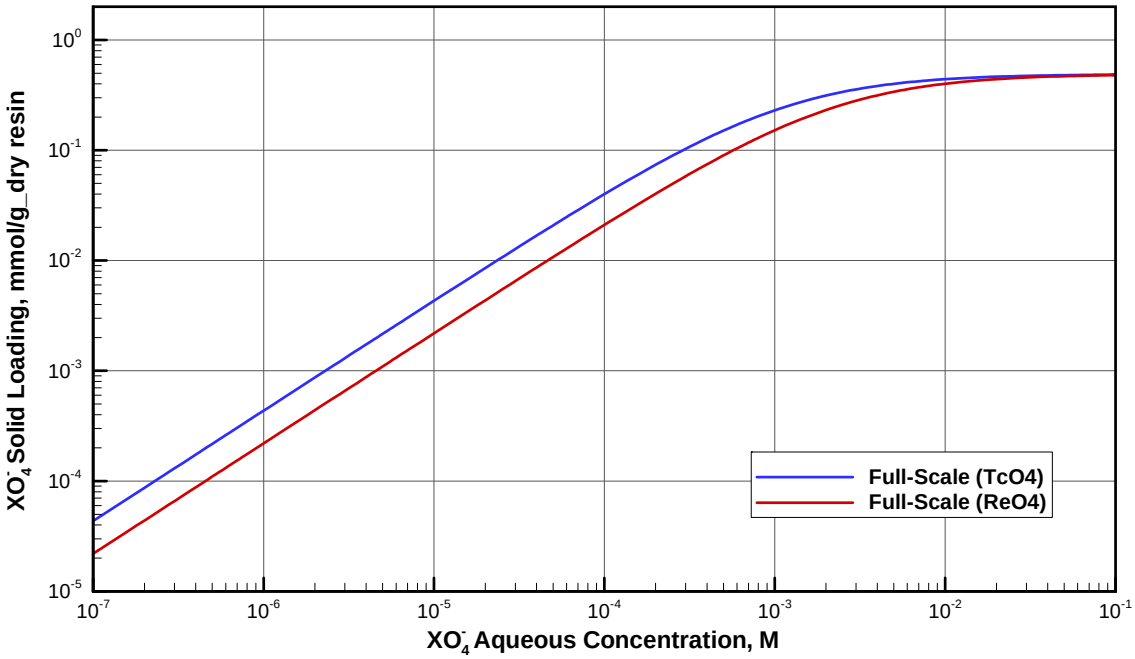

Figure 9-3. A comparison of predicted pertechnetate and perrhenate loadings on SuperLig® 639 resin for the full-scale columns considered with the HTWOS SP6 Avg. Feed.

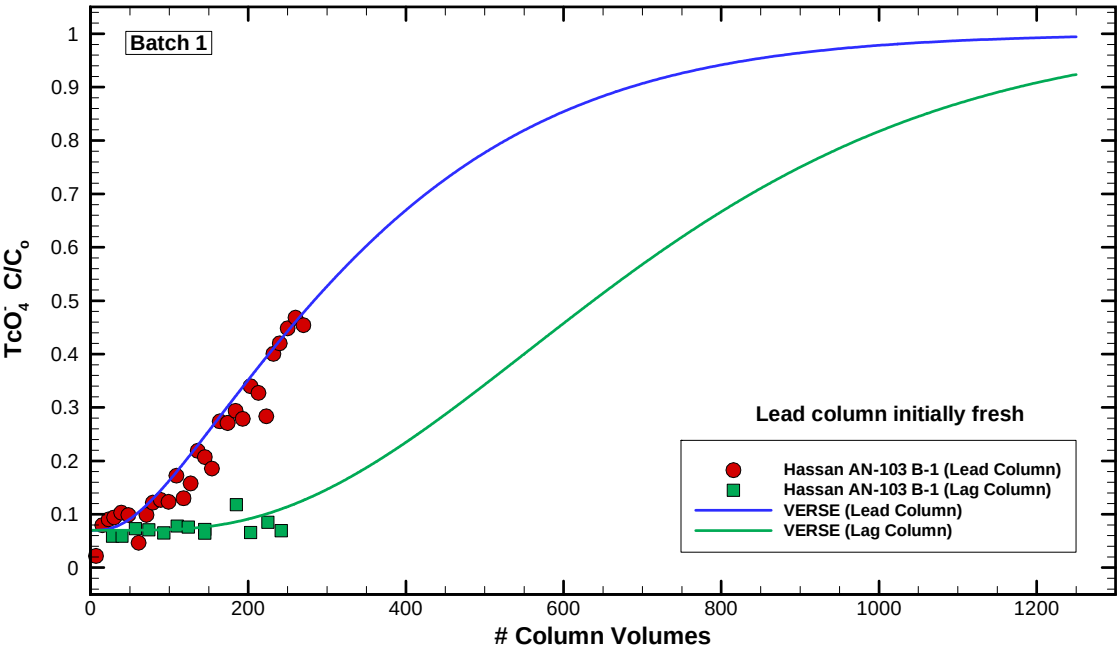

Figure 9-4. VERSE-LC pertechnetate exit breakthrough curve compared to data from Hassan et al., (2000a): AN-103, Batch 1, D = 1.10 cm, L = 10.73 cm, F = 1.50 CV/hr, T = 26°C.

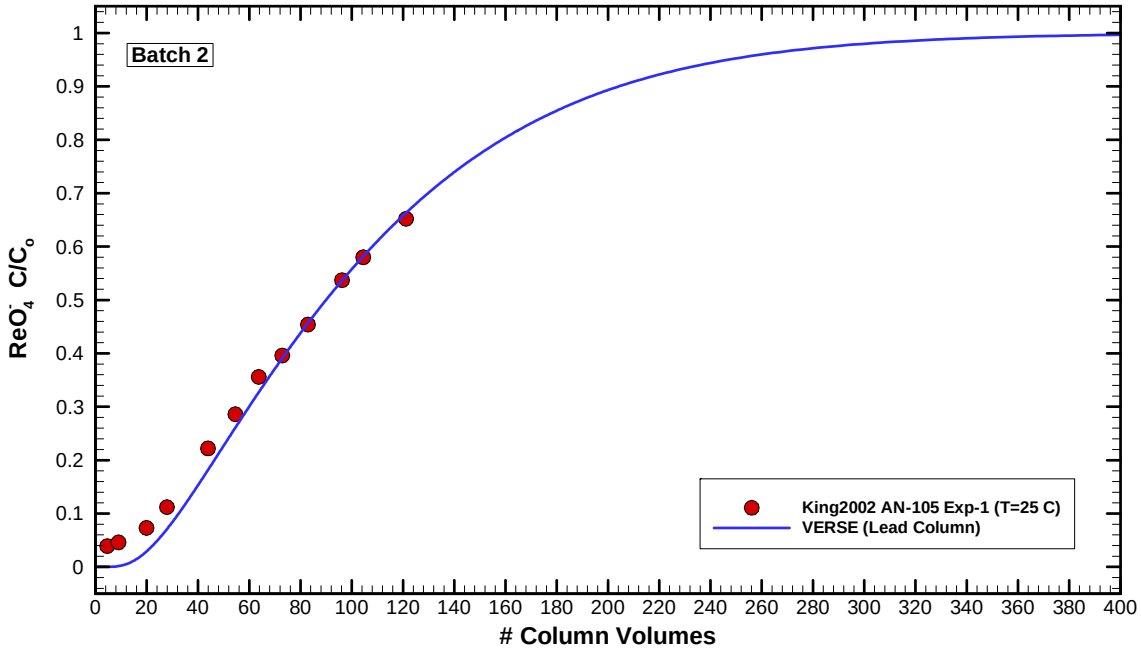

Figure 9-5. VERSE-LC perrhenate exit breakthrough curve compared to Exp-1 data from King et al., (2003): AN-105, Batch 2, D = 1.60 cm, L = 5.02 cm, F = 2.98 CV/hr, T = 25°C.

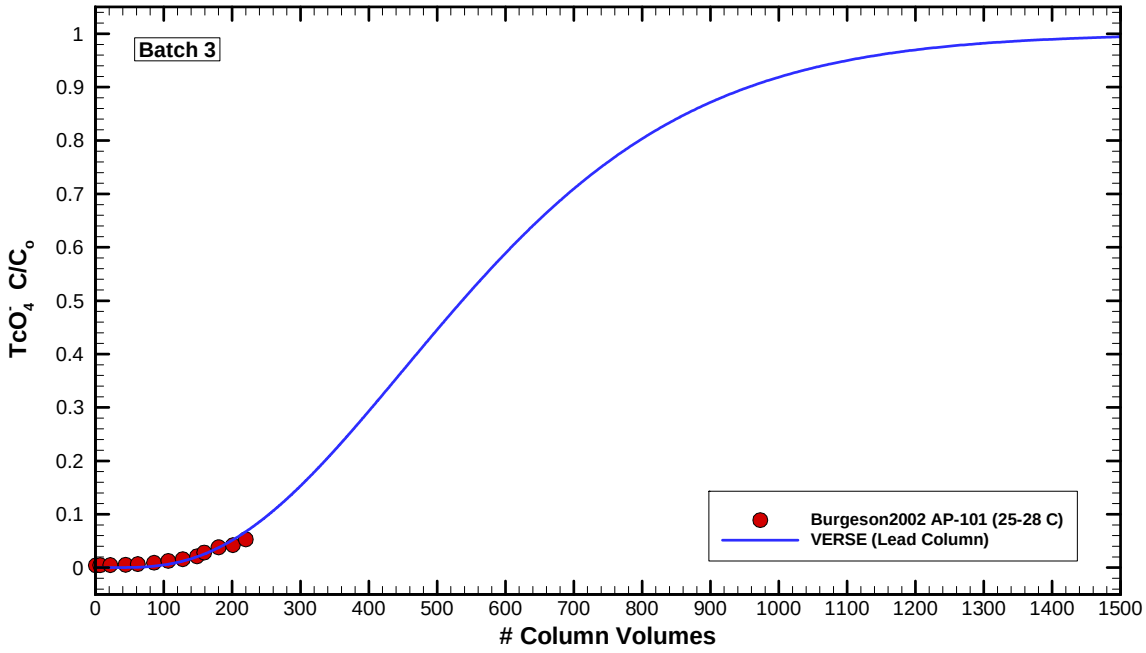

Figure 9-6. VERSE-LC pertechnetate exit breakthrough curve compared to data from Burgeson et al. (2002): AP-101, Batch 3, D = 1.50 cm, L = 3.10 cm, F = 3.00 CV/hr, T = 25-28°C.

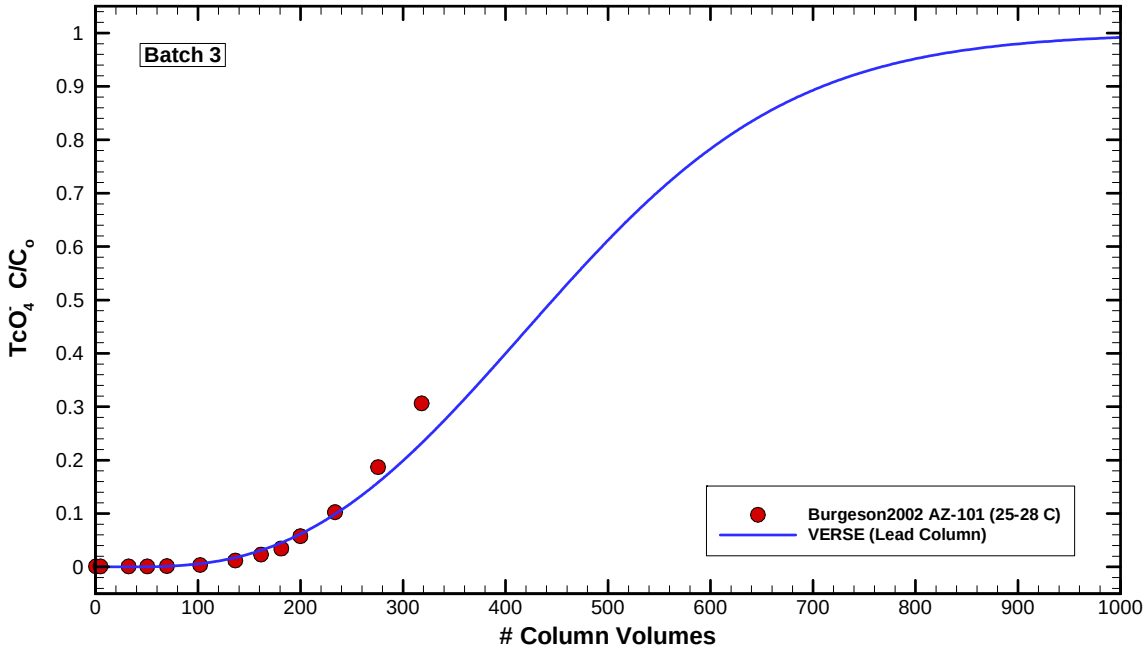

Figure 9-7. VERSE-LC pertechnetate exit breakthrough curve compared to data from Burgeson et al. (2004): AZ-101, Batch 3, D = 1.50 cm, L = 3.10 cm, F = 3.00 CV/hr, T = 25-28°C.

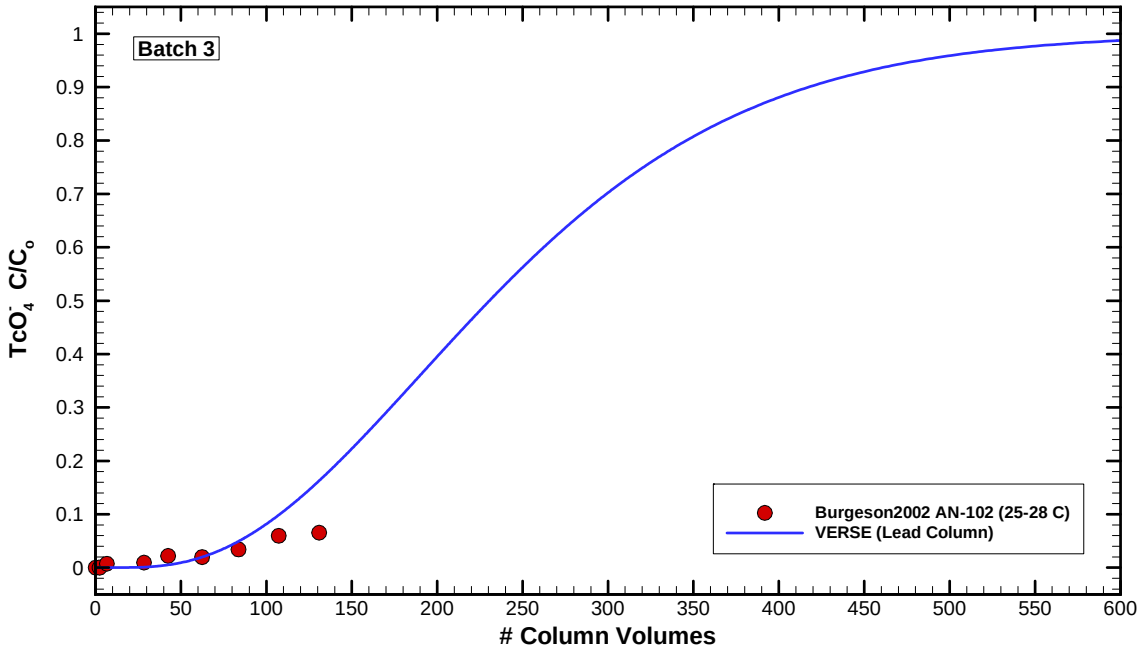

Figure 9-8. VERSE-LC pertechnetate exit breakthrough curve compared to data from Burgeson et al. (2003a): AN-102/C-104, Batch 3, D = 1.50 cm, L = 3.10 cm, F = 3.00 CV/hr, T = 25-28°C.

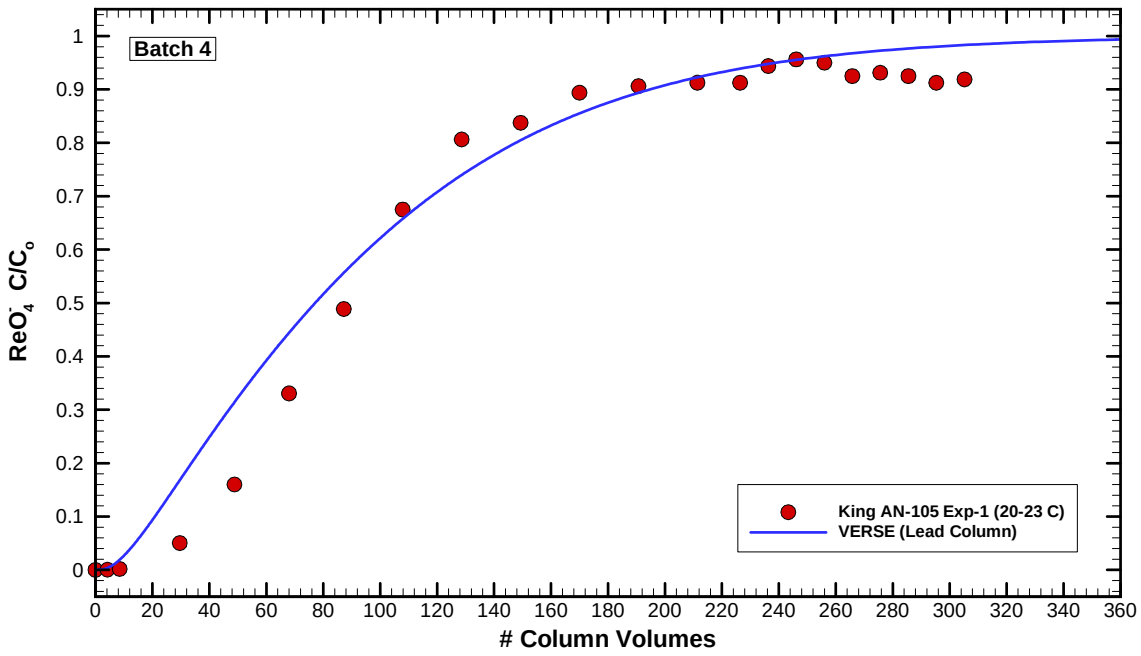

Figure 9-9. VERSE-LC perrhenate exit breakthrough curve compared to Exp-1 data from King et al. (2000a): AN-105, Batch 4, D = 2.69 cm, L = 8.99 cm, F = 3.40 CV/hr, T = 20-23°C.

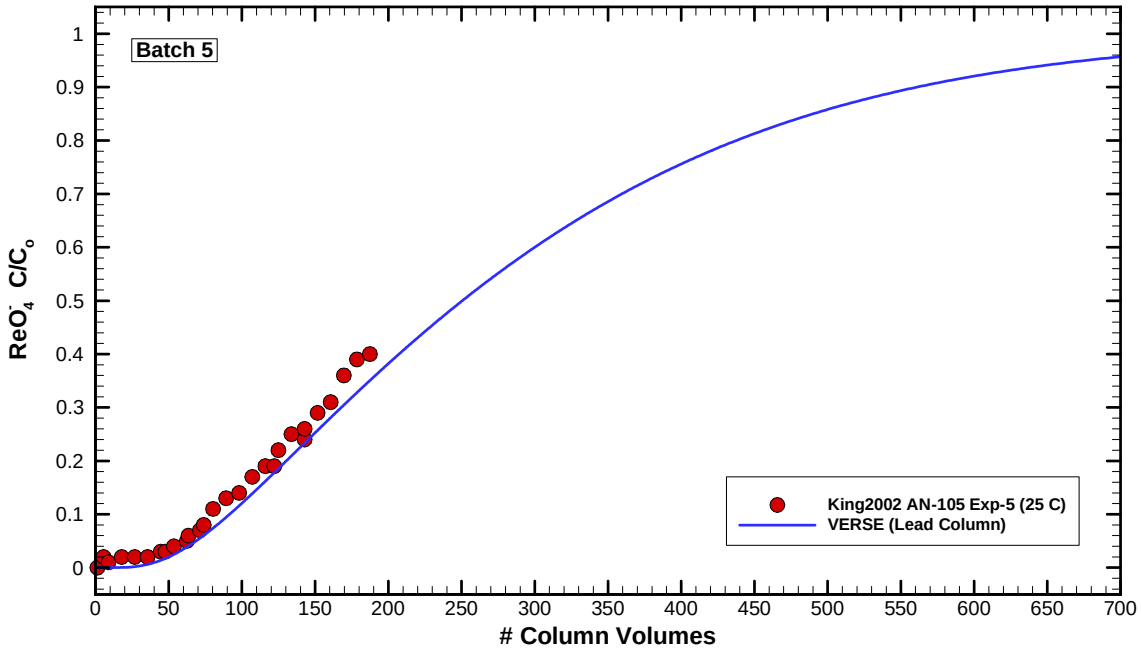

Figure 9-10. VERSE-LC perrhenate exit breakthrough curve compared to Exp-5 data from King et al. (2003): AN-105, Batch 5, D = 1.45 cm, L = 6.10 cm, F = 2.99 CV/hr, T = 25°C.

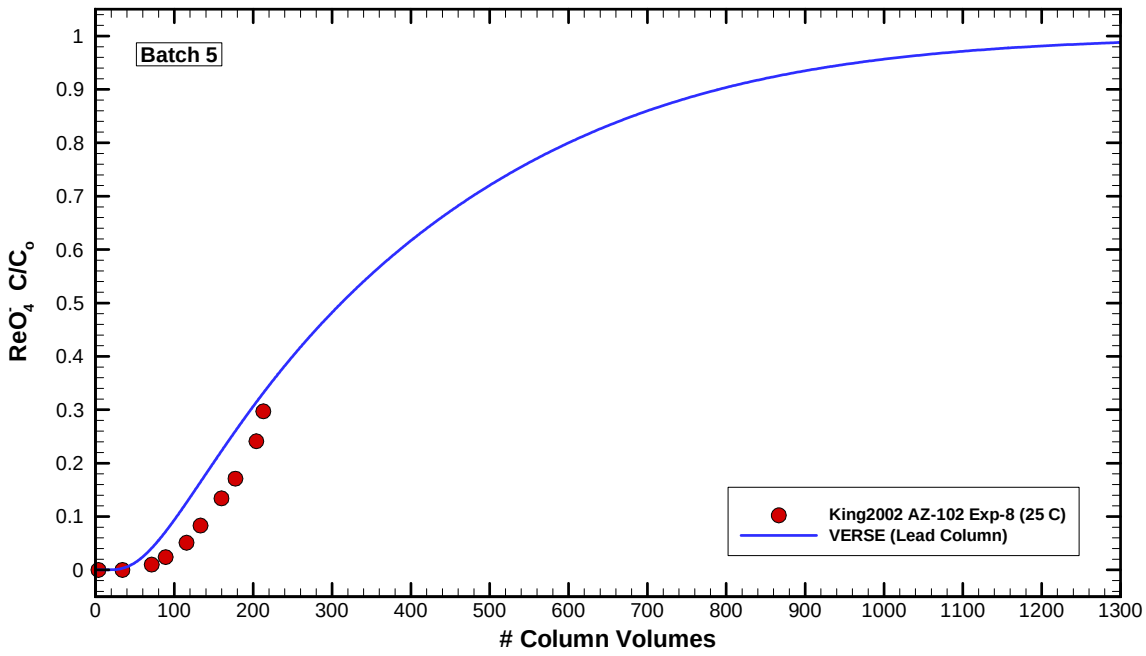

Figure 9-11. VERSE-LC perrhenate exit breakthrough curve compared to Exp-8 data from King et al. (2003): AZ-102, Batch 5, D = 2.50 cm, L = 15.19 cm, F = 2.95 CV/hr, T = 25°C.

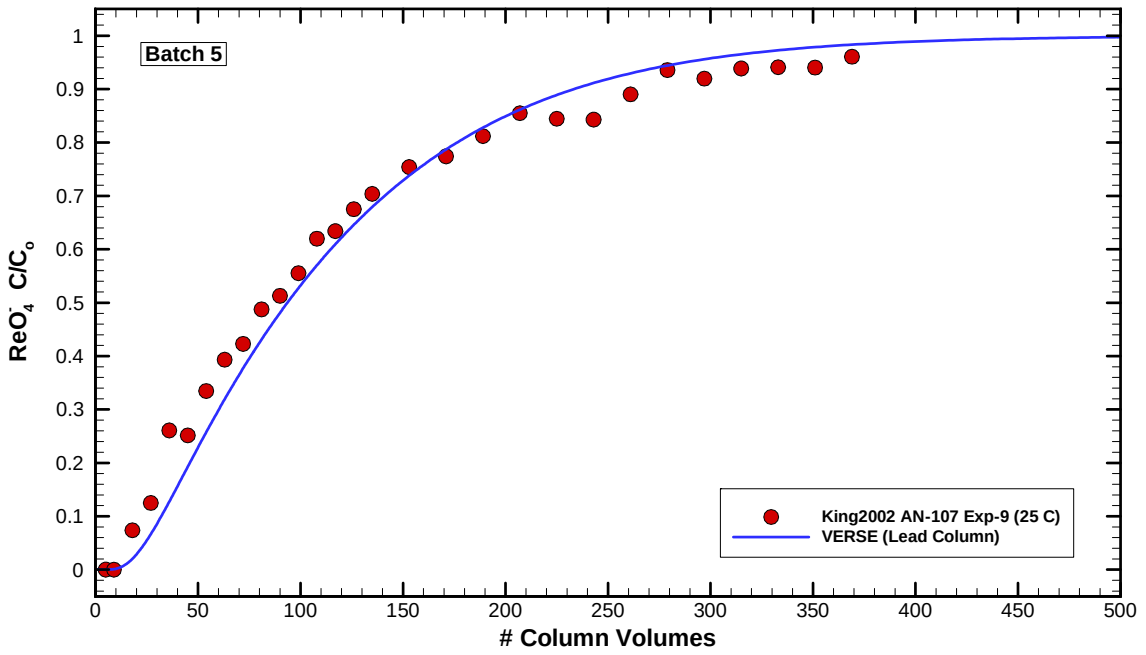

Figure 9-12. VERSE-LC perrhenate exit breakthrough curve compared to Exp-9 data from King et al. (2003): AN-107, Batch 5, D = 2.50 cm, L = 15.19 cm, F = 3.02 CV/hr, T = 25°C.

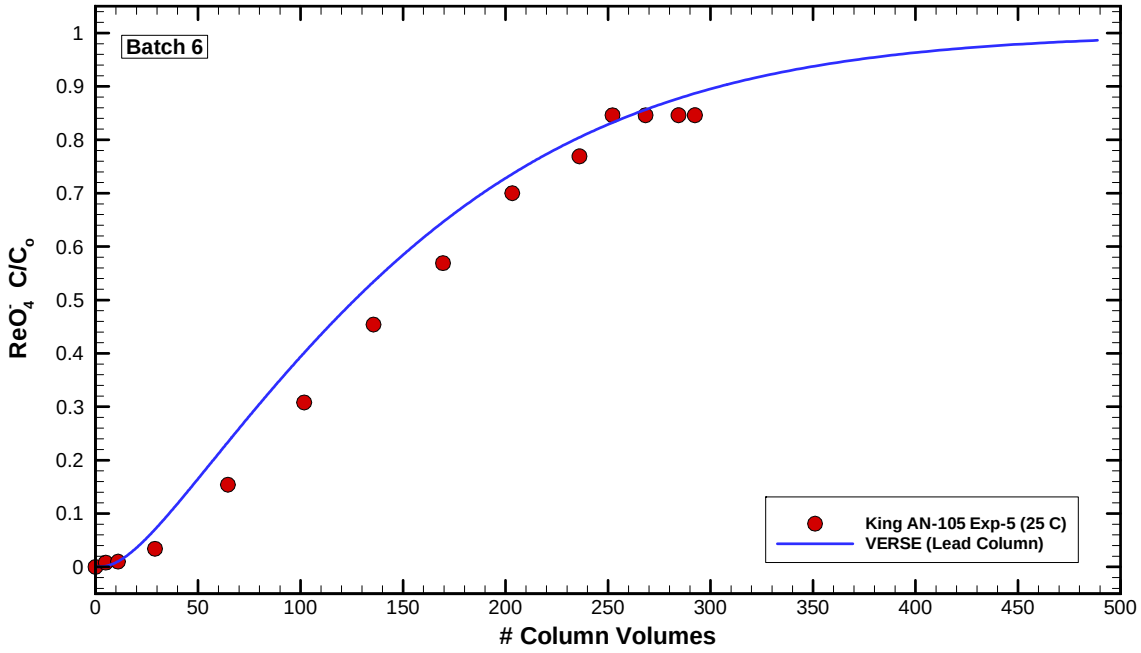

Figure 9-13. VERSE-LC perrhenate exit breakthrough curve compared to Exp-5 data from King et al. (2000a): AN-105, Batch 6, D = 2.69 cm, L = 8.80 cm, F = 2.93 CV/hr, T = 20-23°C.

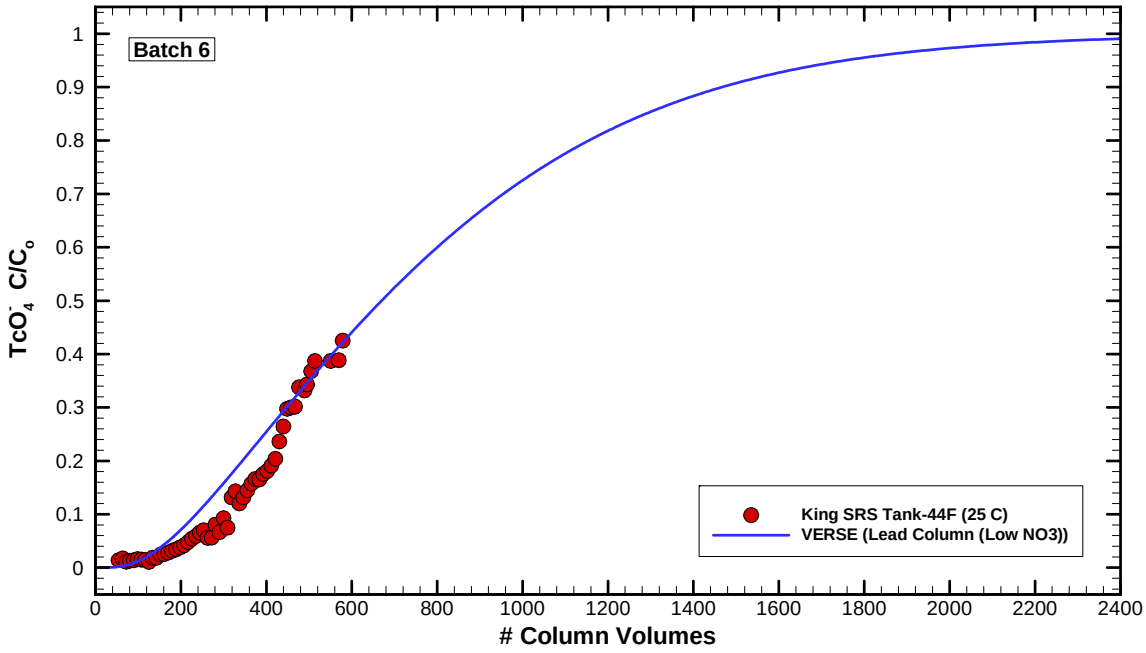

Figure 9-14. VERSE-LC pertechnetate exit breakthrough curve compared to data from King et al. (2000b): SRS Tank-44F, Batch 6, D = 2.70 cm, L = 8.75 cm, F = 3.10 CV/hr, T = 23-27°C.

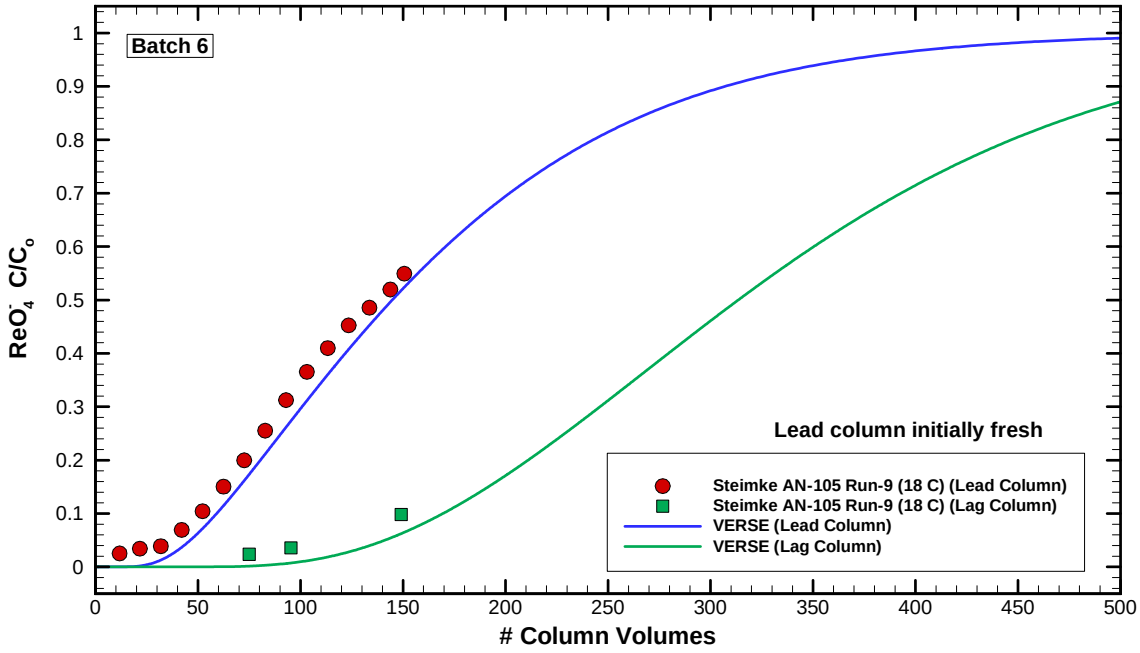

Figure 9-15. VERSE-LC perrhenate exit breakthrough curve compared to Run-9 data from Steimke et al. (2000): AN-105, Batch 6, D = 2.61 cm, L = 223.66 cm, F = 3.36 CV/hr, T = 18°C.

10.0 Full-Scale Column Modeling

The predicted performance of the proposed LAW full-scale ion-exchange facility under best estimate conditions is discussed in this section. The predictions are based on a VERSE-LC model of the lead and lag columns where the column parameter settings are consistent with the values used during the assessment of the laboratory-scale and pilot-scale column experiments and the values used in the previous assessment (Hamm et al., 2000). The chemical composition of the LAW feed was the HTWOS System Plan 6 2013 average baseline case at 5 M [Na^+] with adjustment for solubility and neutrality is shown in Table 9-2. Example VERSE-LC input and output files for one Full-Scale simulation are provided in Appendix D.

10.1 Basic Flowsheet

The key parameters defining the full-scale technetium ion-exchange column are provided in Table 10-1. The performance of two identically sized columns in series (lead and lag columns) was modeled where each column was assumed to have a void headspace that is the same volume as the column. Carousel operation was modeled starting with fresh ion-exchange resin in both columns. When the average concentration of technetium (pertechnetate) in the cumulative effluent volume (bucket average concentration) from the lag column reaches 1.0% of the feed composition, the columns are cycled with the partially loaded lag column moving into the lead position and a fresh column placed in the lag position. Starting with two fresh columns, the first ion-exchange cycle is able to process more feed volume than subsequent cycles. After the first

cycle, as the partially loaded lag columns are placed into the lead position, the ion-exchange capacity for each cycle decreases reaching essentially constant operating conditions by the third cycle. If both columns are eluted, all cycles would behave like the first cycle modeled assuming 100% elution and neglecting resin degradation.

Prior to loading, both columns are pretreated and contain an aqueous solution with an ionic strength of approximately 0.25 M sodium with essentially zero technetium and nitrate present. During the loading phase, the nitrate concentration in the feed solution increases from 0 to 1.62 M and the inlet feed concentration of technetium increases from 0 to 4.5×10^{-5} M. A design flowrate of 15 gpm or ~3.4 CV/hr was used during the technetium loading phase. Upon reaching the lag column exit concentration criterion, the technetium loading phase is terminated and for subsequent loading cycles the lag column is placed in the lead column position with a fresh column placed in the lag position. The loaded lead column is eluted and pretreated for future use. A fresh column implies an essentially technetium-free media. It is assumed that the isotopic feed concentrations on a mole basis are 100% ^{99}Tc. It is also assumed that technetium enters the lead column only in its pertechnetate form and no liquid-phase reactions either create or consume pertechnetate during its residence time within the columns.

The technetium (pertechnetate) and nitrate concentration profiles along the column train vary with time. Due to the significant selectivity for pertechnetate by SuperLig® 639 resin, the column exit breakthrough for nitrate occurs within 5-10 column volumes with the pertechnetate breakthrough significantly retarded. Key concentration points along the facility are numbered from 0 through 4 as shown in Figure 10-1. The inlet conditions correspond to point 0 while the exit product criterion is imposed at point 4. Points 1 and 3 represent the locations where the headspace ends and the active bed begins. Points 2 and 4 represent instantaneous technetium concentrations exiting the lead and lag columns. Point 5 represents the bucket average effluent concentration from the complete processing cycle. When the concentration reaches 1% at point 5, the breakthough criteria has been reached.

10.2 VERSE-LC Model of Full-Scale Facility

The VERSE-LC model representing the full-scale flowsheet is shown in Figure 10-1. To model the full-scale facility using VERSE-LC the headspaces are considered to be continuous stirred tank reactors (CSTRs). In these CSTRs perfect mixing is assumed with no chemical reactions taking place. During a VERSE-LC simulation, exit breakthrough curves at points 2 and 4 are generated along with concentration profiles over both columns at key points in time. During the loading phase, for modeling purposes, constant flow and inlet feed conditions are assumed to apply. The simulations were run out for over a total of 100 column volumes such that a repeating pattern occurs during subsequent cycling.

The first three cycles occurred as shown in Figure 10-2 by the lag-column exit breakthrough curves for technetium. The start of each cycle represents the replacement of the lead-column with the lag-column and insertion of a fully eluted (assumes complete technetium elution) and regenerated column in the lag position. For the results presented in Figure 10-2, cycle initiation occurred when the cumulative average technetium concentration exiting from the lag-column reached 1.0% of its inlet feed concentration to the lead column (only technetium in the pertechnetate form is removed). A technetium-99 activity level of 1 μCi/ml corresponds to a total technetium-99 concentration of 5.957×10^{-4} M where the radioactive half-life of 2.13×10^{5} years for ^{99}Tc is used (see Table 10-1). It is assumed that only technetium in its pertechnetate

from is present and that no liquid-phase reactions occur that create or consume pertechnetate within the timeframe of interest.

By the third cycle, a repeating pattern has been achieved and no additional cycles are necessary to demonstrate the long-term behavior of the facility. This is apparent in Table 10-2 which lists the waste volume processed during the first three cycles. A significantly larger waste volume can be processed before reaching the lag column exit criterion during the first cycle but the volume processed in subsequent cycles is relatively constant. Beyond the third cycle, all subsequent cycles processed approximately 27,000 gallons of waste solution before reaching the 1.0% cumulative average concentration in the effluent.

The breakthrough curves plotted in Figure 10-2 show a relatively gradual increase in the concentration at the lag column outlet. Using the cumulative average instead of the instantaneous concentration at the exit of the lag column to determine the cycling point allows for a significant increase in the volume of waste that can be processed. For the third cycle, which is again representative of all subsequent cycles, column cycling using a concentration at the lag column exit of 1.0% of the feed concentration as the cycling criterion would only allow processing about 17,000 gallons of waste instead of the 27,000 gallons achieved. This is almost a 60% increase in processing volume achieved through use of the cumulative average criterion.

Figure 10-3 plots technetium concentration profiles through the lead and lag columns at the end of the third cycle. At the end of the third cycle (and beyond) the lead-column overall contains, on average, (i.e., its axial average) ~74.1% of its total technetium loading capacity as shown by the technetium concentration profiles presented in Figure 10-3. The fraction of column technetium loading was estimated by integrating the predicted concentration profile over the column's axial length and dividing by column length. The mixing impact associated with the void headspace (i.e., modeled as a CSTR) between the two columns is negligible as seen in Figure 10-3 since there is essentially no break in the profile between the columns. The overall technetium loading (i.e., axial average) for the lag-column is ~17.5% for cycle number 3 and beyond.

Listings of VERSE-LC input and output files for the full-size column simulations are provided in Appendix D. To simulate two columns in series, VERSE-LC requires the total ion-exchange bed length as input. Therefore, the input column length of 450 cm represents two 225 cm long columns in series. The input column diameter is 77 cm giving a column length to diameter ratio of L/D = 2.92 and a column volume of 1.05 m^3. In addition to the output file shown in Appendix D, VERSE-LC writes out other files giving concentration time histories and column profiles as specified by the user. These files were used to generate the plots shown in Figures 10-2 and 10-3. The plot shown in Figure 10-2 required special post processing of VERSE-LC output to implement the cumulative average criterion.

For a linear adsorption isotherm the number of column volumes required to reach a given exit criterion would not vary beyond the second cycle. As shown in Table 10-2, the number of column volumes required to reach a given exit criterion varies during the first three cycles. This characteristic variation where the volume processed initially drops then rises and levels off can be explained by the variations in concentration profile over both columns during different cycles. At the end of the first cycle the highest level of concentrations within the lag-column are experienced due to its initially "technetium-free" state. Therefore, for subsequent cycles the lag-column experiences migration of technetium into its bed at the outset (due to the initial presence

of technetium loading throughout the upstream lead-column) reducing the number of column volumes required to reach the exit criterion. After a few cycles (note that the adsorption isotherm is only slightly non-linear and no more than three cycles is required) the concentration profile throughout both columns becomes repeatable (i.e., repeatable after only three cycles for the technetium-SuperLig® 639 system).

Table 10-1. Key column parameters for the full-scale facility.

Parameter	Lead/Lag column
SuperLig® 639 batch ID, (#6)	50% 981015DHC-720011 50% 990420DHC-720067
Operating Temperature, (°C)	25
Bed density[a], (g/ml)	0.5003
Total ionic exchange capacity, (mmole/g_{resin})	0.4906
Column inner diameter, (cm)	77.0
Active bed length[a], (cm)	225.0
Active column volume[a], (L)	1047.74
Headspace volume, (L)	1047.74
Bed porosity, (-)	0.357
Pore porosity, (-)	0.371
Superficial flow velocity, (cm/min)	12.2
Volumetric flow rate, (ml/min)	56,781.2
Volumetric flow rate, (CV/hr)	3.4
Feed concentrations: **Total Technetium, ^{99}Tc, [M]** **Nitrate, NO_3^-, [M]**	 4.50×10^{-5} 1.62
Column feed non-pertechnetate fraction, (%)[b]	0%
Column exit ^{99}Tc bucket average concentration criterion[c], (%, {µCi/ml}, and [M])	1.0% of feed $\{7.55 \times 10^{-4}\}$ $[4.50 \times 10^{-7}]$

[a] Slight swelling due to feed ionic strength variations can alter the original bed geometry and the numbers provided assume the bed's approximate size during ~5 M [Na^+] loading conditions. Bed density is based on the average measured value for resin Batch 6 as shown in Table 9-1.

[b] The model assumes that non-pertechnetate Tc does not adsorb onto SL-639 and does not impact performance of the resin.

[c] An isotopic mixture on a mole basis of 100% ^{99}Tc is assumed, where the conversion factor 1 µCi/ml equals 5.957×10^{-4} M of ^{99}Tc is used. A radioactive half-life of 2.13×10^5 years for ^{99}Tc is used taken from GE Nuclear Energy (1996).

Table 10-2. Estimated waste volume processed and column loading times during first three ion-exchange cycles.

Cycle	Volume Processed (1000 gal)	Column Loading Time (Days)
1	35.4	1.64
2	25.3	1.17
3	27.2	1.26
Total	87.9	4.07

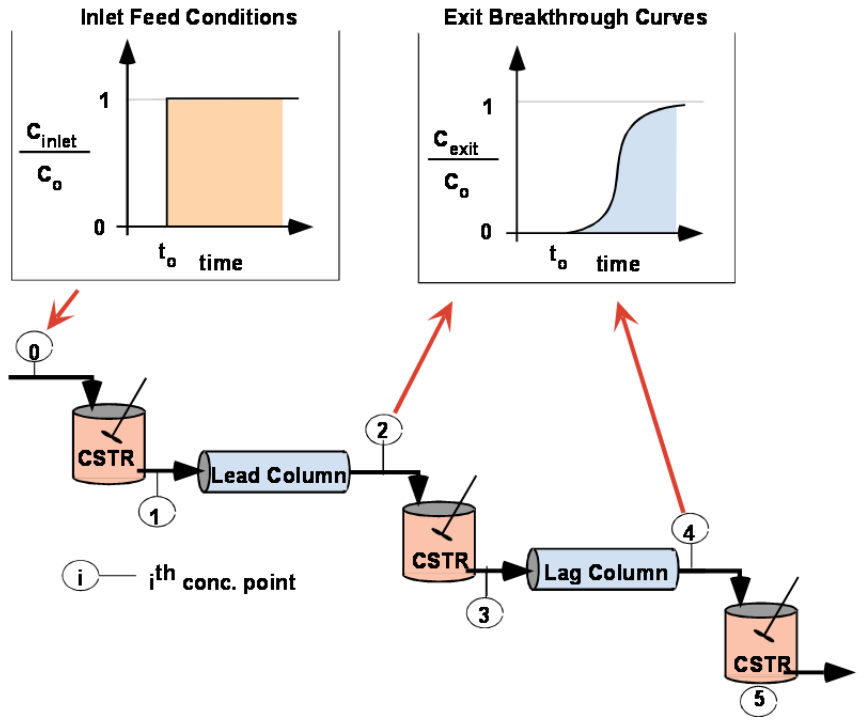

Figure 10-1. VERSE-LC model representing the full-scale flowsheet for removal of technetium (in the pertechnetate form) using SuperLig® 639 resin.

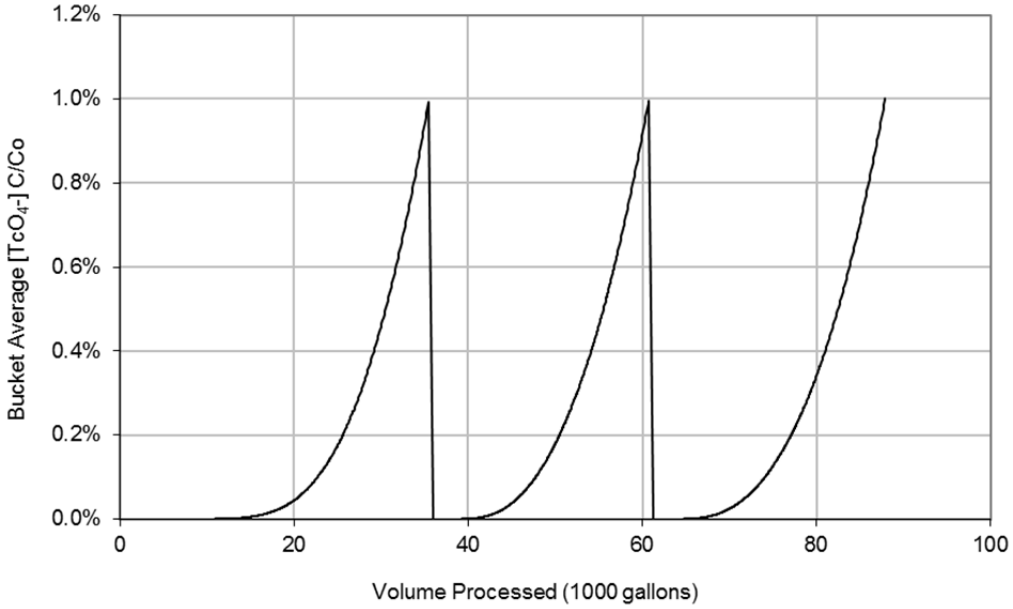

Figure 10-2. VERSE-LC model best estimate predictions for multiple cycling of the full-scale facility for technetium (pertechnetate) removal from LAW using the SuperLig® 639 resin.

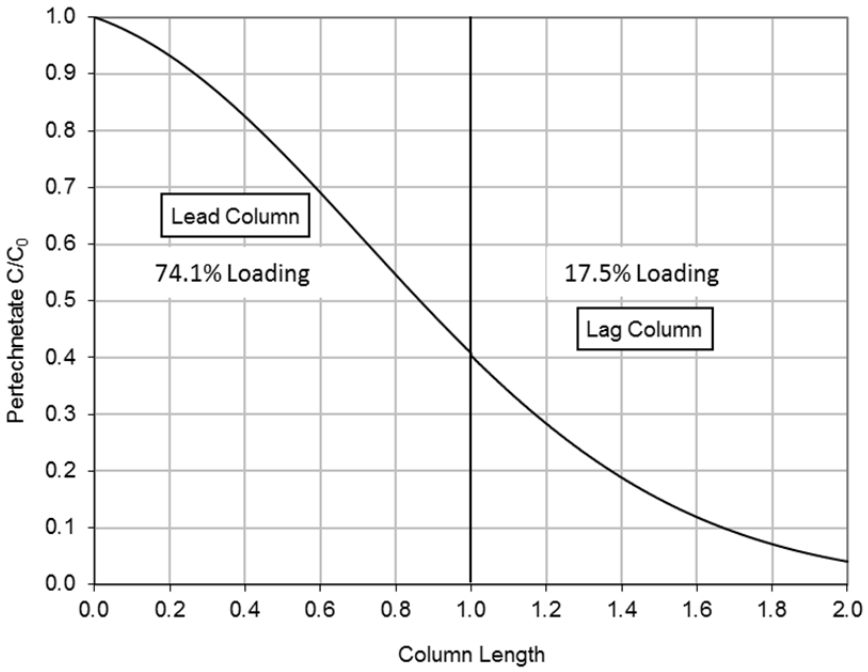

Figure 10-3. VERSE-LC model best estimate prediction of column loading profiles for cycle three of the full-scale facility for technetium (pertechnetate) removal from LAW using the SuperLig® 639 resin.

11.0 Conclusion

This report documents the development and application of computer models to describe the sorption of pertechnetate [TcO_4^-], and its surrogate perrhenate [ReO_4^-], on SuperLig® 639 resin. Two models were developed:

1) A thermodynamic isotherm model, based on experimental data, that predicts [TcO_4^-] and [ReO_4^-] sorption as a function of solution composition. The isotherm model provides a synthesis of experimental data collected from 17 studies to give a best estimate prediction of the behavior of the pertechnetate-SuperLig® 639 system. The model that best predicted the experimental data assumed sorption of neutral species $NaTcO_4$ and $KTcO_4$ on the resin instead of a true ion-exchange system. The current model was limited to predicting system behavior at 25 °C. The model is able to predict sorption behavior over a range of solution compositions and ionic strength.

2) A VERSE-LC column model that uses the isotherm calculated by the thermodynamic model to simulate the performance of a full-scale sorption process. The column model provides a prediction of the expected performance of the plant process by determining the volume of waste solution that can be processed based on design parameters such as column size, flow rate and resin physical properties. The model predicts that a typical lead/lag column cycle using two columns with volumes of one cubic meter and length to diameter ratios of 3:1 is able to process approximately 27,000 gallons of waste (102 bed volumes) when operating at 25 °C. A cycle is terminated when the cumulative average concentration of pertechnetate in the effluent collected from the lag column reaches 1% of the concentration in the feed stream (i.e, a decontamination factor of 100). The column model was validated against twelve column experiments and model predictions closely followed the experimental results.

Other results obtained from this study include:

- The average estimated value for the total sorption capacity for pertechnetate from the five different batches of SL-639 analyzed in this report is ~0.58 mmole [TcO_4^-]/g_{resin}. Sorption capacity varied from 0.30 to 0.96 mmole [TcO_4^-]/g_{resin} for these batches.
- The prediction of overall performance for the Full-Scale column is lower in this report than was estimated in the 2000 Report. The reduced performance is not the result of the newer analysis but is caused by differences between the original projected LAW composition and the current projected composition due to the inclusion of additional waste tanks. The feed compositions used in the 2000 Report (Envelope-A and Envelope-B feeds) had higher K+ (enhancer effect) and Na+ (ionic strength effect) concentrations along with lower NO_3^- (competitor effect) concentrations than the HTWOS System Plan 6 (Certa et al., 2011) average 5 M feed composition employed in this report.
- The modeling study is based on pertechnetate removal data as presented in the experimental studies and assumes that technetium in the non-pertechnetate form does not adsorb onto the SL-639 resin. The calculational strategy presented in the 2000 Report was reviewed and was found to be functionally correct and its implementation consistent. Experimental data shows that the fraction of technetium in the non-pertechnetate form varies widely in samples of actual waste.

12.0 References

Anderson, T. F., D. S. Abrams, and E. A. Grens, II, 1978. "Evaluation of Parameters for Nonlinear Thermodynamic Models," AIChE Journal, Vol. 24, No. 1, pp. 20-29.

Bromley, L. A., 1973. "Thermodynamic Properties of Strong Electrolytes in Aqueous Solutions," AIChE Journal, Vol. 19, No. 2, pp. 313-320.

Certa, P. J., P. A. Empey, and M. N. Wells, 2011. *River Protection Project System Plan*. ORP-11242, Revision 6, Washington River Protection Solutions, LLC, Richland, Washington.

Chung, S. F. and C. Y. Wen, 1968. "Longitudinal Dispersion of Liquid Flowing Through Fixed and Fluidized Beds," AIChE Journal, Vol. 14, No. 6, pp. 857-866.

GE Nuclear Energy, 1996. Nuclides and Isotopes, General Electric Company, Nuclear Energy Operations, 15th Edition, pp.31.

Hamm, L.L., F. G. Smith, and McCabe, D.J., 2000, Preliminary Ion Exchange Modeling for Removal of Technetium from Hanford Waste Using SuperLig 639 Resin, WSRC-TR-2000-00305, SRT-RPP-2000-00011, August.

Hassan, N. M. and D. J. McCabe, 1998. "Hanford Envelope C (hydroxide-adjusted) Tank Waste Batch Distribution Coefficient Study (U)," SRTC-BNFL-027, Rev. 0, January 19.

Hassan, N. M., W. D. King, and D. J. McCabe, 1999a. "SuperLig® Ion Exchange Resin Swelling and Buoyancy Study (U)," BNF-003-98-0051, March 25.

Hassan, N. M., D. A. Kaplan, and D. J. McCabe, 2000c. "Mixing of Process Heels, Process Solutions, and Recycle Streams: Small-Scale Active Tests," BNF-003-98-0246.

Helfferich, 1962. Ion Exchange, McGraw-Hill series in advanced chemistry, McGraw-Hill Book Company, Inc., New York.

Icenhower, J.P., Qafoku, N.P., Martin, W.J., Zachara, J.M., 2008, The Geochemistry of Technetium: A Summary of the Behavior of an Artificial Element in the Natural Environment, PNNL-18139, December.

Icenhower, J.P., Qafoku, N.P., Martin, W.J., Zachara, J.M., 2010, The Biogeochemistry of Technetium: A review of the behavior of an Element in the Natural Environment, October.

McCabe, D. J., 1997. "Hanford Envelope B Tank Waste Ion Exchange Distribution Coefficient Study (U)," SRTC-BNFL-014, Rev. 0, August 15.

McCabe, D. J. and Hamm, L. L., 2012, "Task Technical and Quality Assurance Plan for Technetium Ion Exchange Computer Modeling Update," SRNL-RP-2012-00707, Savannah River National Laboratory, Aiken, SC, October.

Whitley, R. D. and L. N.-H. Wang, 1996. "User's Manual VERSE (VErsatile Reaction SEparation) Simulation for Liquid Phase Adsorption and Chromatography Processes," Purdue University.

Wilson, E. J. and C. J. Geankoplis, 1966. "Liquid Mass Transfer at Very Low Reynolds Numbers in Packed Beds," Industrial and Engineering Chemistry Fundamentals, Vol. 5, No. 1, pp. 9-14.

Zheng, Z., D. Gu, and R. G. Anthony, 1995. "Estimation of Cesium Ion Exchange Distribution Coefficients for Concentrated Electrolytic Solutions When Using Crystalline Silicotitanates," Ind. Eng. Chem. Res., Vol. 34, No. 6, pp. 2142-2147.

Mann, F.M., Puigh, R.J., Khaleel, R., Finfrock, S., McGrail, B.P., Bacon, D.H., Serne, R.J., 2003, Risk Assessment Supporting the Decision on the Initial Selection of Supplemental ILAW Technologies, RPP-17675, Rev. 0, September 29.

12.1 Experimental Data Sources

12.1.1 Data Sources Used in 2000 Preliminary Study and Included in Current Study

Hassan, N. M., D. J. McCabe and W. D. King, 2000a, "Small-Scale Ion Exchange Removal of Cesium and Technetium from Hanford Tank 241-AN-103," BNF-003-98-0146, Rev. 1, April 12.

Hassan, N. M., D. J. McCabe, W. D. King and M. L. Crowder, 2000b, "Small-Scale Ion Exchange Removal of Cesium and Technetium from Hanford Tank 241-AN-102," BNF-003-98-0219, Rev. 0, March 29.

Hassan, N. M., D. J. McCabe, W. D. King and M. L. Crowder, 2000c, "Small-Scale Ion Exchange Removal of Cesium and Technetium from Envelope B Hanford Tank 241-AZ-102," WSRC-TR-2000-00419 (SRT-RPP-2000-00036), Rev. 0, October 17.

King, W. D., D. J. McCabe and N. M. Hassan, 2000a, "Evaluation of SuperLig® 639 Ion Exchange Resin for the Removal of Rhenium from Hanford Envelope A Simulant," BNF-003-98-0140, Rev. 0, April 13.

King, W. D., D. J. McCabe, N. M. Hassan and D. D. Walker, 2000b, "Intermediate-Scale Ion Exchange Removal of Technetium from Savannah River Site Tank 44F Supernate Solution," BNF-003-98-0230, Rev. 0, May 23.

King, W. D., D. J. McCabe and N. M. Hassan, 2000c, "Intermediate-Scale Ion Exchange Removal of Cesium and Technetium from Hanford Tank 241-AN-102", WSRC-TR-2000-00420 (SRT-RPP-2000-00014), Rev. 0, October 17.

King, W. D., D. J. McCabe and N. M. Hassan, 2001, "Intermediate-Scale Ion Exchange Removal of Cesium and Technetium from Hanford Tank 241-AN-102", WSRC-TR-2000-00420 (SRT-RPP-2000-00014), Rev. 1, August 6.

Kurath, D. E., D. L. Blanchard and J. R. Bontha, 1999, "Ion Exchange Distribution Coefficients for ^{137}Cs and ^{99}Tc removal from Hanford Tank Supernatants AW-101 (Envelope A) and AN-107 (Envelope C)," PNWD/BNFL-RPT-009, Rev. 0, Project 29953, Battelle (PNNL), June.

Steimke, J. L., M. A. Norato, T. J. Steeper and D. J. McCabe, 2000, "Summary of Testing of SuperLig® 639 at the TFL Ion Exchange Facility," WSRC-TR-2000-00302 (SRT-RPP-2000-00008), Rev. 0, August 24.

12.1.2 Data Sources Added in Current Study

Blanchard, D. L., D. E. Kurath and J. R. Bontha, 2000a, "Small Column Testing of SuperLiq® 639 for Removing ^{99}Tc from Hanford Tank Waste Envelope A (Tank 241-AW-101)," PNWD-3004 (BNFL-RPT-016), Rev. 0, August.

Blanchard, D. L., D. E. Kurath and B. M. Rapko, 2000b, "Small Column Testing of SuperLiq® 639 for Removing ^{99}Tc from Hanford Tank Waste Envelope C (Tank 241-AN-107)," PNWD-3028 (BNFL-RPT-022), Rev. 0, June.

Burgeson, I. E., D. L. Blanchard and J. R. Deschane, 2002, "Small Column Testing of SuperLiq® 639 for Removing ^{99}Tc from Hanford Tank Waste Envelope A (Tank 241-AP-101)," PNWD-3222 (WTP-RPT-030), Rev. 0, December.

Burgeson, I. E., D. L. Blanchard and J. R. Deschane, 2003a, "Small Column Testing of SuperLiq® 639 for Removing ^{99}Tc from Hanford Tank Waste 241-AN-102 Supernate (Envelope C) Mixed with Tank 241-C-104 Solids (Envelope D) Wash and Permeate Solutions," PNWD-3252 (WTP-RPT-031), Rev. 0, March.

Burgeson, I. E., D. L. Blanchard and J. R. Deschane, 2003b, "Small Column Testing of SuperLiq® 639 for Removing ^{99}Tc from Hanford Tank Waste Envelope B (Tank 241-AZ-101)," PNWD-3281 (WTP-RPT-058), Rev. 0, January.

Burgeson, I. E., D. L. Blanchard and J. R. Deschane, 2004, "Small Column Testing of SuperLiq® 639 for Removing ^{99}Tc from Hanford Tank Waste Envelope B (Tank 241-AZ-101)," PNWD-3281 (WTP-RPT-058), Rev. 1, March.

Duffey, C. E., W. D. King and L. L. Hamm, 2003, "Determination of Perrhenate (ReO_4^-) Adsorption Kinetics from Hanford Waste Simulants using SuperLig® 639 Resin (U)," WSRC-TR-2002-00548 (SRT-RPP-2002-00272), Rev. 0, April.

Hassan, N. M., K. Adu-Wusu and C. A. Nash, 2003, "Multiple Ion Exchange Column Runs for Cesium and Technetium Removal from AW-101 Waste Sample (U)," WSRC-TR-2003-00098 (SRT-RPP-2003-00026), Rev. 0, July.

King, W. D., W. A. Spencer and M. P. Bussey, 2003, "Laboratory-Scale SuperLig® 639 Column Tests with Hanford Waste Simulants (U)", WSRC-TR-2002-00580 (SRT-RPP-2002-00266), Rev. 0, May.

Rapko, B. M., D. L. Blanchard and K. J. Carson, 2003, "Equilibrium Batch Contact Testing of SuperLig® 639," PNWD-3251 (WTP-RPT-026), Rev. 0, March.

13.0 Appendix A (Equilibrium Batch Test Database)

As stated in Appendix A of the 2000 Report:

> "There are future plans to measure the adsorption characteristics of SuperLig® 639 resin in contact with simple binary ionic mixtures. Also future tests are planned to measure the total ionic capacity of the resin under varying conditions."

Testing beyond the 2000 Report included batch contact tests and column loading/elution studies.

The majority of new batch contact tests were performed by Rapko et al. (2003) where a significant amount of their tests were performed using simple ionic mixtures. All tests were taken at 25.8 C. A brief breakdown on those batch contact tests are:

For ReO_4^- tests:

- 2 simple simulants
- 6 AN-105 simulants

For TcO4- tests:

- 4 simple simulants
- 28 AN-105 simulants

A total of 40 batch contact tests were performed. The simple simulants ranged over a wide range of conditions:

- Na^+ (0.03 to 5.31 M)
- K^+ (0.00 to 0.00 M) (no enhancer effects tested)
- NO_2^- (0.00 to 1.21 M)
- NO_3^- (0.00 to 1.80 M) (modest amount of comptetitor effects tested)
- OH^- (0.01 to 4.90 M)
- TcO_4^- ($1.34x10^{-4}$ to $1.36x10^{-3}$ M)
- ReO_4^- ($3.11x10^{-7}$ to $9.56x10^{-4}$ M)

No testing was performed to measure total sorption capacity or "simple" binary contact tests. This total sorption capacity parameter is an important parameter that should be included in future testing plans. Better confidence can be obtained for thermodynamic constants when"simple" binary contact tests are considered; however, the above tests provide a significant improvement for parameter estimations.

13.1 Equilibrium Batch Contact Test Database

Batch contact test data was taken from the 2000 Report and additional data created post 2000 Report was included. A brief summary of the batch contact database is provided in Tables A-1 through A-7 where only those key parameters of interest are listed. The database is arranged by the first (lead) author of each technical report reviewed:

- King (22 Re tests and 2 Tc tests) (see Table A-1)
- Duffey (9 Re tests) (see Table A-2)
- Rapko (8 Re tests and 32 Tc tests) (see Table A-3)

- Hassan (25 Tc tests) (see Table A-4)
- Burgeson (22 Tc tests) (see Table A-5)
- Blanchard (12 Tc tests) (see Table A-6)
- Kurath (15 Tc tests) (see Table A-7)

A total of 147 batch contact tests constitute the database with an additional 12 isotherm points obtained from key column experiments. From this total database of 159 data points, 9 batch contact tests were later excluded from the database due to potential conflicts (outliers) during the optimization process. The 9 outliers are shaded in orange.

13.2 CERMOD Optimization Results

A listing of the CERMOD parameter estimation output results are provided in Table A-8. A detailed discussion of these results is provided in Section 4 of the mainbody.

Table A-1. Batch contact data taken from reports with King as the lead author.

Simulant	Test ID	XO_4^-	Batch ID	K^+ [M]	Na^+ [M]	NO_2^- [M]	NO_3^- [M]	OH^- [M]	XO_4^- [M]	Vol (ml)	Resin (g)	F factor (-)	T (C)	Final XO_4^- [M]	Loading (mmol/g)
AN-105	BNF-SSIX-10-1	Re	1	0.09	4.993	1.13	1.25	1.7914	3.7380E-05	17.88	0.1809	0.986	20	7.4962E-06	2.9956E-03
AN-105	BNF-SSIX-10-1-D	Re	1	0.09	4.993	1.13	1.25	1.7914	3.7380E-05	17.74	0.1801	0.986	20	7.6251E-06	2.9725E-03
AN-105	BNF-SSIX-10-2	Re	1	0.09	4.993	1.13	1.25	1.7910	3.9088E-04	17.76	0.1827	0.986	20	8.6568E-05	3.0002E-02
AN-105	BNF-SSIX-10-2-D	Re	1	0.09	4.993	1.13	1.25	1.7910	3.9088E-04	17.73	0.1816	0.986	20	8.8942E-05	2.9897E-02
AN-105	BNF-SSIX-10-3	Re	1	0.09	4.987	1.13	1.244	1.7914	7.4960E-06	14.63	0.1499	0.986	19	1.4135E-06	6.0207E-04
AN-105	BNF-SSIX-10-3-D	Re	1	0.09	4.9869	1.13	1.2439	1.7914	7.6250E-06	14.3	0.1503	0.986	19	1.4132E-06	5.9941E-04
AN-105	BNF-SSIX-10-5	Re	1	0.09	4.9809	1.13	1.2379	1.7914	1.4140E-06	11.32	0.1113	0.986	20	3.0075E-07	1.1483E-04
AN-105	BNF-SSIX-10-5-D	Re	1	0.09	4.9806	1.13	1.2376	1.7914	1.4130E-06	10.6	0.1184	0.986	20	3.0612E-07	1.0050E-04
AN-105	BNF-SSIX-17-1	Re	4	0.09	4.993	1.13	1.25	1.7913	7.5140E-05	11.96	0.1203	0.986	22	1.9441E-05	5.6161E-03
AN-105	BNF-SSIX-17-1-D	Re	4	0.09	4.993	1.13	1.25	1.7913	7.5140E-05	11.98	0.1213	0.986	22	1.6805E-05	5.8432E-03
AN-105	BNF-SSIX-17-2	Re	4	0.09	4.993	1.13	1.25	1.7910	3.7150E-04	11.95	0.1198	0.986	22	1.3187E-04	2.4242E-02
AN-105	BNF-SSIX-17-2-D	Re	4	0.09	4.993	1.13	1.25	1.7910	3.7150E-04	11.96	0.1202	0.986	22	1.3250E-04	2.4118E-02
AN-105	BNF-SSIX-17-3	Re	4	0.09	4.993	1.13	1.25	1.7906	8.1940E-04	11.96	0.1205	0.986	22	3.3295E-04	4.8967E-02
AN-105	BNF-SSIX-17-3-D	Re	4	0.09	4.993	1.13	1.25	1.7906	8.1940E-04	11.96	0.1206	0.986	22	3.4110E-04	4.8107E-02
AN-105	BNF-SSIX-17-4	Re	4	0.09	4.993	1.13	1.25	1.7902	1.1960E-03	11.96	0.1199	0.986	22	5.4796E-04	6.5560E-02
AN-105	BNF-SSIX-17-4-D	Re	4	0.09	4.993	1.13	1.25	1.7902	1.1960E-03	11.97	0.1205	0.986	22	5.5430E-04	6.4649E-02
AN-105	BNF-SSIX-17-5	Re	4	0.09	4.993	1.13	1.25	1.7914	3.8560E-05	17.9	0.1803	0.986	22	1.2728E-05	2.6010E-03
AN-105	BNF-SSIX-17-5-D	Re	4	0.09	4.993	1.13	1.25	1.7914	3.8560E-05	17.91	0.1803	0.986	22	1.2997E-05	2.5754E-03
AN-105	BNF-SSIX-17-6	Re	2	0.09	4.993	1.13	1.25	1.7914	3.8560E-05	17.93	0.1833	0.987	22	6.0150E-06	3.2254E-03
AN-105	BNF-SSIX-17-6-D	Re	2	0.09	4.993	1.13	1.25	1.7914	3.8560E-05	17.9	0.1832	0.987	22	6.3910E-06	3.1846E-03
AN-105	BNF-SSIX-17-7	Re	4	0.09	4.987	1.13	1.244	1.7914	1.2728E-05	15.65	0.1587	0.986	22	4.2320E-06	8.4972E-04
AN-105	BNF-SSIX-17-7-D	Re	4	0.09	4.987	1.13	1.244	1.7914	1.2997E-05	15.37	0.1573	0.986	22	4.0387E-06	8.8776E-04
Tank 44	SRS-1	Tc	1	0.057	5.4	0.476	0.495	4.1727	0.00003061	13.283	0.1217	0.987	22	2.6856E-06	3.0880E-03
Tank 44	SRS-1-D	Tc	1	0.057	5.4	0.476	0.495	4.1727	0.00003061	13.517	0.1201	0.987	22	2.6681E-06	3.1862E-03

Table A-2. Batch contact data taken from reports with Duffey as the lead author.

Simulant	Test ID	XO_4^-	Batch ID	K^+ [M]	Na^+ [M]	NO_2^- [M]	NO_3^- [M]	OH^- [M]	XO_4^- [M]	Vol (ml)	Resin (g)	F factor (-)	T (C)	Final XO_4^- [M]	Loading (mmol/g)
AN-105	Exp-1	Re	5	0.09	5	1.096	1.077	1.9659	7.4600E-05	120	0.580	1	23.8	2.1200E-05	1.1043E-02
AN-105	Exp-2	Re	5	0.09	5	1.096	1.077	1.9659	7.7300E-05	120	0.583	1	24.7	2.2200E-05	1.1334E-02
AN-105	Exp-05	Re	5	0.09	5	1.096	1.077	1.9659	7.8400E-05	120	0.598	1	24.9	2.5000E-05	1.0718E-02
AN-105	Exp-06	Re	5	0.09	5	1.096	1.077	1.9659	7.3600E-05	120	0.595	1	25	2.2600E-05	1.0286E-02
AN-105	Exp-07	Re	5	0.09	5	1.096	1.077	1.9659	7.3600E-05	120	0.589	1	24.8	2.1700E-05	1.0576E-02
AN-105	Exp-08	Re	5	0.09	5	1.096	1.077	1.9659	7.7900E-05	120	0.580	1	25.2	2.2700E-05	1.1419E-02
AN-105	Exp-09	Re	5	0.09	5	1.096	1.077	1.9659	7.8900E-05	120	0.579	1	25.2	2.3600E-05	1.1465E-02
AZ-102	Exp-10	Re	5	0.153	5	1.137	0.442	0.7601	2.1300E-04	120	0.593	1	24.7	3.4600E-05	3.6089E-02
AN-107	Exp-11	Re	5	0.027	5	0.780	2.209	0.0054	3.5800E-05	120	0.593	1	24.7	1.5200E-05	4.1672E-03
AN-105	Exp-03	Re	5	0.09	5	1.096	1.077	1.9659	7.7300E-05	120	0.5836	1	33.3	2.8600E-05	1.0014E-02
AN-105	Exp-04	Re	5	0.09	5	1.096	1.077	1.9659	7.8400E-05	120	0.5821	1	45.2	3.9600E-05	7.9986E-03

Table A-3. Batch contact data taken from reports with Rapko as the lead author. All new data since 2000 Report. Shaded data not employed in optimization process.

Simulant	Test ID	XO_4^-	Batch ID	K^+ [M]	Na^+ [M]	NO_2^- [M]	NO_3^- [M]	OH^- [M]	XO_4^- [M]	Vol (ml)	Resin (g)	F factor (-)	T (C)	Final XO_4^- [M]	Loading (mmol/g)
AN-105	D-6a	Re	3	0.0951	5.3053	1.21	1.3269	1.72	9.4520E-04	10	0.1059	0.7643	25.8	2.3201E-04	8.8120E-02
AN-105	D-6b	Re	3	0.0951	5.3051	1.21	1.3269	1.72	7.9480E-04	10	0.1066	0.7643	25.8	2.1106E-04	7.1651E-02
AN-105	D-8a	Re	3	0.0951	5.3043	1.21	1.3269	1.72	9.4520E-06	10	0.1179	0.7643	25.8	1.7454E-06	8.5529E-04
AN-105	D-8b	Re	3	0.0951	5.3044	1.21	1.3269	1.72	1.0150E-05	10	0.1054	0.7643	25.8	1.9495E-06	1.0180E-03
AN-105	D-9a	Re	3	0.0951	5.3043	1.21	1.3269	1.72	3.1100E-07	10	0.1051	0.7643	25.8	6.4447E-08	3.0695E-05
AN-105	D-9b	Re	3	0.0951	5.3043	1.21	1.3269	1.72	3.1800E-07	10	0.0974	0.7643	25.8	7.0892E-08	3.3197E-05
5.0/1.8 M Simple	D-10a	Re	3	0	5.001	0	1.8	0.1	9.5600E-04	10	0.0941	0.7643	25.8	3.3781E-04	8.5960E-02
5.0/1.8 M Simple	D-10b	Re	3	0	5.001	0	1.8	0.1	9.0230E-04	10	0.1021	0.7643	25.8	3.0505E-04	7.6541E-02
5.018/4.9 M Simple	B-1a	Tc	3	0	5.018	0	0.018	0.1	3.9870E-04	10	0.1186	0.7643	25.8	1.4150E-05	4.2426E-02
5.018/4.9 M Simple	B-1b	Tc	3	0	5.018	0	0.018	0.1	3.9940E-04	10	0.0988	0.7643	25.8	1.6217E-05	5.0747E-02
5.018/4.0 M Simple	B-2a	Tc	3	0	5.018	0	0.018	1	3.8670E-04	10	0.0994	0.7643	25.8	1.6487E-05	4.8734E-02
5.018/4.0 M Simple	B-2b	Tc	3	0	5.018	0	0.018	1	3.9810E-04	10	0.1142	0.7643	25.8	1.4825E-05	4.3915E-02
5.018/2.5 M Simple	B-3a	Tc	3	0	5.018	0	0.018	2.5	3.9185E-04	10	0.0992	0.7643	25.8	1.7365E-05	4.9395E-02
5.018/2.5 M Simple	B-3b	Tc	3	0	5.018	0	0.018	2.5	4.0200E-04	10	0.104	0.7643	25.8	1.8239E-05	4.8283E-02
5.018/1.0 M Simple	B-4a	Tc	3	0	5.018	0	0.018	4	3.9173E-04	10	0.1021	0.7643	25.8	1.9046E-05	4.7762E-02
5.018/1.0 M Simple	B-4b	Tc	3	0	5.018	0	0.018	4	3.9880E-04	10	0.1127	0.7643	25.8	1.7409E-05	4.4280E-02
5.018/0.1 M Simple	B-5a	Tc	3	0	5.018	0	0.018	4.9	3.9660E-04	10	0.1158	0.7643	25.8	2.3235E-05	4.2188E-02
5.018/0.1 M Simple	B-5b	Tc	3	0	5.018	0	0.018	4.9	4.0970E-04	10	0.1053	0.7643	25.8	2.8662E-05	4.7348E-02
5.0/0.0018 M Simple	D-1a	Tc	3	0	5.0018	0	0.0018	0.1	1.3370E-03	10	0.1125	0.7643	25.8	6.6527E-05	1.4777E-01
5.0/0.0018 M Simple	D-1b	Tc	3	0	5.0018	0	0.0018	0.1	1.3370E-03	10	0.1066	0.7643	25.8	6.9291E-05	1.5561E-01
5.0/0.18 M Simple	D-2a	Tc	3	0	4.98	0	0.18	0.1	1.3070E-03	10	0.1058	0.7643	25.8	7.7100E-05	1.5211E-01
5.0/0.18 M Simple	D-2b	Tc	3	0	4.98	0	0.18	0.1	1.3630E-03	10	0.1062	0.7643	25.8	7.5483E-05	1.5863E-01
5.0/1.8 M Simple	D-3a	Tc	3	0	5	0	1.8	0.1	1.3340E-03	10	0.1069	0.7643	25.8	2.1069E-04	1.3749E-01
5.0/1.8 M Simple	D-3b	Tc	3	0	5	0	1.8	0.1	1.3340E-03	10	0.0974	0.7643	25.8	2.2493E-04	1.4899E-01
5.0/1.8 M Simple	D-4a	Tc	3	0	5	0	1.8	0.1	1.4040E-04	10	0.1093	0.7643	25.8	1.5945E-05	1.4899E-02
5.0/1.8 M Simple	D-4b	Tc	3	0	5	0	1.8	0.1	1.3720E-04	10	0.1015	0.7643	25.8	1.7185E-05	1.5472E-02
AN-105	D-5a	Tc	3	0.0951	5.3043	1.21	1.3269	1.72	1.3230E-03	10	0.1183	0.7643	25.8	1.1462E-04	1.3365E-01
AN-105	D-5b	Tc	3	0.0951	5.3043	1.21	1.3269	1.72	1.3150E-03	10	0.0953	0.7643	25.8	1.7254E-04	1.5686E-01
AN-105	D-7a	Tc	3	0.0951	5.3043	1.21	1.3269	1.72	1.3350E-04	10	0.11	0.7643	25.8	1.1038E-05	1.4567E-02
AN-105	D-7b	Tc	3	0.0951	5.3043	1.21	1.3269	1.72	1.4040E-04	10	0.1015	0.7643	25.8	1.2089E-05	1.6541E-02
5.028 M Simple	F-1a	Tc	3	0	5.028	0	0.018	0.01	1.3100E-03	10	0.1155	0.7643	25.5	6.4783E-05	1.4107E-01
5.028 M Simple	F-1b	Tc	3	0	5.028	0	0.018	0.01	1.3220E-03	10	0.0983	0.7643	25.5	8.1802E-05	1.6508E-01
1.028 M Simple	F-2a	Tc	3	0	1.028	0	0.018	0.01	1.3210E-03	10	0.1095	0.7643	25.5	2.9182E-04	1.2298E-01
1.028 M Simple	F-2b	Tc	3	0	1.028	0	0.018	0.01	1.3120E-03	10	0.1096	0.7643	25.5	3.1595E-04	1.1891E-01
0.528 M Simple	F-3a	Tc	3	0	0.528	0	0.018	0.01	1.3170E-03	10	0.0981	0.7643	25.5	4.6743E-04	1.1332E-01
0.528 M Simple	F-3b	Tc	3	0	0.528	0	0.018	0.01	1.3170E-03	10	0.0974	0.7643	25.5	4.8129E-04	1.1227E-01
0.128 M Simple	F-4a	Tc	3	0	0.128	0	0.018	0.01	1.3150E-03	10	0.1007	0.7643	25.5	7.9218E-04	6.7935E-02

Simulant	Test ID	XO_4^-	Batch ID	K^+ [M]	Na^+ [M]	NO_2^- [M]	NO_3^- [M]	OH^- [M]	XO_4^- [M]	Vol (ml)	Resin (g)	F factor (-)	T (C)	Final XO_4^- [M]	Loading (mmol/g)
0.128 M Simple	F-4b	Tc	3	0	0.128	0	0.018	0.01	1.3240E-03	10	0.0947	0.7643	25.5	7.9326E-04	7.3333E-02
0.028 M Simple	F-5a	Tc	3	0	0.0293	0	0.018	0.01	1.3180E-03	10	0.1104	0.7643	25.5	1.0709E-03	2.9292E-02
0.028 M Simple	F-5b	Tc	3	0	0.0293	0	0.018	0.01	1.3220E-03	10	0.1064	0.7643	25.5	1.0676E-03	3.1285E-02

Table A-4. Batch contact data taken from reports with Hassan as the lead author. Shaded data not employed in optimization process.

Simulant	Test ID	XO_4^-	Batch ID	K^+ [M]	Na^+ [M]	NO_2^- [M]	NO_3^- [M]	OH^- [M]	XO_4^- [M]	Vol (ml)	Resin (g)	F factor (-)	T (C)	Final XO_4^- [M]	Loading (mmol/g)
AN-102	BNF-LC305-S639-1	Tc	1	0.029	5.98	0.832	1.89	1.49	1.9289E-05	17.849	0.1805	0.987	26	5.5146E-06	1.3800E-03
AN-102	BNF-LC305-S639-1D	Tc	1	0.029	5.98	0.832	1.89	1.49	1.9289E-05	18.243	0.1809	0.987	26	4.7558E-06	1.4849E-03
AN-102	BNF-LC305-S639-1R-1	Tc	1	0.029	5.9736	0.832	1.8836	1.49	5.5146E-06	11.309	0.1223	0.987	26	1.2149E-06	4.0283E-04
AN-102	BNF-LC305-S639-SPK-1	Tc	1	0.029	5.9737	0.832	1.8837	1.49	2.5307E-04	10.222	0.1012	0.987	26	6.8221E-05	1.8917E-02
AN-102	BNF-LC305-S639-SPK-1D	Tc	1	0.029	5.9672	0.832	1.8772	1.49	2.5307E-04	9.397	0.1037	0.987	26	5.9642E-05	1.7759E-02
AN-103	BNF-A325-S39-1	Tc	1	0.121	5.25	1.037	1.571	1.876	2.3846E-05	19.39	0.1804	0.987	26	4.3765E-06	2.1202E-03
AN-103	BNF-A325-S39-1D	Tc	1	0.121	5.25	1.037	1.571	1.876	2.3846E-05	17.52	0.1804	0.987	26	3.4767E-06	2.0043E-03
AN-103	BNF-A325-S39-1R-1	Tc	1	0.121	5.2441	1.037	1.5651	1.876	4.3765E-06	11.552	0.1201	0.987	26	4.7593E-07	3.8012E-04
AN-103	BNF-A325-S39-1R-1D	Tc	1	0.121	5.2434	1.037	1.5644	1.876	3.4767E-06	12.402	0.1202	0.987	26	4.9641E-07	3.1155E-04
AN-103	BNF-A325-S39-2R-1	Tc	1	0.121	5.2374	1.037	1.5584	1.876	4.7593E-07	7.957	0.081	0.987	26	8.0550E-08	3.9352E-05
AN-103	BNF-A325-S39-2R-1D	Tc	1	0.121	5.2373	1.037	1.5583	1.876	4.9641E-07	8.39	0.0802	0.987	26	9.8366E-08	4.2189E-05
AN-103	BNF-A325-S39-SPR-1	Tc	1	0.121	5.2310	1.037	1.5519	1.876	2.5074E-04	9.233	0.1018	0.987	26	4.2229E-05	1.9161E-02
AN-103	BNF-A325-S39-SPR-1D	Tc	1	0.121	5.2312	1.037	1.5522	1.876	2.5074E-04	9.195	0.1011	0.987	26	4.2655E-05	1.9175E-02
AZ-102	BNF-B305-S639-1	Tc	1	0.081	2.65	0.832	0.273	0.1369	1.4117E-04	17.877	0.1808	0.987	26	1.3895E-05	1.2750E-02
AZ-102	BNF-B305-S639-1D	Tc	1	0.081	2.65	0.832	0.273	0.1369	1.3936E-04	17.934	0.1801	0.987	26	1.4734E-05	1.2573E-02
AZ-102	BNF-B305-S639-1R-1	Tc	1	0.081	2.6437	0.832	0.2667	0.1369	1.3895E-05	10.643	0.1212	0.987	26	1.3381E-06	1.1172E-03
AZ-102	BNF-B305-S639-1R-1D	Tc	1	0.081	2.6437	0.832	0.2667	0.1369	1.4734E-05	10.745	0.1209	0.987	26	1.0895E-06	1.2286E-03
AZ-102	BNF-A325-S39-2R-1	Tc	1	0.081	2.6364	0.832	0.2594	0.1369	1.3381E-06	7.327	0.1005	0.987	26	1.1914E-07	9.0039E-05
AZ-102	BNF-A325-S39-2R-1D	Tc	1	0.081	2.6365	0.832	0.2595	0.1369	1.0895E-06	7.842	0.1007	0.987	26	2.0541E-07	6.9755E-05
AZ-102	BNF-A325-S39-3R-1	Tc	1	0.081	2.6276	0.832	0.2506	0.1369	1.1914E-07	4.274	0.0526	0.987	26	5.2720E-09	9.3742E-06
AZ-102	BNF-A325-S39-3R-1D	Tc	1	0.081	2.6283	0.832	0.2513	0.1369	2.0541E-07	3.663	0.0512	0.987	26	2.9052E-08	1.2783E-05
AW-101	AW101-Kd39-1-filtrate-1	Tc	5	0.598	4.96	1.13	1.56	2.1006	4.7774E-05	9.55	0.1	0.98	25	4.9562E-06	4.1726E-03
AW-101	AW101-Kd39-1-filtrate-2	Tc	5	0.598	4.96	1.13	1.56	2.1006	4.7774E-05	9.22	0.102	0.98	25	5.1160E-06	3.9346E-03
AW-101	AW101-Kd39-2-filtrate-1	Tc	5	0.598	4.96	1.13	1.56	2.1006	4.7774E-05	9.52	1	0.98	25	1.9251E-06	4.4539E-04
AW-101	AW101-Kd39-2-filtrate-2	Tc	5	0.598	4.96	1.13	1.56	2.1006	4.7774E-05	9.55	1	0.98	25	1.8280E-06	4.4774E-04

Table A-5. Batch contact data taken from reports with Burgeson as the lead author. All new data since 2000 Report.

Simulant	Test ID	XO_4^-	Batch ID	K^+ [M]	Na^+ [M]	NO_2^- [M]	NO_3^- [M]	OH^- [M]	XO_4^- [M]	Vol (ml)	Resin (g)	F factor (-)	T (C)	Final XO_4^- [M]	Loading (mmol/g)
AP-101-1	E-1	Tc	1&2	0.75	4.81	0.78	1.88	1.51	2.7673E-05	5.1050	0.0509	0.9798	24	3.1570E-06	2.5116E-03
AP-101-1D	E-1D	Tc	1&2	0.75	4.81	0.78	1.88	1.51	2.7673E-05	5.1209	0.0518	0.9798	24	3.1618E-06	2.4717E-03
AP-101-2	E-2	Tc	1&2	0.75	4.81	0.78	1.88	1.51	8.9040E-04	5.1288	0.0501	0.9798	24	1.4188E-04	7.8194E-02
AP-101-2D	E-2D	Tc	1&2	0.75	4.81	0.78	1.88	1.51	8.9040E-04	5.1288	0.0499	0.9798	24	1.2806E-04	8.0021E-02
AP-101-3	E-3	Tc	1&2	0.75	4.81	0.78	1.88	1.51	2.4175E-03	5.0971	0.0498	0.9798	24	6.0558E-04	1.8932E-01
AP-101-3D	E-3D	Tc	1&2	0.75	4.81	0.78	1.88	1.51	2.4175E-03	5.1209	0.0502	0.9798	24	5.6806E-04	1.9248E-01
AP-101-4	E-4	Tc	3	0.75	4.81	0.78	1.88	1.51	1.8897E-05	4	0.0423	0.9204	24	1.0320E-06	1.8354E-03
AP-101-4D	E-4D	Tc	3	0.75	4.81	0.78	1.88	1.51	1.8897E-05	4	0.0406	0.9204	24	1.0721E-06	1.9080E-03
AN-102/C-104-1	A-1	Tc	3	0.028	4.78	0.9	1.73	0.18	6.4874E-05	6.0021	0.0559	0.9318	25	9.8799E-06	6.3368E-03
AN-102/C-104-1D	A-1D	Tc	3	0.028	4.78	0.9	1.73	0.18	6.4874E-05	6.0241	0.0566	0.9318	25	9.3442E-06	6.3426E-03
AN-102/C-104-2	A-2	Tc	3	0.028	4.78	0.9	1.73	0.18	7.0230E-04	6.0260	0.0587	0.9318	25	1.0654E-04	6.5634E-02
AN-102/C-104-2D	A-2D	Tc	3	0.028	4.78	0.9	1.73	0.18	7.0230E-04	6.0128	0.0571	0.9318	25	9.4632E-05	6.8670E-02
AN-102/C-104-3	A-3	Tc	3	0.028	4.78	0.9	1.73	0.18	2.2438E-03	6.0386	0.0639	0.9318	25	3.0413E-04	1.9671E-01
AN-102/C-104-3D	A-3D	Tc	3	0.028	4.78	0.9	1.73	0.18	2.2438E-03	6.0094	0.0567	0.9318	25	3.4103E-04	2.1642E-01
AZ-101-1	B-1	Tc	3	0.09	4.26	1.182	0.85	0.63	2.1538E-04	10.060	0.0992	0.9204	~22	1.9156E-05	2.1622E-02
AZ-101-1D	B-1D	Tc	3	0.09	4.26	1.182	0.85	0.63	2.1538E-04	10.015	0.1033	0.9204	~22	1.7059E-05	2.0890E-02
AZ-101-2	B-2	Tc	3	0.09	4.26	1.182	0.85	0.63	3.6042E-04	10.068	0.0979	0.9204	~22	3.2075E-05	3.6690E-02
AZ-101-2D	B-2D	Tc	3	0.09	4.26	1.182	0.85	0.63	3.6042E-04	10.031	0.097	0.9204	~22	3.5866E-05	3.6467E-02
AZ-101-3	B-3	Tc	3	0.09	4.26	1.182	0.85	0.63	1.1881E-03	9.7445	0.1014	0.9204	~22	9.5682E-05	1.1406E-01
AZ-101-3D	B-3D	Tc	3	0.09	4.26	1.182	0.85	0.63	1.1881E-03	9.4093	0.104	0.9204	~22	1.0917E-04	1.0606E-01
AZ-101-4	B-4	Tc	3	0.09	4.26	1.182	0.85	0.63	1.8926E-03	10.072	0.1018	0.9204	~22	2.0306E-04	1.8161E-01
AZ-101-4D	B-4D	Tc	3	0.09	4.26	1.182	0.85	0.63	1.8926E-03	10.042	0.1006	0.9204	~22	2.1033E-04	1.8246E-01

Table A-6. Batch contact data taken from reports with Blanchard as the lead author. Shaded data not employed in optimization process.

Simulant	Test ID	XO_4^-	Batch ID	K^+ [M]	Na^+ [M]	NO_2^- [M]	NO_3^- [M]	OH^- [M]	XO_4^- [M]	Vol (ml)	Resin (g)	F factor (-)	T (C)	Final XO_4^- [M]	Loading (mmol/g)
AW-101-1	A-1	Tc	4	0.39	4.59	1.01	1.5	1.6566	3.9000E-05	5.05	0.0456	0.77	25	6.3100E-06	4.7017E-03
AW-101-1D	A-1D	Tc	4	0.39	4.59	1.01	1.5	1.6566	3.9000E-05	5.05	0.0554	0.77	25	6.6300E-06	3.8321E-03
AW-101-2	A-2	Tc	4	0.39	4.59	1.01	1.5	1.6566	3.7600E-04	5.05	0.0503	0.77	25	6.3900E-05	4.0694E-02
AW-101-2D	A-2D	Tc	4	0.39	4.59	1.01	1.5	1.6566	3.7600E-04	5.03	0.048	0.77	25	8.2900E-05	3.9889E-02
AW-101-3	A-3a	Tc	4	0.39	4.59	1.01	1.5	1.6566	1.3900E-03	5.04	0.0489	0.77	25	4.2200E-04	1.2957E-01
AW-101-3D	A-3D	Tc	4	0.39	4.59	1.01	1.5	1.6566	1.3900E-03	5.04	0.047	0.77	25	4.2600E-04	1.3425E-01
AN-107-1	B-1	Tc	4	0.0214	5.7	0.717	2.06	0.9832	3.2320E-05	5.129	0.0497	0.9605	25	9.5316E-06	2.4485E-03
AN-107-1D	B-1D	Tc	4	0.0214	5.7	0.717	2.06	0.9832	3.2320E-05	5.144	0.0509	0.9605	25	6.1808E-06	2.7503E-03
AN-107-2	B-2	Tc	4	0.019	4.7	0.717	2.06	0.7842	2.8280E-05	5.15	0.0525	0.9605	25	1.0032E-05	1.8636E-03
AN-107-2D	B-2D	Tc	4	0.019	4.7	0.717	2.06	0.7842	2.8280E-05	5.148	0.0521	0.9605	25	9.2600E-06	1.9567E-03
AN-107-3	B-3	Tc	4	0.019	4.84	0.6	1.942	0.94	3.8750E-05	4.997	0.0492	0.956	25	3.0110E-05	9.1792E-04
AN-107-3D	B-3D	Tc	4	0.019	4.84	0.6	1.942	0.94	3.8750E-05	4.997	0.0493	0.956	25	3.4384E-05	4.6285E-04

Table A-7. Batch contact data taken from reports with Kurath as the lead author. Shaded data not employed in optimization process.

Simulant	Test ID	XO_4^-	Batch ID	K^+ [M]	Na^+ [M]	NO_2^- [M]	NO_3^- [M]	OH^- [M]	XO_4^- [M]	Vol (ml)	Resin (g)	F factor (-)	T (C)	Final XO_4^- [M]	Loading (mmol/g)
AW-101/Simulant	Kinetics	Tc	4	0.4300	5.0000	0.7900	1.5200	2.3326	4.6300E-05	5.0000	0.0519	0.9855	21	5.7800E-06	3.9611E-03
AW-101	W39	Tc	4	0.6100	6.5900	1.2800	1.9900	2.7507	5.2725E-05	5.0776	0.0499	0.9855	21	9.8300E-06	4.4291E-03
AW-101	W39-R	Tc	4	0.6100	6.5900	1.2800	1.9900	2.7507	5.3599E-05	5.0776	0.0499	0.9855	21	7.4800E-06	4.7619E-03
AW-101	W39D	Tc	4	0.6100	6.5900	1.2800	1.9900	2.7507	5.2725E-05	5.0876	0.0509	0.9855	21	9.7100E-06	4.3628E-03
AW-101	W39D-R	Tc	4	0.6100	6.5900	1.2800	1.9900	2.7507	5.3599E-05	5.0876	0.0509	0.9855	21	6.9600E-06	4.7303E-03
AW-101	W39-S1	Tc	4	0.6100	6.5900	1.2800	1.9900	2.7504	4.1644E-04	5.0080	0.0510	0.9855	21	6.7800E-05	3.4738E-02
AW-101	W39-S1-R	Tc	4	0.6100	6.5900	1.2800	1.9900	2.7504	4.1644E-04	5.0080	0.0510	0.9855	21	7.9200E-05	3.3603E-02
AW-101	W39-S1D	Tc	4	0.6100	6.5900	1.2800	1.9900	2.7504	4.1644E-04	4.9507	0.0491	0.9855	21	6.6700E-05	3.5782E-02
AW-101	W39-S2	Tc	4	0.6100	6.5900	1.2800	1.9900	2.7492	1.5784E-03	4.9778	0.0502	0.9855	21	4.1000E-04	1.1756E-01
AW-101	W39-S2-R	Tc	4	0.6100	6.5900	1.2800	1.9900	2.7492	1.5784E-03	4.9778	0.0502	0.9855	21	4.0500E-04	1.1807E-01
AW-101	W39-S2D	Tc	4	0.6100	6.5900	1.2800	1.9900	2.7492	1.5784E-03	5.0790	0.0504	0.9855	21	3.3600E-04	1.2704E-01
AN-107	N39	Tc	4	0.0230	5.6100	0.7170	2.0600	0.4706	7.7720E-06	5.2884	0.0503	0.9855	21	3.6200E-06	4.4295E-04
AN-107	N39-R	Tc	4	0.0230	5.6100	0.7170	2.0600	0.4706	7.7720E-06	5.2884	0.0503	0.9855	21	4.1600E-06	3.8534E-04
AN-107	N39D	Tc	4	0.0230	5.6100	0.7170	2.0600	0.4706	7.7720E-06	5.3910	0.0498	0.9855	21	3.5200E-06	4.6706E-04
AN-107	N39D-R	Tc	4	0.0230	5.6100	0.7170	2.0600	0.4706	7.7720E-06	5.3910	0.0498	0.9855	21	2.3700E-06	5.9339E-04

Table A-8. CERMOD output parameter summary showing measured versus computed values along with statistics of the optimization process.

```
********** CERMOD SL-639 Parameter Estimation of Keq, EtaRe and Qtot ******************************

Cost function is log-difference residual
actred, (||f(x)||-||f(x+p)||)/||f(x)||    =  0.0000E+00
prered, (||f(x)||-||f(x)+Jp)||)/||f(x)||  =  0.0000E+00
abs(actred) and prered tolerance          =  1.0000E-08
ratio, actred/prered                      =  0.0000E+00
ratio  tolerance                          =  2.0000E+00

INFO(LMDIF1) =    0
iterations   =     0

Pitzer parameters: binary and ternary

(Y) K11: [Na+:XO4-] electrolyte molal equilibrium constant =  1.436055371E+03 ln =  7.269655308E+00

(Y) K12: [Na+:NO3-] electrolyte molal equilibrium constant =  1.093978074E+00 ln =  8.982066167E-02

(Y) K21: [ K+:XO4-] electrolyte molal equilibrium constant =  1.070942225E+05 ln =  1.158146431E+01

(Y) K22: [ K+:NO3-] electrolyte molal equilibrium constant =  5.104231910E+01 ln =  3.932655075E+00

(N) Qtot:  Total sorption loading  =  6.472000000E-01

(N) EtaRe: Fraction of K11 and K21 for XReO4 reactions =  5.050000000E-01

Batch     Batch ID                Qfrac
  1       981015DHC-720011        1.001
  2       990420DHC-720067        0.498
  3       010227CTC-9-23          1.488
  4       980624001DC             0.459
  5       I-R2-03-27-02-20-45     1.030
  6       50%Batch1 50%Batch2     0.758

********** XO4- Ionic Loadings ************************************************************

                                    Batch Contact                    Q (Observed)  Q (Computed)       Error
                                       Dataset                          (mmol/g)      (mmol/g)        (%)
------------------------------------------------------------------------------- ------------  ------------  -------

SRNL\King\ReO4\25C\AN-105\BNF-SSIX-10-1\BNF-SSIX-10-1.dat              2.9956E-03     3.0575E-03        2.067
SRNL\King\ReO4\25C\AN-105\BNF-SSIX-10-1\BNF-SSIX-10-1-D.dat            2.9725E-03     3.0490E-03        2.573
SRNL\King\ReO4\25C\AN-105\BNF-SSIX-10-2\BNF-SSIX-10-2.dat              3.0002E-02     3.1279E-02        4.256
SRNL\King\ReO4\25C\AN-105\BNF-SSIX-10-2\BNF-SSIX-10-2-D.dat            2.9897E-02     3.1388E-02        4.989
SRNL\King\ReO4\25C\AN-105\BNF-SSIX-10-3\BNF-SSIX-10-3.dat              6.0207E-04     6.0763E-04        0.924
```

SRNL\King\ReO4\25C\AN-105\BNF-SSIX-10-3\BNF-SSIX-10-3-D.dat	5.9941E-04	6.0530E-04	0.983
SRNL\King\ReO4\25C\AN-105\BNF-SSIX-10-5\BNF-SSIX-10-5.dat	1.1483E-04	1.1864E-04	3.314
SRNL\King\ReO4\25C\AN-105\BNF-SSIX-10-5\BNF-SSIX-10-5-D.dat	1.0050E-04	1.0674E-04	6.209
SRNL\King\ReO4\25C\AN-105\BNF-SSIX-17-1\BNF-SSIX-17-1.dat	5.6161E-03	5.0490E-03	-10.098
SRNL\King\ReO4\25C\AN-105\BNF-SSIX-17-1\BNF-SSIX-17-1-D.dat	5.8432E-03	5.0269E-03	-13.970
SRNL\King\ReO4\25C\AN-105\BNF-SSIX-17-2\BNF-SSIX-17-2.dat	2.4242E-02	2.4436E-02	0.799
SRNL\King\ReO4\25C\AN-105\BNF-SSIX-17-2\BNF-SSIX-17-2-D.dat	2.4118E-02	2.4397E-02	1.157
SRNL\King\ReO4\25C\AN-105\BNF-SSIX-17-3\BNF-SSIX-17-3.dat	4.8967E-02	5.1712E-02	5.606
SRNL\King\ReO4\25C\AN-105\BNF-SSIX-17-3\BNF-SSIX-17-3-D.dat	4.8107E-02	5.1687E-02	7.442
SRNL\King\ReO4\25C\AN-105\BNF-SSIX-17-4\BNF-SSIX-17-4.dat	6.5560E-02	7.3098E-02	11.497
SRNL\King\ReO4\25C\AN-105\BNF-SSIX-17-4\BNF-SSIX-17-4-D.dat	6.4649E-02	7.2935E-02	12.817
SRNL\King\ReO4\25C\AN-105\BNF-SSIX-17-5\BNF-SSIX-17-5.dat	2.6010E-03	2.5958E-03	-0.199
SRNL\King\ReO4\25C\AN-105\BNF-SSIX-17-5\BNF-SSIX-17-5-D.dat	2.5754E-03	2.5968E-03	0.830
SRNL\King\ReO4\25C\AN-105\BNF-SSIX-17-7\BNF-SSIX-17-7.dat	8.4972E-04	8.5559E-04	0.691
SRNL\King\ReO4\25C\AN-105\BNF-SSIX-17-7\BNF-SSIX-17-7-D.dat	8.8776E-04	8.6827E-04	-2.196
SRNL\King\ReO4\25C\AN-105\BNF-SSIX-17-6\BNF-SSIX-17-6.dat	3.2254E-03	2.6365E-03	-18.258
SRNL\King\ReO4\25C\AN-105\BNF-SSIX-17-6\BNF-SSIX-17-6-D.dat	3.1846E-03	2.6345E-03	-17.275
SRNL\Duffey\ReO4\25C\AN-105\Exp-01\Exp-01.dat	1.1043E-02	1.1019E-02	-0.216
SRNL\Duffey\ReO4\25C\AN-105\Exp-02\Exp-02.dat	1.1334E-02	1.1373E-02	0.342
SRNL\Duffey\ReO4\25C\AN-105\Exp-05\Exp-05.dat	1.0718E-02	1.1333E-02	5.740
SRNL\Duffey\ReO4\25C\AN-105\Exp-06\Exp-06.dat	1.0286E-02	1.0680E-02	3.827
SRNL\Duffey\ReO4\25C\AN-105\Exp-07\Exp-07.dat	1.0576E-02	1.0759E-02	1.728
SRNL\Duffey\ReO4\25C\AN-105\Exp-08\Exp-08.dat	1.1419E-02	1.1507E-02	0.770
SRNL\Duffey\ReO4\25C\AN-105\Exp-09\Exp-09.dat	1.1465E-02	1.1672E-02	1.810
SRNL\Duffey\ReO4\25C\AZ-102\Exp-10\Exp-10.dat	3.6089E-02	3.4572E-02	-4.204
SRNL\Duffey\ReO4\25C\AN-107\Exp-11\Exp-11.dat	4.1672E-03	3.3409E-03	-19.828
PNNL\Rapco\ReO4\25C\AN-105\D-6\D-6a.dat	8.8120E-02	9.6331E-02	9.318
PNNL\Rapco\ReO4\25C\AN-105\D-6\D-6b.dat	7.1651E-02	8.0808E-02	12.780
PNNL\Rapco\ReO4\25C\AN-105\D-8\D-8a.dat	8.5529E-04	8.9545E-04	4.696
PNNL\Rapco\ReO4\25C\AN-105\D-8\D-8b.dat	1.0180E-03	1.0566E-03	3.794
PNNL\Rapco\ReO4\25C\AN-105\D-9\D-9a.dat	3.0695E-05	3.2472E-05	5.790
PNNL\Rapco\ReO4\25C\AN-105\D-9\D-9b.dat	3.3197E-05	3.5367E-05	6.537
PNNL\Rapco\ReO4\25C\Simple\D-10\D-10a.dat	8.5960E-02	9.4263E-02	9.660
PNNL\Rapco\ReO4\25C\Simple\D-10\D-10b.dat	7.6541E-02	8.4396E-02	10.262
SRNL\King\TcO4\25C\Tank-44F\SRS-1\SRS-1.dat	3.0880E-03	3.2265E-03	4.484
SRNL\King\TcO4\25C\Tank-44F\SRS-1\SRS-1-D.dat	3.1862E-03	3.3236E-03	4.313
SRNL\Hassan\TcO4\25C\AN-102\BNF-LC305-S639\BNF-LC305-S639-1.dat	1.3800E-03	1.6388E-03	18.751
SRNL\Hassan\TcO4\25C\AN-102\BNF-LC305-S639\BNF-LC305-S639-1D.dat	1.4849E-03	1.6662E-03	12.210
SRNL\Hassan\TcO4\25C\AN-102\BNF-LC305-S639-1R\BNF-LC305-S639-1R-1.dat	4.0283E-04	4.4271E-04	9.900
SRNL\Hassan\TcO4\25C\AN-102\BNF-LC305-S639-SPK\BNF-LC305-S639-SPK-1.dat	1.8917E-02	2.1788E-02	15.176
SRNL\Hassan\TcO4\25C\AN-102\BNF-LC305-S639-SPK\BNF-LC305-S639-SPK-1D.dat	1.7759E-02	1.9885E-02	11.972
SRNL\Hassan\TcO4\25C\AN-103\BNF-A325-S39\BNF-A325-S39-1.dat	2.1202E-03	2.2770E-03	7.396
SRNL\Hassan\TcO4\25C\AN-103\BNF-A325-S39\BNF-A325-S39-1D.dat	2.0043E-03	2.0822E-03	3.886
SRNL\Hassan\TcO4\25C\AN-103\BNF-A325-S39-1R\BNF-A325-S39-1R-1.dat	3.8012E-04	3.7913E-04	-0.262
SRNL\Hassan\TcO4\25C\AN-103\BNF-A325-S39-1R\BNF-A325-S39-1R-1D.dat	3.1155E-04	3.2049E-04	2.869
SRNL\Hassan\TcO4\25C\AN-103\BNF-A325-S39-2R\BNF-A325-S39-2R-1.dat	3.9352E-05	4.2025E-05	6.792
SRNL\Hassan\TcO4\25C\AN-103\BNF-A325-S39-2R\BNF-A325-S39-2R-1D.dat	4.2189E-05	4.6339E-05	9.837
SRNL\Hassan\TcO4\25C\AN-103\BNF-A325-S39-SPR\BNF-A325-S39-SPR-1.dat	1.9161E-02	2.0556E-02	7.280
SRNL\Hassan\TcO4\25C\AN-103\BNF-A325-S39-SPR\BNF-A325-S39-SPR-1D.dat	1.9175E-02	2.0606E-02	7.462
SRNL\Hassan\TcO4\25C\AZ-102\BNF-B305-S639\BNF-B305-S639-1.dat	1.2750E-02	1.3078E-02	2.572
SRNL\Hassan\TcO4\25C\AZ-102\BNF-B305-S639\BNF-B305-S639-1D.dat	1.2573E-02	1.2995E-02	3.357

SRNL\Hassan\TcO4\25C\AZ-102\BNF-B305-S639-1R\BNF-B305-S639-1R-1.dat	1.1172E-03	1.1549E-03	3.372
SRNL\Hassan\TcO4\25C\AZ-102\BNF-B305-S639-1R\BNF-B305-S639-1R-1D.dat	1.2286E-03	1.2384E-03	0.799
SRNL\Hassan\TcO4\25C\AZ-102\BNF-A325-S39-2R\BNF-A325-S39-2R-1.dat	9.0039E-05	9.3424E-05	3.760
SRNL\Hassan\TcO4\25C\AZ-102\BNF-A325-S39-3R\BNF-A325-S39-3R-1.dat	9.3742E-06	9.2175E-06	-1.672
SRNL\Hassan\TcO4\25C\AW-101\AW101-Kd39-1\AW101-Kd39-1-filtrate-1.dat	4.1726E-03	4.2920E-03	2.861
SRNL\Hassan\TcO4\25C\AW-101\AW101-Kd39-1\AW101-Kd39-1-filtrate-2.dat	3.9346E-03	4.0796E-03	3.685
PNNL\Rapco\TcO4\25C\Simple\B-1\B-1a.dat	4.2426E-02	4.2773E-02	0.819
PNNL\Rapco\TcO4\25C\Simple\B-1\B-1b.dat	5.0747E-02	5.1163E-02	0.820
PNNL\Rapco\TcO4\25C\Simple\B-2\B-2a.dat	4.8734E-02	4.9073E-02	0.695
PNNL\Rapco\TcO4\25C\Simple\B-2\B-2b.dat	4.3915E-02	4.4216E-02	0.684
PNNL\Rapco\TcO4\25C\Simple\B-3\B-3a.dat	4.9395E-02	4.9672E-02	0.561
PNNL\Rapco\TcO4\25C\Simple\B-3\B-3b.dat	4.8283E-02	4.8773E-02	1.015
PNNL\Rapco\TcO4\25C\Simple\B-4\B-4a.dat	4.7762E-02	4.8257E-02	1.037
PNNL\Rapco\TcO4\25C\Simple\B-4\B-4b.dat	4.4280E-02	4.4725E-02	1.006
PNNL\Rapco\TcO4\25C\Simple\D-1\D-1a.dat	1.4777E-01	1.5052E-01	1.858
PNNL\Rapco\TcO4\25C\Simple\D-1\D-1b.dat	1.5561E-01	1.5856E-01	1.898
PNNL\Rapco\TcO4\25C\Simple\D-2\D-2a.dat	1.5211E-01	1.5424E-01	1.402
PNNL\Rapco\TcO4\25C\Simple\D-2\D-2b.dat	1.5863E-01	1.6021E-01	0.996
PNNL\Rapco\TcO4\25C\Simple\D-3\D-3a.dat	1.3749E-01	1.3670E-01	-0.572
PNNL\Rapco\TcO4\25C\Simple\D-3\D-3b.dat	1.4899E-01	1.4766E-01	-0.892
PNNL\Rapco\TcO4\25C\Simple\D-4\D-4a.dat	1.4899E-02	1.4444E-02	-3.052
PNNL\Rapco\TcO4\25C\Simple\D-4\D-4b.dat	1.5472E-02	1.5038E-02	-2.804
PNNL\Rapco\TcO4\25C\AN-105\D-5\D-5a.dat	1.3365E-01	1.3293E-01	-0.539
PNNL\Rapco\TcO4\25C\AN-105\D-5\D-5b.dat	1.5686E-01	1.5991E-01	1.943
PNNL\Rapco\TcO4\25C\AN-105\D-7\D-7a.dat	1.4567E-02	1.4511E-02	-0.387
PNNL\Rapco\TcO4\25C\AN-105\D-7\D-7b.dat	1.6541E-02	1.6418E-02	-0.745
PNNL\Rapco\TcO4\25C\Simple\F-1\F-1a.dat	1.4107E-01	1.4360E-01	1.795
PNNL\Rapco\TcO4\25C\Simple\F-1\F-1b.dat	1.6508E-01	1.6921E-01	2.500
PNNL\Rapco\TcO4\25C\Simple\F-2\F-2a.dat	1.2298E-01	1.2705E-01	3.310
PNNL\Rapco\TcO4\25C\Simple\F-2\F-2b.dat	1.1891E-01	1.2615E-01	6.090
PNNL\Rapco\TcO4\25C\Simple\F-3\F-3a.dat	1.1332E-01	1.1854E-01	4.602
PNNL\Rapco\TcO4\25C\Simple\F-3\F-3b.dat	1.1227E-01	1.1902E-01	6.009
PNNL\Rapco\TcO4\25C\Simple\F-4\F-4a.dat	6.7935E-02	7.0767E-02	4.169
PNNL\Rapco\TcO4\25C\Simple\F-4\F-4b.dat	7.3333E-02	7.3019E-02	-0.429
PNNL\Rapco\TcO4\25C\Simple\F-5\F-5a.dat	2.9292E-02	2.9408E-02	0.396
PNNL\Rapco\TcO4\25C\Simple\F-5\F-5b.dat	3.1285E-02	2.9844E-02	-4.607
PNNL\Burgeson\TcO4\25C\AP-101\E-1\E-1.dat	2.5116E-03	2.4528E-03	-2.342
PNNL\Burgeson\TcO4\25C\AP-101\E-1\E-1D.dat	2.4717E-03	2.4223E-03	-1.997
PNNL\Burgeson\TcO4\25C\AP-101\E-2\E-2.dat	7.8194E-02	7.8357E-02	0.208
PNNL\Burgeson\TcO4\25C\AP-101\E-2\E-2D.dat	8.0021E-02	7.8613E-02	-1.759
PNNL\Burgeson\TcO4\25C\AP-101\E-3\E-3.dat	1.8932E-01	1.9957E-01	5.414
PNNL\Burgeson\TcO4\25C\AP-101\E-3\E-3D.dat	1.9248E-01	1.9911E-01	3.445
PNNL\Burgeson\TcO4\25C\AP-101\E-4\E-4.dat	1.8354E-03	1.7996E-03	-1.951
PNNL\Burgeson\TcO4\25C\AP-101\E-4\E-4D.dat	1.9080E-03	1.7412E-03	-8.744
PNNL\Burgeson\TcO4\25C\AN-102\A-1\A-1.dat	6.3368E-03	6.1739E-03	-2.570
PNNL\Burgeson\TcO4\25C\AN-102\A-1\A-1D.dat	6.3426E-03	6.2294E-03	-1.785
PNNL\Burgeson\TcO4\25C\AN-102\A-2\A-2.dat	6.5634E-02	6.3706E-02	-2.937
PNNL\Burgeson\TcO4\25C\AN-102\A-2\A-2D.dat	6.8670E-02	6.5035E-02	-5.294
PNNL\Burgeson\TcO4\25C\AN-102\A-3\A-3.dat	1.9671E-01	1.8522E-01	-5.840
PNNL\Burgeson\TcO4\25C\AN-102\A-3\A-3D.dat	2.1642E-01	2.0222E-01	-6.560
PNNL\Burgeson\TcO4\25C\AZ-101\B-1\B-1.dat	2.1622E-02	2.1883E-02	1.208

PNNL\Burgeson\TcO4\25C\AZ-101\B-1\B-1D.dat	2.0890E-02	2.0993E-02	0.492
PNNL\Burgeson\TcO4\25C\AZ-101\B-2\B-2.dat	3.6690E-02	3.7047E-02	0.973
PNNL\Burgeson\TcO4\25C\AZ-101\B-2\B-2D.dat	3.6467E-02	3.7235E-02	2.105
PNNL\Burgeson\TcO4\25C\AZ-101\B-3\B-3.dat	1.1406E-01	1.1393E-01	-0.115
PNNL\Burgeson\TcO4\25C\AZ-101\B-3\B-3D.dat	1.0606E-01	1.0783E-01	1.671
PNNL\Burgeson\TcO4\25C\AZ-101\B-4\B-4.dat	1.8161E-01	1.8496E-01	1.845
PNNL\Burgeson\TcO4\25C\AZ-101\B-4\B-4D.dat	1.8246E-01	1.8644E-01	2.180
PNNL\Blanchard\TcO4\25C\AW-101\A-1\A-1.dat	4.7017E-03	4.1904E-03	-10.875
PNNL\Blanchard\TcO4\25C\AW-101\A-1\A-1D.dat	3.8321E-03	3.6123E-03	-5.736
PNNL\Blanchard\TcO4\25C\AW-101\A-2\A-2.dat	4.0694E-02	3.6450E-02	-10.428
PNNL\Blanchard\TcO4\25C\AW-101\A-2\A-2D.dat	3.9889E-02	3.7580E-02	-5.789
PNNL\Blanchard\TcO4\25C\AW-101\A-3\A-3.dat	1.2957E-01	1.2185E-01	-5.961
PNNL\Blanchard\TcO4\25C\AW-101\A-3\A-3D.dat	1.3425E-01	1.2438E-01	-7.351
PNNL\Blanchard\TcO4\25C\AN-107\B-1\B-1.dat	2.4485E-03	2.2497E-03	-8.118
PNNL\Blanchard\TcO4\25C\AN-107\B-1\B-1D.dat	2.7503E-03	2.2194E-03	-19.303
PNNL\Blanchard\TcO4\25C\AN-107\B-2\B-2.dat	1.8636E-03	1.8127E-03	-2.729
PNNL\Blanchard\TcO4\25C\AN-107\B-2\B-2D.dat	1.9567E-03	1.8210E-03	-6.935
PNNL\Kurath\TcO4\21C\AW-101\Kinetics\K-1.dat	3.9611E-03	3.8003E-03	-4.060
PNNL\Kurath\TcO4\21C\AW-101\W39\W39.dat	4.4291E-03	4.4923E-03	1.427
PNNL\Kurath\TcO4\21C\AW-101\W39\W39-R.dat	4.7619E-03	4.5665E-03	-4.102
PNNL\Kurath\TcO4\21C\AW-101\W39D\W39D.dat	4.3628E-03	4.4266E-03	1.462
PNNL\Kurath\TcO4\21C\AW-101\W39D\W39D-R.dat	4.7303E-03	4.4998E-03	-4.873
PNNL\Kurath\TcO4\21C\AW-101\W39-S1\W39-S1.dat	3.4738E-02	3.3811E-02	-2.670
PNNL\Kurath\TcO4\21C\AW-101\W39-S1\W39-S1R.dat	3.3603E-02	3.3811E-02	0.618
PNNL\Kurath\TcO4\21C\AW-101\W39-S1\W39-S1D.dat	3.5782E-02	3.4528E-02	-3.505
PNNL\Kurath\TcO4\21C\AW-101\W39-S2\W39-S2.dat	1.1756E-01	1.1863E-01	0.912
PNNL\Kurath\TcO4\21C\AW-101\W39-S2\W39-S2R.dat	1.1807E-01	1.1863E-01	0.477
PNNL\Kurath\TcO4\21C\AW-101\W39-S2\W39-S2D.dat	1.2704E-01	1.1986E-01	-5.654
PNNL\Kurath\TcO4\21C\AN-107\N39\N39.dat	4.4295E-04	5.2743E-04	19.072
PNNL\Kurath\TcO4\21C\AN-107\N39\N39D.dat	4.6706E-04	5.3726E-04	15.030
PNNL\Kurath\TcO4\21C\AN-107\N39\N39D-R.dat	5.9339E-04	5.3726E-04	-9.459
SRNL\Hassan\TcO4\25C\AN-103\Bat-1_Column\Hassan-AN-103.dat	1.8445E-02	1.8470E-02	0.137
SRNL\King2002\ReO4\25C\AN-105\Exp-1_Bat-2_Column\King-AN-105.dat	6.4338E-03	6.4972E-03	0.985
PNNL\Burgeson2002\TcO4\25C\AP-101\Bat-3_Column\Burgeson-AP-101.dat	3.6101E-02	3.7870E-02	4.900
PNNL\Burgeson2002\TcO4\25C\AZ-101\Bat-3_Column\Burgeson-AZ-101.dat	2.0358E-01	2.2752E-01	11.761
PNNL\Burgeson2002\TcO4\25C\AN-102\Bat-3_Column\Burgeson-AN-102.dat	1.0208E-02	8.8588E-03	-13.217
SRNL\King\ReO4\25C\AN-105\Exp-1_Bat-4_Column\King-AN-105.dat	1.6554E-02	1.6477E-02	-0.468
SRNL\King2002\ReO4\25C\AN-105\Exp-5_Bat-5_Column\King-AN-105.dat	2.6513E-02	2.9679E-02	11.942
SRNL\King2002\ReO4\25C\AZ-102\Exp-8_Bat-5_Column\King-AZ-102.dat	1.4479E-01	1.2974E-01	-10.397
SRNL\King2002\ReO4\25C\AN-107\Exp-9_Bat-5_Column\King-AN-107.dat	5.6620E-03	5.6919E-03	0.528
SRNL\King\ReO4\25C\AN-105\Exp-5_Bat-6_Column\King-AN-105.dat	2.2951E-02	2.3972E-02	4.448
SRNL\Steimke\ReO4\25C\AN-105\Run-9_Bat-6_Column\Pilot-Scale.dat	1.7354E-02	1.8779E-02	8.212
SRNL\King\TcO4\25C\Tank-44F\Bat-6_Low-NO3_Column\King-Tank-44_Low-NO3.dat	5.6780E-02	5.1161E-02	-9.895

(150)RMS error total = 6.720
(046)RMS error ReO4- = 7.790
(104)RMS error TcO4- = 6.188

(150)Avg error total = 0.902
(046)Avg error ReO4- = 1.570
(104)Avg error TcO4- = 0.607

(030)RMS error batch 1 = 7.054
(030)avg error batch 1 = 5.324

(003)RMS error batch 2 = 14.523
(003)avg error batch 2 = -11.516

(056)RMS error batch 3 = 4.699
(056)avg error batch 3 = 1.416

(037)RMS error batch 4 = 7.985
(037)avg error batch 4 = -1.747

(014)RMS error batch 5 = 7.261
(014)avg error batch 5 = -0.101

(010)RMS error batch 6 = 5.616
(010)avg error batch 6 = -0.301

********** XO4- Ionic Concentrations **********

Batch Contact Dataset	C (Observed) (M)	C (Computed) (M)	Error (%)
SRNL\King\ReO4\25C\AN-105\BNF-SSIX-10-1\BNF-SSIX-10-1.dat	7.4962E-06	6.8788E-06	-8.237
SRNL\King\ReO4\25C\AN-105\BNF-SSIX-10-1\BNF-SSIX-10-1-D.dat	7.6251E-06	6.8595E-06	-10.041
SRNL\King\ReO4\25C\AN-105\BNF-SSIX-10-2\BNF-SSIX-10-2.dat	8.6568E-05	7.3613E-05	-14.965
SRNL\King\ReO4\25C\AN-105\BNF-SSIX-10-2\BNF-SSIX-10-2-D.dat	8.8942E-05	7.3884E-05	-16.930
SRNL\King\ReO4\25C\AN-105\BNF-SSIX-10-3\BNF-SSIX-10-3.dat	1.4135E-06	1.3573E-06	-3.975
SRNL\King\ReO4\25C\AN-105\BNF-SSIX-10-3\BNF-SSIX-10-3-D.dat	1.4132E-06	1.3521E-06	-4.326
SRNL\King\ReO4\25C\AN-105\BNF-SSIX-10-5\BNF-SSIX-10-5.dat	3.0075E-07	2.6389E-07	-12.256
SRNL\King\ReO4\25C\AN-105\BNF-SSIX-10-5\BNF-SSIX-10-5-D.dat	3.0612E-07	2.3742E-07	-22.441
SRNL\King\ReO4\25C\AN-105\BNF-SSIX-17-1\BNF-SSIX-17-1.dat	1.9441E-05	2.5066E-05	28.932
SRNL\King\ReO4\25C\AN-105\BNF-SSIX-17-1\BNF-SSIX-17-1-D.dat	1.6805E-05	2.4954E-05	48.493
SRNL\King\ReO4\25C\AN-105\BNF-SSIX-17-2\BNF-SSIX-17-2.dat	1.3187E-04	1.2996E-04	-1.448
SRNL\King\ReO4\25C\AN-105\BNF-SSIX-17-2\BNF-SSIX-17-2-D.dat	1.3250E-04	1.2974E-04	-2.085
SRNL\King\ReO4\25C\AN-105\BNF-SSIX-17-3\BNF-SSIX-17-3.dat	3.3295E-04	3.0568E-04	-8.190
SRNL\King\ReO4\25C\AN-105\BNF-SSIX-17-3\BNF-SSIX-17-3-D.dat	3.4110E-04	3.0550E-04	-10.436
SRNL\King\ReO4\25C\AN-105\BNF-SSIX-17-4\BNF-SSIX-17-4.dat	5.4796E-04	4.7345E-04	-13.598
SRNL\King\ReO4\25C\AN-105\BNF-SSIX-17-4\BNF-SSIX-17-4-D.dat	5.5430E-04	4.7205E-04	-14.838
SRNL\King\ReO4\25C\AN-105\BNF-SSIX-17-5\BNF-SSIX-17-5.dat	1.2728E-05	1.2779E-05	0.403
SRNL\King\ReO4\25C\AN-105\BNF-SSIX-17-5\BNF-SSIX-17-5-D.dat	1.2997E-05	1.2784E-05	-1.638
SRNL\King\ReO4\25C\AN-105\BNF-SSIX-17-7\BNF-SSIX-17-7.dat	4.2320E-06	4.1733E-06	-1.387
SRNL\King\ReO4\25C\AN-105\BNF-SSIX-17-7\BNF-SSIX-17-7-D.dat	4.0387E-06	4.2354E-06	4.869
SRNL\King\ReO4\25C\AN-105\BNF-SSIX-17-6\BNF-SSIX-17-6.dat	6.0150E-06	1.1957E-05	98.788
SRNL\King\ReO4\25C\AN-105\BNF-SSIX-17-6\BNF-SSIX-17-6-D.dat	6.3910E-06	1.1948E-05	86.946
SRNL\Duffey\ReO4\25C\AN-105\Exp-01\Exp-01.dat	2.1200E-05	2.1313E-05	0.535
SRNL\Duffey\ReO4\25C\AN-105\Exp-02\Exp-02.dat	2.2200E-05	2.2009E-05	-0.858
SRNL\Duffey\ReO4\25C\AN-105\Exp-05\Exp-05.dat	2.5000E-05	2.1932E-05	-12.272
SRNL\Duffey\ReO4\25C\AN-105\Exp-06\Exp-06.dat	2.2600E-05	2.0647E-05	-8.644

SRNL\Duffey\ReO4\25C\AN-105\Exp-07\Exp-07.dat	2.1700E-05	2.0802E-05	-4.140
SRNL\Duffey\ReO4\25C\AN-105\Exp-08\Exp-08.dat	2.2700E-05	2.2274E-05	-1.878
SRNL\Duffey\ReO4\25C\AN-105\Exp-09\Exp-09.dat	2.3600E-05	2.2600E-05	-4.238
SRNL\Duffey\ReO4\25C\AZ-102\Exp-10\Exp-10.dat	3.4600E-05	4.2100E-05	21.675
SRNL\Duffey\ReO4\25C\AN-107\Exp-11\Exp-11.dat	1.5200E-05	1.9285E-05	26.873
PNNL\Rapco\ReO4\25C\AN-105\D-6\D-6a.dat	2.3201E-04	1.6555E-04	-28.643
PNNL\Rapco\ReO4\25C\AN-105\D-6\D-6b.dat	2.1106E-04	1.3646E-04	-35.343
PNNL\Rapco\ReO4\25C\AN-105\D-8\D-8a.dat	1.7454E-06	1.3835E-06	-20.732
PNNL\Rapco\ReO4\25C\AN-105\D-8\D-8b.dat	1.9495E-06	1.6387E-06	-15.945
PNNL\Rapco\ReO4\25C\AN-105\D-9\D-9a.dat	6.4447E-08	5.0175E-08	-22.146
PNNL\Rapco\ReO4\25C\AN-105\D-9\D-9b.dat	7.0892E-08	5.4734E-08	-22.793
PNNL\Rapco\ReO4\25C\Simple\D-10\D-10a.dat	3.3781E-04	2.7810E-04	-17.677
PNNL\Rapco\ReO4\25C\Simple\D-10\D-10b.dat	3.0505E-04	2.4376E-04	-20.092
SRNL\King\TcO4\25C\Tank-44F\SRS-1\SRS-1.dat	2.6856E-06	1.4265E-06	-46.882
SRNL\King\TcO4\25C\Tank-44F\SRS-1\SRS-1-D.dat	2.6681E-06	1.4696E-06	-44.920
SRNL\Hassan\TcO4\25C\AN-102\BNF-LC305-S639\BNF-LC305-S639-1.dat	5.5146E-06	2.9323E-06	-46.827
SRNL\Hassan\TcO4\25C\AN-102\BNF-LC305-S639\BNF-LC305-S639-1D.dat	4.7558E-06	2.9815E-06	-37.307
SRNL\Hassan\TcO4\25C\AN-102\BNF-LC305-S639-1R\BNF-LC305-S639-1R-1.dat	1.2149E-06	7.8918E-07	-35.041
SRNL\Hassan\TcO4\25C\AN-102\BNF-LC305-S639-SPK\BNF-LC305-S639-SPK-1.dat	6.8221E-05	4.0170E-05	-41.117
SRNL\Hassan\TcO4\25C\AN-102\BNF-LC305-S639-SPK\BNF-LC305-S639-SPK-1D.dat	5.9642E-05	3.6481E-05	-38.833
SRNL\Hassan\TcO4\25C\AN-103\BNF-A325-S39\BNF-A325-S39-1.dat	4.3765E-06	2.9366E-06	-32.900
SRNL\Hassan\TcO4\25C\AN-103\BNF-A325-S39\BNF-A325-S39-1D.dat	3.4767E-06	2.6848E-06	-22.778
SRNL\Hassan\TcO4\25C\AN-103\BNF-A325-S39-1R\BNF-A325-S39-1R-1.dat	4.7593E-07	4.8618E-07	2.153
SRNL\Hassan\TcO4\25C\AN-103\BNF-A325-S39-1R\BNF-A325-S39-1R-1D.dat	4.9641E-07	4.1092E-07	-17.222
SRNL\Hassan\TcO4\25C\AN-103\BNF-A325-S39-2R\BNF-A325-S39-2R-1.dat	8.0550E-08	5.3691E-08	-33.345
SRNL\Hassan\TcO4\25C\AN-103\BNF-A325-S39-2R\BNF-A325-S39-2R-1D.dat	9.8366E-08	5.9213E-08	-39.804
SRNL\Hassan\TcO4\25C\AN-103\BNF-A325-S39-SPR\BNF-A325-S39-SPR-1.dat	4.2229E-05	2.7043E-05	-35.962
SRNL\Hassan\TcO4\25C\AN-103\BNF-A325-S39-SPR\BNF-A325-S39-SPR-1D.dat	4.2655E-05	2.7122E-05	-36.417
SRNL\Hassan\TcO4\25C\AZ-102\BNF-B305-S639\BNF-B305-S639-1.dat	1.3895E-05	1.0625E-05	-23.535
SRNL\Hassan\TcO4\25C\AZ-102\BNF-B305-S639\BNF-B305-S639-1D.dat	1.4734E-05	1.0556E-05	-28.358
SRNL\Hassan\TcO4\25C\AZ-102\BNF-B305-S639-1R\BNF-B305-S639-1R-1.dat	1.3381E-06	9.1451E-07	-31.656
SRNL\Hassan\TcO4\25C\AZ-102\BNF-B305-S639-1R\BNF-B305-S639-1R-1D.dat	1.0895E-06	9.8079E-07	-9.978
SRNL\Hassan\TcO4\25C\AZ-102\BNF-A325-S39-2R\BNF-A325-S39-2R-1.dat	1.1914E-07	7.3317E-08	-38.462
SRNL\Hassan\TcO4\25C\AZ-102\BNF-A325-S39-3R\BNF-A325-S39-3R-1.dat	5.2720E-09	7.1753E-09	36.103
SRNL\Hassan\TcO4\25C\AW-101\AW101-Kd39-1\AW101-Kd39-1-filtrate-1.dat	4.9562E-06	3.7308E-06	-24.725
SRNL\Hassan\TcO4\25C\AW-101\AW101-Kd39-1\AW101-Kd39-1-filtrate-2.dat	5.1160E-06	3.5446E-06	-30.715
PNNL\Rapco\TcO4\25C\Simple\B-1\B-1a.dat	1.4150E-05	1.1003E-05	-22.241
PNNL\Rapco\TcO4\25C\Simple\B-1\B-1b.dat	1.6217E-05	1.3078E-05	-19.354
PNNL\Rapco\TcO4\25C\Simple\B-2\B-2a.dat	1.6487E-05	1.3911E-05	-15.627
PNNL\Rapco\TcO4\25C\Simple\B-2\B-2b.dat	1.4825E-05	1.2199E-05	-17.715
PNNL\Rapco\TcO4\25C\Simple\B-3\B-3a.dat	1.7365E-05	1.5266E-05	-12.087
PNNL\Rapco\TcO4\25C\Simple\B-3\B-3b.dat	1.8239E-05	1.4343E-05	-21.362
PNNL\Rapco\TcO4\25C\Simple\B-4\B-4a.dat	1.9046E-05	1.5178E-05	-20.308
PNNL\Rapco\TcO4\25C\Simple\B-4\B-4b.dat	1.7409E-05	1.3577E-05	-22.014
PNNL\Rapco\TcO4\25C\Simple\D-1\D-1a.dat	6.6527E-05	4.2898E-05	-35.518
PNNL\Rapco\TcO4\25C\Simple\D-1\D-1b.dat	6.9291E-05	4.5203E-05	-34.763
PNNL\Rapco\TcO4\25C\Simple\D-2\D-2a.dat	7.7100E-05	5.9832E-05	-22.398
PNNL\Rapco\TcO4\25C\Simple\D-2\D-2b.dat	7.5483E-05	6.2676E-05	-16.966
PNNL\Rapco\TcO4\25C\Simple\D-3\D-3a.dat	2.1069E-04	2.1716E-04	3.070
PNNL\Rapco\TcO4\25C\Simple\D-3\D-3b.dat	2.2493E-04	2.3484E-04	4.405
PNNL\Rapco\TcO4\25C\Simple\D-4\D-4a.dat	1.5945E-05	1.9743E-05	23.819

PNNL\Rapco\TcO4\25C\Simple\D-4\D-4b.dat	1.7185E-05	2.0547E-05	19.562
PNNL\Rapco\TcO4\25C\AN-105\D-5\D-5a.dat	1.1462E-04	1.2118E-04	5.720
PNNL\Rapco\TcO4\25C\AN-105\D-5\D-5b.dat	1.7254E-04	1.5034E-04	-12.866
PNNL\Rapco\TcO4\25C\AN-105\D-7\D-7a.dat	1.1038E-05	1.1513E-05	4.306
PNNL\Rapco\TcO4\25C\AN-105\D-7\D-7b.dat	1.2089E-05	1.3046E-05	7.913
PNNL\Rapco\TcO4\25C\Simple\F-1\F-1a.dat	6.4783E-05	4.2406E-05	-34.542
PNNL\Rapco\TcO4\25C\Simple\F-1\F-1b.dat	8.1802E-05	5.0823E-05	-37.870
PNNL\Rapco\TcO4\25C\Simple\F-2\F-2a.dat	2.9182E-04	2.5777E-04	-11.667
PNNL\Rapco\TcO4\25C\Simple\F-2\F-2b.dat	3.1595E-04	2.5533E-04	-19.185
PNNL\Rapco\TcO4\25C\Simple\F-3\F-3a.dat	4.6743E-04	4.2831E-04	-8.370
PNNL\Rapco\TcO4\25C\Simple\F-3\F-3b.dat	4.8129E-04	4.3107E-04	-10.435
PNNL\Rapco\TcO4\25C\Simple\F-4\F-4a.dat	7.9218E-04	7.7038E-04	-2.752
PNNL\Rapco\TcO4\25C\Simple\F-4\F-4b.dat	7.9326E-04	7.9553E-04	0.286
PNNL\Rapco\TcO4\25C\Simple\F-5\F-5a.dat	1.0709E-03	1.0699E-03	-0.096
PNNL\Rapco\TcO4\25C\Simple\F-5\F-5b.dat	1.0676E-03	1.0793E-03	1.098
PNNL\Burgeson\TcO4\25C\AP-101\E-1\E-1.dat	3.1570E-06	3.7112E-06	17.553
PNNL\Burgeson\TcO4\25C\AP-101\E-1\E-1D.dat	3.1618E-06	3.6648E-06	15.909
PNNL\Burgeson\TcO4\25C\AP-101\E-2\E-2.dat	1.4188E-04	1.4044E-04	-1.012
PNNL\Burgeson\TcO4\25C\AP-101\E-2\E-2D.dat	1.2806E-04	1.4099E-04	10.098
PNNL\Burgeson\TcO4\25C\AP-101\E-3\E-3.dat	6.0558E-04	5.0699E-04	-16.280
PNNL\Burgeson\TcO4\25C\AP-101\E-3\E-3D.dat	5.6806E-04	5.0502E-04	-11.097
PNNL\Burgeson\TcO4\25C\AP-101\E-4\E-4.dat	1.0320E-06	1.3809E-06	33.805
PNNL\Burgeson\TcO4\25C\AP-101\E-4\E-4D.dat	1.0721E-06	2.6308E-06	145.384
PNNL\Burgeson\TcO4\25C\AN-102\A-1\A-1.dat	9.8799E-06	1.1295E-05	14.322
PNNL\Burgeson\TcO4\25C\AN-102\A-1\A-1D.dat	9.3442E-06	1.1397E-05	21.967
PNNL\Burgeson\TcO4\25C\AN-102\A-2\A-2.dat	1.0654E-04	1.2406E-04	16.441
PNNL\Burgeson\TcO4\25C\AN-102\A-2\A-2D.dat	9.4632E-05	1.2683E-04	34.023
PNNL\Burgeson\TcO4\25C\AN-102\A-3\A-3.dat	3.0413E-04	4.1746E-04	37.264
PNNL\Burgeson\TcO4\25C\AN-102\A-3\A-3D.dat	3.4103E-04	4.6591E-04	36.618
PNNL\Burgeson\TcO4\25C\AZ-101\B-1\B-1.dat	1.9156E-05	1.6775E-05	-12.429
PNNL\Burgeson\TcO4\25C\AZ-101\B-1\B-1D.dat	1.7059E-05	1.6079E-05	-5.742
PNNL\Burgeson\TcO4\25C\AZ-101\B-2\B-2.dat	3.2075E-05	2.8868E-05	-9.998
PNNL\Burgeson\TcO4\25C\AZ-101\B-2\B-2D.dat	3.5866E-05	2.9020E-05	-19.088
PNNL\Burgeson\TcO4\25C\AZ-101\B-3\B-3.dat	9.5682E-05	9.6935E-05	1.310
PNNL\Burgeson\TcO4\25C\AZ-101\B-3\B-3D.dat	1.0917E-04	9.1111E-05	-16.542
PNNL\Burgeson\TcO4\25C\AZ-101\B-4\B-4.dat	2.0306E-04	1.7187E-04	-15.360
PNNL\Burgeson\TcO4\25C\AZ-101\B-4\B-4D.dat	2.1033E-04	1.7357E-04	-17.478
PNNL\Blanchard\TcO4\25C\AW-101\A-1\A-1.dat	6.3100E-06	9.8648E-06	56.336
PNNL\Blanchard\TcO4\25C\AW-101\A-1\A-1D.dat	6.6300E-06	8.4865E-06	28.001
PNNL\Blanchard\TcO4\25C\AW-101\A-2\A-2.dat	6.3900E-05	9.6443E-05	50.928
PNNL\Blanchard\TcO4\25C\AW-101\A-2\A-2D.dat	8.2900E-05	9.9866E-05	20.466
PNNL\Blanchard\TcO4\25C\AW-101\A-3\A-3.dat	4.2200E-04	4.7971E-04	13.675
PNNL\Blanchard\TcO4\25C\AW-101\A-3\A-3D.dat	4.2600E-04	4.9688E-04	16.638
PNNL\Blanchard\TcO4\25C\AN-107\B-1\B-1.dat	9.5316E-06	1.1381E-05	19.404
PNNL\Blanchard\TcO4\25C\AN-107\B-1\B-1D.dat	6.1808E-06	1.1226E-05	81.635
PNNL\Blanchard\TcO4\25C\AN-107\B-2\B-2.dat	1.0032E-05	1.0530E-05	4.969
PNNL\Blanchard\TcO4\25C\AN-107\B-2\B-2D.dat	9.2600E-06	1.0579E-05	14.240
PNNL\Kurath\TcO4\21C\AW-101\Kinetics\K-1.dat	5.7800E-06	7.4252E-06	28.464
PNNL\Kurath\TcO4\21C\AW-101\W39\W39.dat	9.8300E-06	9.2176E-06	-6.230
PNNL\Kurath\TcO4\21C\AW-101\W39\W39-R.dat	7.4800E-06	9.3723E-06	25.298
PNNL\Kurath\TcO4\21C\AW-101\W39D\W39D.dat	9.7100E-06	9.0806E-06	-6.482

PNNL\Kurath\TcO4\21C\AW-101\W39D\W39D-R.dat	6.9600E-06	9.2330E-06	32.659
PNNL\Kurath\TcO4\21C\AW-101\W39-S1\W39-S1.dat	6.7800E-05	7.7112E-05	13.734
PNNL\Kurath\TcO4\21C\AW-101\W39-S1\W39-S1R.dat	7.9200E-05	7.7112E-05	-2.637
PNNL\Kurath\TcO4\21C\AW-101\W39-S1\W39-S1D.dat	6.6700E-05	7.8963E-05	18.386
PNNL\Kurath\TcO4\21C\AW-101\W39-S2\W39-S2.dat	4.1000E-04	3.9937E-04	-2.593
PNNL\Kurath\TcO4\21C\AW-101\W39-S2\W39-S2R.dat	4.0500E-04	3.9937E-04	-1.391
PNNL\Kurath\TcO4\21C\AW-101\W39-S2\W39-S2D.dat	3.3600E-04	4.0628E-04	20.917
PNNL\Kurath\TcO4\21C\AN-107\N39\N39.dat	3.6200E-06	2.8282E-06	-21.874
PNNL\Kurath\TcO4\21C\AN-107\N39\N39D.dat	3.5200E-06	2.8810E-06	-18.154
PNNL\Kurath\TcO4\21C\AN-107\N39\N39D-R.dat	2.3700E-06	2.8810E-06	21.560
SRNL\Hassan\TcO4\25C\AN-103\Bat-1_Column\Hassan-AN-103.dat	2.4015E-05	2.3996E-05	-0.078
SRNL\King2002\ReO4\25C\AN-105\Exp-1_Bat-2_Column\King-AN-105.dat	2.9430E-05	2.9424E-05	-0.022
PNNL\Burgeson2002\TcO4\25C\AP-101\Bat-3_Column\Burgeson-AP-101.dat	2.9997E-05	2.9959E-05	-0.126
PNNL\Burgeson2002\TcO4\25C\AZ-101\Bat-3_Column\Burgeson-AZ-101.dat	2.2498E-04	2.2475E-04	-0.101
PNNL\Burgeson2002\TcO4\25C\AN-102\Bat-3_Column\Burgeson-AN-102.dat	1.6248E-05	1.6239E-05	-0.055
SRNL\King\ReO4\25C\AN-105\Exp-1_Bat-4_Column\King-AN-105.dat	8.5929E-05	8.5913E-05	-0.019
SRNL\King2002\ReO4\25C\AN-105\Exp-5_Bat-5_Column\King-AN-105.dat	6.2700E-05	6.2670E-05	-0.047
SRNL\King2002\ReO4\25C\AZ-102\Exp-8_Bat-5_Column\King-AZ-102.dat	2.0700E-04	2.0687E-04	-0.063
SRNL\King2002\ReO4\25C\AN-107\Exp-9_Bat-5_Column\King-AN-107.dat	3.0600E-05	3.0594E-05	-0.019
SRNL\King\ReO4\25C\AN-105\Exp-5_Bat-6_Column\King-AN-105.dat	7.5188E-05	7.5164E-05	-0.032
SRNL\Steimke\ReO4\25C\AN-105\Run-9_Bat-6_Column\Pilot-Scale.dat	5.9613E-05	5.9595E-05	-0.031
SRNL\King\TcO4\25C\Tank-44F\Bat-6_Low-NO3_Column\King-Tank-44_Low-NO3.dat	3.1232E-05	3.1180E-05	-0.165

```
                                                    (150)RMS error total   =     27.644
                                                    (046)RMS error ReO4-   =     24.859
                                                    (104)RMS error TcO4-   =     28.790

                                                    (150)Avg error total   =     -2.429
                                                    (046)Avg error ReO4-   =     -0.976
                                                    (104)Avg error TcO4-   =     -3.071

                                                    (030)RMS error batch 1 =     29.470
                                                    (030)avg error batch 1 =    -23.211

                                                    (003)RMS error batch 2 =     75.980
                                                    (003)avg error batch 2 =     61.904

                                                    (056)RMS error batch 3 =     20.133
                                                    (056)avg error batch 3 =     -7.366

                                                    (037)RMS error batch 4 =     25.125
                                                    (037)avg error batch 4 =     11.811

                                                    (014)RMS error batch 5 =     14.667
                                                    (014)avg error batch 5 =     -2.751

                                                    (010)RMS error batch 6 =     47.105
                                                    (010)avg error batch 6 =     16.033

****************************************** XO4- Kds ************************************************************
```

Batch Contact Dataset	Kd (Observed) (ml/g)	Kd (Computed) (ml/g)	Error (%)
SRNL\King\ReO4\25C\AN-105\BNF-SSIX-10-1\BNF-SSIX-10-1.dat	3.9962E+02	4.4449E+02	11.229
SRNL\King\ReO4\25C\AN-105\BNF-SSIX-10-1\BNF-SSIX-10-1-D.dat	3.8983E+02	4.4449E+02	14.021
SRNL\King\ReO4\25C\AN-105\BNF-SSIX-10-2\BNF-SSIX-10-2.dat	3.4657E+02	4.2491E+02	22.604
SRNL\King\ReO4\25C\AN-105\BNF-SSIX-10-2\BNF-SSIX-10-2-D.dat	3.3614E+02	4.2484E+02	26.387
SRNL\King\ReO4\25C\AN-105\BNF-SSIX-10-3\BNF-SSIX-10-3.dat	4.2594E+02	4.4767E+02	5.101
SRNL\King\ReO4\25C\AN-105\BNF-SSIX-10-3\BNF-SSIX-10-3-D.dat	4.2415E+02	4.4768E+02	5.548
SRNL\King\ReO4\25C\AN-105\BNF-SSIX-10-5\BNF-SSIX-10-5.dat	3.8181E+02	4.4956E+02	17.745
SRNL\King\ReO4\25C\AN-105\BNF-SSIX-10-5\BNF-SSIX-10-5-D.dat	3.2830E+02	4.4958E+02	36.939
SRNL\King\ReO4\25C\AN-105\BNF-SSIX-17-1\BNF-SSIX-17-1.dat	2.8888E+02	2.0143E+02	-30.272
SRNL\King\ReO4\25C\AN-105\BNF-SSIX-17-1\BNF-SSIX-17-1-D.dat	3.4771E+02	2.0144E+02	-42.065
SRNL\King\ReO4\25C\AN-105\BNF-SSIX-17-2\BNF-SSIX-17-2.dat	1.8383E+02	1.8802E+02	2.280
SRNL\King\ReO4\25C\AN-105\BNF-SSIX-17-2\BNF-SSIX-17-2-D.dat	1.8202E+02	1.8805E+02	3.311
SRNL\King\ReO4\25C\AN-105\BNF-SSIX-17-3\BNF-SSIX-17-3.dat	1.4707E+02	1.6917E+02	15.026
SRNL\King\ReO4\25C\AN-105\BNF-SSIX-17-3\BNF-SSIX-17-3-D.dat	1.4103E+02	1.6919E+02	19.960
SRNL\King\ReO4\25C\AN-105\BNF-SSIX-17-4\BNF-SSIX-17-4.dat	1.1964E+02	1.5439E+02	29.045
SRNL\King\ReO4\25C\AN-105\BNF-SSIX-17-4\BNF-SSIX-17-4-D.dat	1.1663E+02	1.5451E+02	32.473
SRNL\King\ReO4\25C\AN-105\BNF-SSIX-17-5\BNF-SSIX-17-5.dat	2.0435E+02	2.0313E+02	-0.600
SRNL\King\ReO4\25C\AN-105\BNF-SSIX-17-5\BNF-SSIX-17-5-D.dat	1.9815E+02	2.0313E+02	2.510
SRNL\King\ReO4\25C\AN-105\BNF-SSIX-17-7\BNF-SSIX-17-7.dat	2.0078E+02	2.0501E+02	2.107
SRNL\King\ReO4\25C\AN-105\BNF-SSIX-17-7\BNF-SSIX-17-7-D.dat	2.1981E+02	2.0500E+02	-6.737
SRNL\King\ReO4\25C\AN-105\BNF-SSIX-17-6\BNF-SSIX-17-6.dat	5.3623E+02	2.2050E+02	-58.880
SRNL\King\ReO4\25C\AN-105\BNF-SSIX-17-6\BNF-SSIX-17-6-D.dat	4.9829E+02	2.2050E+02	-55.749
SRNL\Duffey\ReO4\25C\AN-105\Exp-01\Exp-01.dat	5.2090E+02	5.1700E+02	-0.747
SRNL\Duffey\ReO4\25C\AN-105\Exp-02\Exp-02.dat	5.1054E+02	5.1672E+02	1.211
SRNL\Duffey\ReO4\25C\AN-105\Exp-05\Exp-05.dat	4.2872E+02	5.1674E+02	20.532
SRNL\Duffey\ReO4\25C\AN-105\Exp-06\Exp-06.dat	4.5513E+02	5.1726E+02	13.651
SRNL\Duffey\ReO4\25C\AN-105\Exp-07\Exp-07.dat	4.8737E+02	5.1720E+02	6.121
SRNL\Duffey\ReO4\25C\AN-105\Exp-08\Exp-08.dat	5.0304E+02	5.1662E+02	2.699
SRNL\Duffey\ReO4\25C\AN-105\Exp-09\Exp-09.dat	4.8581E+02	5.1649E+02	6.316
SRNL\Duffey\ReO4\25C\AZ-102\Exp-10\Exp-10.dat	1.0430E+03	8.2119E+02	-21.269
SRNL\Duffey\ReO4\25C\AN-107\Exp-11\Exp-11.dat	2.7416E+02	1.7324E+02	-36.809
PNNL\Rapco\ReO4\25C\AN-105\D-6\D-6a.dat	3.7981E+02	5.8187E+02	53.199
PNNL\Rapco\ReO4\25C\AN-105\D-6\D-6b.dat	3.3948E+02	5.9215E+02	74.429
PNNL\Rapco\ReO4\25C\AN-105\D-8\D-8a.dat	4.9003E+02	6.4722E+02	32.078
PNNL\Rapco\ReO4\25C\AN-105\D-8\D-8b.dat	5.2219E+02	6.4481E+02	23.483
PNNL\Rapco\ReO4\25C\AN-105\D-9\D-9a.dat	4.7628E+02	6.4718E+02	35.882
PNNL\Rapco\ReO4\25C\AN-105\D-9\D-9b.dat	4.6828E+02	6.4617E+02	37.988
PNNL\Rapco\ReO4\25C\Simple\D-10\D-10a.dat	2.5446E+02	3.3896E+02	33.206
PNNL\Rapco\ReO4\25C\Simple\D-10\D-10b.dat	2.5091E+02	3.4623E+02	37.987
SRNL\King\TcO4\25C\Tank-44F\SRS-1\SRS-1.dat	1.1498E+03	2.2617E+03	96.702
SRNL\King\TcO4\25C\Tank-44F\SRS-1\SRS-1-D.dat	1.1942E+03	2.2616E+03	89.384
SRNL\Hassan\TcO4\25C\AN-102\BNF-LC305-S639\BNF-LC305-S639-1.dat	2.5024E+02	5.5886E+02	123.327
SRNL\Hassan\TcO4\25C\AN-102\BNF-LC305-S639\BNF-LC305-S639-1D.dat	3.1223E+02	5.5884E+02	78.983
SRNL\Hassan\TcO4\25C\AN-102\BNF-LC305-S639-1R\BNF-LC305-S639-1R-1.dat	3.3157E+02	5.6097E+02	69.185
SRNL\Hassan\TcO4\25C\AN-102\BNF-LC305-S639-SPK\BNF-LC305-S639-SPK-1.dat	2.7729E+02	5.4238E+02	95.602
SRNL\Hassan\TcO4\25C\AN-102\BNF-LC305-S639-SPK\BNF-LC305-S639-SPK-1D.dat	2.9776E+02	5.4508E+02	83.061
SRNL\Hassan\TcO4\25C\AN-103\BNF-A325-S39\BNF-A325-S39-1.dat	4.8445E+02	7.7538E+02	60.054

SRNL\Hassan\TcO4\25C\AN-103\BNF-A325-S39\BNF-A325-S39-1D.dat	5.7649E+02	7.7555E+02	34.529
SRNL\Hassan\TcO4\25C\AN-103\BNF-A325-S39-1R\BNF-A325-S39-1R-1.dat	7.9869E+02	7.7981E+02	-2.364
SRNL\Hassan\TcO4\25C\AN-103\BNF-A325-S39-1R\BNF-A325-S39-1R-1D.dat	6.2761E+02	7.7993E+02	24.270
SRNL\Hassan\TcO4\25C\AN-103\BNF-A325-S39-2R\BNF-A325-S39-2R-1.dat	4.8854E+02	7.8272E+02	60.216
SRNL\Hassan\TcO4\25C\AN-103\BNF-A325-S39-2R\BNF-A325-S39-2R-1D.dat	4.2890E+02	7.8259E+02	82.465
SRNL\Hassan\TcO4\25C\AN-103\BNF-A325-S39-SPR\BNF-A325-S39-SPR-1.dat	4.5374E+02	7.6013E+02	67.525
SRNL\Hassan\TcO4\25C\AN-103\BNF-A325-S39-SPR\BNF-A325-S39-SPR-1D.dat	4.4954E+02	7.5976E+02	69.010
SRNL\Hassan\TcO4\25C\AZ-102\BNF-B305-S639\BNF-B305-S639-1.dat	9.1760E+02	1.2309E+03	34.143
SRNL\Hassan\TcO4\25C\AZ-102\BNF-B305-S639\BNF-B305-S639-1D.dat	8.5333E+02	1.2311E+03	44.269
SRNL\Hassan\TcO4\25C\AZ-102\BNF-B305-S639-1R\BNF-B305-S639-1R-1.dat	8.3492E+02	1.2628E+03	51.253
SRNL\Hassan\TcO4\25C\AZ-102\BNF-B305-S639-1R\BNF-B305-S639-1R-1D.dat	1.1277E+03	1.2627E+03	11.972
SRNL\Hassan\TcO4\25C\AZ-102\BNF-A325-S39-2R\BNF-A325-S39-2R-1.dat	7.5574E+02	1.2743E+03	68.610
SRNL\Hassan\TcO4\25C\AZ-102\BNF-A325-S39-3R\BNF-A325-S39-3R-1.dat	1.7781E+03	1.2846E+03	-27.754
SRNL\Hassan\TcO4\25C\AW-101\AW101-Kd39-1\AW101-Kd39-1-filtrate-1.dat	8.4190E+02	1.1504E+03	36.646
SRNL\Hassan\TcO4\25C\AW-101\AW101-Kd39-1\AW101-Kd39-1-filtrate-2.dat	7.6908E+02	1.1509E+03	49.651
PNNL\Rapco\TcO4\25C\Simple\B-1\B-1a.dat	2.9983E+03	3.8874E+03	29.655
PNNL\Rapco\TcO4\25C\Simple\B-1\B-1b.dat	3.1292E+03	3.9120E+03	25.015
PNNL\Rapco\TcO4\25C\Simple\B-2\B-2a.dat	2.9559E+03	3.5277E+03	19.345
PNNL\Rapco\TcO4\25C\Simple\B-2\B-2b.dat	2.9622E+03	3.6246E+03	22.361
PNNL\Rapco\TcO4\25C\Simple\B-3\B-3a.dat	2.8445E+03	3.2538E+03	14.388
PNNL\Rapco\TcO4\25C\Simple\B-3\B-3b.dat	2.6472E+03	3.4005E+03	28.455
PNNL\Rapco\TcO4\25C\Simple\B-4\B-4a.dat	2.5077E+03	3.1794E+03	26.785
PNNL\Rapco\TcO4\25C\Simple\B-4\B-4b.dat	2.5435E+03	3.2943E+03	29.518
PNNL\Rapco\TcO4\25C\Simple\D-1\D-1a.dat	2.2212E+03	3.5087E+03	57.963
PNNL\Rapco\TcO4\25C\Simple\D-1\D-1b.dat	2.2457E+03	3.5078E+03	56.196
PNNL\Rapco\TcO4\25C\Simple\D-2\D-2a.dat	1.9729E+03	2.5779E+03	30.668
PNNL\Rapco\TcO4\25C\Simple\D-2\D-2b.dat	2.1015E+03	2.5562E+03	21.633
PNNL\Rapco\TcO4\25C\Simple\D-3\D-3a.dat	6.5257E+02	6.2951E+02	-3.534
PNNL\Rapco\TcO4\25C\Simple\D-3\D-3b.dat	6.6238E+02	6.2878E+02	-5.073
PNNL\Rapco\TcO4\25C\Simple\D-4\D-4a.dat	9.3440E+02	7.3162E+02	-21.702
PNNL\Rapco\TcO4\25C\Simple\D-4\D-4b.dat	9.0032E+02	7.3190E+02	-18.707
PNNL\Rapco\TcO4\25C\AN-105\D-5\D-5a.dat	1.1660E+03	1.0970E+03	-5.920
PNNL\Rapco\TcO4\25C\AN-105\D-5\D-5b.dat	9.0912E+02	1.0636E+03	16.996
PNNL\Rapco\TcO4\25C\AN-105\D-7\D-7a.dat	1.3197E+03	1.2603E+03	-4.500
PNNL\Rapco\TcO4\25C\AN-105\D-7\D-7b.dat	1.3683E+03	1.2585E+03	-8.023
PNNL\Rapco\TcO4\25C\Simple\F-1\F-1a.dat	2.1776E+03	3.3864E+03	55.511
PNNL\Rapco\TcO4\25C\Simple\F-1\F-1b.dat	2.0180E+03	3.3293E+03	64.977
PNNL\Rapco\TcO4\25C\Simple\F-2\F-2a.dat	4.2142E+02	4.9288E+02	16.955
PNNL\Rapco\TcO4\25C\Simple\F-2\F-2b.dat	3.7636E+02	4.9406E+02	31.275
PNNL\Rapco\TcO4\25C\Simple\F-3\F-3a.dat	2.4243E+02	2.7675E+02	14.157
PNNL\Rapco\TcO4\25C\Simple\F-3\F-3b.dat	2.3327E+02	2.7610E+02	18.360
PNNL\Rapco\TcO4\25C\Simple\F-4\F-4a.dat	8.5757E+01	9.1860E+01	7.117
PNNL\Rapco\TcO4\25C\Simple\F-4\F-4b.dat	9.2445E+01	9.1786E+01	-0.713
PNNL\Rapco\TcO4\25C\Simple\F-5\F-5a.dat	2.7353E+01	2.7487E+01	0.492
PNNL\Rapco\TcO4\25C\Simple\F-5\F-5b.dat	2.9304E+01	2.7650E+01	-5.643
PNNL\Burgeson\TcO4\25C\AP-101\E-1\E-1.dat	7.9557E+02	6.6092E+02	-16.925
PNNL\Burgeson\TcO4\25C\AP-101\E-1\E-1D.dat	7.8174E+02	6.6097E+02	-15.448
PNNL\Burgeson\TcO4\25C\AP-101\E-2\E-2.dat	5.5113E+02	5.5792E+02	1.233
PNNL\Burgeson\TcO4\25C\AP-101\E-2\E-2D.dat	6.2487E+02	5.5757E+02	-10.770
PNNL\Burgeson\TcO4\25C\AP-101\E-3\E-3.dat	3.1263E+02	3.9364E+02	25.913
PNNL\Burgeson\TcO4\25C\AP-101\E-3\E-3D.dat	3.3884E+02	3.9426E+02	16.357

PNNL\Burgeson\TcO4\25C\AP-101\E-4\E-4.dat	1.7785E+03	1.3032E+03	-26.722
PNNL\Burgeson\TcO4\25C\AP-101\E-4\E-4D.dat	1.7797E+03	6.6184E+02	-62.811
PNNL\Burgeson\TcO4\25C\AN-102\A-1\A-1.dat	6.4138E+02	5.4661E+02	-14.776
PNNL\Burgeson\TcO4\25C\AN-102\A-1\A-1D.dat	6.7877E+02	5.4659E+02	-19.474
PNNL\Burgeson\TcO4\25C\AN-102\A-2\A-2.dat	6.1605E+02	5.1352E+02	-16.642
PNNL\Burgeson\TcO4\25C\AN-102\A-2\A-2D.dat	7.2565E+02	5.1278E+02	-29.336
PNNL\Burgeson\TcO4\25C\AN-102\A-3\A-3.dat	6.4680E+02	4.4369E+02	-31.402
PNNL\Burgeson\TcO4\25C\AN-102\A-3\A-3D.dat	6.3461E+02	4.3404E+02	-31.605
PNNL\Burgeson\TcO4\25C\AZ-101\B-1\B-1.dat	1.1287E+03	1.3045E+03	15.573
PNNL\Burgeson\TcO4\25C\AZ-101\B-1\B-1D.dat	1.2246E+03	1.3056E+03	6.614
PNNL\Burgeson\TcO4\25C\AZ-101\B-2\B-2.dat	1.1439E+03	1.2833E+03	12.189
PNNL\Burgeson\TcO4\25C\AZ-101\B-2\B-2D.dat	1.0168E+03	1.2831E+03	26.192
PNNL\Burgeson\TcO4\25C\AZ-101\B-3\B-3.dat	1.1921E+03	1.1753E+03	-1.406
PNNL\Burgeson\TcO4\25C\AZ-101\B-3\B-3D.dat	9.7151E+02	1.1835E+03	21.822
PNNL\Burgeson\TcO4\25C\AZ-101\B-4\B-4.dat	8.9437E+02	1.0762E+03	20.327
PNNL\Burgeson\TcO4\25C\AZ-101\B-4\B-4D.dat	8.6749E+02	1.0742E+03	23.823
PNNL\Blanchard\TcO4\25C\AW-101\A-1\A-1.dat	7.4512E+02	4.2478E+02	-42.991
PNNL\Blanchard\TcO4\25C\AW-101\A-1\A-1D.dat	5.7799E+02	4.2565E+02	-26.357
PNNL\Blanchard\TcO4\25C\AW-101\A-2\A-2.dat	6.3684E+02	3.7795E+02	-40.653
PNNL\Blanchard\TcO4\25C\AW-101\A-2\A-2D.dat	4.8117E+02	3.7630E+02	-21.794
PNNL\Blanchard\TcO4\25C\AW-101\A-3\A-3.dat	3.0704E+02	2.5400E+02	-17.274
PNNL\Blanchard\TcO4\25C\AW-101\A-3\A-3D.dat	3.1514E+02	2.5033E+02	-20.567
PNNL\Blanchard\TcO4\25C\AN-107\B-1\B-1.dat	2.5688E+02	1.9767E+02	-23.049
PNNL\Blanchard\TcO4\25C\AN-107\B-1\B-1D.dat	4.4497E+02	1.9769E+02	-55.572
PNNL\Blanchard\TcO4\25C\AN-107\B-2\B-2.dat	1.8577E+02	1.7214E+02	-7.333
PNNL\Blanchard\TcO4\25C\AN-107\B-2\B-2D.dat	2.1131E+02	1.7214E+02	-18.536
PNNL\Kurath\TcO4\21C\AW-101\Kinetics\K-1.dat	6.8531E+02	5.1180E+02	-25.318
PNNL\Kurath\TcO4\21C\AW-101\W39\W39.dat	4.5057E+02	4.8736E+02	8.166
PNNL\Kurath\TcO4\21C\AW-101\W39\W39-R.dat	6.3662E+02	4.8724E+02	-23.465
PNNL\Kurath\TcO4\21C\AW-101\W39D\W39D.dat	4.4931E+02	4.8748E+02	8.495
PNNL\Kurath\TcO4\21C\AW-101\W39D\W39D-R.dat	6.7964E+02	4.8735E+02	-28.292
PNNL\Kurath\TcO4\21C\AW-101\W39-S1\W39-S1.dat	5.1236E+02	4.3846E+02	-14.423
PNNL\Kurath\TcO4\21C\AW-101\W39-S1\W39-S1R.dat	4.2428E+02	4.3846E+02	3.343
PNNL\Kurath\TcO4\21C\AW-101\W39-S1\W39-S1D.dat	5.3646E+02	4.3726E+02	-18.491
PNNL\Kurath\TcO4\21C\AW-101\W39-S2\W39-S2.dat	2.8673E+02	2.9705E+02	3.599
PNNL\Kurath\TcO4\21C\AW-101\W39-S2\W39-S2R.dat	2.9153E+02	2.9705E+02	1.893
PNNL\Kurath\TcO4\21C\AW-101\W39-S2\W39-S2D.dat	3.7810E+02	2.9501E+02	-21.975
PNNL\Kurath\TcO4\21C\AN-107\N39\N39.dat	1.2236E+02	1.8649E+02	52.410
PNNL\Kurath\TcO4\21C\AN-107\N39\N39D.dat	1.3269E+02	1.8649E+02	40.545
PNNL\Kurath\TcO4\21C\AN-107\N39\N39D-R.dat	2.5038E+02	1.8649E+02	-25.518
SRNL\Hassan\TcO4\25C\AN-103\Bat-1_Column\Hassan-AN-103.dat	7.6806E+02	7.6971E+02	0.215
SRNL\King2002\ReO4\25C\AN-105\Exp-1_Bat-2_Column\King-AN-105.dat	2.1861E+02	2.2082E+02	1.007
PNNL\Burgeson2002\TcO4\25C\AP-101\Bat-3_Column\Burgeson-AP-101.dat	1.2035E+03	1.2641E+03	5.032
PNNL\Burgeson2002\TcO4\25C\AZ-101\Bat-3_Column\Burgeson-AZ-101.dat	9.0488E+02	1.0123E+03	11.874
PNNL\Burgeson2002\TcO4\25C\AN-102\Bat-3_Column\Burgeson-AN-102.dat	6.2826E+02	5.4552E+02	-13.170
SRNL\King\ReO4\25C\AN-105\Exp-1_Bat-4_Column\King-AN-105.dat	1.9265E+02	1.9178E+02	-0.449
SRNL\King2002\ReO4\25C\AN-105\Exp-5_Bat-5_Column\King-AN-105.dat	4.2285E+02	4.7358E+02	11.995
SRNL\King2002\ReO4\25C\AZ-102\Exp-8_Bat-5_Column\King-AZ-102.dat	6.9947E+02	6.2714E+02	-10.341
SRNL\King2002\ReO4\25C\AN-107\Exp-9_Bat-5_Column\King-AN-107.dat	1.8503E+02	1.8604E+02	0.547
SRNL\King\ReO4\25C\AN-105\Exp-5_Bat-6_Column\King-AN-105.dat	3.0525E+02	3.1893E+02	4.481
SRNL\Steimke\ReO4\25C\AN-105\Run-9_Bat-6_Column\Pilot-Scale.dat	2.9111E+02	3.1511E+02	8.245

```
SRNL\King\TcO4\25C\Tank-44F\Bat-6_Low-NO3_Column\King-Tank-44_Low-NO3.dat 1.8180E+03      1.6408E+03         -9.746

                                                                    (150)RMS error total   =     35.319
                                                                    (046)RMS error ReO4-   =     26.861
                                                                    (104)RMS error TcO4-   =     38.471

                                                                    (150)Avg error total   =     11.840
                                                                    (046)Avg error ReO4-   =      8.422
                                                                    (104)Avg error TcO4-   =     13.351

                                                                    (030)RMS error batch 1 =     57.560
                                                                    (030)avg error batch 1 =     45.141

                                                                    (003)RMS error batch 2 =     46.818
                                                                    (003)avg error batch 2 =    -37.874

                                                                    (056)RMS error batch 3 =     28.645
                                                                    (056)avg error batch 3 =     14.307

                                                                    (037)RMS error batch 4 =     24.891
                                                                    (037)avg error batch 4 =     -7.745

                                                                    (014)RMS error batch 5 =     21.648
                                                                    (014)avg error batch 5 =      5.729

                                                                    (010)RMS error batch 6 =     23.895
                                                                    (010)avg error batch 6 =     -5.947
```

14.0 Appendix B (CERMOD Isotherm Code)

An improved method for the prediction of multicomponent ion exchange equilibria has been an ongoing research topic for decades. One of the more notable approaches was undertaken by Shallcross et al. (1988) and later upgraded by Mehablia et al. (1994). The detailed thermodynamic isotherm model developed for handling the high caustic DOE HLW solutions presented within this report has its origins within these earlier approaches. The code input and output structure has its origins from the ZAM code by Zheng et al. (1997) which is use to model DOE HLW in contact with CST material.

A Cation Exchange Resin Model (CERMOD v1.0 and 2.0) was developed by the Savannah River National Laboratory to simulate cation-exchange equilibria of electrolytic solutions in direct contact with SuperLig® 644 and Resorcinol-Formaldehyde resins. The current version of CERMOD, Version 3.0, was updated to model the strong-electrolyte absorption of $NaXO_4$, $NaNO_3$, KXO_4 and KNO_3 with SuperLig® 639. X referes to either Tc or Re.

CERMOD is written in Fortran 90 and compiled with Intel® Visual Fortran Composer XE 2013 for Windows XP Professional SP3 and Windows 7. This report contains or references the necessary material for using version 3.0 of CERMOD.

14.1 Model Description

The CERMOD model solves a set of equations for solid-liquid equilibrium (SLE). This model includes the competitive strong-electrolyte absorption of the following neutal species: $NaXO_4$, $NaNO_3$, KXO_4 and KNO_3. Nonidealities within the aqueous phase are handled using Pitzer's model for calculating ionic activity coefficients and water activity. Since Pitzer only established modeling parameters for some of the most common ions up to an ionic strength of ~6 molal, growing errors may occur when one uses the CERMOD code beyond 6 molal or when addressing solutions containing ions whose Pitzer parameters are currently not contained within CERMOD. A listing of the currently available ionic species contained within the CERMOD database is provided in Table B-1.

Table B-1. Aqueous-phase ionic species available within CERMOD Version 3.0.

ID	Cation	MW	ID	Anion	MW
1	Al^{+++}	26.9815	22	$Al(OH)_4^-$	95.0107
2	Ba^{++}	137.327	23	Br^-	79.904
3	Ca^{++}	40.078	24	$C_2O_4^{--}$	88.019
4	Cd^{++}	112.411	25	CH_3COO^-	59.0439
5	Co^{++}	58.9332	26	Cl^-	35.453
6	Cr^{+++}	51.9961	27	$COOH^-$	45.0174
7	Cs^+	132.905	28	CO_3^{--}	60.0089
8	Cu^{++}	63.546	29	F^-	18.9984
9	Fe^{+++}	55.845	30	HCO_3^-	61.0168
10	H^+	1.0079	31	HPO_4^{--}	95.9793
11	K^+	39.0983	32	I^-	126.90447
12	Li^+	6.941	33	NO_2^-	46.0055
13	Mg^{++}	24.305	34	NO_3^-	62.0049
14	Mn^{++}	54.938	35	OH^-	17.0073
15	Na^+	22.9898	36	PO_4^{---}	94.9714
16	Ni^{++}	58.6934	37	ReO_4^-	250.2046
17	Pb^{++}	207.2	38	SO_4^{--}	96.0626
18	Rb^+	85.4678	39	TcO_4^-	162.9046

ID	Cation	MW	ID	Anion	MW
19	Sr^{++}	87.62			
20	UO_2^{++}	270.028			
21	Zn^{++}	65.409			

Surface nonidealities on the solid phase resin are handled by assuming that the solid-phase is ideal. In future upgrades, solid-phase nonidealities may be handled by applying the Wilson's model to account for surface adsorption species interactions (Wilson, 1964). The Wilson's model appears to be a good basis for handling solution nonidealities on solids (based on low heat of reactions and used several times successfully in the literature; see Shallcross et al., 1988 and Mehablia et al., 1994). Another method of handling solid-phase non-idealities is the grouping of neighboring sites into a "super-site" model as was done for Crystalline Silicotitanates (CST) material by Zheng, et al. (1995, 1996, and 1997) where the super-site behave as ideal identities.

Mass-action relationships are written for each of the potential competitors ($NaXO_4$, $NaNO_3$, KXO_4 and KNO_3). Also species material balance equations are written relating the amount of each species within the liquid and solid phases in the initial state to amounts in the equilibrium state. To obtain these material balances the mass of SuperLig® 639 and mass of liquid (i.e., volume of liquid and its density) must also be specified. Solution of this set of nonlinear algebraic equations is achieved using a modified Powell hybrid algorithm and a finite-difference approximation to the Jacobian.

The solid-liquid equilibrium model solves the various mass-action equations involving strong-electrolyte absorption in conjunction with the appropriate material balance equations. At a specified operating temperature, CERMOD performs a numerical batch contact where the quantity of the following variables at their initial state must be specified:

- Initial composition of aqueous solution
- Pitzer temperature correction (yes or no)
- Pitzer ternary parameters (yes or no)
- Liquid density
- Sorbed species of interest (either TcO_4^- or ReO_4^-)
- SuperLig® 639 resin batch number
- Amount of SuperLig® 639 material present in wet form, dry mass is computed using the input value of the f-factor
- Initial loading of SuperLig® 639 (loading fractions in $NaXO_4$, $NaNO_3$, KXO_4 and KNO_3; typically resin is not loaded)

Upon solving the numerical batch contact, CERMOD outputs the following detailed information:

- Configuration header
- Dataset filename (parameter estimation)
- Title
- SuperLig® 639 resin batch number and id
- Liquid temperature and initial solution density
- Species name (cations to anions), molecular weight, valence and initial molar concentration
- Initial moles and activity of water

- Initial ionic strength of solution and initial pH
- Equilibrium constants
- Liquid volume, dry resin mass and phase ratio
- Total absorption capacity
- Fraction of total electrolyte sorption capacity
- $NaXO_4$, $NaNO_3$, KXO_4 and KNO_3 initial electrolyte solid loadings
- Nonlinear solver error flag and tolerance for L2 norm
- Species equilibrium molarities, molalities and ionic activity coefficients
- Equilibrium moles of water and water activity
- Equilibrium ionic strength and pH
- Equilibrium Na^+, K^+, XO_4^- and NO_3^- aqueous concentration, K_d, solid loading and fractional loading
- Unoccupied sites, total sorption sites, and total sites
- Estimate of Fruendlich/Langmuir hybrid isotherm parameters (optional)

In order to mathematically predict the state of the solid-electrolyte system, there are three essential steps involved. These are

1. Formulating a proper set of nonlinear algebraic equations in order to represent the system.
2. Obtaining, via published material and/or nonlinear regression, the required coefficients for the equilibrium constants and species interaction parameters for activity coefficient calculations.
3. Solving the nonlinear algebraic system numerically.

14.2 Model Formulation

Formulating a model for an isothermal solid-electrolyte system requires stating in mathematical expressions the following

1. Mass-action or reaction equilibria
2. Phase equilibria
3. Material balances
4. Electroneutrality

For each strong electrolyte (i.e. neutral species) that can possibly absorb onto the resin a mass-action equation is required. The following for strong electrolytes are currently being considered:

mass-action
$$K_{11}(T) = \frac{\hat{\gamma}_{NaXO_4} Q_{NaXO_4}}{\xi Q_L \gamma_{Na^+} m_{Na^+} \gamma_{XO_4^-} m_{XO_4^-}} \tag{B-1}$$

mass-action
$$K_{12}(T) = \frac{\hat{\gamma}_{NaNO_3} Q_{NaNO_3}}{Q_L \gamma_{Na^+} m_{Na^+} \gamma_{NO_3^-} m_{NO_3^-}} \tag{B-2}$$

mass-action $$K_{21}(T) = \frac{\hat{\gamma}_{KXO_4} Q_{KXO_4}}{\xi Q_L \gamma_{K^+} m_{K^+} \gamma_{XO_4^-} m_{XO_4^-}} \quad \text{(B-3)}$$

mass-action $$K_{22}(T) = \frac{\hat{\gamma}_{KNO_3} Q_{KNO_3}}{Q_L \gamma_{K^+} m_{K^+} \gamma_{NO_3^-} m_{NO_3^-}} \quad \text{(B-4)}$$

Material balances for the four ionic species loaded onto the solid (i.e., operating lines) are:

ionic solid loading $$Q_{Na^+} = Q^{\circ}_{Na^+} + (c^{\circ}_{Na^+} - c_{Na^+})\phi \quad \text{(B-5)}$$

ionic solid loading $$Q_{K^+} = Q^{\circ}_{K^+} + (c^{\circ}_{K^+} - c_{K^+})\phi \quad \text{(B-6)}$$

ionic solid loading $$Q_{XO_4^-} = Q^{\circ}_{XO_4^-} + (c^{\circ}_{XO_4^-} - c_{XO_4^-})\phi \quad \text{(B-7)}$$

ionic solid loading $$Q_{NO_3^-} = Q^{\circ}_{NO_3^-} + (c^{\circ}_{NO_3^-} - c_{NO_3^-})\phi \quad \text{(B-8)}$$

Only three of these ionic loading equations are independent. Four ionic balances on the solid-phase are:

ion balance $$Q_{Na^+} = Q_{NaXO_4} + Q_{NaNO_3} \quad \text{(B-9)}$$

ion balance $$Q_{K^+} = Q_{KXO_4} + Q_{KNO_3} \quad \text{(B-10)}$$

ion balance $$Q_{XO_4^-} = Q_{NaXO_4} + Q_{KXO_4} \quad \text{(B-11)}$$

ion balance $$Q_{NO_3^-} = Q_{NaNO_3} + Q_{KNO_3} \quad \text{(B-12)}$$

Only three of these ionic balances are independent. The solid-phase charge balance becomes:

solid phase charge balance $$Q_{Na^+} + Q_{K^+} = Q_{XO_4^-} + Q_{NO_3^-} \quad \text{(B-13)}$$

The liquid-phase charge balance becomes:

liquid phase charge balance $$\sum_{i=1}^{\text{cations}} z_i m_i = \sum_{j=1}^{\text{anions}} z_j m_j \quad \text{(B-14)}$$

The total number of resin sites becomes:

total resin sites $$Q_T = Q_L + Q_{Na^+} + Q_{K^+} \quad \text{(B-15)}$$

The dissociation reaction for water becomes:

dissociation water $$K_w(T) = \frac{\gamma_{H^+} m_{H^+} \gamma_{OH^-} m_{OH^-}}{a_w} \quad \text{(B-16)}$$

An overall (solid plus liquid phase) hydrogen balance becomes:

$$2n_w^o + V_L\left(c^\circ_{H^+} + c^\circ_{OH^-} + 4c^\circ_{Al(OH)_4^-} + 3c^\circ_{CH_3O_2^-} + c^\circ_{COOH^-} + c^\circ_{HCO_3^-} + c^\circ_{HPO_4^-}\right)$$

$$\text{H-balance} \quad = 2n_w + \frac{n_w}{\Omega}\left(m_{H^+} + m_{OH^-} + 4m_{Al(OH)_4^-} + 3m_{CH_3O_2^-} + m_{COOH^-} + m_{HCO_3^-} + m_{HPO_4^-}\right) \tag{B-17}$$

From the above list of equations 16 of them are independent and the following is a list of the 16 unknowns:

$$\text{16 unknowns} \left[\begin{array}{l} n_w, m_{H^+}, m_{OH^-}, m_{Na^+}, m_{K^+}, m_{XO_4^-}, m_{NO_3^-}, Q_{Na^+}, Q_{K^+}, Q_{XO_4^-}, Q_{NO_3^-}, Q_L, \\ Q_{NaXO_4}, Q_{NaNO_3}, Q_{KXO_4}, Q_{KNO_3} \end{array}\right] \tag{B-18}$$

The liquid-phase nonideality factors are computed using the Pitzer correlation and available correlation coefficients taken from the literature. The equilibrium constant for the dissociation reaction of water is specified from literature values.

For closure in the above set of equations the following parameters must also be specified in order to perform a numerical batch contact simulation:

$K_{11}(T)$ - Equilibrium constant for $NaXO_4$ sorption (B-19a)

$K_{12}(T)$ - Equilibrium constant for $NaNO_3$ sorption (B-19b)

$K_{21}(T)$ - Equilibrium constant for KXO_4 sorption (B-19c)

$K_{22}(T)$ - Equilibrium constant for KNO_3 sorption (B-19d)

Q_T - Total sorption capacity (batch dependent) (B-19e)

Q_L - Number of unoccupied sites (B-19f)

ξ - Selectivity ratio between ReO_4^- versus TcO_4^- (B-19g)

14.3 Pitzer Activity Coefficient Model

In an ideal-solution the local and long-range intermolecular forces between differing species are identical to those of similar molecules. For solutions containing ionic species charged particles interact with coulombic forces at small separations and, because of the formation of ionic clouds around each ion, damped coulombic forces exist at larger separation distances. These forces are much longer ranged than those involved in the interactions of neutral molecules, so that solute ions in solution interact at very low concentrations. Consequently, electrolyte solutions are nonideal even at very low concentrations resulting in electrolyte activity coefficients significantly different from unity at very low electrolyte concentrations. Debye and Hückel (1923), using a statistical mechanical model derived an adequate model to address electrolytes at very low concentrations (i.e., typically referred to as the Debye-Hückel limiting law). In their derivation they defined one key parameter to addressing nonideality within electrolyte solutions, the "ionic strength" defined as:

$$I = \frac{1}{2}\sum_i z_i^2 m_i$$

Unfortunately, this theoretically based law breaks down for electrolyte solutions with ionic strengths excessing ~0.01 molal. To extent the range of predicting nonideal behavior (i.e., ionic activity coefficients) to higher ionic strengths, many notable attempts have been made since 1923, all of which have been empirical in nature. There are two models that have been employed extensively for addressing electrolyte solutions at high ionic strengths: (1) Bromley's Model (Bromley, 1973) and (2) Pitzer's Model (Pitzer, 1973). We have chosen Pitzer's Model since more effort has recently been made in addressing electrolytic solutions of a high caustic nature. Both of these approaches added empirical terms to better account for the ionic strength dependence to the short-range forces effect in binary interactions (i.e., and sometimes in ternary interactions).

14.3.1 Overview

The derivation of the Pitzer activity coefficient model is based on Appendix C of "Aspen Physical Property System Physical Property Methods and Models 11.1" (2001, Aspen Technology, Inc).

14.3.2 Working Equations

Fürst and Renon (1982) propose the following expression as the Pitzer equation for the excess Gibbs energy:

$$\frac{G^E}{RT} = n_w \left[\begin{array}{l} f(I) + \sum_i \sum_j B_{ij} m_i m_j + \sum_i \sum_j \theta_{ij} m_i m_j + \tfrac{1}{2} \sum_i \sum_j \left(\sum_k m_k |z_k| \right) C_{ij} m_i m_j \\ + \tfrac{1}{6} \sum_i \sum_j \sum_k \Psi_{ijk} m_i m_j m_k \end{array} \right] \quad \text{(B-20)}$$

$$B_{ij} = f(\beta_{ij}^{(0)}, \beta_{ij}^{(1)}, \beta_{ij}^{(2)}) \quad \text{(B-21a)}$$

$$C_{ij} = f(C_{ij}^{\phi}, z_i, z_j) \quad \text{(B-21b)}$$

where

G^E .....excess Gibbs energy
R .....gas constant
T .....temperature
n_w .....kilograms of water
z_i .....charge number of ion i
m_i .....molality of ion i
i, j, k .....indices over all cations and anions

B, **C**, **θ** and **Ψ** are interaction parameters, f(I) is an electrostatic term that expresses the effect of long-range electrostatic forces between ions. This takes into account the hard-core effects of the Debye-Hückel theory. The cation-anion parameters **B** and **C** are characteristic for an aqueous single-electrolyte system. These parameters can be

determined by the properties of pure (apparent) electrolytes. **B** is expressed as a function of **β** (Eqs. (B-32) and (B-33)). **C** is expressed as a function of C^{ϕ} and z.

The parameters **θ** and **Ψ** are for the difference of interaction of unlike ions of the same sign from the mean of like ions. These parameters can be measured from common-ion mixtures.

The modified Pitzer expression for the excess Gibbs energy orders cations before anions. Fürst and Renon do not. All summations are taken over all ions i and j (both cations and anions). This involves making the parameter matrices B_{ij}, C_{ij}, θ_{ij} and Ψ_{ij} symmetric as follows:

Second-order parameters are written B_{ij} if i and j are ions of different sign. $B_{ij} = 0$ if the sign of z_i = sign of z_j, and $B_{ii} = 0$. Since cations are not ordered before anions, $B_{ij} = B_{ji}$. Second-order parameters are written θ_{ij} if i and j are ions of same sign. Thus $\theta_{ij} = 0$ if the sign of z_i is different from the sign of z_j, and $\theta_{ii} = 0$ with $\theta_{ij} = \theta_{ji}$.

Third-order parameters are written C_{ij} if i and j are ions of different sign. $C_{ij} = 0$ if the sign of z_i = sign of z_j, and $C_{ii} = 0$ with $C_{ij} = C_{ji}$. The matrix **C** is symmetric and $\sum_k m_k|z_k|$ is extended to all ions to make the equation symmetric.

Ψ_{ijk} is written for three different ions $\Psi_{ijk} = \Psi_{kij} = \Psi_{jki}$, and $\Psi_{ikk} = 0$. $\Psi_{ijk} = 0$ if the sign of z_i = sign of z_j = sign of z_k. Fürst and Renon's expression, Eq. (B-22), calculates the expressions for the activity coefficients and osmotic coefficients.

14.3.3 Calculation of Activity Coefficients

Taking the partial derivative of the expression for G^E yields expressions for the ionic activity coefficient

$$\begin{aligned}\ln\gamma_i &= \frac{\partial\left(G^E/RT\right)}{\partial n_i} \\ &= \tfrac{1}{2} z_i^2 f' + 2\sum_j B_{ij} m_j + \tfrac{1}{2} z_i^2 \sum_j \sum_k B'_{jk} m_j m_k + 2\sum_j \theta_{ij} m_j \\ &+ \tfrac{1}{2}|z_i| \sum_j \sum_k C_{jk} m_j m_k + \sum_j \left(\sum_k m_k |z_k| \right) C_{ij} m_j + \tfrac{1}{2} \sum_j \sum_k \Psi_{ijk} m_j m_k\end{aligned} \qquad \text{(B-22)}$$

where $B'_{jk} = dB_{jk}/dI$, $f' = df/dI$, and where the dependence of θ_{ij} on ionic strength is neglected $\left(\theta'_{ij} = 0\right)$. f and parameters B_{ij} are functions of ionic strength.

For water the logarithm of the activity is calculated as follows:

$$\ln a_w = \ln x_w + \ln \gamma_w \qquad \text{(B-23)}$$

The mole fraction of water x_w is computed as

$$x_w = \frac{\Omega}{\Omega + \sum_i m_i} \tag{B-24}$$

where $\Omega = 1000/M_w$ and M_w is the molecular weight of water. For water the logarithm of the activity coefficient is calculated as follows:

$$\ln \gamma_w = \frac{\partial\left(G^E/RT\right)}{\partial N_w} = \frac{\partial\left(G^E/RT\right)}{\Omega \partial n_w} \tag{B-25}$$

where N_w is the number of moles of water. Rearranging Eqn. (B-25) yields

$$\begin{aligned} \Omega \ln \gamma_w = f - If' - \sum_i \sum_j B_{ij} m_i m_j - I \sum_i \sum_j B'_{ij} m_i m_j - \sum_i \sum_j \theta_{ij} m_i m_j \\ - \sum_i \sum_j \left(\sum_k m_z |z_k| \right) C_{ij} m_i m_j - \tfrac{1}{3} \sum_i \sum_j \sum_k \Psi_{ijk} m_i m_j m_k \end{aligned} \tag{B-26}$$

$f(I)$ is the function describing the long-range electrostatic effects as a function of ionic strength as

$$f(I) = -A^{DH}\left(\frac{4I}{b}\right)\ln\left(1 + b\sqrt{I}\right) \tag{B-27}$$

where I is the ionic strength, defined as

$$I = \tfrac{1}{2} \sum_i m_i z_i^2 \tag{B-28}$$

b is an adjustable parameter, which has been optimized in this model to equal 1.2. Taking the derivative of Eq. (B-27) with respect to I, gives

$$f'(I) = \frac{df}{dI} = -2A^{DH}\left[\frac{\sqrt{I}}{1 + b\sqrt{I}} + \frac{2}{b}\ln\left(1 + b\sqrt{I}\right)\right] \tag{B-29}$$

so that

$$f - If' = \frac{2A^{DH} I^{3/2}}{1 + b\sqrt{I}} \tag{B-30}$$

This equation is used in Eq. (B-26). In Eqs. (B-27) and (B-29), A^{DH} is the Debye-Hückel constant for the osmotic coefficient on a log e basis, computed as

$$A^{DH} = \tfrac{1}{3}\left(\frac{2\pi N_A d_w}{1000}\right)^{1/2}\left(\frac{e}{\sqrt{DkT}}\right)^3 \tag{B-31}$$

where

N_A .....Avogadro's number
d_w .....water density
e .....electronic charge
D .....dielectric constant of solvent
k .....Boltzmann's constant
T .....absolute temperature

B_{ij} and B'_{ij} need expressions so that Eqs. (B-22) and (B-26) can be completely solved for the activity coefficients. The parameter B_{ij} is determined differently for different electrolyte pairings. For 1-N electrolytes (1-1, 1-2, 2-1, and so on) the following expression gives the parameter B_{ij}:

$$B_{ij} = \beta_{ij}^{(0)} + \frac{2\beta_{ij}^{(1)}}{\alpha_1^2 I}\left[1 - \left(1 + \alpha_1 I^{1/2}\right)e^{-\alpha_1 I^{1/2}}\right] \tag{B-32}$$

with $\alpha_1 = 2.0$.

For 2-2 electrolytes, B_{ij} is determined by the following expression:

$$B_{ij} = \beta_{ij}^{(0)} + \frac{2\beta_{ij}^{(1)}}{\alpha_1^2 I}\left[1 - \left(1 + \alpha_1 I^{1/2}\right)e^{-\alpha_1 I^{1/2}}\right] + \frac{2\beta_{ij}^{(2)}}{\alpha_2^2 I}\left[1 - \left(1 + \alpha_2 I^{1/2}\right)e^{-\alpha_2 I^{1/2}}\right] \tag{B-33}$$

with $\alpha_1 = 1.4$ and $\alpha_2 = 12.0$.

By taking appropriate derivatives, expressions for B'_{ij} can be derived for 1-N electrolytes:

$$B'_{ij} = \frac{2\beta_{ij}^{(1)}}{(\alpha_1 I)^2}\left[-1 + \left(1 + \alpha_1 I^{1/2} + 0.5\alpha_1^2 I\right)e^{-\alpha_1 I^{1/2}}\right] \tag{B-34}$$

and for 2-2 electrolytes:

$$\begin{aligned} B'_{ij} = {} & \frac{2\beta_{ij}^{(1)}}{(\alpha_1 I)^2}\left[-1 + \left(1 + \alpha_1 I^{1/2} + 0.5\alpha_1^2 I\right)e^{-\alpha_1 I^{1/2}}\right] \\ & + \frac{2\beta_{ij}^{(2)}}{(\alpha_2 I)^2}\left[-1 + \left(1 + \alpha_2 I^{1/2} + 0.5\alpha_2^2 I\right)e^{-\alpha_2 I^{1/2}}\right] \end{aligned} \tag{B-35}$$

The parameters $\beta_{ij}^{(0)}$, $\beta_{ij}^{(1)}$, $\beta_{ij}^{(2)}$ and also C_{ij}^{ϕ}, θ_{ij}, and Ψ_{ijk} can be found in Pitzer's articles (Pitzer, 1991) and other relevant publications (Weber, 2001, and Zemaitis et al., 1986).

14.3.4 Pitzer Parameters

The Pitzer model in the CERMOD code involves user-supplied parameters. These parameters are used in the calculation of binary and ternary parameters for the electrolyte system. These parameters include the binary cation-anion parameters $\beta_{ij}^{(0)}$, $\beta_{ij}^{(1)}$, $\beta_{ij}^{(3)}$ and C_{ij} in Table B-2 at 25°C, ternary cation-cation parameters θ_{ij} in Table B-3, ternary anion-anion parameters θ_{ij} in Table B-4, ternary cation-anion-anion parameters Ψ_{ijk} in Table B-5, and ternary cation-cation-anion parameters Ψ_{ijk} in Table A-6.

Table B-2. Binary Pitzer Cation-Anion Parameters at 25°C.

Cation	Anion	β_0	β_1	β_2	C
Al^{3+}	Cl^-	0.6993	5.845	0.0	0.7794E-03
Ba^{2+}	Cl^-	0.2628	1.496	0.0	-.6859E-02
	NO_3^-	-.3230E-01	0.8025	0.0	0.000
	OH^-	0.1717	1.200	0.0	0.000
Ca^{2+}	Cl^-	0.3159	1.614	0.0	-.1202E-03
	NO_3^-	0.2108	1.409	0.0	-.7106E-02
	SO_4^{2-}	0.2000	2.650	-55.70	0.000
Cd^{2+}	NO_3^-	0.2865	1.668	0.0	-.9051E-02
	SO_4^{2-}	0.2053	2.617	-48.07	0.2850E-02
Co^{2+}	Cl^-	0.3643	1.475	0.0	-.4388E-02
	NO_3^-	0.3119	1.690	0.0	-.2194E-02
	SO_4^{2-}	0.2000	2.700	-30.7	0.000
Cr^{3+}	Cl^-	0.7364	5.255	0.0	-.1302E-01
	NO_3^-	0.7040	5.185	0.0	-.1703E-01
Cs^+	Br^-	0.0279	0.0139	0.0	0.2000E-04
	$CH_3CO_2^-$	0.1628	0.3605	0.0	-.2775E-02
	Cl^-	0.3000E-01	0.5580E-01	0.0	0.1900E-03
	F^-	0.1306	0.2570	0.0	-.2150E-02
	I^-	0.0244	0.0262	0.0	-.1825E-02
	NO_2^-	0.4270E-01	0.6000E-01	0.0	-.2550E-02
	NO_3^-	-.7580E-01	-.6690E-01	0.0	0.000
	OH^-	0.1500	0.3000	0.0	0.000
	SO_4^{2-}	0.8880E-01	1.111	0.0	-.2121E-02
	ReO_4^-	-0.1884	-0.1588	0.0	0.000
	TcO_4^-	-0.1884	-0.1588	0.0	0.000
Cu^{2+}	Cl^-	0.2966	1.391	0.0	-.1273E-01
	NO_3^-	0.3168	1.430	0.0	-.7743E-02
	SO_4^{2-}	0.2340	2.527	-48.33	0.1100E-02
H^+	Br^-	0.1960	0.3564	0.0	0.4135E-02
	Cl^-	0.1775	0.2945	0.0	0.4000E-03
	I^-	0.2362	0.3920	0.0	0.5500E-03
	NO_3^-	0.1119	0.3206	0.0	0.5000E-03
K^+	$Al(OH)_4^-$	0.1276	0.9700E-01	0.0	-.6000E-02
	Br^-	0.0569	0.2212	0.0	-.9000E-03
	$C_2O_4^{2-}$	0.6430E-01	1.524	0.0	0.5000E-03
	$CH_3CO_2^-$	0.1587	0.3251	0.0	-.3300E-02
	Cl^-	0.4750E-01	0.2148	0.0	-.3000E-03
	CO_3^{2-}	0.1288	1.433	0.0	-.1800E-03
	F^-	0.8089E-01	0.2021	0.0	0.4650E-03
	HCO_3^-	-.1071E-01	0.4780E-01	0.0	0.000
	HPO_4^{2-}	0.2480E-01	1.274	0.0	0.5798E-02
	I^-	0.0746	0.2517	0.0	-0.2070E-02
	NO_2^-	0.1280E-01	0.6680E-01	0.0	-.5000E-03
	NO_3^-	-.8060E-01	0.7640E-01	0.0	0.2500E-02
	OH^-	0.1632	0.9700E-01	0.0	-.7000E-03
	PO_4^{3-}	0.3729	3.972	0.0	-.2506E-01

Cation	Anion	β_0	β_1	β_2	C
	SO_4^{2-}	0.4995E-01	0.7793	0.0	0.000
	ReO_4^-	-0.0578	0.0060	0.0	0.000
	TcO_4^-	-0.0578	0.0060	0.0	0.000
Li^+	Br^-	0.1748	0.2547	0.0	0.265E-02
	$CH_3CO_2^-$	0.1124	0.2483	0.0	-.2625E-02
	Cl^-	0.1494	0.3074	0.0	0.1795E-02
	I^-	0.2104	0.3730	0.0	0.000
	NO_2^-	0.1336	0.3250	0.0	-.2650E-02
	NO_3^-	0.1420	0.2780	0.0	-.2755E-02
	OH^-	0.1500E-01	0.1400	0.0	0.000
	SO_4^{2-}	0.1363	1.270	0.0	-.1414E-02
Mg^{2+}	Cl^-	0.3524	1.681	0.0	0.1838E-02
	NO_3^-	0.3671	1.585	0.0	-.7283E-02
	SO_4^{2-}	0.2210	3.343	-37.23	0.6250E-02
	ReO_4^-	0.3138	1.8400	0.0	0.4030E-02
	TcO_4^-	0.3138	1.8400	0.0	0.4030E-02
Mn^{2+}	Cl^-	0.3272	1.550	0.0	-.7248E-02
	SO_4^{2-}	0.2010	2.980	0.0	0.4550E-02
Na^+	$Al(OH)_4^-$	0.5130E-01	0.2481	0.0	0.1300E-02
	Br^-	0.0973	0.2791	0.0	0.5800E-03
	$C_2O_4^{2-}$	0.1621	1.453	0.0	-.8220E-01
	$CH_3CO_2^-$	0.1426	0.3237	0.0	-.3145E-02
	Cl^-	0.7430E-01	0.2744	0.0	0.8000E-03
	$COOH^-$	0.8200E-01	0.2872	0.0	-.2615E-02
	CO_3^{2-}	0.3620E-01	1.510	0.0	0.1840E-02
	F^-	0.3300E-01	0.2456	0.0	0.2810E-02
	HCO_3^-	0.2800E-01	0.4400E-01	0.0	0.000
	HPO_4^{2-}	-.3045E-01	1.350	0.0	0.3590E-02
	I^-	0.1195	0.3439	0.0	0.9000E-03
	NO_2^-	0.4980E-01	0.2177	0.0	-.1200E-02
	NO_3^-	0.2040E-02	0.2368	0.0	0.8000E-04
	OH^-	0.8640E-01	0.2530	0.0	0.2200E-02
	PO_4^{3-}	0.2534	3.738	0.0	-.2260E-01
	ReO_4^-	0.0111	0.1595	0.0	0.1180E-02
	SO_4^{2-}	0.2620E-01	1.028	0.0	0.1260E-02
	TcO_4^-	0.0111	0.1595	0.0	0.1180E-02
Ni^{2+}	Cl^-	0.3479	1.581	0.0	-.1308E-02
	SO_4^{2-}	0.1702	2.907	-40.06	0.9150E-02
Pb^{2+}	NO_3^-	-.3610E-01	0.2850	0.0	0.1874E-02
Rb^+	Br^-	0.0396	0.1530	0.0	-0.7200E-03
	$CH_3CO_2^-$	0.1622	0.3353	0.0	-0.2755E-02
	Cl^-	4.410E-02	1.483E-01	0.0	-0.5050E-03
	F^-	1.141E-01	2.842E-01	0.0	-0.5250E-02
	I^-	0.0397	0.1330	0.0	-0.5400E-03
	NO_2^-	2.690E-02	-1.553E-01	0.0	-0.1830E-02
	NO_3^-	-7.890E-02	-1.720E-02	0.0	0.2645E-02
	SO_4^{2-}	5.790E-02	1.1107	0.0	-0.3562E-04
Sr^{2+}	Cl^-	0.2857	1.667	0.0	-.4596E-03
	NO_3^-	0.1346	1.380	0.0	-.7036E-02
UO_2^{2+}	Cl^-	0.4607	1.613	0.0	-.1115E-01
	CO_3^{2-}	0.4607	1.613	0.0	-.1115E-01
	HCO_3^-	0.3220	1.827	0.0	-.1760E-01
	NO_3^-	0.4607	1.613	0.0	-.1115E-01
	OH^-	0.4274	1.644	0.0	-.1303E-01
	SO_4^{2-}	0.3220	1.827	0.0	-.4400E-02
Zn^{2+}	Cl^-	0.2602	1.643	0.0	-.3111E-01
	NO_3^-	0.3481	1.691	0.0	-.5551E-02
	SO_4^{2-}	0.1949	2.883	-32.81	0.7250E-02

Table B-3. Ternary Pitzer Cation-Cation Parameters.

Cation	Cation	θ
Ba^{2+}	Cs^{+}	-.1500
	H^{+}	-.3600E-01
	K^{+}	-.7200E-01
	Li^{+}	-.7000E-01
	Na^{+}	-.3000E-02
Ca^{2+}	Co^{2+}	-.5500E-01
	K^{+}	-.4000E-01
	Mg^{2+}	0.1000E-01
Co^{2+}	Na^{+}	-.1600E-01
Cs^{+}	H^{+}	-.4400E-01
	Li^{+}	-.9500E-01
	Na^{+}	-.3300E-01
H^{+}	K^{+}	0.5000E-02
	Li^{+}	0.1500E-01
	Na^{+}	0.3600E-01
	Sr^{2+}	-.2000E-01
K^{+}	Na^{+}	-.1200E-01
Li^{+}	Na^{+}	0.1200E-01

Table B-4. Ternary Pitzer Anion-Anion Parameters.

Anion	Anion	θ
$Al(OH)_4^{-}$	NO_2^{-}	0.1970E-02
	NO_3^{-}	-.2720E-01
	OH^{-}	0.1400E-01
Br^{-}	OH^{-}	-.6500E-01
$C_2O_4^{2-}$	NO_3^{-}	-.1093
	OH^{-}	-.1118
Cl^{-}	CO_3^{2-}	-.5300E-01
	F^{-}	-.1000E-01
	HCO_3^{-}	0.3600E-01
	NO_3^{-}	0.1600E-01
	OH^{-}	-.5000E-01
	PO_4^{3-}	0.2559
	ReO_4^{-}	0.0670
	SO_4^{2-}	0.3000E-01
	TcO_4^{-}	0.0670
CO_3^{2-}	HCO_3^{-}	0.9000E-01
	OH^{-}	-.1632
	SO_4^{2-}	0.2000E-01
F^{-}	OH^{-}	0.1193
	PO_4^{3-}	0.5500
HCO_3^{-}	SO_4^{2-}	0.1000E-01
NO_2^{-}	PO_4^{3-}	0.1047
NO_3^{-}	OH^{-}	-.5470E-01
	SO_4^{2-}	0.6730E-01
OH^{-}	PO_4^{3-}	0.1000
	SO_4^{2-}	-.1300E-01
SO_4^{2-}	ReO_4^{-}	0.1790
	TcO_4^{-}	0.1790

Table B-5. Ternary Pitzer Cation-Anion-Anion Parameters.

Cation	Anion	Anion	Ψ
Cs^+	ReO_4^-	Cl^-	-0.0010E+00
		SO_4^{2-}	0.0240E+00
	TcO_4^-	Cl^-	-0.0010E+00
		SO_4^{2-}	0.0240E+00
K^+	Cl^-	CO_3^{2-}	0.4000E-02
		F^-	-.1350E-01
		HCO_3^-	-.1500E-01
		SO_4^{2-}	-.5000E-02
	CO_3^{2-}	SO_4^{2-}	-.9000E-02
	HCO_3^-	SO_4^{2-}	0.5000E-02
	NO_3^-	Cl^-	-.3100E-02
		OH^-	-.3200E-02
	OH^-	$C_2O_4^{2-}$	0.5000E-01
		Cl^-	-.3200E-02
		CO_3^{2-}	-.1000E-01
		SO_4^{2-}	-.5000E-01
	ReO_4^-	Cl^-	-0.0010E+00
		SO_4^{2-}	0.0020E+00
	TcO_4^-	Cl^-	-0.0010E+00
		SO_4^{2-}	0.0020E+00
Mg^{2+}	ReO_4^-	Cl^-	-0.0115E+00
		SO_4^{2-}	-0.0300E+00
	TcO_4^-	Cl^-	-0.0115E+00
		SO_4^{2-}	-0.0300E+00
Na^+	Cl^-	CO_3^{2-}	0.8500E-02
		F^-	-.2180E-02
	CO_3^{2-}	HCO_3^-	0.2000E-02
		SO_4^{2-}	-.5000E-02
	HCO_3^-	SO_4^{2-}	-.5000E-02
	NO_2^-	$Al(OH)_4^-$	0.5400E-02
		$C_2O_4^{2-}$	0.2300
	NO_3^-	$Al(OH)_4^-$	0.4700E-02
		$C_2O_4^{2-}$	0.1895
		Cl^-	-.6000E-02
		OH^-	0.2000E-03
		SO_4^{2-}	0.3350E-02
	OH^-	$Al(OH)_4^-$	-.4800E-02
		$C_2O_4^{2-}$	0.1000
		Cl^-	-.6300E-02
		CO_3^{2-}	0.1720E-01
		F^-	-.3500E-01
		PO_4^{3-}	0.3000E-01
		SO_4^{2-}	-.9000E-02
	PO_4^{3-}	NO_2^-	0.5370E-01
	ReO_4^-	Cl^-	-0.0085E+00
		SO_4^{2-}	-0.0030E+00
	TcO_4^-	Cl^-	-0.0085E+00
		SO_4^{2-}	-0.0030E+00

Table B-6. Ternary Pitzer Cation-Cation-Anion Parameters.

Cation	Cation	Anion	Ψ
Ca^{2+}	Co^{2+}	Cl^-	0.1300E-01
Cs^+	H^+		-0.1900E-01
	K^+		-0.1000E-02
	Li^+		-0.9000E-02
	Na^+		-0.3000E-02
H^+	Ba^{2+}		0.2400E-01
	K^+	Br^-	-0.2100E-01
	Na^+	Br^-	-0.1200E-01
	Sr^{2+}	Cl^-	0.1800E-01
K^+	Ca^{2+}		-0.1500E-01
	H^+		-0.1100E-01
		NO_3^-	-0.1030E-01
	Li^+	Cl^-	-0.1000E-01
Li^+	Ba^{2+}		0.1900E-01
Na^+	Co^{2+}		-0.1100E-01
	Cu^{2+}		-0.1400E-01
		SO_4^{2-}	-0.1400E-01
	H^+	Cl^-	-0.4000E-02
		NO_3^-	-0.2740E-02
	K^+	Br^-	-0.2200E-02
		Cl^-	-0.1800E-02
		CO_3^{2-}	0.3000E-02
		HCO_3^-	0.3000E-02
		NO_3^-	-0.6000E-02
		OH^-	0.4000E-02
		SO_4^{2-}	-0.1000E-01
	Li^+	Cl^-	-0.3000E-02
		NO_3^-	-0.7000E-02
	Mn^{2+}	Cl^-	-0.3000E-02
	UO_2^{2+}	NO_3^-	0.3879E+00
		OH^-	-0.2556E+00

14.3.5 Benchmarking of the Pitzer Activity Coefficient Model

The Pitzer activity coefficient model implemented in CERMOD is benchmarked against mean activity coefficients of single/double strong electrolytes derived from experimental measurements. In general, there is excellent agreement between the CERMOD Pitzer model and experimental results at low to moderate electrolyte concentrations. The Pitzer parameters are typically valid up to 6 molal or lower depending on the experiment data. Beyond 6 molal the CERMOD Pitzer model begins to over-predict the experimental mean activity coefficients. The benchmark cases were chosen to include the five main competing cations for ion-exchange (i.e., H^+, K^+, Na^+, Rb+ and Cs^+).

The activity of water in a sodium hydroxide solution at 25ºC is show in Figure B-1. There is excellent agreement between the model and data (Stokes, 1945) up to 14 molal. The CERMOD Pitzer model under-predicts the Stokes data beyond 14 molal. The reason for this is not understood.

The experimental data for Figures B-9, B-10, B-15, B-17, B-18, B-28, B-30, B-35, B-36, and B-37 are provided in Chapter IV (Single Strong Electrolytes) of the "Handbook of Aqueous Electrolyte Thermodynamics" by Zemaitis, et al. (1986). NBS in the plot legend refers to the National Bureau of Standards fit to experimental data using the following equation:

$$\log \gamma_{\pm} = -\frac{A|z_+ z_-|\sqrt{I}}{1 + B^* \sqrt{I}} + \beta I + CI^2 + DI^3 + EI^4 + FI^5 + GI^6 + \cdots \qquad \text{(B-36)}$$

where

$\gamma_{\pm}$ .....experimental mean activity coefficient of molecular species
A .....Debye-Hückel constant
I .....ionic strength of electrolyte solution
z_+ .....number of charges on cation
z_- .....number of charges on anion

The constants C, D, E, F, G, etc., as well as B* and β are taken as empirical and are not considered to have physical significance. These empirical parameters can be found in the paper by Hamer and Wu (1972).

The NBS parameters used in Figures B-2 through B-41 (excluding those listed above) were obtained from the paper by Hamer and Wu.

Figures B-40 and B-41 show the variation of the mean activity coefficients of RbCl and $RbNO_3$, respectively, in a mixture of both as a function of fractional molality of $RbNO_3$.

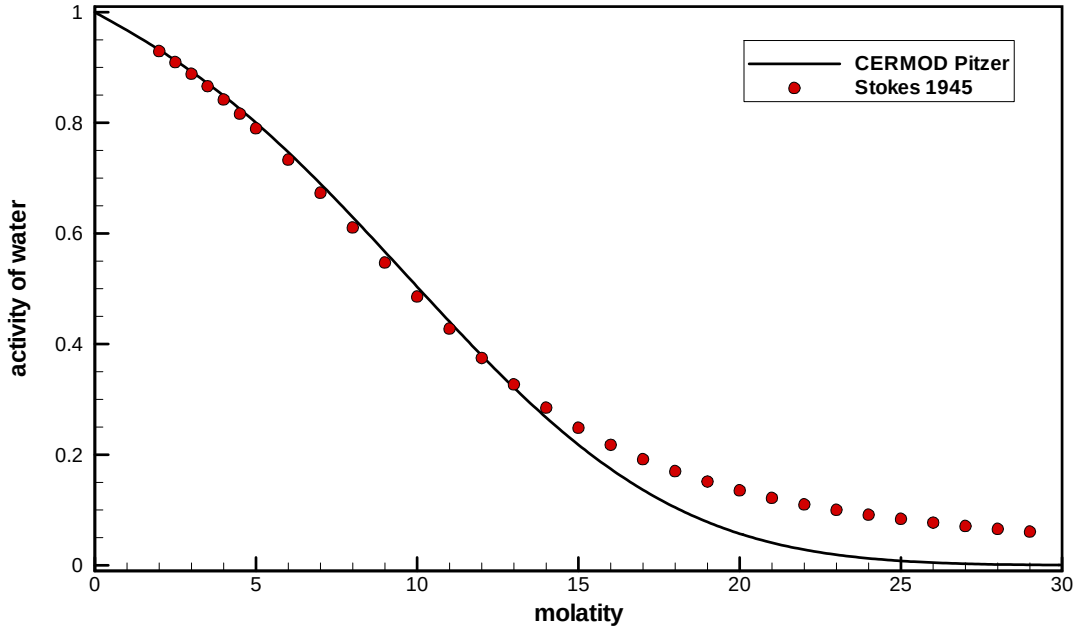

Figure B-1. Activity of water in NaOH at 25°C.

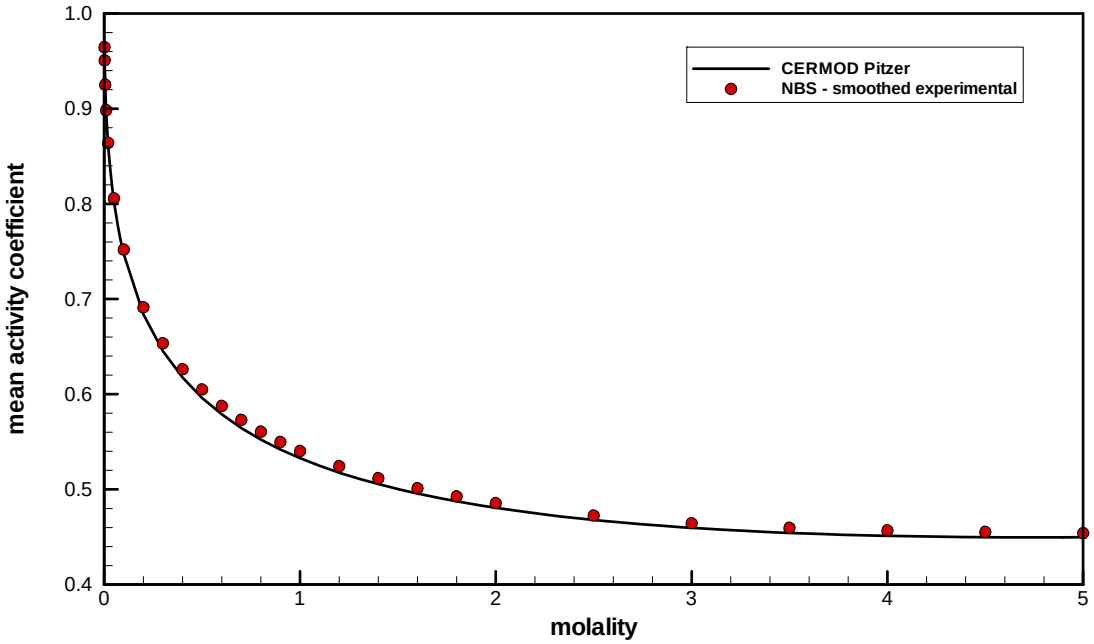

Figure B-2. CsBr at 25°C.

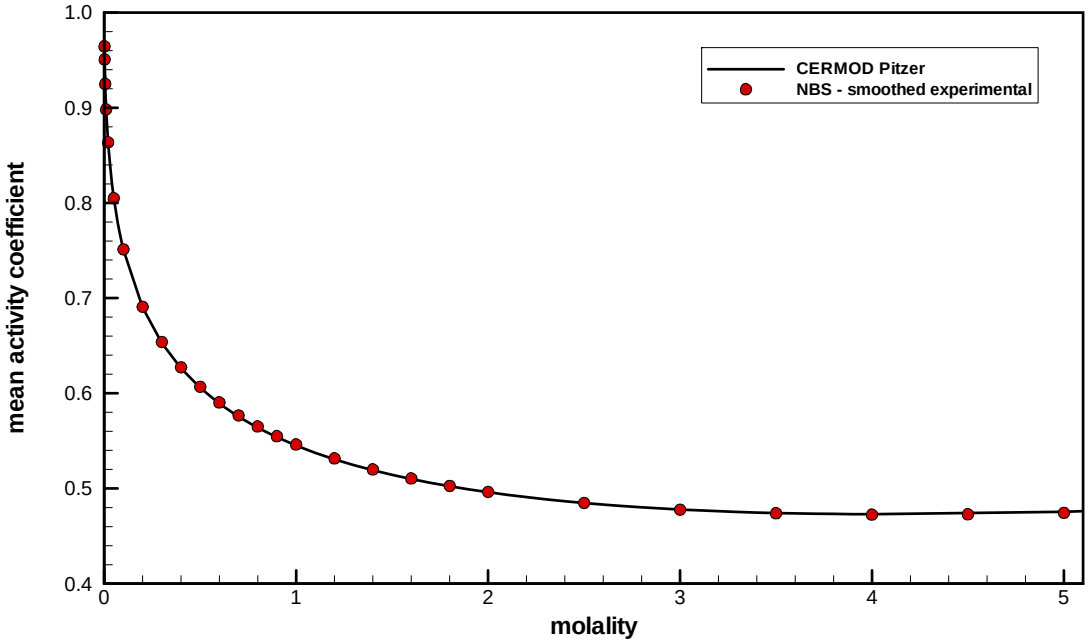

Figure B-3. CsCl at 25°C.

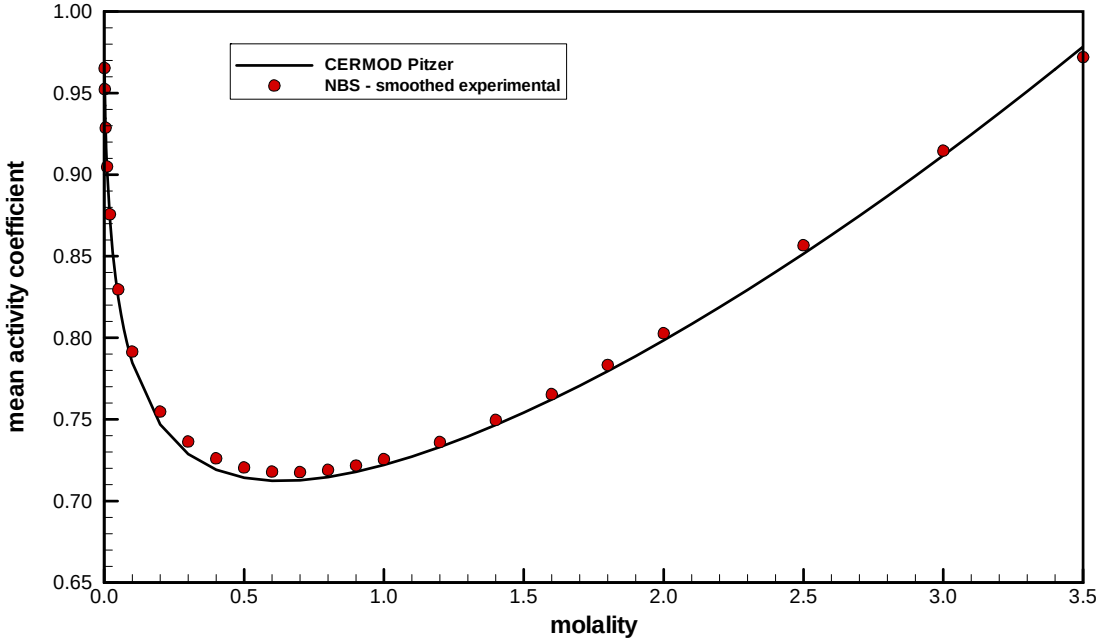

Figure B-4. CsF at 25°C.

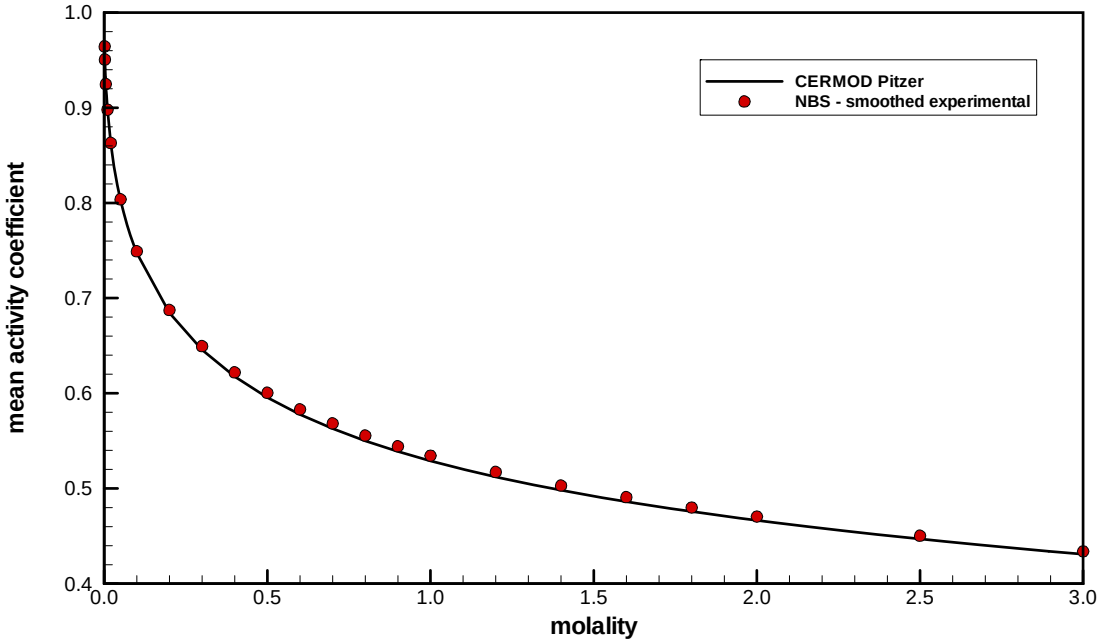

Figure B-5. CsI at 25°C.

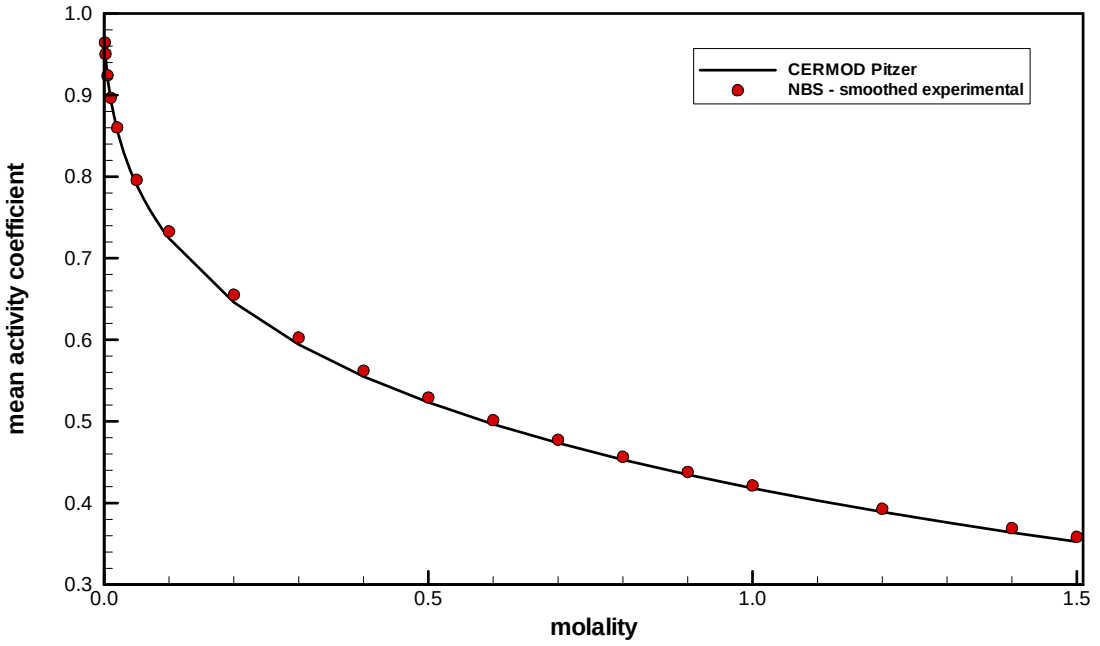

Figure B-6. $CsNO_3$ at 25°C.

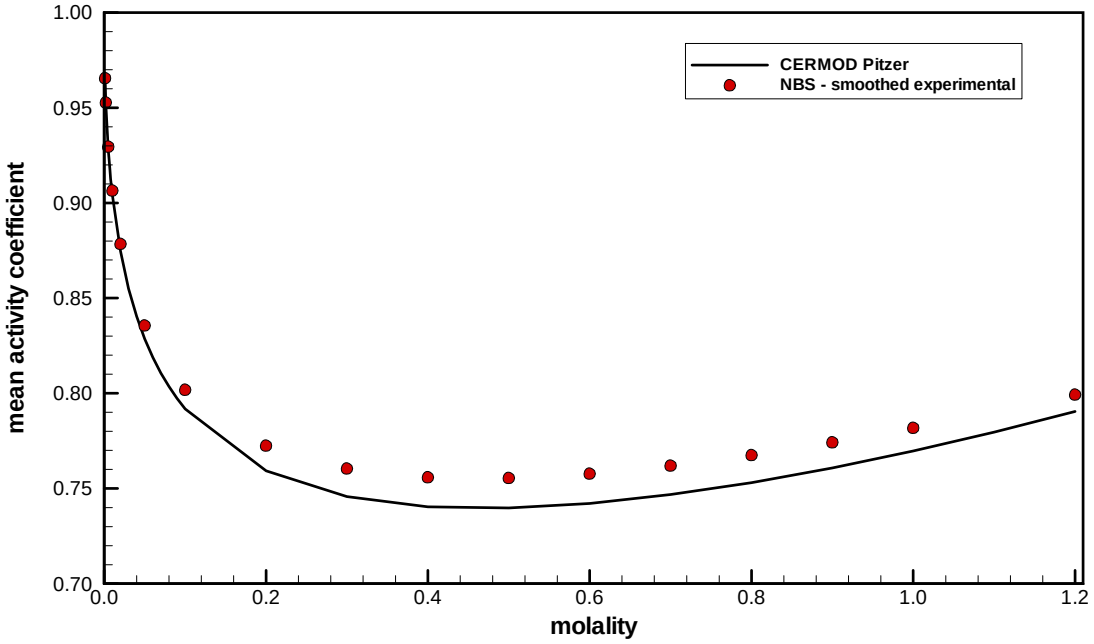

Figure B-7. CsOH at 25°C.

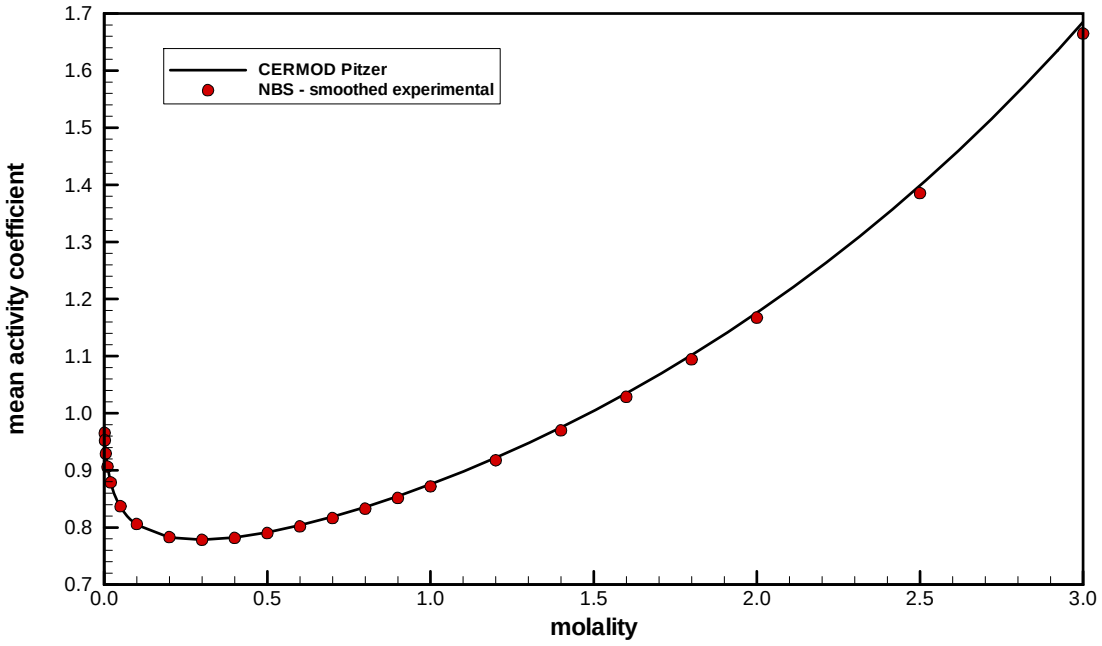

Figure B-8. HBr at 25°C.

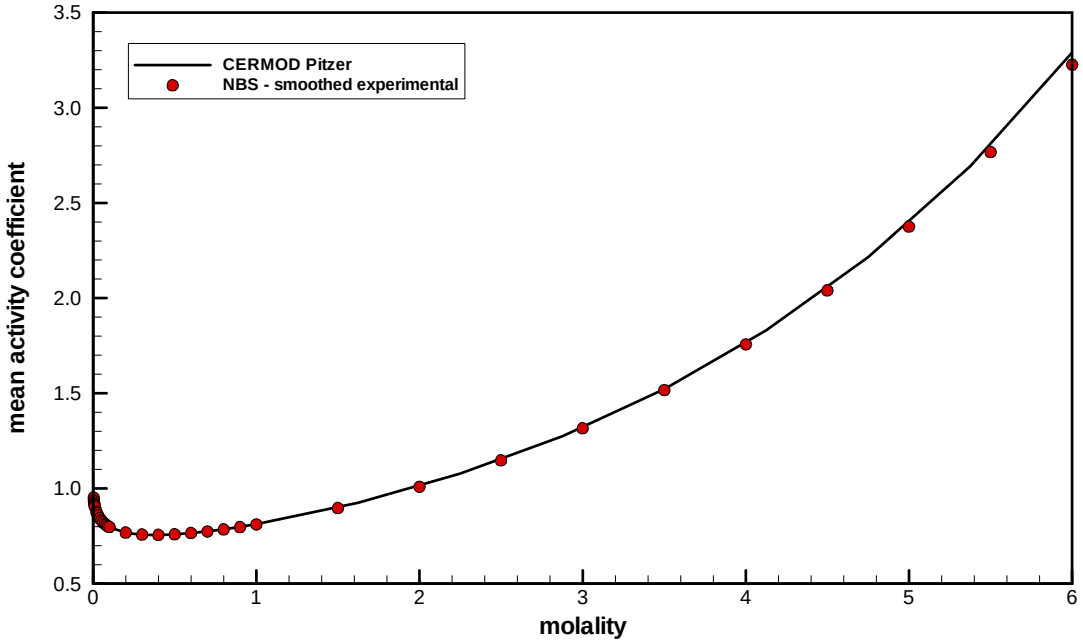

Figure B-9. HCl at 25°C (0 to 6 molal).

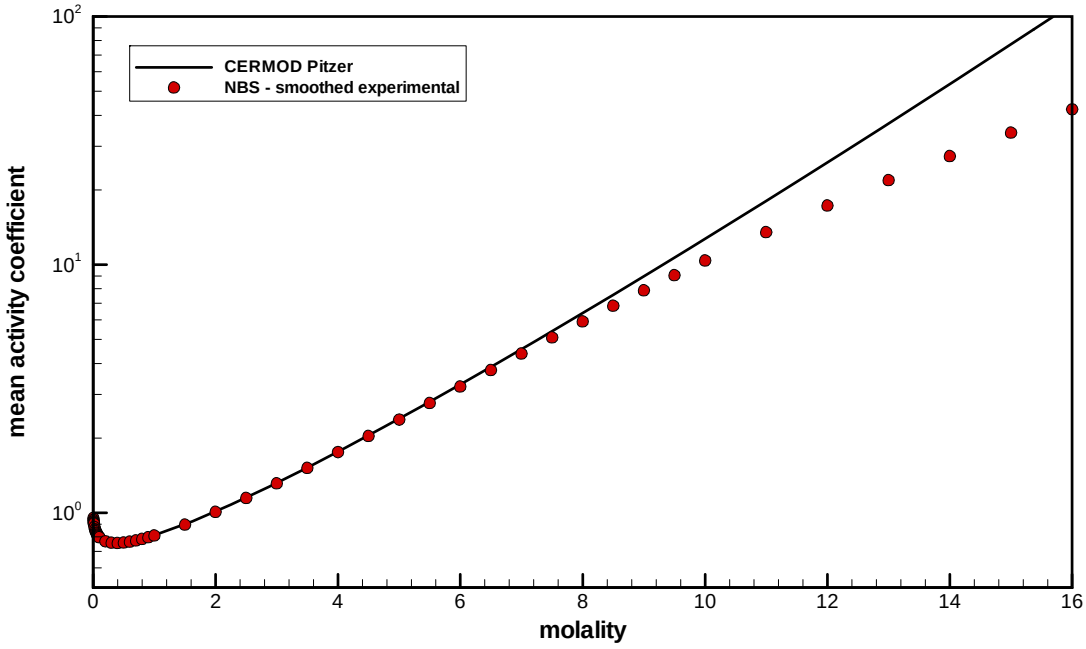

Figure B-10. HCl at 25°C (0 to 16 molal).

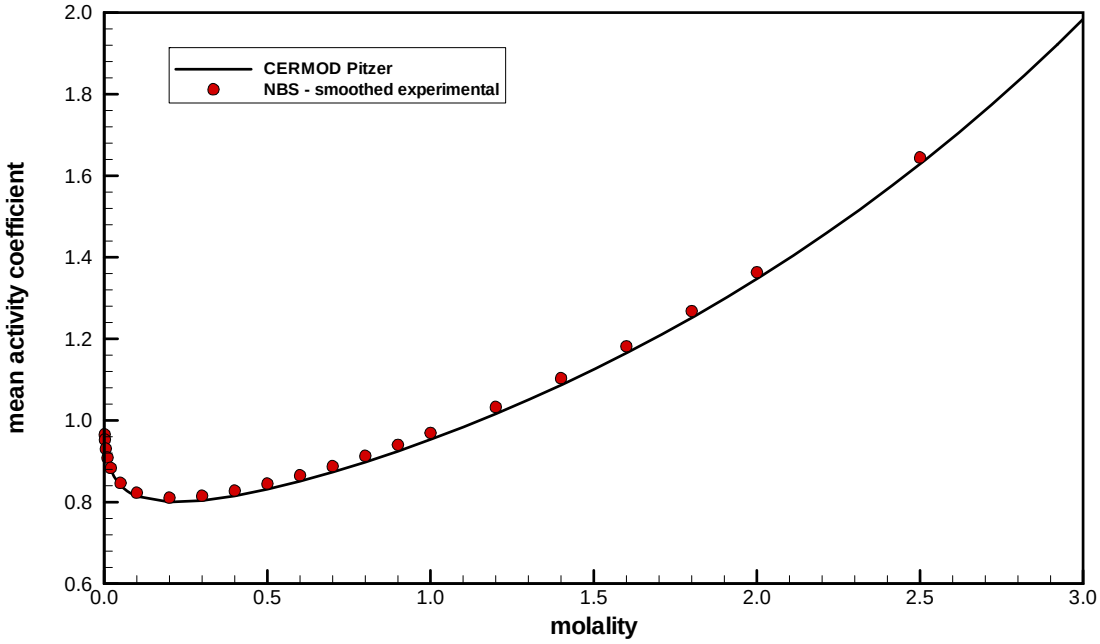

Figure B-11. HI at 25°C.

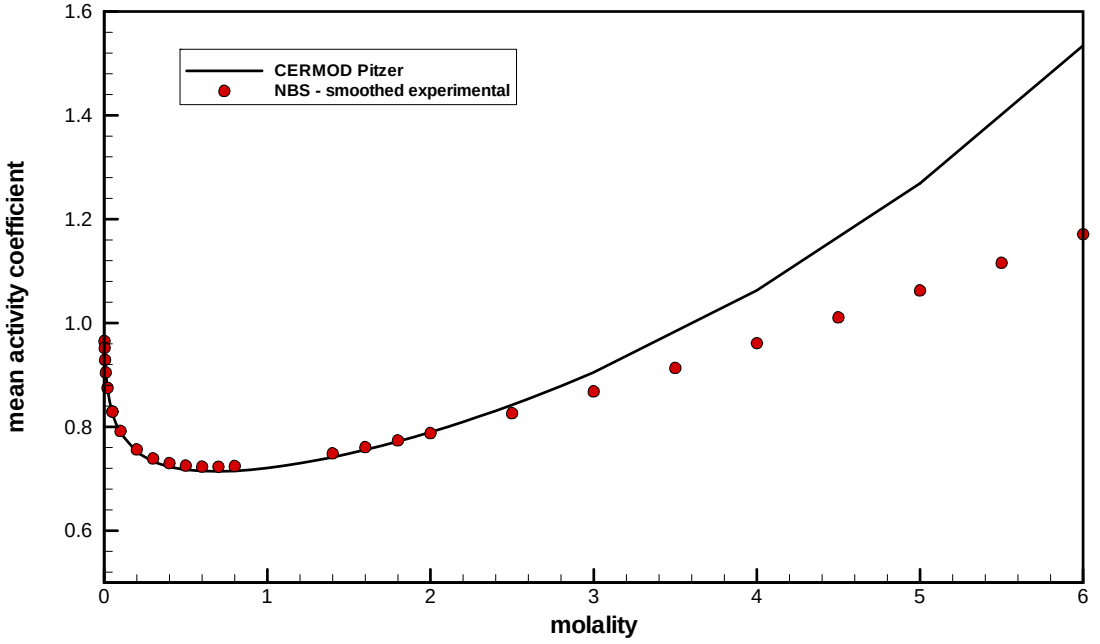

Figure B-12. HNO_3 at 25°C (0 to 6 molal).

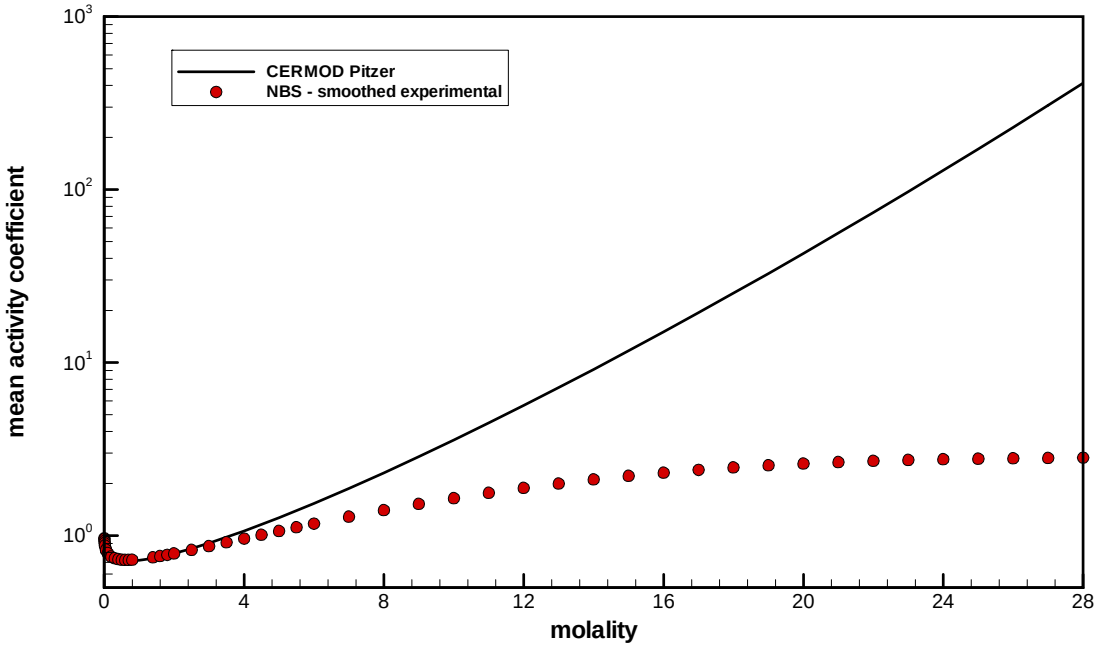

Figure B-13. HNO_3 at 25°C (0 to 28 molal).

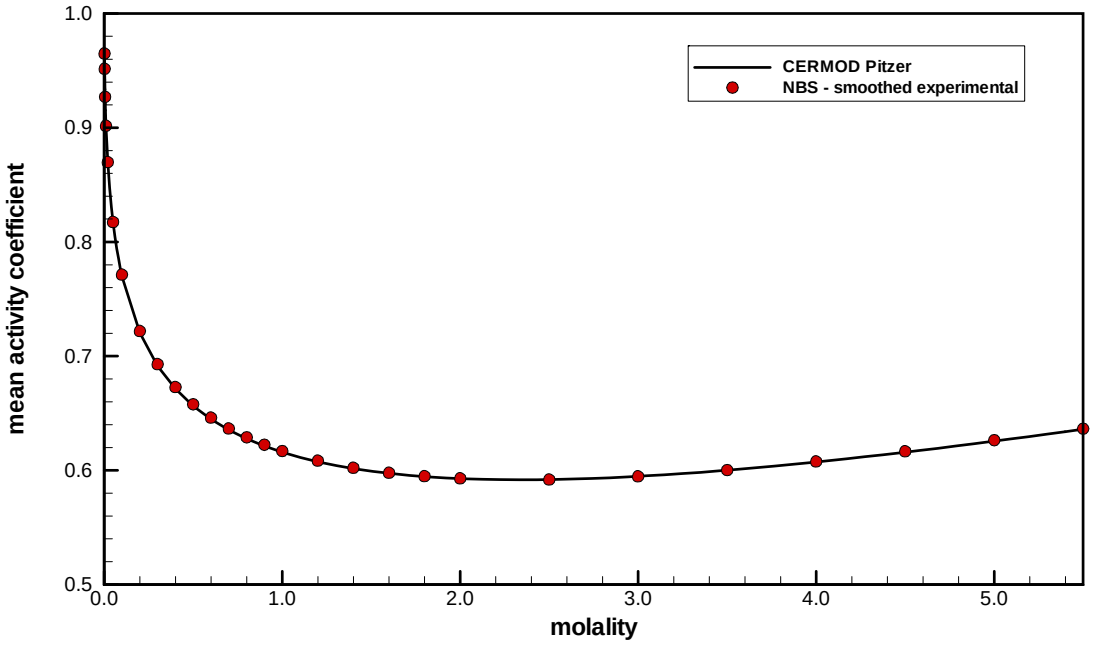

Figure B-14. KBr at 25°C.

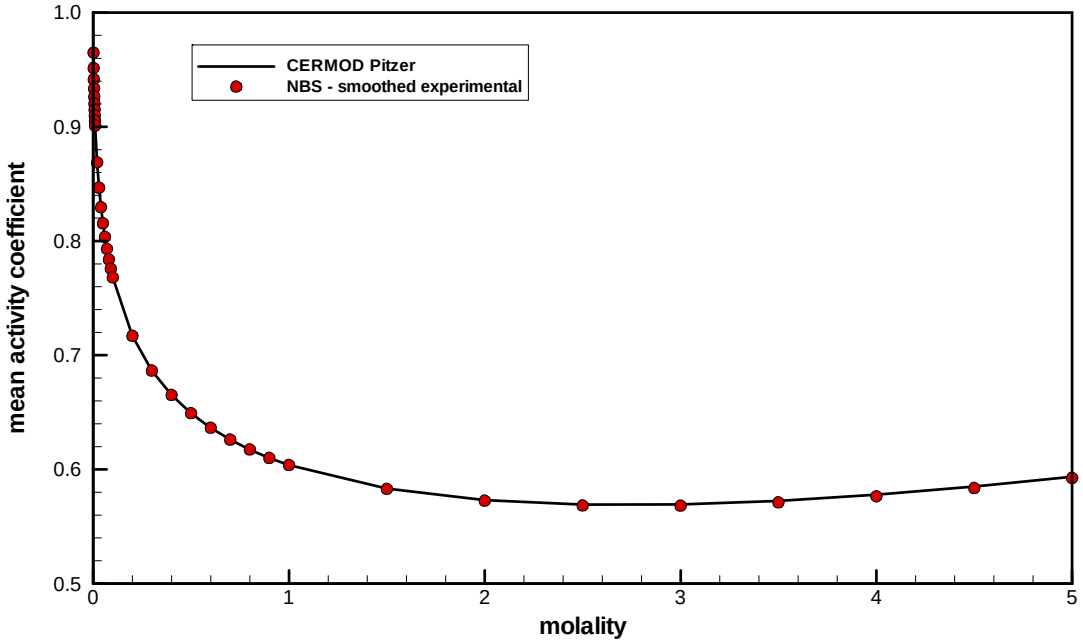

Figure B-15. KCl at 25°C.

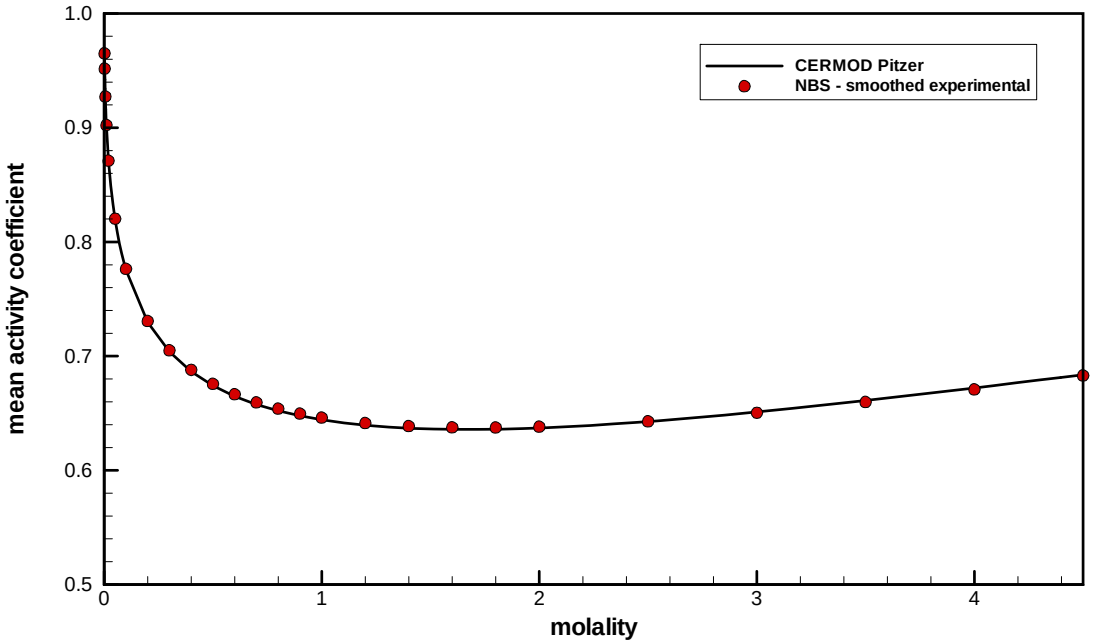

Figure B-16. KI at 25°C.

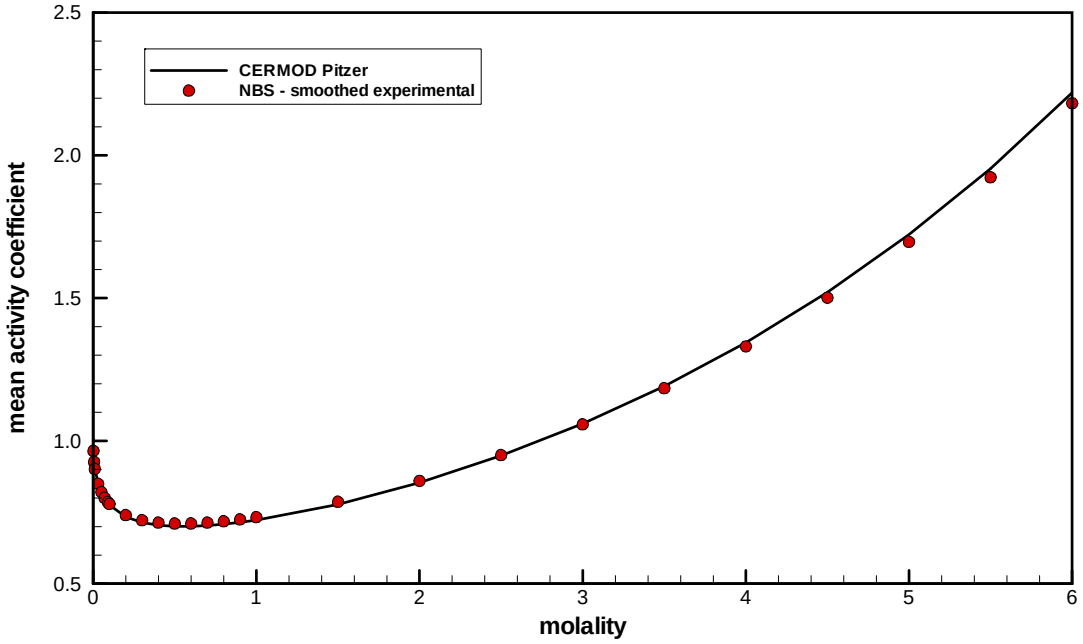

Figure B-17. KOH at 25°C (0 to 6 molal).

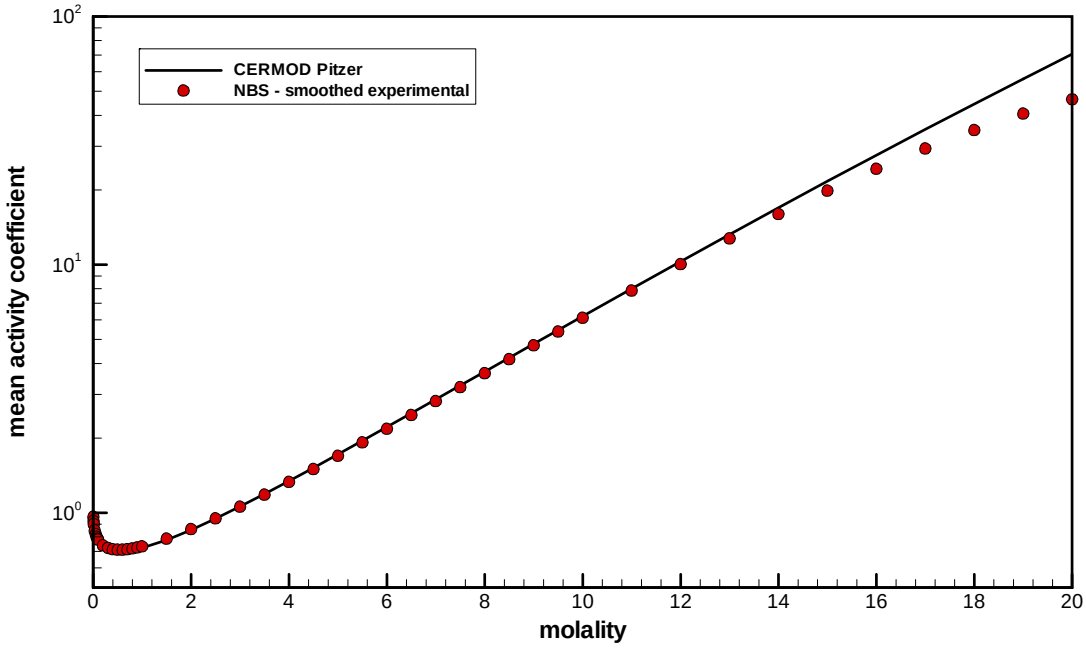

Figure B-18. KOH at 25°C (0 to 20 molal).

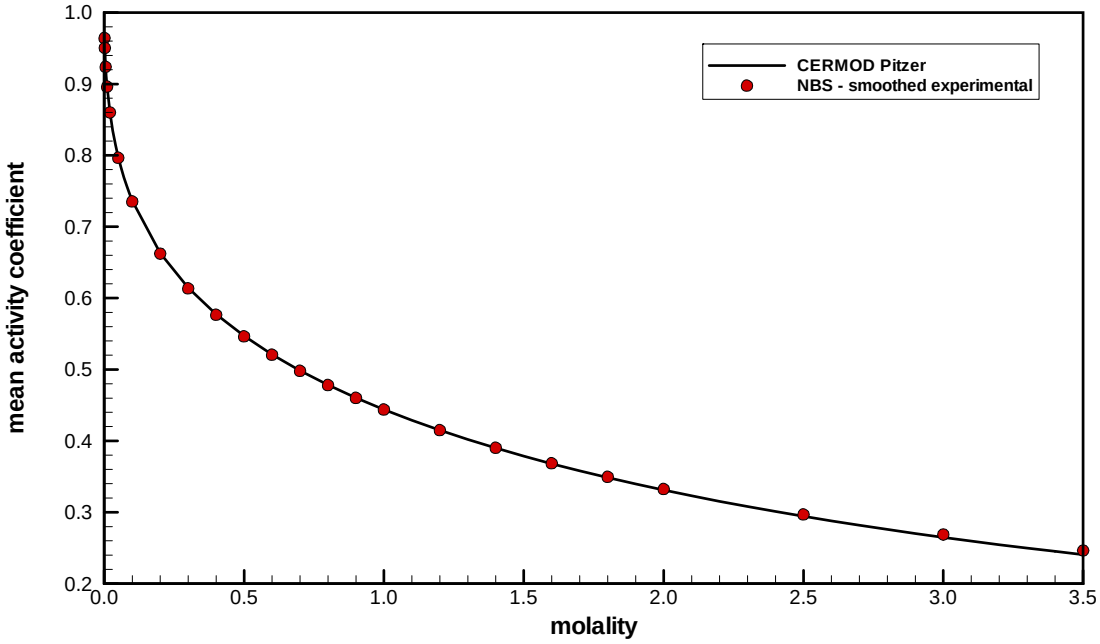

Figure B-19. KNO_3 at 25°C (0 to 3.5 molal).

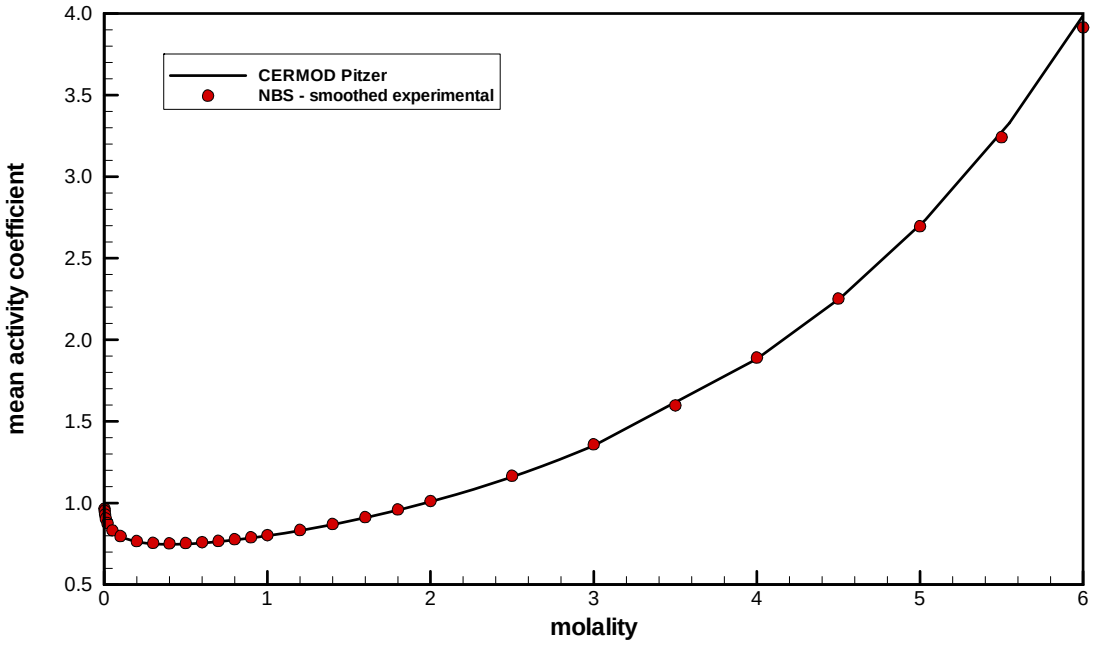

Figure B-20. LiBr at 25°C (0 to 6 molal).

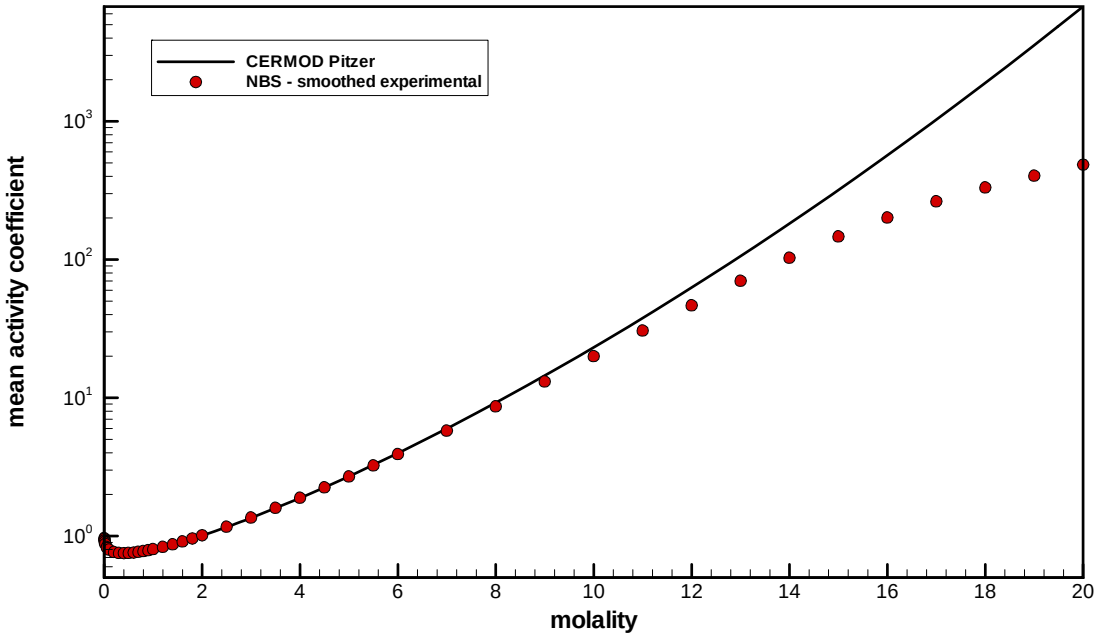

Figure B-21. LiBr at 25°C (0 to 20 molal).

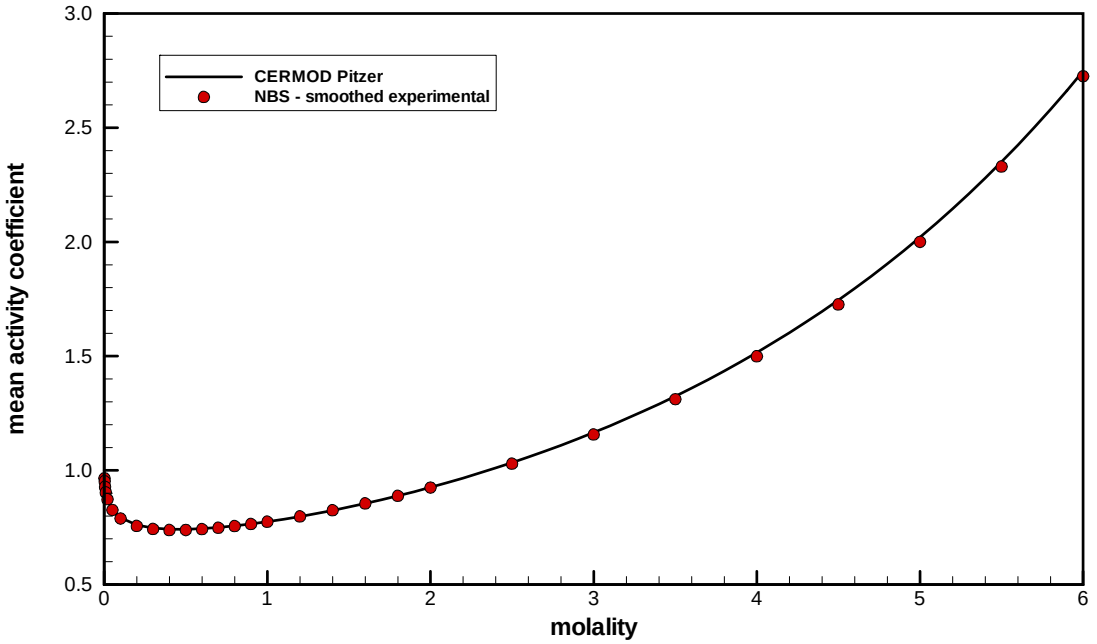

Figure B-22. LiCl at 25°C (0 to 6 molal).

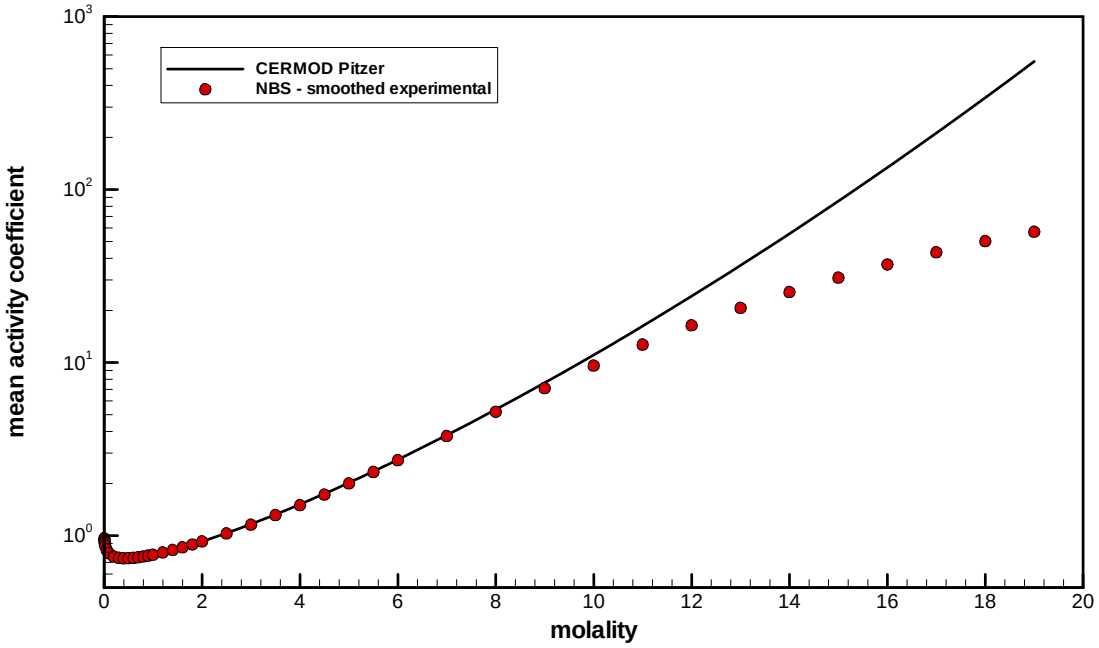

Figure B-23. LiCl at 25°C (0 to 19 molal).

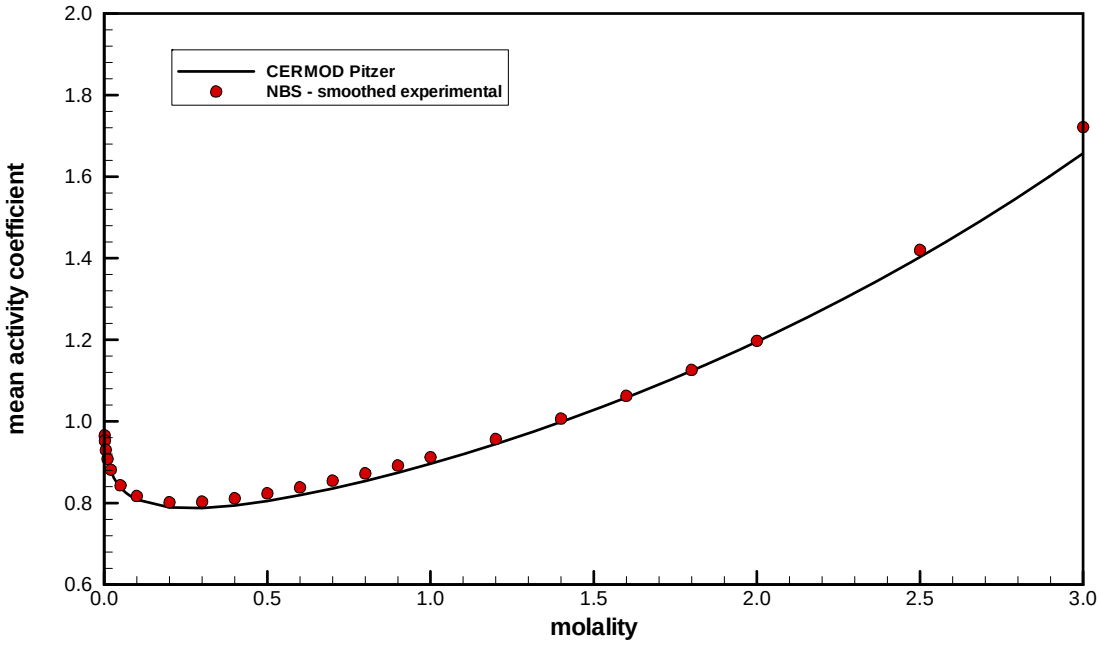

Figure B-24. LiI at 25°C.

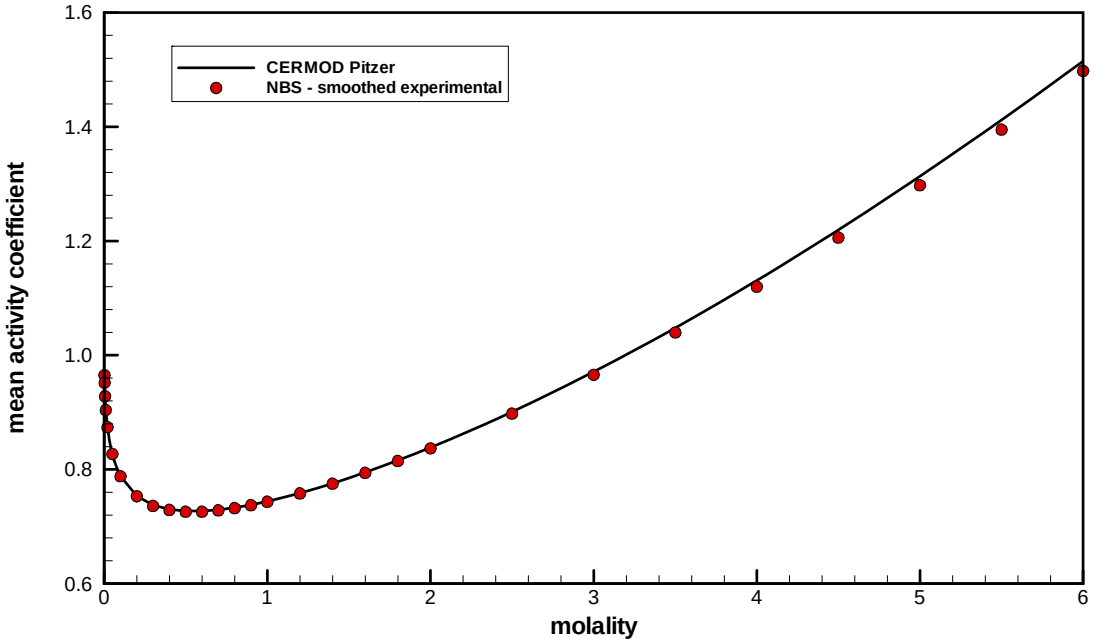

Figure B-25. $LiNO_3$ at 25°C (0 to 6 molal).

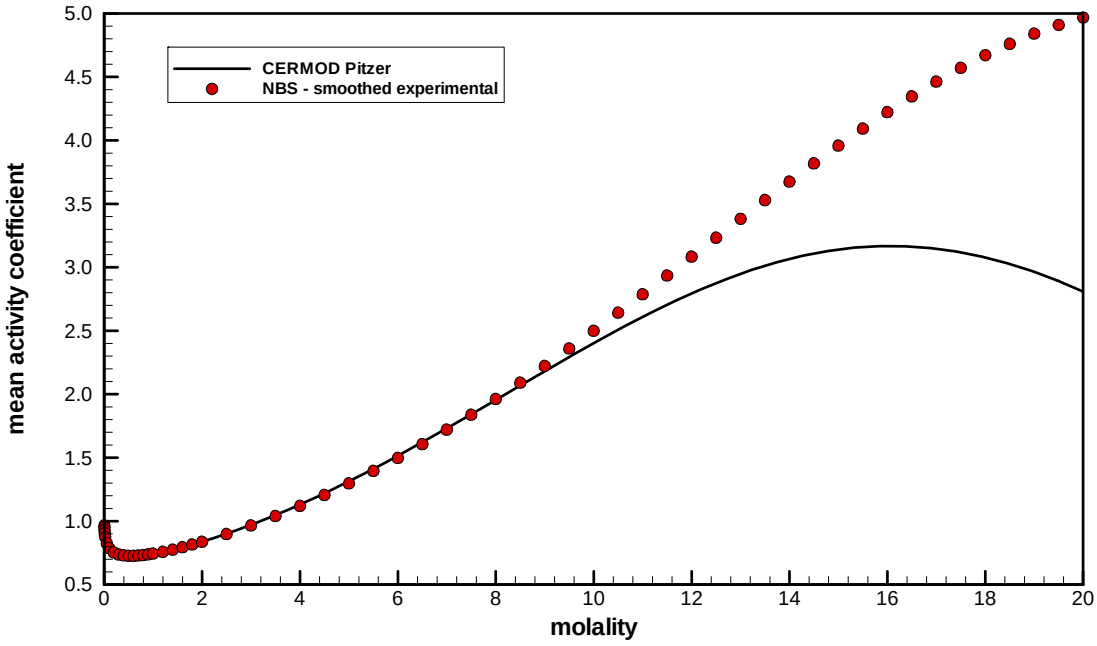

Figure B-26. $LiNO_3$ at 25°C (0 to 20 molal).

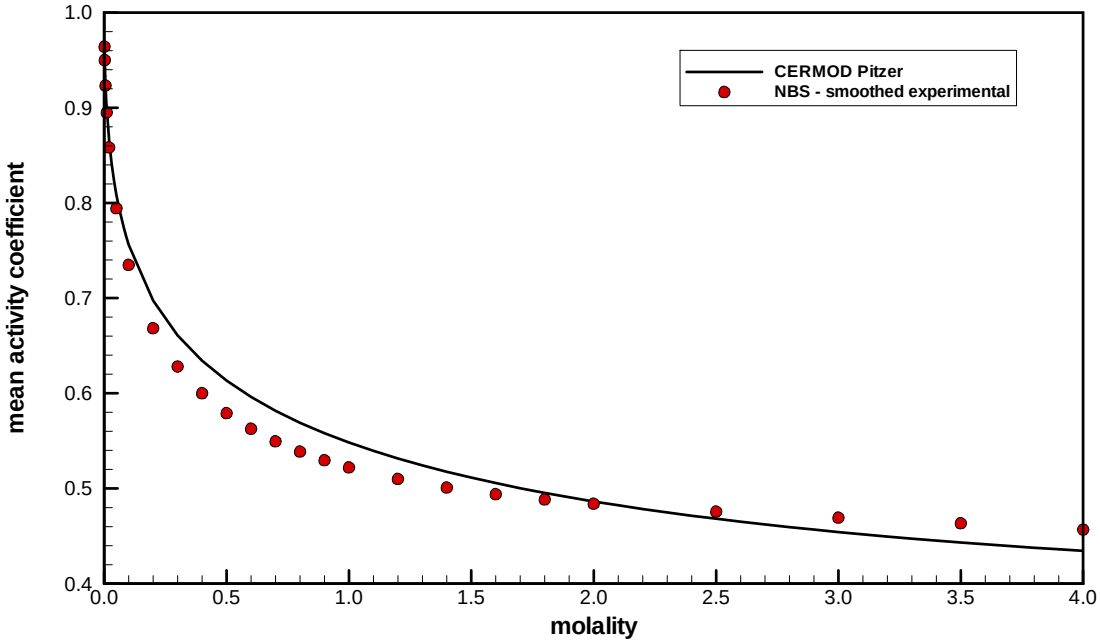

Figure B-27. LiOH at 25°C.

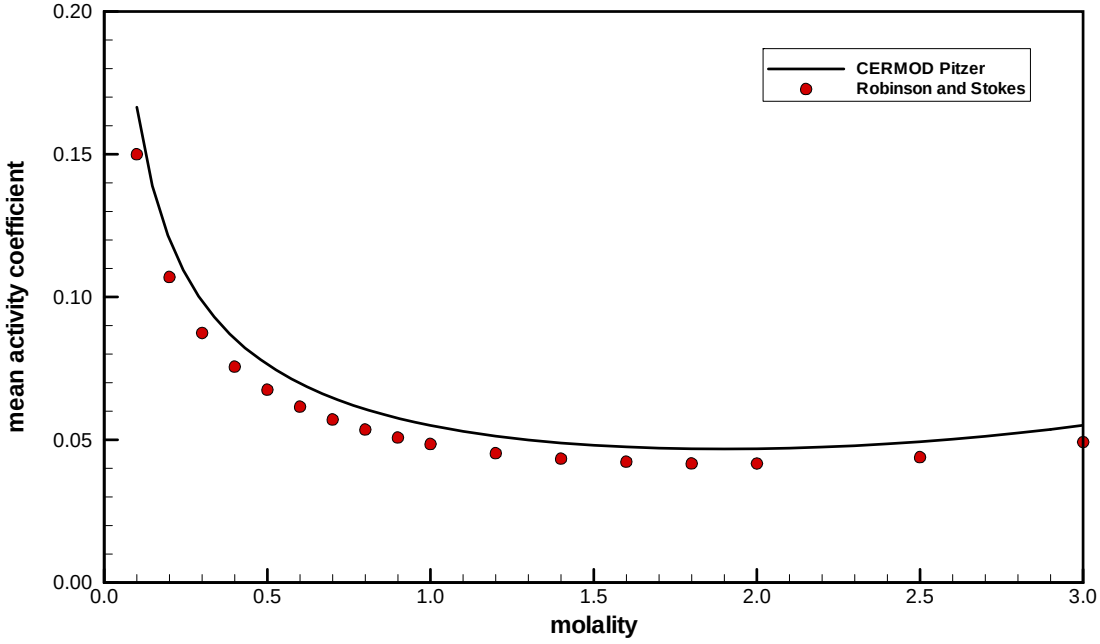

Figure B-28. $MgSO_4$ at 25°C.

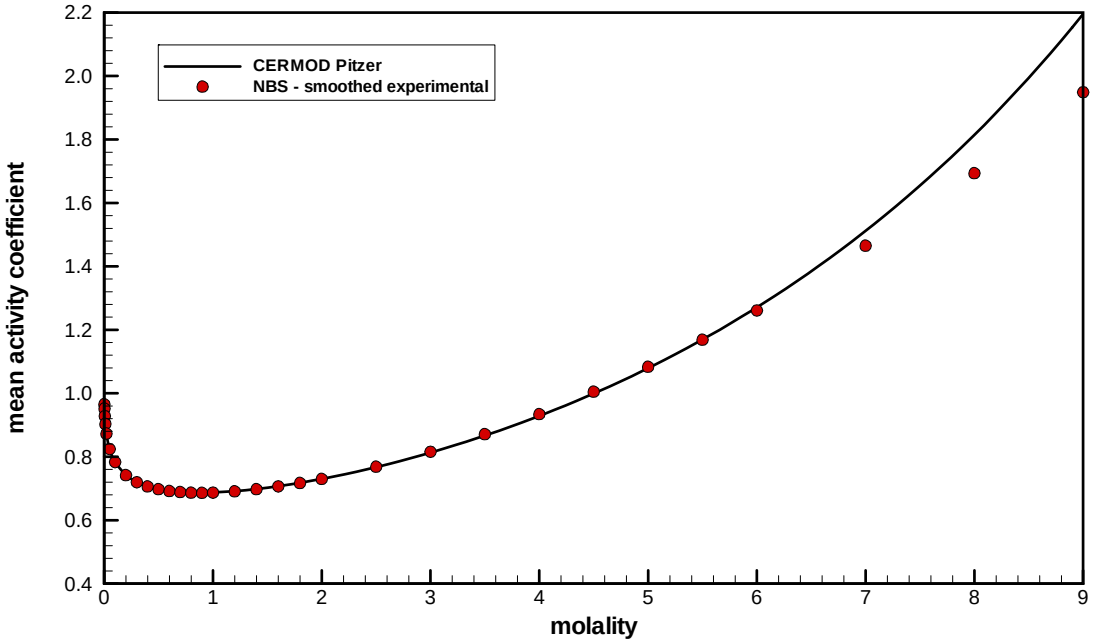

Figure B-29. NaBr at 25°C.

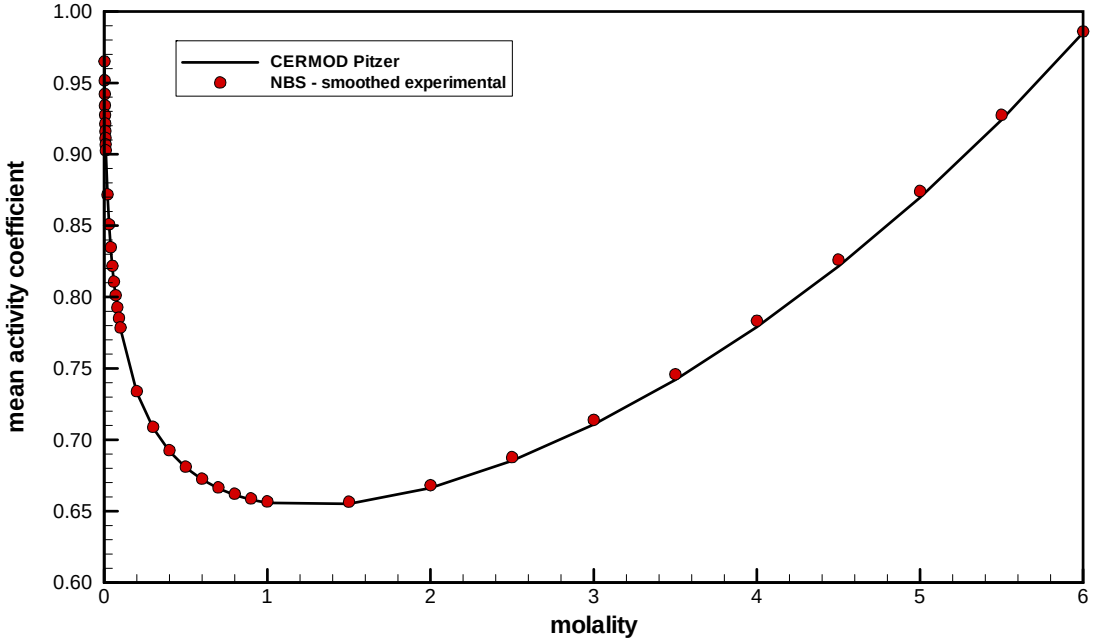

Figure B-30. NaCl at 25°C.

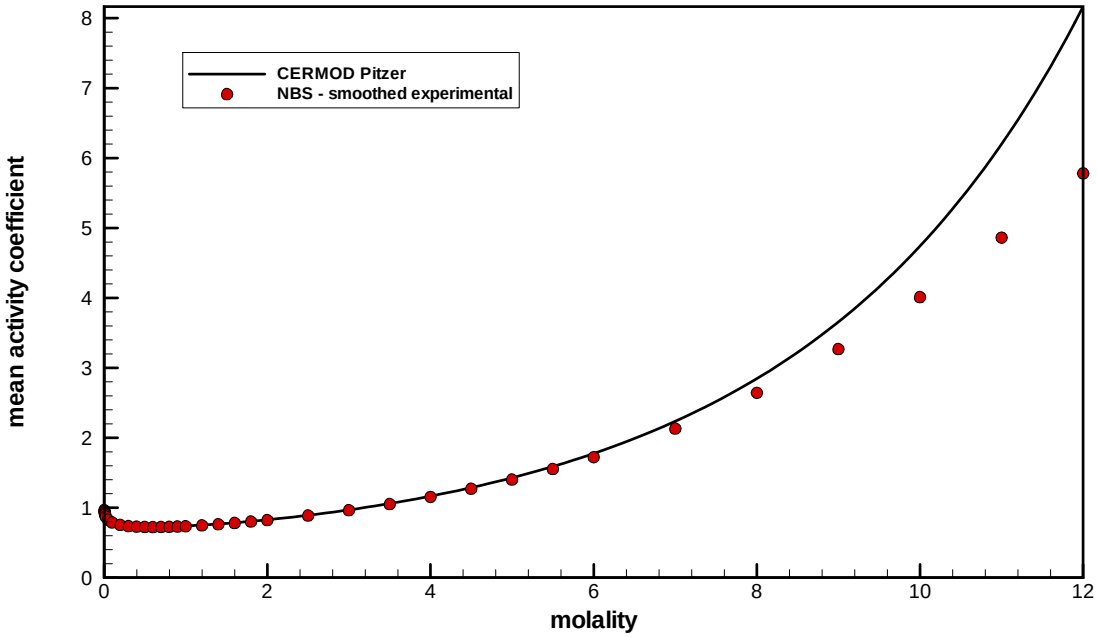

Figure B-31. NaI at 25°C.

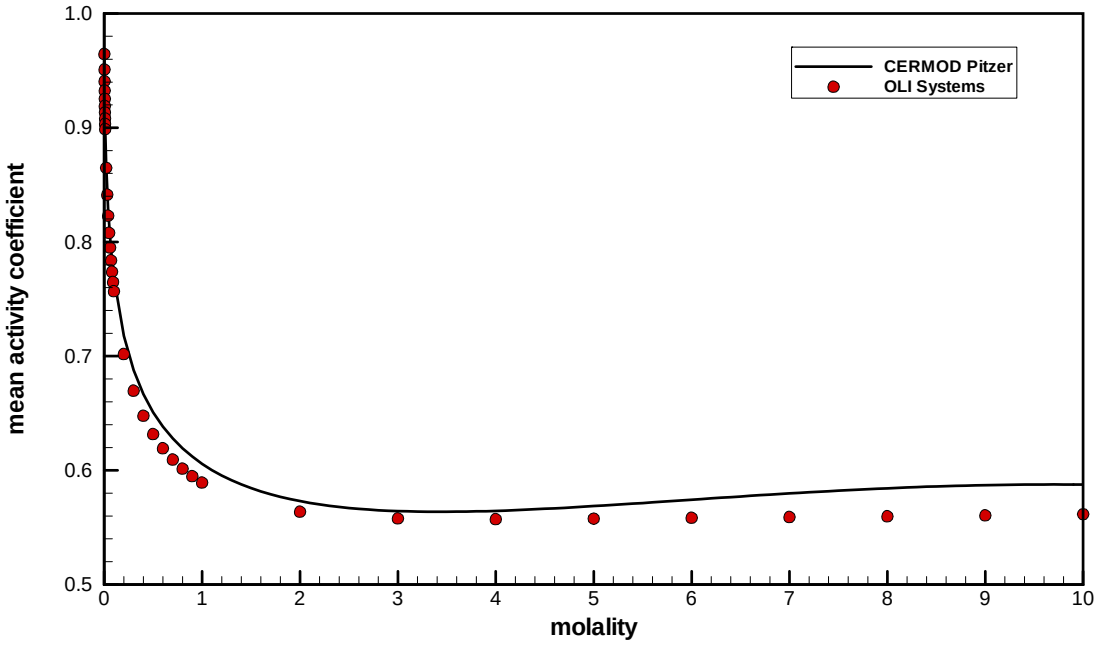

Figure B-32. $NaNO_2$ at 25°C (0 to 10 molal).

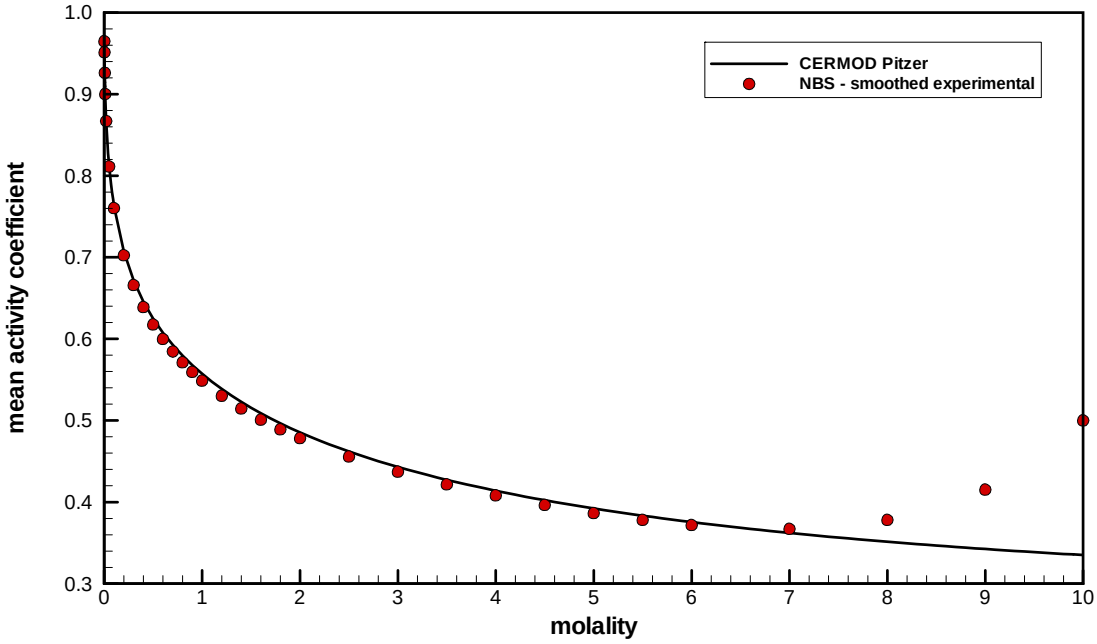

Figure B-33. $NaNO_3$ at 25°C (0 to 10 molal).

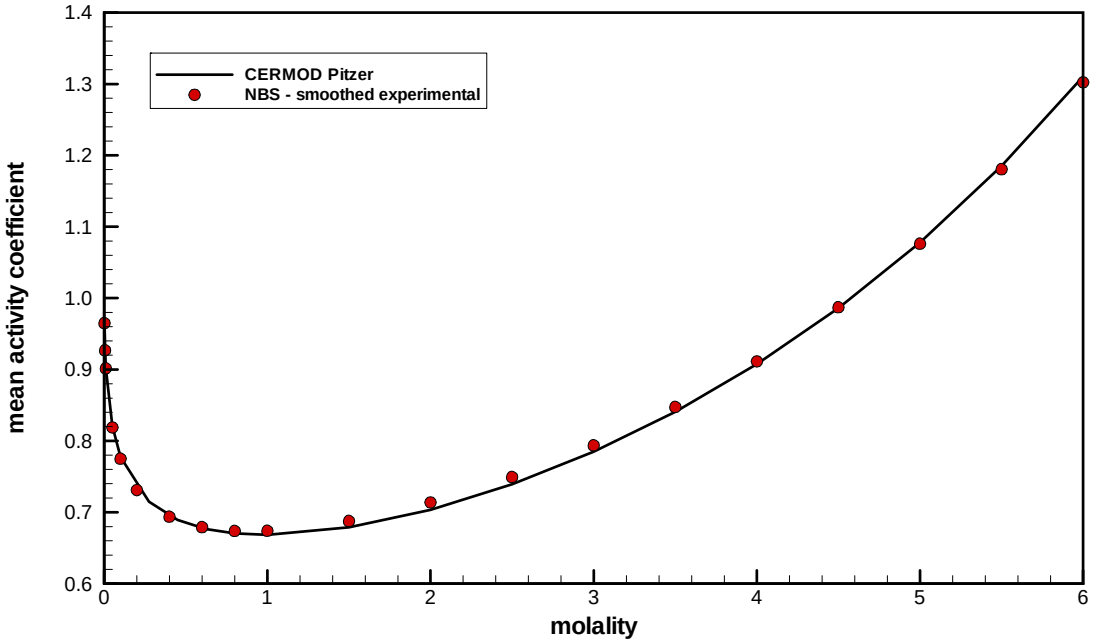

Figure B-34. NaOH at 25°C (0 to 6 molal).

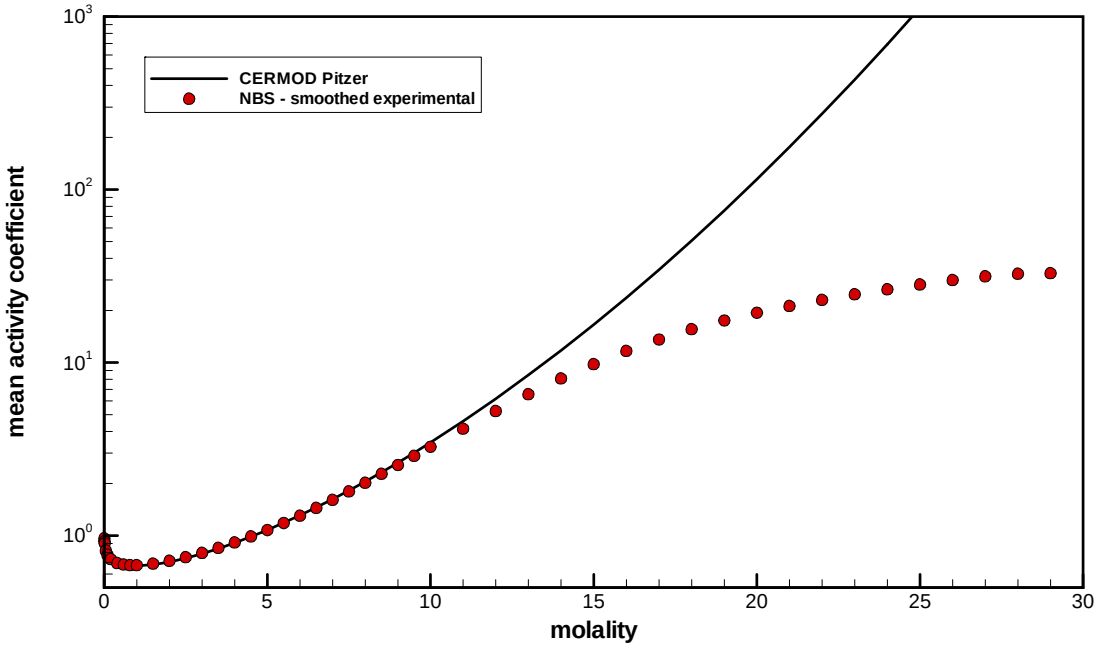

Figure B-35. NaOH at 25°C (0 to 30 molal).

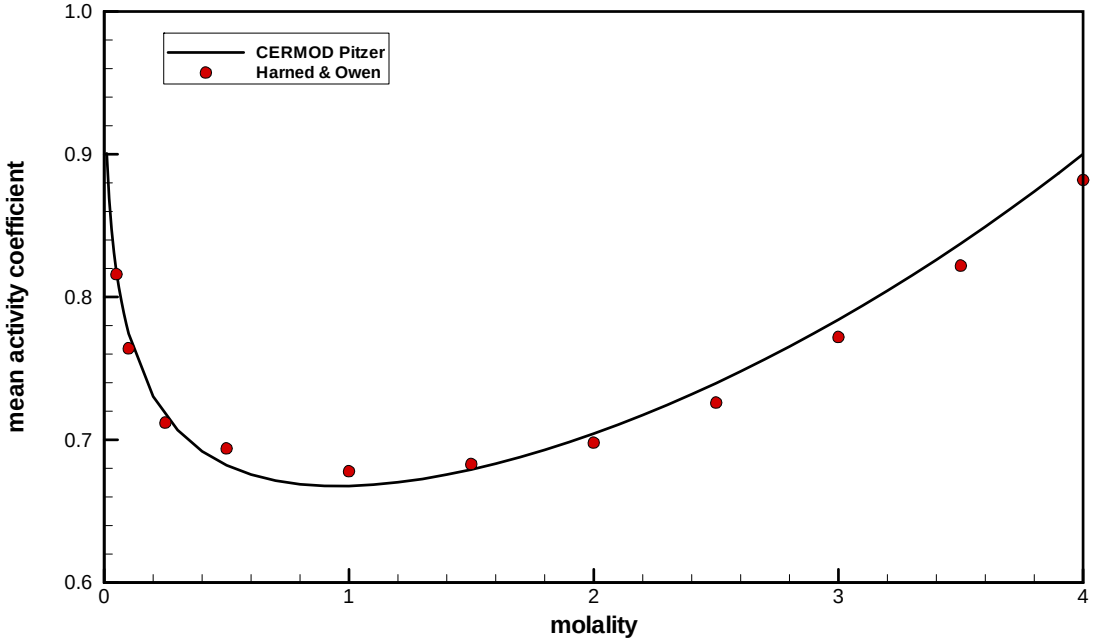

Figure B-36. NaOH at 35°C.

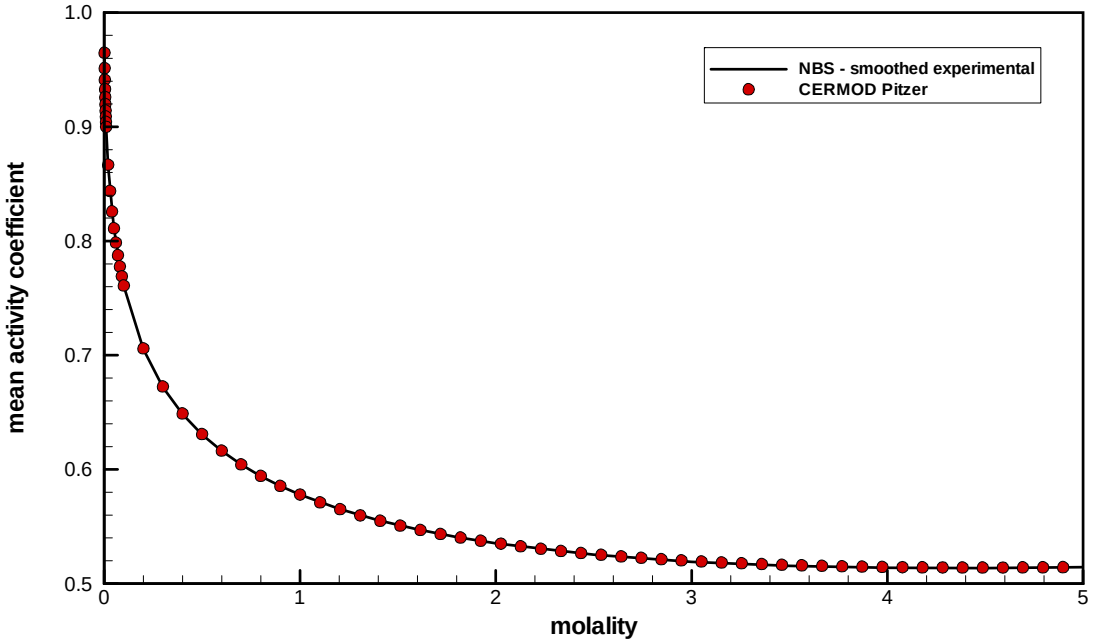

Figure B-37. RbBr at 25°C.

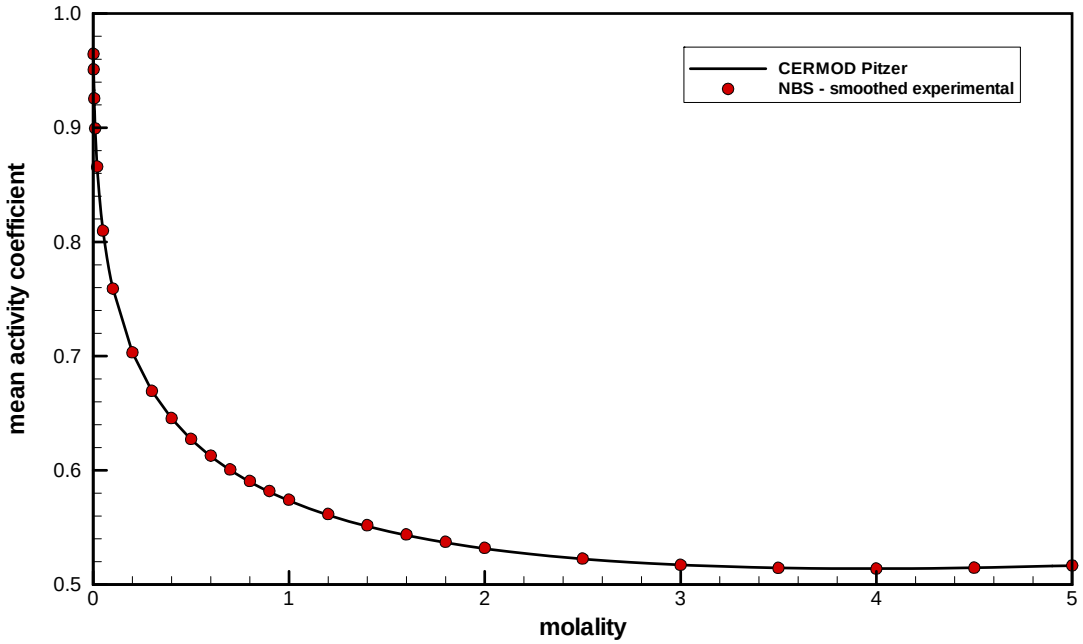

Figure B-38. RbI at 25°C.

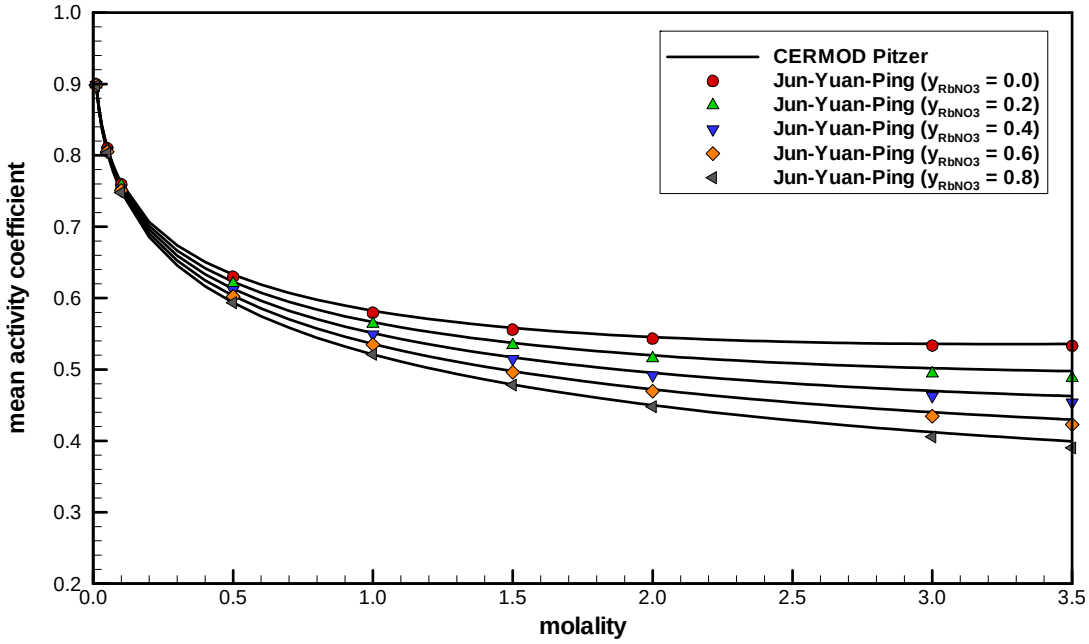

Figure B-39. RbCl in a mixture of RbCl and $RbNO_3$ at 25°C.

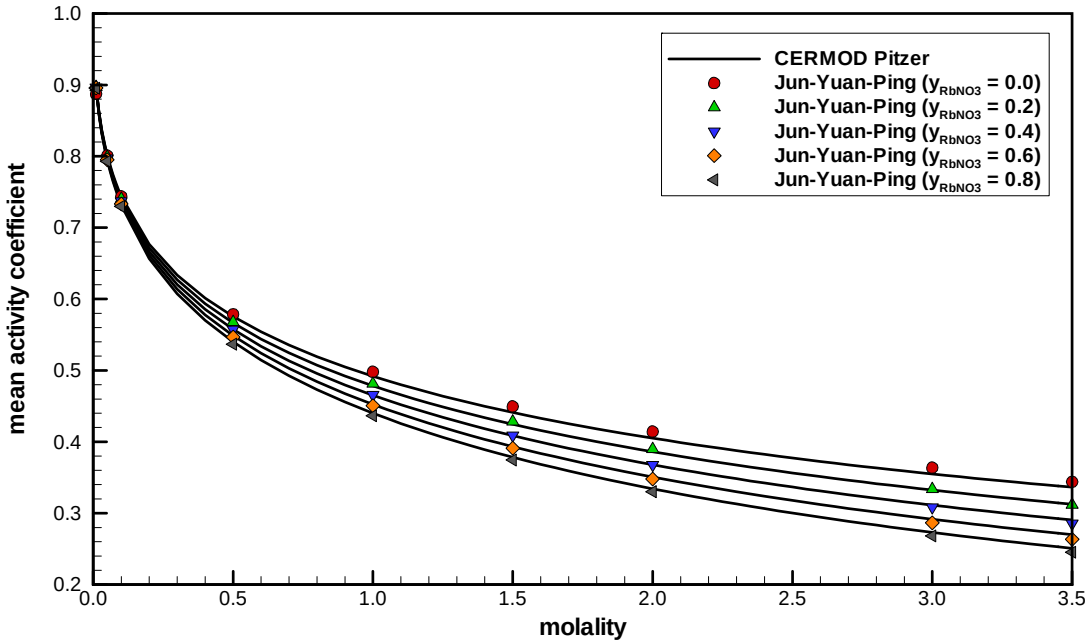

Figure B-40. $RbNO_3$ in a mixture of RbCl and $RbNO_3$ at 25°C.

14.4 Data Structure

The input and output files associated with the CERMOD code and their contents are described below.

14.4.1 Super File

The CERMOD super file is a special type of file used to organize the individual files for input and output operations. The super file is a text file that contains the names of input/output files. The super file is read from standard input (UNIT=5). The first line of the super file is an identifier card, CERMODSup RESIN LiqAct. RESIN is either Solution or SL639. LiqAct is either Ideal or NonIdeal. After the identifier line, each subsequent line is preceded by a four-letter category code and a filename. The category code and filename have to be enclosed in single or double quotes. The MAIN, SPEC, PIT1, EQUL, RESN and TOLS categories are required. The other categories are specified based on the type of simulation, spline specifications, and output options. Table B-7 shows the format of a typical super file.

Table B-7. CERMOD Super File Format.

Category	File Name
CERMODSup	SL639 NonIdeal
'MAIN'	'AN-105-5M-25C.dat'
'SPLN'	'AN-105-5M-25C.spl'
'SPEC'	'..\..\databank\Species-Data.dat'
'PIT1'	'..\..\databank\Pitzer-Cation-Anion.dat'
'PIT2'	'..\..\databank\Pitzer-Cation-Cation.dat'
'PIT3'	'..\..\databank\Pitzer-Anion-Anion.dat'
'PIT4'	'..\..\databank\Pitzer-Cation-Anion-Anion.dat'
'PIT5'	'..\..\databank\Pitzer-Cation-Cation-Anion.dat'
'EQUL'	'..\..\databank\Equilibrium-Constants-SL639.dat'
'RESN'	'..\..\databank\SL639-batch-Info.dat'
'TOLS'	'..\..\databank\HYBRD1-LMDIF1 Tolerances.dat'
'FLHI'	'AN-105-5M-25C.opt'
'PRNT'	'AN-105-5M-25C.out'
'DIAG'	'AN-105-5M-25C.log'
'PLOT'	'AN-105-5M-25C.plt'
'ISOP'	'AN-105-5M-25C-iso.plt'

14.4.2 File Content and Organization

Table B-8 summarizes the input and output (I/O) files specified within the CERMOD super file. The detailed content and organization of each file is presented in the next section.

CERMOD uses list-directed **READ** statements to process numeric data in the main input, species data, Pitzer parameters, equilibrium constants and spline profile data file. Therefore, there are no data formatting requirements and the data associated with a given **READ** statement may occupy multiple lines in the main input file. Data groups are delineated by required comment lines that serve the purpose of annotating the input.
Besides a main output file and optional diagnostic file, CERMOD can create an additional output file intended for Tecplot™ post-processing.

Table B-8. Summary of CERMOD Input and Output Files.

File	Name	I/O	Category
super file	user-specified	input	-
main input	user-specified in super file	input	MAIN
spline data	user-specified in super file	input	SPLN
species data	user-specified in super file	input	SPEC
Pitzer cation-anion parameters	user-specified in super file	input	PIT1
Pitzer cation-cation parameters	user-specified in super file	input	PIT2
Pitzer anion-anion parameters	user-specified in super file	input	PIT3
Pitzer cation-anion-anion parameters	user-specified in super file	input	PIT4
Pitzer cation-cation-anion parameters	user-specified in super file	input	PIT5
equilibrium constants	user-specified in super file	input	EQUL
SL639 batch resin data	user-specified in super file	input	RESN
MINPACK solvers (HYBRD1 and LMDIF1) tolerances	user-specified in super file	input	TOLS
Fruenlich/Langmuir hybrid isotherm fit	user-specified in super file	input	FLHI
print file	user-specified in super file	output	PRNT
plot file	user-specified in super file	output	PLOT
diagnostic file	user-specified in super file	output	DIAG
Fruenlich/Langmuir hybrid isotherm plot	user-specified in super file	output	ISOP

14.4.3 Main Input File

The main input file is divided into 10 groups and arranged as follows:

1. Problem description
2. Simulation options
3. Number of cations and anions
4. List of cations
5. List of anions
6. Cation concentrations
7. Anion concentrations
8. Solution properties
9. Resin properties
10. Initial fractional solid loadings

The above sequence must be strictly followed, although not every item will be present for all simulations. Groups 9 and 10 are not required for the solution chemistry only option. A description of the input variables and data formats is presented below. The user should keep in mind the following items when preparing the main input file.

- The data associated with a given **READ** statement is termed a "data record" in the discussion below.
- A comment line is required before most data records as described below. A comment line cannot be greater than 80 characters.
- CERMOD uses list-directed **READ** statements to process numeric data. Therefore, there are no data formatting requirements and the data associated with a given **READ** statement may occupy multiple lines in the main input file.

The following data records are required as indicated:

Group 1

1. Problem description

A comment line followed by ntitle+1 data records:

```
comment
ntitle
title(1)
   :
title(ntitle)
```

ntitle: Number of title lines.

title: Title character array **(**$1 \le i \le$ ntitle**)** . Each title line cannot be greater than 80 characters and must be enclosed in single or double quotes.

Group 2

2. Simulation options

A comment line followed by one data record:

```
comment
icor    iter    Tc
```

icor: Parameter indicating temperature correction of Pitzer parameters;
= 0 no,
= 1 yes.

iter: Parameter indicating the type of Pitzer parameters;
= 0 binary Pitzer parameters only,
= 1 binary and ternary Pitzer parameters.

Tc: Equilibrium temperature (ºC).

Group 3

3. Number of cations and anions

A comment line followed by one data record:

comment	
ncation	nanion

ncation: Number of cations: A minimum of one cation, H^+, is required for solution chemistry option. A minimum of three cations, H^+, K^+, and Na^+, are required for the SL639 option.

nanion: Number of anions: A minimum of one anion, OH^-, is required for the solution chemistry option. A minimum of three anions, OH^-, NO_3^-, and ReO_4^- or TcO_4^-, are required for the SL639 option.

Group 4

4. List of cations

A comment line followed by ncation data records:

comment
cation(1)
:
cation(ncation)

cation: Name of each cation. The cation name is a character string enclosed within quotes and must be a member of the cation list in Table B-1. The minimum cation list is H^+, K^+, and Na^+ for the SL639 option.

Group 5

5. List of anions

A comment line followed by nanion data records:

comment
anion(1)
:
anion(nanion)

anion: Name of each anion. The anion name is a character enclosed within quotes and must be a member of the anion list in Table **B**-1. The minimum anion list is OH^-, NO_3^-, and ReO_4^- or TcO_4^- for the SL639 option.

Group 6

6. Cation concentrations

A comment line followed by ncation data records:

```
comment
cinmlt(1)                icinxy(1)
   :                        :
cinmlt(ncation)  icinxy(ncation)
```

cinmlt: Cation input concentration (icinxy = 0) or concentration multiplier (icinxy > 0) to the spline dataset specified by the file given in the 'SPLN' category of the CERMOD super file. Here the concentrations should be listed in the same order as the cation list in Group 4. Zero concentrations can be used. If the solution is neutral or basic, set the concentration of H^+ to zero and CERMOD will internally correct the H^+ concentration. Otherwise, specified the H^+ concentration if the solution is acidic.

icinxy: Parameter array indicating which spline dataset to use for computing cation concentration.

- = 0 no spline dataset used (no 'SPLN' category required), cinmlt is the input concentration,
- > 0 integer indicating the index of the spline dataset specified by the file given in the 'SPLN' category of the CERMOD super file.

Group 7

7. Anion concentrations

A comment line followed by nanion data records:

```
comment
cinmlt(ncation+1)                icinxy(ncation+1)
      :                                :
cinmlt(ncation+nanion)  icinxy(ncation+nanion)
```

cinmlt: Anion input concentration (icinxy = 0) or concentration multiplier (icinxy > 0) to the spline dataset specified by the file given in the 'SPLN' category of the CERMOD super file. Here the concentrations should be listed in the same order as the anion list in Group 5. Zero concentrations can be used. If the solution is neutral or acidic, set the concentration of OH^- to zero and CERMOD will internally correct the OH^- concentration. Otherwise, specified the OH^- concentration if the solution is basic.

icinxy: Parameter array indicating which spline dataset to use for computing anion concentration.

- = 0 no spline dataset used (no 'SPLN' category required), cinmlt is the input concentration,
- > 0 integer indicating the index of the spline dataset specified

by the file given in the 'SPLN' category of the CERMOD super file.

Group 8

8. Solution properties

A comment line followed by one data record:

comment			
vol_liq	rhoin	H2Oin	

vol_liq: Volume of liquid (ml).

rhoin: Parameter indicating the method for computing liquid density;
- < 0 liquid density computed using HTWOS model in g/ml,
- > 0 liquid density specified in g/ml.

H2Oin: Parameter indicating the method for computing initial moles of water;
- = 0 compute using liquid density specified above,
- > 0 initial moles of water specified.

Group 9

9. Resin properties (SL639)

A comment line followed by one data record:

comment	
ffactor	wetmass

ffactor: Ratio of dry-to-wet resin mass (-). The resin reference state is dry.

wetmass: Mass of wet resin (g).

A comment line followed by one data record:

comment	
Sion	Batnum

Scion: Sorbed species (either ReO_4^- or TcO_4^-).

Batnum: SL639 resin batch number specified in "RESN" category file.

Group 10

10. Initial fractional solid loadings (SL639)

A comment line followed by one data record:

comment			
Qin(1)	Qin(2)	Qin(3)	Qin(4)

Qin(1): Initial fractional solid loading of $NaXO_4$.

Qin(2): Initial fractional solid loading of $NaNO_3$.

Qin(3): Initial fractional solid loading of KXO_4.

Qin(4): Initial fractional solid loading of KNO_3.

14.4.4 Spline Data File

The spline data file is specified in the CERMOD super file under the 'SPLN' category (Table B-8). This data file is used to vary the concentrations of cations and anions in order to generate multiple numerical batch contacts within a single simulation run. Otherwise, CERMOD computes a single numerical batch contact. Each spline dataset within the file is indexed starting at 1. To access the spline dataset, the user must set the icinxy (Groups 6 and 7) variable to the spline index of interest. Note, the spline data for cations and anions should be set up to maintain electroneutrality at each spline data point. One common example of utilizing the spline data would be the generation of data points along a XO4- isotherm (loading curve) as a function of aqueous equilibrium XO4- concentration. The structure of the spline data file is as follows:

A comment line followed by one data record:

comment
nspl nk

nspl: Number of spline datasets (≥ 1).

nk: Number of knots per spline.

The following block of data is repeated nspl times:

comment
itype() ninv
The following block of data is repeated ninv times:
ylo yhi n

itype(): Parameter integer array indicating the type of spline,
= 0 Linear spline.

ninv: Number of spline intervals per spline dataset.

ylo: Lower concentration value of spline interval.

yhi: Upper concentration value of spline interval.

n: Number of spline data points in spline interval (includes endpoints). For example, if n = 3 CERMOD would generate y values at ylo, 0.5*(ylo+yhi) and yhi.

14.4.5 Species Data File

The species data file is specified in the CERMOD super file under the 'SPEC' category (Table B-8). This data file is used primarily to provide cation and anion names, molecular weights, and valences. In addition, the molecular weight of water (H_2O) is specified at the end of the file. The current species data file includes 21 cations and 18 anions. The structure of the species data file is as follows:

A comment line followed by one data record:

comment
nc na

nc: Number of cations.

na: Number of anions.

A comment line followed by nc data records:

```
comment
ion(1)      MW(1) z(1)
   :           :        :
ion(nc)     MW(nc)     z(nc)
```

A comment line followed by na data records:

```
comment
ion(nc+1)      MW(nc+1)          z(nc+1)
   :              :                 :
ion(nc+na)     MW(nc+na)         z(nc+na)
```

ion(): Array of ion names. Ion name must be enclosed within quotes.

MW(): Array of ion molecular weights.

z(): Array of ion valences.

A comment line followed by one data record:

```
comment
MWw
```

MWw: Molecular weight of water (g/gmole).

14.4.6 Pitzer Cation-Anion Parameter File

The Pitzer cation-anion parameter file is specified in the CERMOD super file under the 'PIT1' category (Table B-8). This parameter file provides the temperature dependent parameters for computing the binary Pitzer parameters. This file is always required. The structure of the Pitzer cation-anion parameter file is as follows:

A comment line followed by one data record:

```
comment
ncap
```

ncap: Number of Pitzer cation-anion binary parameter records.

The following block of data is repeated ncap times:

comment					
ion1		ion2		etype	ref
comment					
A(1)	A(2)	A(3)	A(4)	A(5)	// $\beta_{ij}^{(0)}$ parameters //
A(1)	A(2)	A(3)	A(4)	A(5)	// $\beta_{ij}^{(1)}$ parameters //
A(1)	A(2)	A(3)	A(4)	A(5)	// $\beta_{ij}^{(2)}$ parameters, etype = '2-2' //
A(1)	A(2)	A(3)	A(4)	A(5)	// C_{ij}^{ϕ} parameters, C_{ij} parameters if ref = 2//

ion1: Cation name. Cation name must be enclosed within quotes.

ion2: Anion name. Anion name must be enclosed within quotes.

etype: Electrolyte type. For example, barium chloride would be considered a '2-1' electrolyte pair and calcium sulfate would be considered a '2-2' electrolyte pair. etype must be enclosed within quotes.

ref: Parameter integer indicating reference source for Pitzer parameters.
= 1 K.S. Pitzer (1979),
= 2 C. F. Weber (2001),
= 3 V. Neck et al. (1998)

A(1:5): Coefficients to temperature dependent functional form of Pitzer parameter. The functional form is:

$$A(1) + A(2)(T - T_{ref}) + A(3)(1/T_{ref} - 1/T) + A(4)\ln(T/T_{ref}) + A(5)(T^2 - T_{ref}^2)$$

$T_{ref} = 298.15\ K$.

14.4.7 Pitzer Cation-Cation Parameter File

The Pitzer cation-cation parameter file is specified in the CERMOD super file under the 'PIT2' category (Table B-8). This parameter file provides the temperature dependent parameters for computing the ternary Pitzer cation-cation parameters. This file is required if iter = 1 in the main input file. The structure of the Pitzer cation-cation parameter file is as follows:

A comment line followed by one data record:

comment
nccp

nccp: Number of Pitzer cation-cation ternary parameter records.

The following block of data is repeated nccp times:

comment ion1 ion2 comment A(1) A(2) A(3) A(4) A(5) // θ_{ij} parameters //

ion1: Cation 1 name. Cation 1 name must be enclosed within quotes.

ion2: Cation 2 name. Cation 2 name must be enclosed within quotes .

A(1:5): Coefficients to temperature dependent functional form of Pitzer θ_{ij} parameter. The functional form is:

$$A(1) + A(2)(T - T_{ref}) + A(3)(1/T_{ref} - 1/T) + A(4)\ln(T/T_{ref}) + A(5)(T^2 - T_{ref}^2)$$

$T_{ref} = 298.15$ K .

14.4.8 Pitzer Anion-Anion Parameter File

The Pitzer anion-anion parameter file is specified in the CERMOD super file under the 'PIT3' category (Table B-8). This parameter file provides the temperature dependent parameters for computing the ternary Pitzer anion-anion parameters. This file is required if iter = 1 in the main input file. The structure of the Pitzer anion-anion parameter file is as follows:

A comment line followed by one data record:

comment naap

naap: Number of Pitzer anion-anion ternary parameter records.

The following block of data is repeated naap times:

comment ion1 ion2 comment A(1) A(2) A(3) A(4) A(5) // θ_{ij} parameters //

ion1: Anion 1 name. Anion 1 name must be enclosed within quotes.

ion2: Anion 2 name. Anion 2 name must be enclosed within quotes.

A(1:5): Coefficients to temperature dependent functional form of Pitzer θ_{ij} parameter. The functional form is:

$$A(1) + A(2)(T - T_{ref}) + A(3)(1/T_{ref} - 1/T) + A(4)\ln(T/T_{ref}) + A(5)(T^2 - T_{ref}^2)$$

$T_{ref} = 298.15$ K .

14.4.9 Pitzer Cation-Anion-Anion Parameter File

The Pitzer cation-anion-anion parameter file is specified in the CERMOD super file under the 'PIT4' category (Table B-8). This parameter file provides the temperature dependent parameters for computing the ternary Pitzer cation-anion-anion parameters.

This file is required if iter = 1 in the main input file. The structure of the Pitzer cation-anion-anion parameter file is as follows:

A comment line followed by one data record:

comment ncaap

nccap: Number of Pitzer cation-anion-anion ternary parameter records.

The following block of data is repeated ncaap times:

comment ion1 ion2 ion3 comment A(1) A(2) A(3) A(4) A(5) // ψ_{ijk} parameters //

ion1: Cation name. Cation name must be enclosed within quotes and not exceed 8 characters.

ion2: Anion 1 name. Anion 1 name must be enclosed within quotes.

ion3: Anion 2 name. Anion 2 name must be enclosed within quotes.

A(1:5): Coefficients to temperature dependent functional form of Pitzer ψ_{ijk} parameter. The functional form is:

$$A(1) + A(2)(T - T_{ref}) + A(3)(1/T_{ref} - 1/T) + A(4)\ln(T/T_{ref}) + A(5)(T^2 - T_{ref}^2)$$

$T_{ref} = 298.15\,K$.

14.4.10 Pitzer Cation-Cation-Anion Parameter File

The Pitzer cation-cation-anion parameter file is specified in the CERMOD super file under the 'PIT5' category (Table B-8). This parameter file provides the temperature dependent parameters for computing the ternary Pitzer cation-cation-anion parameters. This file is required if iter = 1 in the main input file. The structure of the Pitzer cation-cation-anion parameter file is as follows:

A comment line followed by one data record:

comment nccap

nccap: Number of Pitzer cation-cation-anion ternary parameter records.

The following block of data is repeated nccap times:

comment ion1 ion2 ion3 comment A(1) A(2) A(3) A(4) A(5) // ψ_{ijk} parameters //

ion1: Cation 1 name. Cation 1 name must be enclosed within quotes.

ion2: Cation 2 name. Cation 2 name must be enclosed within quotes.

ion3: Anion name. Anion name must be enclosed within quotes.

A(1:5): Coefficients to temperature dependent functional form of Pitzer ψ_{ijk} parameter. The functional form is:

$$A(1) + A(2)(T - T_{ref}) + A(3)(1/T_{ref} - 1/T) + A(4)\ln(T/T_{ref}) + A(5)(T^2 - T_{ref}^2)$$

$T_{ref} = 298.15\ K$.

14.4.11 Equilibrium Constants Parameter File

The equilibrium constant parameter file is specified in the CERMOD super file under the 'EQUL' category (Table B-8). This parameter file provides the temperature dependent parameters for computing equilibrium constants for the dissociation of water reaction and the mass action equations. The number of entries is simulation dependent. One entry is required for the solution chemistry option: parameters for the dissociation of water reaction (Eqn. B-16). The SuperLig® 639 requires 5 entries: the dissociation of water reaction and parameters for the four mass action reactions (Eqns. (B-1) to (B-4)). The structure of the equilibrium constant parameter file is as follows:

A comment line followed by one data record:

comment nek

nek: Number of equilibrium constants;
= 1 solution chemistry only,
= 5 SL639 resin.

A comment line followed by nek data records:

comment				
coef(1,1)	coef(2,1)	coef(3,1)	coef(4,1)	// Eqn. B-16 //
coef(1,2)	coef(2,2)	coef(3,2)	coef(4,2)	// Eqn. B-1 //
coef(1,3)	coef(2,3)	coef(3,3)	coef(4,3)	// Eqn. B-2 //
coef(1,4)	coef(2,4)	coef(3,4)	coef(4,4)	// Eqn. B-3 //
coef(1,5)	coef(2,5)	coef(3,5)	coef(4,5)	// Eqn. B-4 //

coef(): Matrix of coefficients to temperature dependent parameters used to compute equilibrium constants. The equilibrium constants are computed as:

$$K_j = \exp\left(coef(1,j)1/T + coef(2,j)\ln(T) + coef(3,j)T + coef(4,j)\right)$$

where j = w, 11, 12, 21, 22.

14.4.12 SL639 Batch Resin Data File

The SL639 batch resin data file is specified in the CERMOD super file under the 'RESN' category (Table B-8). This data file provides the total electrolyte sorption capacity for XO4-, fraction of equilibrium constants used for $NaReO_4$ and $KReO_4$ mass action equations, SL639 resin batch id and fraction of total electrolyte sorption capacity for each resin batch. The structure of the SL639 batch resin data file is as follows:

A comment line followed by one data record:

comment
Qtot EtaRe

Qtot: Total electrolyte sorption capacity for XO4-.

EtaRe: fraction of equilibrium constants used for $NaReO_4$ and $KReO_4$ mass action equations.

A comment line followed by one data record:

comment
nbat

nbat: Number of different SL639 resin batches.

A comment line followed by nbat data records:

comment	
Batnum BatID(0)	Qfrac(0)
Batnum BatID(1)	Qfrac(1)
Batnum BatID(nbat-1)	Qfrac(nbat-1)

Batnum Resin batch number (not stored).

BatID() Array of SL639 resin batch id's.

Qfrac() Array of fractions of total electrolyte sorption capacity for each resin batch.

14.4.13 MINPACK Solvers (HYBRD1 and LMDIF1) Tolerances File

The MINPACK solvers tolerances file is specified in the CERMOD super file under the 'TOLS' category (Table B-8). This file provides convergence tolerances for the nonlinear solver HYBRD1 and the parameter estimation solver LMDIF1. The structure of the MINPACK solvers tolerances file is as follows:

A comment line followed by one data record:

comment	
tolHY	tolLM

tolHY: The relative error between X and the solution (HYBRD1).

tolLM: The relative error in the sum of squares (LMDIF1).

14.4.14 Fruenlich/Langmuir Hybrid Isotherm Parameter Estimation

The Fruenlich/Langmuir (F/L) hybrid isotherm parameter estimation file is specified in the CERMOD super file under the 'FLHI' category (Table B-8). If only a single batch contact run is being executed, then no isotherm parameter estimation is performed. The Fruenlich/Langmuir hybrid isotherm is an empirical combination of the Langmuir and Fruenlich isotherms. The isotherm is multicomponent but here it is fitted as a two-parameter single component isotherm for XO4- absorption. The user must utilize the

spline feature to vary the concentration of NaXO4 over several orders of magnitude in order to estimate the parameters for the F/L isotherm. In its binary Langmuir functional form, the isotherm reduces to the following:

$$Q_{XO_4^-} = \frac{CTFL[XO_4^-]_e}{bFL + [XO_4^-]_e} \quad \text{(A-31)}$$

where

$Q_{XO_4^-}$ .....equilibrium XO4- solid-phase loading, mmol/g_{resin},

$[XO_4^-]_e$ .....equilibrium XO4- liquid-phase concentration, [M],

CTFL .....total absorption capacity of resin, mmol/g_{resin},

bFL .....beta parameter which is temperature and composition dependent, [M].

The structure of the Fruendlich/Langmuir hybrid isotherm parameter file is:

comment	
iP(1)	iP(2)
comment	
CTFL	bFL

iP(i): Parameter indicating whether to estimate or use values in next record where i=1 for CTFL and i=2 for bFL;
= 0 use value provided,
= 1 estimate parameter

CTFL: Initial guess or value of total absorption capacity, mmol/g_{resin}.

bFL: Initial guess or value of beta isotherm parameter, [M].

14.4.15 Printed Output File

The printed output file is specified in the CERMOD super file under the 'PRNT' category (Table B-8). This file provides the following information:
Input parameters, conditions and settings

- Configuration header
- Dataset filename (parameter estimation)
- Title
- SuperLig® 639 resin batch number and id
- Liquid temperature and initial solution density
- Species name (cations to anions), molecular weight, valence and initial molar concentration
- Initial moles and activity of water
- Initial ionic strength of solution and initial pH
- Equilibrium constants
- Liquid volume, dry resin mass and phase ratio
- Total absorption capacity
- Fraction of total electrolyte sorption capacity

- $NaXO_4$, $NaNO_3$, KXO_4 and KNO_3 initial electrolyte solid loadings

Output results at equilibrium (final state)

- Nonlinear solver error flag and tolerance for L2 norm
- Species equilibrium molarities, molalities and ionic activity coefficients
- Equilibrium moles of water and water activity
- Equilibrium ionic strength and pH
- Equilibrium Na^+, K^+, XO_4^- and NO_3^- aqueous concentration, K_d, solid loading and fractional loading
- Unoccupied sites, total sorption sites, and total sites
- Estimate of Fruendlich/Langmuir hybrid isotherm parameters (optional)

14.4.16 Tecplot Datafile

The Tecplot datafile is specified in the CERMOD super file under the 'PLOT' category (Table B-8). The output of the Tecplot datafile is simulation dependent. For a solution chemistry only simulation (iopt=0), the Tecplot datafile will dump the following variables at each numerical liquid-phase solution point:

- Equilibrium concentrations in molarities and molalities of ionic species provided in Groups 4 and 5
- Activity of water
- Ionic strength of solution
- pH of solution
- osmotic coefficient of solution

The Tecplot data file will dump the following variables at each numerical batch contact point:

- Equilibrium concentrations in molarities and molalities of ionic species provided in Groups 4 and 5
- Equilibrium ionic solid loadings of Na^+, K^+, XO_4^-, and NO_3^-
- Equilibrium electrolyte solid loadings of $NaXO_4$, $NaNO_3$, KXO_4 and KNO_3.

14.4.17 Diagnostic Log File

The diagnostic log file is specified in the CERMOD super file under the 'DIAG' category (Table B-8). This file provides the following diagnostic information:

- Pitzer binary cation-anion parameters (evaluated at the simulation temperature)
- Spline profile data (and coefficients)
- Species charge balance summary (ionic molarities for each numerical batch contact point or solution chemistry point)

14.4.18 Fruendlich/Langmuir Hybrid Isotherm Tecplot File

The Fruendlich/Langmuir hybrid cesium isotherm Tecplot file is specified in the CERMOD super file under the 'ISOP' category (Table B-8). This option is only available if the 'FLHI' category is selected. A Tecplot datafile is generated showing a comparison of the numerical batch contact points generated (i.e., XO_4^- solid-phase versus

liquid-phase concentrations) and the fit of this numerical batch contact data to the F/L cesium isotherm model.

15.0 Appendix C (Column Test Input Files)

For reference the VERSE-LC input files for the laboratory-scale, bench-scale, and pilot-scale column benchmarking are provided in this appendix. Some of the column tests were performed using perrhenate while the remainder used pertechnetate. Twelve column simulation models were run. The input files for each case are listed below:

VERSE Input for Lab-Scale Pertechnetate Column (Hassan, 2000a) Test

```
NH Run-A Simulation of Tc removal on small-scale Superlig 639 column (5.1 ml)
1 component (93% TcO4) isotherm (NO3- set to 0.998 M) (BNFL Envelope A Salt Solution)
1, 100, 3, 6                    ncomp, nelem, ncol-bed, ncol-part
FCWNA                           isotherm,axial-disp,film-coef,surf-diff,BC-col
NNNNN                           input-only,perfusable,feed-equil,datafile.yio
MM                              comp-conc units
10.7331, 1.1, 0.255, 5.1   Length(cm),Diam(cm),Q-flow(ml/min),CSTR-vol(ml)
377.0, 0.357, 0.371, 0.0        part-rad(um), bed-void, part-void, sorb-cap()
  0.0, 0.0                      init-conc [M]
S                               COMMAND - conc step change in TcO4- (Tc-total =
2.58224d-5)
1, 0.0, 2.40148d-5, 1, 0.0      spec id, time(min), conc(mg/ml), freq, dt(min)
V                               COMMAND - viscosity/density change
0.0261255, 1.223549             fluid viscosity(posie), density(g/cm^3)
m                               COMMAND - subcolumns
50, 100, 0, 1, 2.95d+8, 0.0, 50000.0  elem-shift,elem-watch,pp-watch,c-watch,c-thresh,t-
e,t-ee
h                               COMMAND - effluent history dump
1, 1.0, 1.0, 0.25, 0.1          unit op#, ptscale(1-4) filtering
h                               COMMAND - effluent history dump
2, 1.0, 1.0, 0.25, 0.1          unit op#, ptscale(1-4) filtering
h                               COMMAND - effluent history dump
3, 1.0, 1.0, 0.25, 0.1          unit op#, ptscale(1-4) filtering
h                               COMMAND - effluent history dump
4, 1.0, 1.0, 0.25, 0.1          unit op#, ptscale(1-4) filtering
D
-1, 25000, 1, 0.0
-                               end of commands
25000, 1.0                       end time(min), max dt in B.V.s
1.0d-7, 1.0d-4                  abs-tol(mg/ml), rel-tol
-                               non-negative conc constraint
1.0d0      , 1.0d0              size exclusion factor
1.002d-4   , 1.126d-4           part-pore diffusivities(cm^2/min) 50% of free values
2.004d-4   , 2.252d-4           Brownian diffusivities(cm^2/min)
3.03170E-01 , 3.38024d-4         Freundlich/Langmuir Hybrid a    (moles/L B.V.)
rhob=0.468 (mix)
1.0         , 1.36300d-3         Freundlich/Langmuir Hybrid b    (1/M)  Batch specific
isotherm
1.0         , 1.0                Freundlich/Langmuir Hybrid Ma   (-)    ccap=1.1379
1.0         , 1.0                Freundlich/Langmuir Hybrid Mb   (-)
8.17736E-04 , 0.0                Freundlich/Langmuir Hybrid beta (-) "eff" isotherm NO3
= 0.998 M
------------------------------------------------------------------------------
```

VERSE Input for Lab-Scale Perrhenate Column (King 2002 Exp-1) Test

```
WK Env-A(25 C; Exp-1) Simulation of Re removal on small Superlig 639 column (10.07 ml)
1 component (Re) isotherm (NO3- set to 1.243 M) (BNFL Envelope A Salt Solution)
1, 50, 3, 6                     ncomp, nelem, ncol-bed, ncol-part
FCWNA                           isotherm,axial-disp,film-coef,surf-diff,BC-col
NNNNN                           input-only,perfusable,feed-equil,datafile.yio
M                               comp-conc units
5.02333, 1.60, 0.50163, 5.0         Length(cm),Diam(cm),Q-flow(ml/min),CSTR-vol(ml)
225.0, 0.366, 0.315, 0.0        part-rad(um), bed-void, part-void, sorb-cap()
  0.0                           init-conc [M]
S                               COMMAND - conc step change in ReO4-
```

```
1, 0.0, 2.943d-5, 1, 0.0         spec id, time(min), conc(mg/ml), freq, dt(min)
V                                COMMAND - viscosity/density change
0.0298, 1.234                    fluid viscosity(posie), density(g/cm^3)
h                                COMMAND - effluent history dump
2, 1.0, 1.0, 0.25, 0.1           unit op#, ptscale(1-4) filtering
D
-1, 10000, 1, 0.0
-                                end of commands
10000, 1.0                        end time(min), max dt in B.V.s
1.0d-7, 1.0d-4                   abs-tol(mg/ml), rel-tol
-                                non-negative conc constraint
1.0d0      , 1.0d0               size exclusion factor
3.984d-5   , 2.815d-5            part-pore diffusivities(cm^2/min) 12.5% of free values
3.188d-4   , 2.252d-4            Brownian diffusivities(cm^2/min)
1.54382E-01  , 3.38024d-4          Freundlich/Langmuir Hybrid a    (moles/L B.V.)
rhob=0.6286, ccap=0.855
1.0          , 1.36300d-3          Freundlich/Langmuir Hybrid b    (1/M)  a_Re =
2.48000d-1
1.0          , 1.0                 Freundlich/Langmuir Hybrid Ma   (-) 3.06463d-1
1.0          , 1.0                 Freundlich/Langmuir Hybrid Mb   (-)
1.43021E-03  , 0.0                 Freundlich/Langmuir Hybrid beta (-) effective isotherm
NO3 =
--------------------------------------------------------------------------------
```

VERSE Input for Lab-Scale Pertechnetate Column (Burgeson-A 2002) Test

```
IB(PNNL) Env-A[AP-101] (25 C) Simulation of TcO4 removal on small Superlig 639 column
(5.478 ml)
1 component (TcO4) isotherm (NO3- set to 1.88 M) (AP-101 Envelope A Salt Solution)
1, 50, 3, 6                      ncomp, nelem, ncol-bed, ncol-part
FCWNA                            isotherm,axial-disp,film-coef,surf-diff,BC-col
NNNNN                            input-only,perfusable,feed-equil,datafile.yio
M                                comp-conc units
3.10, 1.5, 0.2739, 2.7           Length(cm),Diam(cm),Q-flow(ml/min),CSTR-vol(ml)
240.0, 0.366, 0.315, 0.0         part-rad(um), bed-void, part-void, sorb-cap()
  0.0                            init-conc [M]
S                                COMMAND - conc step change in ReO4-
1, 0.0, 2.9997d-5, 1, 0.0        spec id, time(min), conc(mg/ml), freq, dt(min)
V                                COMMAND - viscosity/density change
0.0268, 1.234                    fluid viscosity(posie), density(g/cm^3)
h                                COMMAND - effluent history dump
2, 1.0, 1.0, 0.25, 0.1           unit op#, ptscale(1-4) filtering
D
-1, 30000, 1, 0.0
-                                end of commands
30000, 1.0                        end time(min), max dt in B.V.s
1.0d-7, 1.0d-4                   abs-tol(mg/ml), rel-tol
-                                non-negative conc constraint
1.0d0      , 1.0d0               size exclusion factor
1.098d-4   , 2.815d-5            part-pore diffusivities(cm^2/min) 35.05% of free values
3.137d-4   , 2.252d-4            Brownian diffusivities(cm^2/min)
4.39513E-01 , 3.38024d-4          Freundlich/Langmuir Hybrid a    (moles/L B.V.)
rhob=0.453, ccap=1.80
1.0          , 1.36300d-3          Freundlich/Langmuir Hybrid b    (1/M)  a_Re = 2.48000d-
1, ccap=0.6472
1.0          , 1.0                 Freundlich/Langmuir Hybrid Ma   (-) 3.06463d-1,
rhob=0.50, ccap=0.855
1.0          , 1.0                 Freundlich/Langmuir Hybrid Mb   (-)
7.31694E-04 , 0.0                 Freundlich/Langmuir Hybrid beta (-) effective isotherm
NO3 =
--------------------------------------------------------------------------------
```

VERSE Input for Lab-Scale Pertechnetate Column (Burgeson-B 2002) Test

```
IB(PNNL) Env-B[AZ-101] (25 C) Simulation of TcO4 removal on small Superlig 639 column
(5.478 ml)
1 component (TcO4) isotherm (NO3- set to 0.85 M) (AP-101 Envelope A Salt Solution)
1, 50, 3, 6                      ncomp, nelem, ncol-bed, ncol-part
```

```
FCWNA                          isotherm,axial-disp,film-coef,surf-diff,BC-col
NNNNN                          input-only,perfusable,feed-equil,datafile.yio
M                              comp-conc units
3.10, 1.5, 0.2739, 2.7         Length(cm),Diam(cm),Q-flow(ml/min),CSTR-vol(ml)
240.0, 0.366, 0.315, 0.0       part-rad(um), bed-void, part-void, sorb-cap()
  0.0                          init-conc [M]
S                              COMMAND - conc step change in ReO4-
1, 0.0, 2.2498d-4, 1, 0.0      spec id, time(min), conc(mg/ml), freq, dt(min)
V                              COMMAND - viscosity/density change
0.0268, 1.234                  fluid viscosity(posie), density(g/cm^3)
h                              COMMAND - effluent history dump
2, 1.0, 1.0, 0.25, 0.1         unit op#, ptscale(1-4) filtering
D
-1, 30000, 1, 0.0
-                              end of commands
30000, 1.0                      end time(min), max dt in B.V.s
1.0d-7, 1.0d-4                 abs-tol(mg/ml), rel-tol
-                              non-negative conc constraint
1.0d0      , 1.0d0             size exclusion factor
1.098d-4   , 2.815d-5          part-pore diffusivities(cm^2/min) 35.0% of free values
3.137d-4   , 2.252d-4          Brownian diffusivities(cm^2/min)
4.39468E-01 , 3.38024d-4        Freundlich/Langmuir Hybrid a    (moles/L B.V.)
rhob=0.453, ccap=0.855
1.0         , 1.36300d-3        Freundlich/Langmuir Hybrid b    (1/M)  a_Re = 2.48000d-
1, ccap=0.6472
1.0         , 1.0               Freundlich/Langmuir Hybrid Ma   (-) 3.06463d-1,
rhob=0.50
1.0         , 1.0               Freundlich/Langmuir Hybrid Mb   (-)
7.26774E-04 , 0.0               Freundlich/Langmuir Hybrid beta (-) effective isotherm
NO3 =
-------------------------------------------------------------------------------
```

VERSE Input for Lab-Scale Pertechnetate Column (Burgeson-C 2002) Test

```
IB(PNNL) Env-C [AN-102] (25 C) Simulation of TcO4 removal on small Superlig 639 column
(5.478 ml)
1 component (TcO4) isotherm (NO3- set to 1.73 M) (AP-101 Envelope A Salt Solution)
1, 50, 3, 6                    ncomp, nelem, ncol-bed, ncol-part
FCWNA                          isotherm,axial-disp,film-coef,surf-diff,BC-col
NNNNN                          input-only,perfusable,feed-equil,datafile.yio
M                              comp-conc units
3.10, 1.5, 0.2739, 2.7         Length(cm),Diam(cm),Q-flow(ml/min),CSTR-vol(ml)
240.0, 0.366, 0.315, 0.0       part-rad(um), bed-void, part-void, sorb-cap()
  0.0                          init-conc [M]
S                              COMMAND - conc step change in ReO4-
1, 0.0, 1.6248d-5, 1, 0.0      spec id, time(min), conc(mg/ml), freq, dt(min)
V                              COMMAND - viscosity/density change
0.0268, 1.234                  fluid viscosity(posie), density(g/cm^3)
h                              COMMAND - effluent history dump
2, 1.0, 1.0, 0.25, 0.1         unit op#, ptscale(1-4) filtering
D
-1, 30000, 1, 0.0
-                              end of commands
20000, 1.0                      end time(min), max dt in B.V.s
1.0d-7, 1.0d-4                 abs-tol(mg/ml), rel-tol
-                              non-negative conc constraint
1.0d0      , 1.0d0             size exclusion factor
1.098d-4   , 2.815d-5          part-pore diffusivities(cm^2/min) 35.0% of free values
3.137d-4   , 2.252d-4          Brownian diffusivities(cm^2/min)
4.39559E-01 , 3.38024d-4        Freundlich/Langmuir Hybrid a    (moles/L B.V.)
rhob=0.453, ccap=0.855
1.0         , 1.36300d-3        Freundlich/Langmuir Hybrid b    (1/M)  a_Re = 2.48000d-
1, ccap=0.6472
1.0         , 1.0               Freundlich/Langmuir Hybrid Ma   (-) 3.06463d-1,
rhob=0.50
1.0         , 1.0               Freundlich/Langmuir Hybrid Mb   (-)
1.74938E-03 , 0.0               Freundlich/Langmuir Hybrid beta (-) effective isotherm
-------------------------------------------------------------------------------
```

VERSE Input for Lab-Scale Perrhenate Column (King 2000a Exp-1) Test

```
WK Exp-1 Simulation of Re removal on small Superlig 639 column (51.1 ml)
1 component (Re) isotherm (NO3- set to 1.25 M) (BNFL Envelope A Salt Solution)
1, 100, 3, 6                    ncomp, nelem, ncol-bed, ncol-part
FUWNA                           isotherm,axial-disp,film-coef,surf-diff,BC-col
NNNNN                           input-only,perfusable,feed-equil,datafile.yio
MM                              comp-conc units
8.991, 2.69, 2.898442, 51.1     Length(cm),Diam(cm),Q-flow(ml/min),CSTR-vol(ml)
377.0, 0.357, 0.371, 0.0        part-rad(um), bed-void, part-void, sorb-cap()
  0.0, 0.0                      init-conc [M]
S                               COMMAND - conc step change in ReO4-
1, 0.0, 8.5929d-5, 1, 0.0       spec id, time(min), conc(mg/ml), freq, dt(min)
V                               COMMAND - viscosity/density change
0.0261255, 1.223549             fluid viscosity(posie), density(g/cm^3)
h                               COMMAND - effluent history dump
2, 1.0, 1.0, 0.25, 0.1          unit op#, ptscale(1-4) filtering
D
-1, 9200, 1, 0.0
-                               end of commands
9200, 1.0                       end time(min), max dt in B.V.s
1.0d-7, 1.0d-4                  abs-tol(mg/ml), rel-tol
-                               non-negative conc constraint
1.0d0      , 1.0d0              size exclusion factor
1.03185                         Axial dispersion coef (cm2/min) [correlation = 0.18933]
1.002d-4   , 1.126d-4           part-pore diffusivities(cm^2/min) 50% of free values
2.004d-4   , 2.252d-4           Brownian diffusivities(cm^2/min)
1.45282E-01 , 3.38024d-4         Freundlich/Langmuir Hybrid a    (moles/L B.V.)
rhob=0.489, ccap=0.5071
1.0         , 1.36300d-3         Freundlich/Langmuir Hybrid b    (1/M)  a_Re = 2.48000d-
1
1.0         , 1.0                Freundlich/Langmuir Hybrid Ma   (-)
1.0         , 1.0                Freundlich/Langmuir Hybrid Mb   (-)
1.46318E-03  , 0.0                Freundlich/Langmuir Hybrid beta (-) effective isotherm
NO3
--------------------------------------------------------------------------------
```

VERSE Input for Lab-Scale Perrhenate Column (King 2002 Exp-5) Test

```
WK Env-A(25 C; Exp-5) Simulation of Re removal on small Superlig 639 column (10.07 ml)
1 component (Re) isotherm (NO3- set to 1.243 M) (BNFL Envelope A Salt Solution)
1, 50, 3, 6                     ncomp, nelem, ncol-bed, ncol-part
FCWNA                           isotherm,axial-disp,film-coef,surf-diff,BC-col
NNNNN                           input-only,perfusable,feed-equil,datafile.yio
M                               comp-conc units
6.09823, 1.45, 0.50163, 5.0         Length(cm),Diam(cm),Q-flow(ml/min),CSTR-vol(ml)
225.0, 0.366, 0.315, 0.0        part-rad(um), bed-void, part-void, sorb-cap()
  0.0                           init-conc [M]
S                               COMMAND - conc step change in ReO4-
1, 0.0, 6.270d-5, 1, 0.0        spec id, time(min), conc(mg/ml), freq, dt(min)
V                               COMMAND - viscosity/density change
0.0298, 1.234                   fluid viscosity(posie), density(g/cm^3)
h                               COMMAND - effluent history dump
2, 1.0, 1.0, 0.25, 0.1          unit op#, ptscale(1-4) filtering
D
-1, 20000, 1, 0.0
-                               end of commands
20000, 1.0                       end time(min), max dt in B.V.s
1.0d-7, 1.0d-4                  abs-tol(mg/ml), rel-tol
-                               non-negative conc constraint
1.0d0      , 1.0d0              size exclusion factor
3.984d-5   , 2.815d-5           part-pore diffusivities(cm^2/min) 12.5% of free values
3.188d-4   , 2.252d-4           Brownian diffusivities(cm^2/min)
4.14625E-01 , 3.38024d-4         Freundlich/Langmuir Hybrid a    (moles/L B.V.)
rhob=0.6286, ccap=0.855
1.0         , 1.36300d-3         Freundlich/Langmuir Hybrid b    (1/M)  a_Re = 2.48000d-
1
1.0         , 1.0                Freundlich/Langmuir Hybrid Ma   (-) 3.06463d-1
```

```
1.0         , 1.0                Freundlich/Langmuir Hybrid Mb   (-)
1.34504E-03 , 0.0                Freundlich/Langmuir Hybrid beta (-) effective isotherm
NO3 =
-------------------------------------------------------------------------------
```

VERSE Input for Lab-Scale Perrhenate Column (King 2002 Exp-8) Test

```
WK Env-B (25 C: Exp-8) Simulation of Re removal on small Superlig 639 column (75.1 ml)
1 component (Re) isotherm (NO3- set to 0.515 M) (BNFL Envelope A Salt Solution)
1, 50, 3, 6                      ncomp, nelem, ncol-bed, ncol-part
FCWNA                            isotherm,axial-disp,film-coef,surf-diff,BC-col
NNNNN                            input-only,perfusable,feed-equil,datafile.yio
M                                comp-conc units
15.19331, 2.50, 3.66685, 35.0            Length(cm),Diam(cm),Q-flow(ml/min),CSTR-vol(ml)
287.0, 0.366, 0.315, 0.0         part-rad(um), bed-void, part-void, sorb-cap()
  0.0                            init-conc [M]
S                                COMMAND - conc step change in ReO4-
1, 0.0, 2.070d-4, 1, 0.0         spec id, time(min), conc(mg/ml), freq, dt(min)
V                                COMMAND - viscosity/density change
0.0305, 1.232                    fluid viscosity(posie), density(g/cm^3)
h                                COMMAND - effluent history dump
2, 1.0, 1.0, 0.25, 0.1           unit op#, ptscale(1-4) filtering
D
-1, 30000, 1, 0.0
-                                end of commands
30000, 1.0                        end time(min), max dt in B.V.s
1.0d-7, 1.0d-4                   abs-tol(mg/ml), rel-tol
-                                non-negative conc constraint
1.0d0      , 1.0d0               size exclusion factor
4.109d-5   , 1.126d-4            part-pore diffusivities(cm^2/min) 50% of free values
3.287d-4   , 2.252d-4            Brownian diffusivities(cm^2/min)
4.14563E-01 , 3.38024d-4          Freundlich/Langmuir Hybrid a    (moles/L B.V.)
rhob=0.525, ccap=0.751
1.0         , 1.36300d-3          Freundlich/Langmuir Hybrid b    (1/M)  a_Re = 2.48000d-
1
1.0         , 1.0                 Freundlich/Langmuir Hybrid Ma   (-) 3.06463d-1
1.0         , 1.0                 Freundlich/Langmuir Hybrid Mb   (-)
8.56092E-04 , 0.0                 Freundlich/Langmuir Hybrid beta (-) effective isotherm
NO3 =
-------------------------------------------------------------------------------
```

VERSE Input for Lab-Scale Perrhenate Column (King 2002 Exp-9) Test

```
WK Env-C (25 C: Exp-9) Simulation of Re removal on small Superlig 639 column (75.1 ml)
1 component (Re) isotherm (NO3- set to 2.625 M) (BNFL Envelope A Salt Solution)
1, 50, 3, 6                      ncomp, nelem, ncol-bed, ncol-part
FCWNA                            isotherm,axial-disp,film-coef,surf-diff,BC-col
NNNNN                            input-only,perfusable,feed-equil,datafile.yio
M                                comp-conc units
15.19331, 2.5, 3.75386, 35.0            Length(cm),Diam(cm),Q-flow(ml/min),CSTR-vol(ml)
225.0, 0.366, 0.315, 0.0         part-rad(um), bed-void, part-void, sorb-cap()
  0.0                            init-conc [M]
S                                COMMAND - conc step change in ReO4-
1, 0.0, 3.060d-5, 1, 0.0         spec id, time(min), conc(mg/ml), freq, dt(min)
V                                COMMAND - viscosity/density change
0.0337, 1.255                    fluid viscosity(posie), density(g/cm^3)
h                                COMMAND - effluent history dump
2, 1.0, 1.0, 0.25, 0.1           unit op#, ptscale(1-4) filtering
D
-1, 15000, 1, 0.0
-                                end of commands
15000, 1.0                        end time(min), max dt in B.V.s
1.0d-7, 1.0d-4                   abs-tol(mg/ml), rel-tol
-                                non-negative conc constraint
1.0d0      , 1.0d0               size exclusion factor
3.188d-5  , 1.126d-4            part-pore diffusivities(cm^2/min) 12.5% of free
values3.5775d-5 1.431d-5
2.550d-4   , 2.252d-4            Brownian diffusivities(cm^2/min)
```

```
4.14687E-01 , 3.38024d-4          Freundlich/Langmuir Hybrid a    (moles/L B.V.)
rhob=0.525, ccap=0.855
1.0         , 1.36300d-3          Freundlich/Langmuir Hybrid b    (1/M)  a_Re = 2.48000d-
1
1.0         , 1.0                 Freundlich/Langmuir Hybrid Ma   (-) 3.06463d-1
1.0         , 1.0                 Freundlich/Langmuir Hybrid Mb   (-)
3.55316E-03 , 0.0                 Freundlich/Langmuir Hybrid beta (-) effective isotherm
NO3 =
-------------------------------------------------------------------------------
```

VERSE Input for Lab-Scale Perrhenate Column (King 2000a Exp-5) Test

```
WK Exp-5 Simulation of Re removal on small Superlig 639 column (50.0 ml)
1 component (Re) isotherm (NO3- set to 1.25 M) (BNFL Envelope A Salt Solution)
1, 100, 3, 6                      ncomp, nelem, ncol-bed, ncol-part
FUWNA                             isotherm,axial-disp,film-coef,surf-diff,BC-col
NNNNN                             input-only,perfusable,feed-equil,datafile.yio
MM                                comp-conc units
8.798, 2.69, 2.443784, 51.1       Length(cm),Diam(cm),Q-flow(ml/min),CSTR-vol(ml)
377.0, 0.357, 0.371, 0.0          part-rad(um), bed-void, part-void, sorb-cap()
  0.0, 0.0                        init-conc [M]
S                                 COMMAND - conc step change in ReO4-
1, 0.0, 7.5188d-5, 1, 0.0         spec id, time(min), conc(mg/ml), freq, dt(min)
V                                 COMMAND - viscosity/density change
0.0261255, 1.223549               fluid viscosity(posie), density(g/cm^3)
h                                 COMMAND - effluent history dump
2, 1.0, 1.0, 0.25, 0.1            unit op#, ptscale(1-4) filtering
D
-1, 10000, 1, 0.0
-                                 end of commands
10000, 1.0                         end time(min), max dt in B.V.s
1.0d-7, 1.0d-4                    abs-tol(mg/ml), rel-tol
-                                 non-negative conc constraint
1.0d0      , 1.0d0                size exclusion factor
0.87527                           Axial dispersion coef (cm2/min) [correlation = 0.16060]
1.002d-4   , 1.126d-4             part-pore diffusivities(cm^2/min) 50% of free values
2.004d-4   , 2.252d-4             Brownian diffusivities(cm^2/min)
2.32299E-01 , 3.38024d-4           Freundlich/Langmuir Hybrid a    (moles/L B.V.)
rhob=0.489, ccap=0.5071
1.0         , 1.36300d-3           Freundlich/Langmuir Hybrid b    (1/M)  a_Re = 2.48000d-
1
1.0         , 1.0                  Freundlich/Langmuir Hybrid Ma   (-) 3.06463d-1
1.0         , 1.0                  Freundlich/Langmuir Hybrid Mb   (-)
1.46316E-03 , 0.0                  Freundlich/Langmuir Hybrid beta (-) effective isotherm
NO3 =
-------------------------------------------------------------------------------
```

VERSE Input for Lab-Scale Pertechnetate Column (King 2000b Tk-44F) Test

```
Tank44F Simulation of Tc removal on small-scale Superlig 639 column (50.1 ml)
1 component (Tc) isotherm (NO3- set to 0.370 M) (SRS Tank 44F Salt Solution)
1, 50, 3, 6                       ncomp, nelem, ncol-bed, ncol-part
FCWNA                             isotherm,axial-disp,film-coef,surf-diff,BC-col
NNNNN                             input-only,perfusable,feed-equil,datafile.yio
MM                                comp-conc units
8.75, 2.7, 2.5885, 50.1           Length(cm),Diam(cm),Q-flow(ml/min),CSTR-vol(ml)
377.0, 0.357, 0.371, 0.0          part-rad(um), bed-void, part-void, sorb-cap()
  0.0, 0.0                        init-conc [M]
S                                 COMMAND - conc step change in ReO4-
1, 0.0, 3.12316d-5, 1, 0.0        spec id, time(min), conc(mg/ml), freq, dt(min)
V                                 COMMAND - viscosity/density change
0.0261255, 1.202                  fluid viscosity(posie), density(g/cm^3)
h                                 COMMAND - effluent history dump
2, 1.0, 1.0, 0.25, 0.1            unit op#, ptscale(1-4) filtering
D
-1, 55000, 1, 0.0
-                                 end of commands
55000, 1.0                        end time(min), max dt in B.V.s
```

```
1.0d-7, 1.0d-4                  abs-tol(mg/ml), rel-tol
-                               non-negative conc constraint
1.0d0      , 1.0d0              size exclusion factor
1.002d-4   , 1.126d-4           part-pore diffusivities(cm^2/min) 50% of free values
2.004d-4   , 2.252d-4           Brownian diffusivities(cm^2/min)
2.32252E-01 , 3.38024d-4         Freundlich/Langmuir Hybrid a    (moles/L B.V.)
rhob=0.4735 (mix)
1.0         , 1.36300d-3         Freundlich/Langmuir Hybrid b    (1/M)  Batch specific
isotherm
1.0         , 1.0                Freundlich/Langmuir Hybrid Ma   (-)    ccap=0.64723
1.0         , 1.0                Freundlich/Langmuir Hybrid Mb   (-)
2.67865E-04 , 0.0                Freundlich/Langmuir Hybrid beta (-) "eff" isotherm NO3
=
-------------------------------------------------------------------------
```

VERSE Input for Lab-Scale Perrhenate Column (Steimke 2000) Test

```
TFL Run-9 Simulation of Re removal on pilot-scale Superlig 639 column (1200.0 ml)
1 component (Re) isotherm (NO3- set to 1.247 M) (BNFL Envelope A Salt Solution)
1, 100, 3, 6                    ncomp, nelem, ncol-bed, ncol-part
FCWNA                           isotherm,axial-disp,film-coef,surf-diff,BC-col
NNNNN                           input-only,perfusable,feed-equil,datafile.yio
MM                              comp-conc units
447.325, 2.61366, 67.167, 1200.0 Length(cm),Diam(cm),Q-flow(ml/min),CSTR-vol(ml)
377.0, 0.269, 0.371, 0.0        part-rad(um), bed-void, part-void, sorb-cap()
  0.0, 0.0                      init-conc [M]
S                               COMMAND - conc step change in ReO4- 12.8=6.87433d-5
1, 0.0, 5.96133d-5, 1, 0.0      spec id, time(min), conc(mg/ml), freq, dt(min)
V                               COMMAND - viscosity/density change
0.0261255, 1.223549             fluid viscosity(posie), density(g/cm^3)
m                               COMMAND - subcolumns
50, 100, 0, 1, 2.95d+8, 0.0, 50000.0  elem-shift,elem-watch,pp-watch,c-watch,c-thresh,t-
e,t-ee
h                               COMMAND - effluent history dump
1, 1.0, 1.0, 0.25, 0.1          unit op#, ptscale(1-4) filtering
h                               COMMAND - effluent history dump
2, 1.0, 1.0, 0.25, 0.1          unit op#, ptscale(1-4) filtering
h                               COMMAND - effluent history dump
3, 1.0, 1.0, 0.25, 0.1          unit op#, ptscale(1-4) filtering
h                               COMMAND - effluent history dump
4, 1.0, 1.0, 0.25, 0.1          unit op#, ptscale(1-4) filtering
D
-1, 9430, 1, 0.0
-                               end of commands
9430, 1.0                       end time(min), max dt in B.V.s  [2690] [6430]
1.0d-7, 1.0d-4                  abs-tol(mg/ml), rel-tol
-                               non-negative conc constraint
1.0d0      , 1.0d0              size exclusion factor
1.002d-4   , 1.126d-4           part-pore diffusivities(cm^2/min) 50% of free values
2.004d-4   , 2.252d-4           Brownian diffusivities(cm^2/min)
2.58546E-01 , 3.38024d-4         Freundlich/Langmuir Hybrid a    (moles/L B.V.)
rhob=0.527 (mix)
1.0         , 1.36300d-3         Freundlich/Langmuir Hybrid b    (1/M)  Batch specific
isotherm
1.0         , 1.0                Freundlich/Langmuir Hybrid Ma   (-)    ccap=0.64723
1.0         , 1.0                Freundlich/Langmuir Hybrid Mb   (-)
1.49735E-03 , 0.0                Freundlich/Langmuir Hybrid beta (-) "eff" isotherm NO3
=
-------------------------------------------------------------------------
```

16.0 Appendix D (Full-Scale Facility Input and Output Files)

For reference VERSE-LC input and output files for full-scale column simulations are provided in this appendix. The case presented here corresponds to an "effective" single component isotherm modeling approach where the pertechnetate ion is modeled assuming the nitrate concentration remains essentially constant throughout the columns. Note that the maximum number of internal collocation points within the pores allowed by VERSE-LC was used. Early numerical testing to establish the minimum usable number of finite elements and collocation points that maintains acceptable accuracy indicated that radial concentration gradients within the particle pores were large and sharp.

Table D-1. Key parameter settings[a] for VERSE-LC simulation of the "effective" single component anion exchange processes for the full-scale column.

Parameter	Parameter settings
Number of finite elements within bed	50 for lead 50 for lag
Number of internal collocation points per finite element within bed	4 for lead 4 for lag
Number of internal collocation points within pores	6 for lead 6 for lag
Components explicitly modeled:	pertechnetate
Axial dispersion, E_b (cm^2/min)	Chung and Wen (1968) correlation
Film coefficient, k_f (cm/min)	Wilson and Geankoplis (1966) correlation
Active column lengths, L	225.0 cm for lead 225.0 cm for lag
Column diameters, D	77.0 cm for lead 77.0 cm for lag
Headspace volumes	1047.74 L for lead 1047.74 L for lag
Bed porosities, ε_b (-)	0.357 for lead 0.357 for lag
Particle porosities, ε_p (-)	0.371 for lead 0.371 for lag
Fluid dynamic viscosity, μ_w	0.0261255 poise
Fluid density, ρ_w	1.223549 g/ml
Lag column switching exit technetium concentration criterion (none for lead)	1.0% of feed concentration as bucket average
Native (initial) concentration	0.0 M
Feed (loading) concentration	4.50×10^{-5} M
Molecular diffusion coefficient	2.004×10^{-4} cm^2/min
Particle pore diffusion coefficient	1.002×10^{-4} cm^2/min
Freundlich-Langmuir Hybrid **a** coefficient	2.45447×10^{-1} gmoles/L_{BV}
Freundlich-Langmuir Hybrid **b** coefficient	1.0 M^{-1}
Freundlich-Langmuir Hybrid $\mathbf{M_a}$ coefficient	1.0 (-)
Freundlich-Langmuir Hybrid $\mathbf{M_b}$ coefficient	1.0 (-)
Freundlich-Langmuir Hybrid β "effective" coefficient for pertechnetate	1.49735×10^{-3} (-)

[a] Isotherm model parameters are based on a bed density of 0.468 g_{resin}/ml and a total ionic exchange capacity of 0.6472 mmole/g_{resin} consistent with batch ID (# 981015DHC720011).

VERSE Input for Full-Scale Column

```
[Full-Scale] Simulation of TcO4 removal on 1047.74 L Full-Scale Superlig 639 lead/lag
columns
1 component (TcO4) isotherm (Avg-Feed: Average feed over broad range of Salt Solutions)
1, 100, 4, 6                      ncomp, nelem, ncol-bed, ncol-part
FCWNA                             isotherm,axial-disp,film-coef,surf-diff,BC-col  FCUNA
NNNYY                             input-only,perfusable,feed-equil,datafile.yio
M                                 comp-conc units
450.0, 77.0, 56781.18, 1.04774d+6 Length(cm),Diam(cm),Q-flow(ml/min),CSTR-vol(ml)
377.0, 0.357, 0.371, 0.0          part-rad(um), bed-void, part-void, sorb-cap()
0.0                               initial concentrations (M)
S                                 COMMAND - conc step change
1, 0.0, 4.50d-5, 1, 0.0           spec id, time(min), conc(M), freq, dt(min)
V                                 COMMAND - viscosity/density change
0.0261255, 1.223549               fluid viscosity(posie), density(g/cm^3)
m                                 COMMAND - subcolumns
50, 100, 0, 1, 0.1, 0.0, 10000.0 elem-shift,elem-watch,pp-watch,c-watch,c-thresh,t-e,t-ee
h                                 COMMAND - effluent history dump
1, 1.0, 1.0, 0.25, 0.1            unit op#, ptscale(1-4) filtering
h                                 COMMAND - effluent history dump
2, 1.0, 1.0, 0.25, 0.1            unit op#, ptscale(1-4) filtering
h                                 COMMAND - effluent history dump
3, 1.0, 1.0, 0.25, 0.1            unit op#, ptscale(1-4) filtering
h                                 COMMAND - effluent history dump
4, 1.0, 1.0, 0.25, 0.1            unit op#, ptscale(1-4) filtering
D
-1, 1811.4, 1, 0.0
D
-1, 1811.4, 1, 0.0
D
-1, 1811.4, 1, 0.0
-                  end of commands
 1811.4, 1.0       end time(min), max dt in B.V.s
1.0d-7, 1.0d-4     abs-tol, rel-tol
-                  non-negative conc constraint
1.0d0              size exclusion factor
1.002d-4           part-pore diffusivities(cm^2/min) 50% of free values
2.004d-4           Brownian diffusivities(cm^2/min)
2.45447E-01        Freundlich/Langmuir Hybrid a    (moles/L B.V.) rhob=0.5003 (Batch-6)
1.0                Freundlich/Langmuir Hybrid b    (1/M)          Batch specific isotherm
1.0                Freundlich/Langmuir Hybrid Ma   (-)            ccap=0.4906
1.0                Freundlich/Langmuir Hybrid Mb   (-)
1.49735E-03        Freundlich/Langmuir Hybrid beta (-)            "eff" isotherm
```

VERSE Output for Full-Scale Column

```
================================================================================
 VERSE v7.80  by R. D. Whitley and N.-H. L. Wang, c1999 PRF
 ================================================================================
 Input file: case
 [Full-Scale] Simulation of TcO4 removal on 1047.74 L Full-Scale Superlig 63
 1 component (TcO4) isotherm (Avg-Feed: Average feed over broad range of Sal
 Begin Run:  16:11:07 on 03-04-2013   running under Windows 95/8
 Finite elements    - axial:100  particle: 1
 Collocation points - axial:  4  particle: 6 => Number of eqns:  4019
 Inlet species at equilib.? N   Perfusable sorbent? N   Feed profile only? N
 Use Profile File? Y   Generate Profile File? Y
 Axial dispersion correlation:   Chung & Wen (1968)
 Film mass transfer correlation: Wilson & Geankoplis (1966)
 Sub-Column Boundary Conditions: Axial Dispersion and CSTR
 ================================================================================
 SYSTEM PARAMETERS (at initial conditions):

 t(stop)        =   1811.40000 min         dtheta max     =      1.00000 BV
 abs. tol.      =       .10000E-06         rel. tol.      =       .10000E-03
 Total Length   =    450.00000 cm          D              =     77.00000 cm
 Tot. Capacity  =       .00000 eq/L solid  Col. Vol.      =2095481.56985 mL
```

```
F              =  56781.18000 mL/min      Uo (linear)    =     34.15583 cm/min
R              =    377.00000 microns     L/R            =  11936.33952
Bed Void frac. =       .35700             Pcl. Porosity  =       .37100
Spec. Area     =     51.16711 1/cm        Time/BV        =      6.58745 min
Vol CSTRs      =1047740.00000 mL

Component no.  =      1
Ke  [-]        =  .10000E+01
Eb  [cm2/min]  =  .43910E+01
Dp  [cm2/min]  =  .10020E-03
Doo [cm2/min]  =  .20040E-03
kf  [cm/min]   =  .13484E+00
Ds  [cm2/min]  =  .00000E+00

Dimensionless Groups:
Re             =  .71765E+00
Sc(i)          =  .63929E+04
Peb(i)         =  .17502E+04
Bi(i)          =  .13675E+03
Nf(i)          =  .12731E+03
Np(i)          =  .17230E+00
Pep(i)         =  .34639E+05

Isotherm       =  Freundlich/Langmuir Hybrid
Iso. Const. 1  =  .24545E+00
Iso. Const. 2  =  .10000E+01
Iso. Const. 3  =  .10000E+01
Iso. Const. 4  =  .10000E+01
Iso. Const. 5  =  .14973E-02
Init. Conc.    =  .00000E+00
Conc. at eqb.  =  .00000E+00
Conc. units           M
================================================================================
COMMAND LIST:
  1: Step conc. of component 1 at .0000     min to .4500E-04 M
     Execute   1 times, every .0000     mins.
  2: User set viscosity to .2613E-01 poise and density to 1.224     g/cm3
  3: Carousel (conc.). Active between t = .0000     and .1000E+05 min.
     When comp.  1 reaches .1000     M     at end of node 100,
     shift  50 axial elements out the feed end
  4: Monitor conc. history at stream  1.  Filename = case.h01
     Output density adjustments:
     1.0    *default abs conc delta,      1.0    *default rel conc delta,
     .25    *default force w/ conc delta, .10    *default force w/o conc delta
  5: Monitor conc. history at stream  2.  Filename = case.h02
     Output density adjustments:
     1.0    *default abs conc delta,      1.0    *default rel conc delta,
     .25    *default force w/ conc delta, .10    *default force w/o conc delta
  6: Monitor conc. history at stream  3.  Filename = case.h03
     Output density adjustments:
     1.0    *default abs conc delta,      1.0    *default rel conc delta,
     .25    *default force w/ conc delta, .10    *default force w/o conc delta
  7: Monitor conc. history at stream  4.  Filename = case.h04
     Output density adjustments:
     1.0    *default abs conc delta,      1.0    *default rel conc delta,
     .25    *default force w/ conc delta, .10    *default force w/o conc delta
  8: Dump full profile file at  1811.     min
     Execute   1 times, every .0000     mins.
  9: Dump full profile file at  1811.     min
     Execute   1 times, every .0000     mins.
 10: Dump full profile file at  1811.     min
     Execute   1 times, every .0000     mins.
================================================================================
VERSE-LC finished in  1370 steps.  Average step size 1.322     minutes
End run:  16:17:29 on 03-04-2013
Integrated Areas in History Files:
case.h01                   .815130E-01
case.h02                   .156146E-01
case.h03                   .152789E-01
case.h04                   .815017E-03
```

Distribution:

R.A. Robbins, WRPS
S. E. Aleman, 735-A
J. V. Odum, 735-A
M. B. Gorensek, 703-41A
L. L. Hamm, 703-41A
F. G. Smith, III, 703-41A
F. M. Pennebaker, 773-42A
D. J. McCabe, 773-42A
W. D. King. 773-42A
C. A. Nash, 773-42A
S. L. Marra, 773-A
W. R. Wilmarth, 773-A